STUDIES OF THE ELECTROCHEMISTRY OF LEAD DIOXIDE

APPENDIX

by

James Peter Carr

CONTENTS

APPENDIX 1. THE LEAD DIOXIDE ELECTRODE - A REVIEW

CONTENTS

(v) Electrode Reactions in Sulphate Solutions

(a) Thermodynamics of the lead dioxide | $PbSO_4$ H_2SO_4 electrode

(b) Kinetics of the lead dioxide | $PbSO_4$, H_2SO_4 electrode

(vi) Electrode Reactions in Phosphate Solutions

6. NUCLEATION OF LEAD DIOXIDE (and associated processes)

(i) The Deposition of Lead Dioxide onto an Inert Basis from Lead Acetate Solution

(ii) The Nucleation of Lead Dioxide onto $PbSO_4$

(iii) The Oxidation of Lead to Lead Dioxide

(iv) Linear Sweep Voltammetry

7. OXYGEN EVOLUTION ON LEAD DIOXIDE ELECTRODES

8. THE USE OF ELECTRODEPOSITED LEAD DIOXIDE FOR PREPARATIVE ELECTRODES

9. THE SELF-DISCHARGE OF LEAD DIOXIDE ELECTRODES

INTRODUCTION

Current technological developments, for instance in electrochemical power sources, are creating fresh interest in the fundamental properties of solid oxide electrodes. Of these lead dioxide has attracted considerable attention due to its use as the active material in the positive plate of the lead-acid cell and there exists a considerable amount of literature concerning electrode behaviour. Several past reviews[1-5] have devoted limited sections to the consideration of the lead dioxide electrode. However, since papers describing phenomena have been largely technological and experimental techniques have not always provided kinetic data adequate to test theories of mechanism, experimental papers are discussed, in which it seems that the measurements have been significant in understanding the processes at the lead dioxide electrodes.

For measurements on any solid electrodes the experimental requirements are severe. In the present case lead dioxide should be carefully prepared and manipulated, both mechanically and electrochemically; a rigorous standard of electrolyte cleanliness is necessary and consequently special techniques of measurements are required. The interpretations of the resulting measurements have often left a good deal of speculation and suggested many more experiments rather than providing final conclusions.

Adequate techniques and satisfactory experimental standards have sometimes resulted from the recognition of the inadequacies of early experiments. A very selective review may do less than justice to much good work however it seems that a more rational approach is required than to accumulate measurements from poorly controlled experiments.

In general oxides are non-conducting or semi-conducting, however, there exists a limited number which show electrical conductivity and bear close similarities to metals. Lead dioxide is such an oxide and consequently an electrical double layer forms in the interphase between the lead dioxide electrode and an electrolyte solution in much

the same was as at a metal electrode. Since exchange proceeds through this electrical double layer it is desirable that its properties should be known and understood. In general quantitative interpretation of double layer measurements at solid oxide electodes, comparable with the established knowledge of the ideal polarizable electrode, as exemplified by Hg, is not available. Capacitance measurements seem most promising, but experimental difficulties are considerable. Many oxides carry adsorbed films which, once formed, are relatively permanent even where a range of quasi-ideal polarizability exists. These cause "hysteresis" effects in capacitance measurements made after an electrode has been subjected to quite small potential excursions. Such adsorption also results in frequency dependence of the electrode impedance. However, some frequency dependence in electrode impedances is found even with metals of high hydrogen overvoltage with macroscopically smooth surfaces in exhaustively cleaned solutions of indifferent electrolytes. At present it is suggested that this small residual frequency dependence is a spurious effect. De Levie[6] has reviewed these effects.

The difficulties encountered with solid metal electrodes will also be expected to apply in the case of solid oxide electrodes. In addition, there are several further factors to be considered related to the structure of oxides* . These include the participation in

---

*Footnote The requirements of an 'ideal' oxide electrode can be summarized as:-

1. Perfect lattice containing no holes, fissures, grain boundaries, impermeable to the electrolyte.
2. Readily obtainable in a reproducible state of minimum free energy.
3. Non-reactive nature, so that it is stable in the electrolyte and free from films.
4. No adsorption of reactant ions at the interphase or the presence of adsorbed intermediates and/or reaction products on the surface which will cause the concentration of soluble electroactive ions in the bulk to differ from that at the interphase.
5. Small size difference between the metal atom and oxygen atom in the lattice.

electrode reactions of both oxygen and metal atoms which differ from each other in size. The electronegativity of each atom is also generally different which infers that the bonding electrons are not equally shared between the metal and oxygen atoms. Metals can exist in more than one oxidation state, due to the presence of partially filled orbitals, and hence various stoichiometries have also to be considered.

PREPARATION OF LEAD DIOXIDE

In most of the earlier reported preparations of lead dioxide no attention was paid to the polymorphic form of the product. However, in some more recent papers details of preparations are given in which careful control of the product morphology has been achieved. The various methods[7-30] for the preparation of lead dioxide that have been proposed from time to time may be subdivided into chemical preparations and electrolytic preparations.

Lead dioxide has been prepared chemically by methods in which Pb(II) compounds are oxidised to lead dioxide in the solution phase, in melts or by heating at elevated temperatures in oxygen. It was reported that lead dioxide could be prepared by the thermal oxidation of PbO[7] or Pb_3O_4[8], however, White and Roy[9] examined the products by x-ray diffraction and found that the oxide produced corresponded to an oxide with an active oxygen content of $PbO_{1.582}$, i.e. it was not possible to produce an oxide by this method with oxygen in excess of $Pb_{12}O_{19}$. Lead dioxide may also be prepared by the hydrolysis of lead (IV) salts[31], for example lead tetrachloride may be hydrolysed in cold hydrochloric acid solution[10] or the hydrolysis of a saturated solution of lead tetracetate in glacial acetic acid. The majority of preparations, however, involve the oxidation of lead (II) salts. Chemical oxidations of sodium plumbite solution in alkali are readily achieved with chlorine, bromine and hydrogen peroxide[10] and simple lead (II) salts may be oxidised with 37 M nitric acid[10]. Anodic oxidations may be carried out with alkaline solutions of sodium plumbite or acid solutions of nitrates, perchlorates,

fluoborates or fluosilicates. The anodic oxidation of lead sulphate is well known[11].

Pure Lead Dioxide

The use of lead dioxide in electrolytic systems, particularly for thermodynamic measurements, has indicated that irreproducible results are often obtained and this imposes stringent purity requirements on the materials involved. For example, in the work of Hamer[12], who studied the galvanic cell:-

$$H_2\ (1\ atm),\ Pt\ |H_2SO_4\ (m),\ PbSO_4,\ |\ lead\ dioxide,\ Pt$$

methods for preparing lead dioxide in a suitably stable form were investigated since commercial samples gave erratic e.m.f. results no matter how they were treated before use. The products of the oxidation of alkaline plumbite solutions by chlorine, bromine or hydrogen peroxide were similarly unsatisfactory. Hamer[12] suggested the electrolysis of an aqueous solution containing lead nitrate and concentrated nitric acid, maintained at 93°C, with use of a platinum gauze anode, produced the most consistent potential values. A platinum wire cathode, surrounded by a porous cup, was used and the solution continuously stirred. In agreement with previous observations[13] it was found essential to digest the black powder so formed at 100°C with 3 mol l^{-1} sulphuric acid for 7 days. This apparently converted the dioxide to its most stable form and removed any lower oxide by conversion to sulphate. Chemical analysis, of which the work of Bagshaw et al[14] is typical of may investigations, has shown that lead dioxide, as prepared by any method so far investigated, always contains a deficiency of oxygen from that required for stoichiometry.

Conformation of Lead Dioxide to PbO_2

A considerable amount of effort has been made into forcing lead dioxide to con-

form to exact stoichiometry. The methods used include chemical oxidation, direct oxidation at high temperatures using high oxygen pressures and the crystal growth of stoichiometric lead dioxide in the solution phase. The starting material for these experiments has in the main been lead dioxide of "normal composition".

The most exhaustive attempts to form stoichiometric lead dioxide have been made by Duisman and Giaque[10]. These include oxidation of lead dioxide at elevated temperatures and high oxygen pressures, for example, a slurry of chemically prepared lead dioxide in 5 mol l^{-1} sodium hydroxide was treated with oxygen at pressures up to ~ 8×10^7 Nm^2 and temperatures up to 320°C for as long as two weeks. It was reported[10] that at the extreme conditions small crystals were formed but analysis showed the oxygen content to be only ~ 98% of the theoretical for lead dioxide. In every case it was found that the product had a deficiency of active oxygen. The addition of solid oxidants and oxidising melts to lead dioxide dispersions followed by reaction at high temperatures and oxygen pressures as high as ~ 4×10^7 Nm^2 also failed to yield stoichiometric lead dioxide[10].

Duisman and Giaque[10] also attempted to convert powdered lead dioxide into the crystalline form by dissolving lead dioxide in a suitable solvent and slowly recrystallising out lead dioxide under a pressure of 1 atm. The starting material for all of these experiments was commercial lead dioxide, and the solvent concentrated nitric acid, in 1:2, 1:1, and 2:1 dilutions with water. The lead dioxide/nitric acid mixture was mechanically agitated for periods up to 6 months at 35°C. The lead dioxide was inspected under a microscope before and after this treatment and no evidence of increased particle size was observed, but analysis indicated that the active oxygen content of the material had decreased. Experiments at 100°C for shorter periods of time showed a similar decrease in active oxygen. Other solvents were investigated - perchloric acid ($HClO_4.2H_2O$), hydrofluoric acid (48%), sodium hydroxide (various concentrations), formic acid, acetic acid (various concentrations), and acetic acid with 10% acetic anhydride, but were

found to be unsuccessful. Liquid ammonia was also tested as a solvent since lead dioxide has properties in common with metals but it was found that lead dioxide did not result from this treatment.

Electrolytic Preparations

Of the various inert materials available as anodes for the electrodeposition of lead dioxide, Pt and Au are the most suitable. Various electrolytes have been employed. A nearly saturated solution of lead perchlorate in perchloric acid water eutectic[15] was electrolysed at anode current densities of 1 and 2 mA/cm^2, using a platinum anode and a graphite cathode at temperatures near $-50^{\circ}C$. Analysis of the product gave 96.4% of the theoretical active oxygen for lead dioxide, with no significant difference between materials prepared at the different current densities. Also employed have been solutions of lead perchlorate in water, lead acetate in water and in glacial acetic acid, lead nitrate in with various nitric acid concentrations, and solutions of sodium plumbite at various concentrations of plumbite and sodium hydroxide.

The effect of hydrogen ion concentration on the lead dioxide electrodeposit was investigated by Duisman and Giaque[10] using lead nitrate-nitric acid solutions in water. Neutral lead nitrate solution was added to the electrolysis solution at such a rate to maintain the concentration of nitric acid at a fixed value. Experiments were made in the range from nearly neutral solutions to a hydrogen ion concentration of 2 mol l^{-1}. At the highest acidities, the active oxygen content of the product declined, however, there was no clear evidence that a solution of 0.1 mol l^{-1} HNO_3 engendered a different product than one with 1.0 mol l^{-1} HNO_3. It was suspected that NO_2^- ions, formed at the cathode by reduction may have an adverse effect on the oxygen content of the sample. This possibility was investigated and eliminated through the use of a solution of lead nitrate and copper nitrate as electrolyte, since Collat and Lingane[32] have shown that electrolytic reduction of nitrate ions proceeds all the way to NH_4^+ in the presence

of Cu^{2+}. No change in the active oxygen content of the samples produced was observed. However, there is no doubt of the complications caused by the NO_3^-/NO_2^- process which results in a very serious decline in deposition efficiency if the NO_3^-/NO_2^- concentration ratio falls below 99%. In the case of the lead nitrate solutions Duisman and Giaque[10] also examined the effect of rotating the anode at different speeds. It was observed that at high speeds the porosity of the sample was slightly decreased. The products, prepared at speeds higher than 100 rpm, all had essentially the same active oxygen content. Current density has no significant effect on the active oxygen content of the lead dioxide deposit. However, the samples prepared at low current densities had a more crystalline appearance and are generally of much better mechanical strength.

From the efforts of a number of workers[10,32-35] formula in the region of $PbO_{1.98}$ appears to best represent lead dioxide although it should be emphasised that the analysis of lead dioxide specimen by x-ray techniques may be complicated[14] and the suggested formation of a new phase at $PbO_{1.9}$[33,36] and also that Pb_5O_8 and lead dioxide have essentially the same diagonal lattice[37,38].

The Preparation of α and β Lead Dioxide

The existence of the two polymorphs α and β lead dioxide has been studied in great detail[14]. The following methods have been used successfully for the production of the two polymorphs.

α Lead Dioxide

(i) Oxidation of yellow lead monoxide by a fused sodium chlorate-sodium nitrate mixture.

Yellow lead monoxide (50g), sodium chlorate (20g) and sodium nitrate (40g) were mixed and heated in a nickel crucible to 340° for 10 minutes. The resulting black melt

was treated with water to remove soluble salts. After drying, the dark brown powder was mixed with the same quantities of sodium chlorate and sodium nitrate and the fusion repeated. This product was washed with water to remove any soluble material and then suspended in 500 ml of 3 mol l^{-1} nitric acid solution to remove the divalent lead ions from the lattice. After being kept overnight, the suspension was heated to 60°, filtered and washed with water. It was important that the temperature did not rise above 340° for any length of time as this reduced the material to minimum, Pb_3O_4. The divalent lead in the fusion product was removed by nitric acid and not by ammonium/acetic acid solution, as the latter also produced mixtures of α- and β-lead dioxide[39,40].

(ii) Oxidation of sodium plumbite by chlorine dioxide.

Yellow lead monoxide (50g) was added to 500 ml of water containing 20g of sodium hydroxide. The mixture was stirred and chlorine dioxide blown in by a stream of air for 4 hrs. The resulting sodium chlorite/lead dioxide mixture was filted, washed with water and finally boiled with 3 mol l^{-1} nitric acid for 45 mins. to remove any lead monoxide. The product was then washed with water and dried.

(iii) Oxidation of lead acetate by ammonium persulphate[39,40].

Ammonium persulphate (250g) was added to 250 ml water and 1l of saturated ammonium acetate solution. An aqueous saturated lead acetate solution, containing 325g of lead acetate was then added slowly, simultaneously with 300 ml of 58% NH_4OH. The reaction proceeded slowly. After 6 hrs. an additional quantity of 50g of ammonium persulphate was added and the solution stirred for 24 hrs. It was then heated to $70^{\circ}C$ for a short period of time to drive off excess NH_3 and to dissolve any precipitated divalent lead compounds. The precipitate was filted and washed with ammonium acetate solution and water and finally dried at room temperature.

(iv) Alkaline formation of lead battery positive plates (Voss and Freundlich)[41].

(v) Electro-oxidation of lead acetate in an alkaline solution (Zaslavsky)[42,43].

β-Lead Dioxide

(i) Acid formation of lead battery positive plates[24].

(ii) Electro-oxidation of lead perchlorate[14].

Yellow lead monoxide (195g) was added to 500 ml of 2 mol l^{-1} perchloric acid solution. A platinum anode and a lead cathode were suspended in the solution and a current of density 2.5 mA cm^{-2} was passed. The deposit was removed, ground and washed with water.

(iii) Electro-oxidation of lead acetate in acid solution[14].

Lead acetate (100 g) was dissolved in 0.5 mol l^{-1} acetic acid solution. A platinum anode and lead cathode were suspended in the solution and a current of density mA cm^{-2} was passed. The deposit was ground and washed with water.

PHYSICAL CHARACTERISTICS AND PROPERTIES

Crystal Structure

Following the work of Kameyama and Fukumoto[42], , Zaslavskii and co-workers[43,44,45], Thomas[46], Darbyshire[8] and Huggins[47], the structures of α- and β-lead dioxide are now generally agreed.

α-lead dioxide has the orthorhombic structure of columbite[25,26], and has the space group Pbcn (V_h^{14}). β-lead dioxide has the tetragonal rutile structure[8,46-48] which belongs to the space group P4/mnm (D_{4h}^{14}). It was shown first by Pauling and Sturdivant[49] that a close relationship exists between the two lattices. In both cases,

each metal ion is in the centre of a distorted octehedron. The essential difference is in the way in which the octahedra are packed, as is illustrated in figure 1. In β-lead dioxide, neighbouring octahedra share opposite edges, which results in the formation of linear chains of octahedra. Each chain is connected with the next one by sharing corners. In α-lead dioxide, neighbouring octahedra share non-opposing edges in such a way that zig-zag chains are formed. Each chain is connected with the next one by sharing corners. The general relationship for the polymorphism of pairs of similar oxides has been discussed elsewhere[50-53].

Only in the case of β-lead dioxide have the oxygen positions actually been determined[54], however, the Pb-O distances are thought to be the same in both modifications[55].

α- and β-lead dioxide may be distinguished from each other by means of x-ray analysis. This method has been used extensively to estimate the proportion of polymorphs in a mixture of the two by means of the standard diffraction patterns.

The technique of x-ray analysis is straightforward in principle[20,57] but in the case of lead dioxide it presents certain problems. These arise due to small crystallite size, lattice distortion, preferred orientation, superposition or diffraction peaks, and internal adsorption effects as described by a number of workers[14,58-62]. In standard mixtures of the two polymorphs, which contain measured amounts of each compound, the intensity of the diffraction pattern of α-lead dioxide is weaker than it should be, relative to the known amount of this phase present. Federova et al[58,59] attributed the abnormally low intensity to a coating-over of crystallites of α-lead dioxide by the softer β-lead dioxide during preparative grinding and mixing. Burbank et al[5] suggests that it is possible that a recrystallization to the stable β-lead dioxide takes place in the superficial layers of the metastable crystals of α-lead dioxide, perhaps initiated by the presence of crystals of the stable phase in the mixtures. This mechanism, in the light of the findings of White et al[53], who could not preserve the alpha structure upon quenching to room temperature

Table 1

Standard diffraction pattern for α-lead dioxide[56]

Interplanar Spacing	Relative Intensity	Indices h k l
3.83	12	110
3.12	100	111
2.97	15	020
2.74	70	002
2.63	70	021
2.48	20	200
2.23	6	112
2.02	6	022
1.89	30	220
1.84	45	130, 202
1.79	30	221
1.64	15	113
1.56	17	222, 023
1.53	30	311, 132
1.43	20	041, 312
1.37	15	312
1.31	15	233
1.26	20	330
1.24	30	241, 400
1.20	40	204, 313

Table 1.2

Standard diffraction pattern for β-lead dioxide[56]

Interplanar Spacing	Relative Intensity	Indices h k l
3.50	100	110
2.80	100	101
2.48	70	200
2.21	10	210
1.856	100	211
1.754	60	220
1.693	40	002
1.569	60	310
1.527	70	112
1.486	70	301
1.399	50	202
1.276	70	321
1.240	20	400
1.220	50	222
1.170	20	330
1.152	70	312

and pressure in the presence of moisture, is interesting. Dickens[63] calculated the structure factors from the diffraction pattern and these corresponded with structure factors derived for the α-lead dioxide structure proposed by Zaslavsky and Tolkachev[45]. Good agreement confirmed the random orientation of the sample prepared in this way, and left little doubt that the different intensity ratios in the powder pattern of the electrodeposited samples were due to preferred orientation effects. The intensity ratios of the diffraction patterns from the powdered samples obtained by electrodeposition differed from those for the other samples. This suggested that the powder was packing in the holder in a non-random fashion. Changes in the intensity ratios when the samples were milled was further evidence that preferred orientation effects were present. When the samples obtained by the other methods were milled, the intensity ratios of their diffraction patterns showed no change, suggesting that these samples were completely randomly orientated.

Acton[64] has reported a method of making thin optically transparent sections of lead dioxide deposits which when examined with polarized light proved partially successful in distinguishing between α- and β-lead dioxide.

A number of descriptions for the chemical analysis of lead dioxide are given in the literature and for examples the reader is referred to the papers of Bagshaw et al[14] and Duisman and Giaque[10].

γ-lead Dioxide

The existence of a pseudo tetragonal form (γ), has been suggested by a number of workers[65-68]. Perrault and Brenet[68] studied the decomposition of Pb_3O_4 in nitric acid and acetic acid. X-ray, chemical and thermogravimetric analyses indicated a second polymorph other than the normally expected β-polymorph. As yet further evidence for the existence of a γ-form is awaited.

Stability and Interconversion of α- and β-lead Dioxide

Under normal laboratory conditions β-lead dioxide is the more stable polymorph, however, under pressure β-lead dioxide may be transformed to α-lead dioxide[53-59,69], ~ 4500 MN/m^2 [69] is required[69]. When the pressure was released, the β-form had not reappeared even after a year at room temperature[53], however, at 100°C some β-lead dioxide was detected after two weeks. At 290°C lead dioxide begins to lose oxygen[9,70]. White et al[53] records the heat of transition of α-lead dioxide to β as 11 cal/mole at 1 atm pressure and 32°C. Burbank[71] reports that α-lead dioxide is converted to β-lead dioxide just before the β-form is thermally decomposed and the conversion temperature lies between 296 and 301°C. Thermogravimetric studies of α- and β-lead dioxide have been made by a number of workers[72-77].

Conductivity

Lead dioxide is highly conducting. Thomas[47] recorded the resistance of lead dioxide in pellet form as 2×10^{-4} ohm-cm and in compacted battery plate active material as 74×10^{-4} ohm-cm. This is in agreement with the earlier measurement of 0.95×10^{-4} ohm-cm reported by Palmaer[78] for the microporous battery plate lead dioxide. Aguf et al[79] determined the resistivity of both α- and β-lead dioxide as 10^{-3} and 4×10^{-3} Ω cm respectively. Hall effect measurements carried out on lead dioxide samples[47,80] indicated a Hall coefficient of between -1.7 and -3.4×10^{-2} cm^2/coulomb, showing that the charge carriers are electrons. Carrier concentrations of from 10^{20} to 10^{21} electrons/cm^3 were recorded.

Nuclear magnetic resonance (NMR) studies of lead dioxide have been reported[81-83] using ^{207}Pb. The value of +0.63 to +0.65% for the Knight shift (the Knight shift in lead dioxide resonance is dependent on the density of electrons at the top of the Fermi distribution[83] and hence is a qualitative measure of the conductivity of the sample,) with respect to metallic lead showed that lead dioxide behaves as a metal in this respect.

Since the lattice relaxation resonance time is short, Piette and Weaver[81] concluded that chemical shift for the magnetic resonances in lead dioxide is due to the conduction of electrons.

A number of workers[47,80,84] have suggested that the conductivity of lead dioxide is associated with the excess lead present in the non-stoichiometric compound. Frey and Weaver[83] showed that as oxygen is removed from lead dioxide, the Knight shift increases, thus showing a decrease in conductivity. Ruetschi and Cahan[85] point out that the reported conductivity decreased as oxygen was removed from lead dioxide and that the Hall coefficient increased showing a decrease in the number of charge carriers. If the conductivity is caused by the deficiency of oxygen, the opposite effect should have been observed, although the stability range of lead dioxide with respect to oxygen content is very narrow before a change of phase sets in. The appearance of a poorly conducting phase in the partially reduced lead dioxide could well explain the loss of conductivity as oxygen is removed. Optical absorption measurements by Lappe[80] of thin films of lead dioxide (~ 100 Å thick) produced by sputtering Pb in O_2/Ar atmosphere on quartz surfaces showed that when the O_2 content was below 3%, the films were composed of pure Pb and when between 3 and 25%, low conducting film of Pb_3O_4 was formed, but when above 25%, a highly conducting film of lead dioxide was obtained containing both the tetragonal and orthorhombic modifications. It was suggested in this work that lead dioxide is a highly doped semiconductor with excess Pb and a band width of about 1.5 eV.

In many cases the oxygen content of α-lead dioxide is less than that of β-lead dioxide, therefore, if oxygen deficiency is the cause of the conductivity of lead dioxide, the α-form should be a slightly better electronic conductor than the β-form. This conclusion is supported by the NMR measurements of Frey and Weaver[83] who report that the Knight shift for the α-form is 0.48%, whereas the shift for the β-form is 0.63% indicating that the conductivity of α-lead dioxide is slightly better than that of β-lead dioxide. Ruetschi and Cahan[69] have also suggested that free electrons in lead dioxide

may be due in part to OH groups substituting for oxygen in the lattice. This is supported by analytical evidence of appreciable amounts of bound hydrogen in electrodeposited lead dioxide[14,84,86-88]. Hydrogen is known to play a similar role in other oxide semiconductors, e.g. in ZnO[89]. The presence of hydrogen is not necessary to explain high electron concentrations as was shown in experiments with sputtered lead dioxide films by Lappe[80], these films did not contain hydrogen and also had a carrier density of 10^{21} cm^{-3}. The influence of impurities other than hydrogen on conductivity is small, since high concentrations are necessary to cause significant relative changes in the carrier concentration. It is for the same reason that doping of lead dioxide with 3- or 5-valent ions has little influence on the conductivity (c.f. SnO_2). Mindt[90] found it impossible to decide whether electrons in electrodeposited lead dioxide were due mainly to nonstoichiometry or to incorporation of hydrogen. The carrier concentration of 1.4×10^{21} cm^{-3} found in the α-lead dioxide films corresponded to a composition of $PbO_{1.971}$ if electrons are due only to ionized oxygen vacancies, and to $PbO_{1.942}(OH)_{0.058}$ if they are due only to OH groups substituting for oxygen. Chemical analytical methods are not sufficiently exact to distinguish between the two cases. In particular, the determination of hydrogen involves a large error[14], and it is difficult to distinguish between hydrogen bound in OH groups in the lattice and hydrogen which is part of adsorbed water.

The decomposition of electrodeposited lead dioxide at room temperature can be interpreted in terms of the generation of oxygen vacancies or the incorporation of hydrogen due to oxidation of water. In both cases, oxygen was evolved and the electron concentration increased. The overall reaction is considered by Mindt[90] to be:-

$$(2\,O^{2-})_{latt} \longrightarrow (2\,\square\,O + 4e^-)_{latt} + (O_2)_{gas} \qquad [1]$$

$$(4\,O^{2-})_{latt} + 2H_2O \longrightarrow (4\,OH^- + 4e^-)_{latt} + (O_2)_{gas} \qquad [2]$$

where ◻ O denotes an interstitial oxygen vacancy.

The result that moisture in the air increases the decomposition rate makes reaction [2] more probable although a similar effect may result if adsorbed water increases the rate of one step of reaction [1]. The different electron mobilities in α- and β-lead dioxide are the result of several factors. The lower mobility in the β-lead dioxide films may be due in part to the smaller size of the crystallites in this modification. The average size of the α-lead dioxide crystallites is about 20000 Å, compared with 5000 Å for the β-modification. There is certainly also an influence of the higher carrier density in α-lead dioxide, since this corresponded to a larger number of lattice defects at which electrons are scattered. Since the α-lead dioxide films have a high degree of orientation (the (100) axis is perpendicular to the substrate), an anisotrophy of the mobility in α-lead dioxide might also influence the results.

Morphologies of α- and β-lead Dioxide

Prior to the detection by Kameyama and Fukumoto[42,43] of α-lead dioxide it is clear that most of the previous studies of structure concern the β-polymorph. Several examinations of the surface morphology of lead dioxide deposits have been made[64, 91-100] but in general the deposits concerned have been in the form of battery plates, for which it has been shown that the strength and durability of the plates depends markedly on the morphology of the crystal mass. Simon and Jones[95,96] for example, showed that maximum lifespan was obtained for a lead dioxide lattice containing large euhedral crystals which they concluded were of α-lead dioxide. It has been shown that different methods of preparation produce different morphologies and crystallinities of α-lead dioxide. A number of different preparations of α- and β-lead dioxide and positive active material from battery plates were examined by Kordes[60] using x-ray diffraction, small-angle scattering, and neutron diffraction. It was found that the interior of a battery plate was well crystallized, whereas the outer layers were less well

crystallized. The small-angle scattering investigations showed that the shape factor for the lead dioxide particles was 1.2 - 1.3, however it could not be determined whether they were of the form of rods or platelets. The average particle size was between 0.38 and 0.56 μ, from which the specific surface area was calculated as 15 and 24 m^2/g. Surface area determinations using gas absorption methods show lower values ($\sim 7\ m^2/g$)[60,41].

Mineral deposits of lead dioxide do not generally occur as well developed crystals, but as nodular masses. Synthetic crystals exhibit more crystallinity but most preparations do not produce crystals large enough to be studied by optical methods. Astakhov et al[94] examined electrodeposits of α- and β-lead dioxide and found that α-lead dioxide was deposited as a low surface area deposit of densely packed large crystals ($\sim 1\ \mu$ in diameter), whereas the β-lead dioxide formed a high surface area deposit of a porous mass of needles. Work by Burbank[98] has shown that the initial deposit of lead dioxide on pure lead by anodisation in H_2SO_4 appeared to be prismatic but thickening of the deposit caused the lead dioxide to lose the prismatic character and Feitknecht and Gauman[101] have shown that the surface of cycled (alternatively reduced to $PbSO_4$ and then re-oxidised) lead dioxide becomes covered with nodular masses of lead dioxide. Burbank[98] determined the size of these particles as 0.1 μ in diamter which agreed with Feitknecht and Gauman[101] however x-ray studies of Feitknecht[102] estimate the particle diameter to be $\sim$ 100 Å. The structure of battery plates immediately following oxidation in dilute H_2SO_4[103] indicated compound spikes of 0.5 μ crystals covered with a layer of sessile crystallites 0.1 μ or less in diameter together with rodlike crystallites or whiskers. During the course of charge and discharge Kordes[60] has shown that crystal size increases to $\sim$ 0.55 - 0.6 but the shape factor is reduced to $\sim$ 0.9 indicating a gradual crystal growth of the lead dioxide particles.

It is clear from work concerning the morphology of lead dioxide that both polymorphs are far from smooth.

Mechanical Properties

Bakhchisaraits'yan et al[104] investigated a number of physico-mechanical properties of lead dioxide including microhardness, brittleness and internal tensions, of lead dioxide electrodes electrodeposited on nickel bases from alkaline plumbite electrolytes. These workers studied the relationship between the properties of lead dioxide and (a) the conditions of its formation, (b) the current density and (c) the presence of organic additions in the electrolyte (ethylene glycol). It was observed that the introduction into the forming electrolyte of ethylene glycol, in concentrations above 4 ml l^{-1}, leads to a fall in the microhardness, brittleness and brilliance. With organic additive the internal stresses become compression stresses which reach a comparatively high value. For higher concentrations of additive an increase in current density also causes compression stresses in the deposit. In organic free electrolytes the properties of the deposit, apart from brilliance, depended upon current density to only a small extent. Bakhchisaraits'yan et al[104] connected the changes in properties with the changes in micro-structure and the composition of the deposits. The occurrence and growth of high internal compression stresses was particularly linked with changes in volume of the deposit[105-107] and with the lead oxide content in the deposit which increased with increasing ethylene glycol. In a later paper Bakhchisaraits'yan et al[108-109] reported investigations of the anodic stability of electrodeposited α-lead dioxide in some acid solutions. It was found that α-lead dioxide is fairly stable in nitric and perchloric acid solutions up to concentrations of 40 - 50%. Any instability was associated with the transformation of orthorhombic α-lead dioxide to tetragonal β-lead dioxide. In highly concentrated solutions of H_2SO_4 breakdown of electrodes was ~ 3 - 4 times higher than in nitric and perchloric acid leading to the formation of salts of Pb(II) and Pb(IV). Stability increased with higher temperatures and in the presence of oxidising agents. The increased breakdown in H_2SO_4 solutions was associated[108] with the presence of H_2O_2 (formed on electrolysis

of H_2SO_4).

$$PbO_2 + H_2O_2 + 2H^+ = Pb(II) + O_2 + H_2O \qquad [3]$$

For both nitric and perchloric acid no H_2O_2 is formed by electrolysis at the electrode.

Electrodeposits of lead dioxide are frequently stressed[110-112] causing cracking and detachment of the deposit from the substrate and inferior discharge properties under galvanostatic conditions. The development of stress in electrodeposits (mainly metals) has been investigated[113] and it is well known that the match/mismatch of the deposited lattice on the lattice of the substrate is not the only factor involved although it may be important in certain cases. Bushrod and Hampson[110] investigated stress set up in lead dioxide electrodeposited from lead nitrate solutions and reported the presence of high compressive stress. At low Pb(II) ion concentrations, the addition of acetate, citrate and tartrate ions was investigated, figure 2.

It was suggested that the adsorbed anions participated in the packing of the structural units that form the deposit. The greater is the surface concentration of the adsorbed ion, the greater is the proportion of the electrode surface which cannot be used in the crystal growth process without displacing the adsorbate. A more open crystal structure then occurs, and the compressive stress is reduced and eventually reversed to become tensile as more adsorbate covers the surface. No change in the $\alpha:\beta$ ratio of the lead dioxide deposit was observed for varying deposit stress indicating that the parameters which determine the α or β arrangement are more fundamental than those which determine the nature of the stress. Analysis of electrodeposits did not preclude the possibility of the presence of hydrogen and additional oxygen in the deposit giving rise to stresses. Hydrogen inclusion in the lattice could arise via a mechanism similar to that proposed[114] for the formation of lead dioxide:-

$$Pb^{2+} + 2OH^- = Pb(OH)_2 \quad [4]$$

$$Pb(OH)_2 = Pb(OH)_2^{2+} + 2e \quad [5]$$

$$Pb(OH)_2^{2+} = PbO_2 + 2H^+ \quad [6]$$

The effect of very high current densities on the stress was considered complementary to the other observations, since at the higher positive potentials involved at higher current densities, the adsorption of anions would be favoured. Shibasaki[115] investigated the textures of electrodeposits of lead dioxide from $Pb(NO_3)_2$ solutions and its relation to strength and deposition conditions. Slightly coarse lead dioxide which was brittle and easily cracked was formed under low current density at normal temperatures. At lower current densities in the presence of certain impurities stronger, dull, smooth lead dioxide was obtained. The most suitable conditions for obtaining a strong bright form of lead dioxide were, (a) smooth substrate surface, (b) low temperatures, (c) presence of one or more of Al^{3+}, Mn^{2+}, polyoxyethelenealkyl ether, paratoluenesulfonamide, (d) absence of iron and cobalt, (e) high concentration of Pb(II).

STANDARD ELECTRODE POTENTIALS

The potential of the Pb|lead dioxide electrode, which corresponds in acid solutions to:-

$$\beta\text{-}PbO_2 + 4H^+ + 4e \rightleftharpoons Pb + 2H_2O \quad [7]$$

has been determined as 0.666 V, by Lander[116], and 0.665 V by Ruetschi and Cahan[69].

For the reaction:-

$$3\ \alpha\text{-}PbO_2 + 2H_2O + 2e \rightleftharpoons Pb_3O_4 + 4OH^- \quad [8]$$

E_o was found to be 1.22 V in acid solution and 0.294 V in alkaline solution[117].

The $PbO_2/PbSO_4$ reaction:-

$$PbO_2 + SO_4^{2} + 4H^+ + 2e \rightleftharpoons PbSO_4 + 2H_2O \qquad [9]$$

is of the most interest because of the commercial applications. Vosburgh and Craig[13] describe the construction of an electrode in which a paste is made in H_2SO_4 solution of equal quantities of $PbSO_4$ and lead dioxide obtained from the electrolysis of $Pb(NO_3)_2$. Electrical contact was made with a Pt wire, and the E_o potential of the electrode corresponding to equation 9 at 25°C was recorded as 1.681 V.

Hamer[12] considered that determinations of the potential of the lead dioxide$|PbSO_4$ electrode reported to 1935, were subject to errors because inferior reference electrodes had apparently been used. Using a Pt/H_2 reference electrode, the potential of the lead dioxide$|PbSO_4$ electrode, as a function of temperature (0 - 60°C) and H_2SO_4 concentration (0.0005 - 7 mol l^{-1}) was found to be:-

$$E_o = 1.67699 + 2.85 \times 10^{-4}T + 1.2467 \times 10^{-6}T^2 \qquad [10]$$

Thus at 25°C, E_o = 1.68597 V.

Comparison of E_o values using the activities of H_2SO_4 and H_2O, determined[118] from the emf data reported by Hamer[12] and the corresponding values calculated from vapour pressure measurements for a series of H_2SO_4 solutions indicate a discrepancy of about 2 mV[119,120]. Beck and co-workers[121,122] considered Hamer's[13] emf data unreliable; the potential of the $PbO_2/PbSO_4$ electrode was studied over a range of H_2SO_4 concentrations from 0.1 to 8 mol l^{-1} and over a temperature range 5 to 55°C. The results of Beck and co-workers[121,122] obey the Nernst relationship, and the temperature coefficient conforms to calorimetric data[120]. The activities obtained from Stoke's data[120] yield a constant value of 1.687 V for E_o[123] as determined experimentally for E_o[121,122].

The electrode system was reversible over the experimental range studied, and the lead dioxide$|PbSO_4$ electrode was found to be a good reference electrode as emphasised by Ives and Janz[124]. No easy explanation of the discrepancy is apparent. The data of Beck et al.[121,122] are shown in Table 3.

Table 3.

Temperature coefficient of e.m.f. and heat of cell reaction at 25°C

H_2SO_4 mol l^{-1}	$-\frac{dE}{dT} \times 10^3$ V °K	$-\Delta H$ (kcal)
0.1000	0.4320	78.156
0.1996	0.3967	78.490
0.2917	0.3721	78.604
0.4717	0.3290	78.604
1.129	0.2570	78.834
2.217	0.2122	79.485
3.900	0.2104	81.065
4.973	0.2314	82.309
6.095	0.2417	83.385
7.199	0.2512	84.397

Bode and Voss[125] reported that the potential of lead dioxide$|PbSO_4$ was different for α-lead dioxide than for β-lead dioxide. The β-form has a more negative potential of approximately 30 mV. Ruetschi and co-workers[84,126] found a potential of 1.7085 V for the α-lead dioxide$|PbSO_4$ electrode and 1.7015 V for the β-lead dioxide$|PbSO_4$ electrode with respect to a Pt/H_2 reference electrode at 25°C in 4.4 mol l^{-1} H_2SO_4*

*Footnote Ruetschi and Cahan showed that although in acid solutions the α-lead dioxide electrode has a potential 7 mV above that of β-lead dioxide there is a cross over in the pH region 1-2 where the β-lead dioxide electrode potential becomes more positive than that of α-lead dioxide.

E_o values of 1.698 V for α-lead dioxide and 1.690 V for β-lead dioxide are reported[127]. From considerations of the physical and chemical properties of α- and β-lead dioxide[84, 126,127] the results obtained by Bode and Voss[125] are probably in error. Bone and co-workers[128] also found the potential of α-lead dioxide electrodes to be about 10 mV more positive than that of β-lead dioxide electrodes in confirmation of Ruetschi et al[127].

Duisman and Giaque[10] have studied the heat capacity of an electrolytic sample of lead dioxide in the temperature range from 15 to 318°K. (The composition was PbO_2 : 1.519×10^{-2} PbO : 2.558×10^{-2} H_2O.) After correction, the entropy of lead dioxide was 17.16 gibbs/mol at 298.15°K. The entropy change in the cell reaction

$$H_2 + PbO_2 + H_2SO_4 = 2H_2O + PbSO_4 \qquad [11]$$

calculated from the third law of thermodynamics, was in excellent agreement with the value dE/dT of Beck, Singh and Wynne-Jones[129], and supports the use of third-law data for lead dioxide, Pb, $PbSO_4$ and H_2SO_4 (x mol l^{-1}) to calculate the temperature coefficient of the lead storage cell. Duisman and Giaque[10] also computed values of the change of potential of the lead storage cell over the range 0 - 60° and from 0.1 to 14 mol l^{-1} H_2SO_4 using the third law of thermodynamics. For the reaction

$$Pb + PbO_2 + 2H_2SO_4\,(pure) = 2PbSO_4 + 2H_2O(pure) \qquad [12]$$

ΔG° = -120,200 cal/mol and ΔH° = -121.160 cal/mol at 298.15°K.

The enthalpy data for the lead dioxide electrode referred to the standard hydrogen electrode and also in conjunction with the lead electrode in sulphuric acid (the most important applications) are shown in figure 3. Duisman and Giaque[10] have presented a large amount of detailed information regarding the thermodynamic data of lead dioxide. An abstract of such thermodynamic data is given in Table 4.

Table 4.

	α -PbO_2	β -PbO_2
Free energy of formation ΔG° per mol.	-51.94 Kcal	-52.34 Kcal
Enthalpy of ΔH° formation	-63.52 Kcal	-66.12 Kcal
Entropy S		18.3 cal/°C 76.44 joule/°C
Heat capacity Cp		15.45 cal/°C 64 joule/°C

Pourbaix Diagrams

Delahay et al[117] have constructed a potential -pH diagram[130] for lead in the presence of sulphate ions. This has been extended by Reutschi et al, Barnes and Matheson[131] and Ness[2] to include the basic lead sulphates. By using the data of Bode and Voss[125] a potential -pH diagram was constructed showing the ranges of thermodynamic stability of the materials of interest: Pb, PbO, Pb_3O_4, lead dioxide, $PbSO_4$, $PbO.PbSO_4$ and $3PbO.PbSO_4.H_2O$. Diabasic and tetrabasic lead sulphates were also considered.

Figure 4 shows the potential -pH diagram of lead, in aqueous solutions containing a total sulphate ion activity ($a_{SO_4^{2-}} + a_{HSO_4^-}$) equal to one gram-ion per litre, constructed from the data given by Barnes and Matheson[131].

Notes to diagram

1. Thermodynamic formulae. Following Barnes et al[131], the potential E for the equilibrium $ox + mH^+ + ne = y_{red} + zH_2O$ at 25°C is given by:-

$$E = \frac{G^{\circ}_{ox} - yG^{\circ}_{red} - zG^{\circ}_{H_2O}}{23\,070\,n} - 0.0591\,\frac{m}{n}\,pH + \frac{0.0591}{n}\log\frac{a_{ox}}{a^{y}_{red}}$$

where G° = standard free energies of formation of the reactants

a = activity of the reactants.

The equilibrium constant K for the reaction $pA + mH^{+} = qB + zH_2O$ is given by:-

$$\log K = \frac{pG^{\circ}_{A} - qG^{\circ}_{B} - zG^{\circ}_{H_2O}}{2.3\,RT}$$

2. Standard free energies of formation. All values were taken from Pourbaix[117,130] except those for the basic sulphate which were taken from Bode and Voss[125].

Table 5

Compound	Standard free energy of formation (cal)*
H_2O	-56,690
Pb	0
PbO	-45,250
Pb_3O_4	-147,600
PbO_2	-50,860
$PbSO_4$	-192,532
$PbO.PbSO_4$	-243,200
$3PbO.PbSO_4.H_2O$	-397,300
Pb^{2+}	-5810
$HPbO_2^{-}$	-81,000
Pb^{4+}	72,300
PbO_3^{2-}	-66,340
SO_4^{2-}	-177,340
HSO_4^{-}	-179,940

*1 cal = 4.184J

Reactions

(a) $2H^+ + 2e = H_2$

$$E = -0.0591\ pH - 0.0295 \log p_{H_2}$$

(b) $O_2 + 4H^+ + 4e = 2H_2O$

$$E = 1.228 - 0.0591\ pH + 0.0147 \log p_O$$

(c) $SO_4^{2-} + H^+ = HSO_4^-$

$$\log \frac{a_{HSO_4^-}}{a_{SO_4^{2-}}} = -1.92 + pH$$

(d) $Pb^{2+} + 2H_2O = HPbO_2^- + 3H^+$

$$\log \frac{a_{HPbO_2^-}}{a_{Pb^{2+}}} = -28.02 + 3\ pH$$

(e) $Pb^{4+} + 3H_2O = PbO_3^{2-} + 6H^+$

$$\log \frac{a_{PbO_3^{2-}}}{a_{Pb^{4+}}} \equiv -23.06 + 6\ pH$$

(f) $Pb^{2+} = Pb^{4+} + 2e$

$$E = 1.694 + 0,0295 \log \frac{a_{Pb^{4+}}}{a_{Pb^{2+}}}$$

(g) $Pb^{2+} + 2H_2O = PbO_3^{2-} + 6H^+ + 2e$

$$E = 2.375 - 0.1771\ pH + 0.0295 \log \frac{a_{PbO_3^{2+}}}{a_{Pb^{2+}}}$$

(h) $HPbO_2^- + H_2O = PbO_3^{2-} + 3H^+ + 2e$

$$E = 1.547 - 0.0886\,pH + 0.0295 \log \frac{a_{PbO_3^{2-}}}{a_{HPbO_2^-}}$$

Limits of domains of predominance of soluble lead ions

(d') $Pb^{2+}/HPbO_2^-$ $\quad pH = 9.34$

(e') Pb^{4+}/PbO_3^{2-} $\quad pH = 3.84$

(f') Pb^{2+}/Pb^{4+} $\quad E = 1.694$

(g') Pb^{2+}/PbO_3^{2-} $\quad E = 2.375 - 0.1773\,pH$

(h') $HPbO_2^-/PbO_3^{2-}$ $\quad E = 1.547 - 0.0886\,pH$

Limits of domains of stability of two phases without oxidation

(i) $4PbO + SO_4^{2-} + 2H^+ = 3PbO.PbSO_4.H_2O$

$$pH = 14.6 + \tfrac{1}{2} \log a_{SO_4^{2-}}$$

(j) $3PbO.PbSO_4.H_2O + SO_4^{2-} + 2H^+ = 2(PbO.PbSO_4) + 2H_2O$

$$pH = 9.6 + \tfrac{1}{2} \log a_{SO_4^{2-}}$$

(k) $PbO.PbSO_4 + SO_4^{2-} + 2H^+ = 2PbSO_4 + H_2O$

$$pH = 8.4 + \tfrac{1}{2} \log a_{SO_4^{2-}}$$

Limits of domains of stability of two solid phases with oxidation

(l) $PbSO_4 + H^+ + 2e = Pb + HSO_4^-$

$$E = -0.300 - 0.0295\,pH - 0.0295\,\log a_{HSO_4^-}$$

(m) $PbSO_4 + 2e = Pb + SO_4^{2-}$

$$E = -0.356 - 0.0295\,\log a_{SO_4^{2-}}$$

(n) $PbO.PbSO_4 + 4e + 2H^+ = 2Pb + SO_4^{2-} + H_2O$

$$E = -0.113 - 0.0295\,pH - 0.0148\,\log a_{SO_4^{2-}}$$

(o) $3PbO.PbSO_4.H_2O + 8e + 6H^+ = 4Pb + SO_4^{2-} + 4H_2O$

$$E = 0.030 - 0.044\,pH - 0.0074\,\log a_{SO_4^{2-}}$$

(p) $PbO + 2e + 2H^+ = Pb + H_2O$

$$E = 0.248 - 0.0591\,pH$$

(q) $PbO_2 + HSO_4^- + 2e + 3H^+ = PbSO_4 + 2H_2O$

$$E = 1.655 - 0.0886\,pH + 0.0295\,\log a_{HSO_4^-}$$

(r) $PbO_2 + SO_4^{2-} + 4H^+ + 4e = PbSO_4 + 2H_2O$

$$E = 1.712 - 0.1182\,pH + 0.0295\,\log a_{SO_4^{2-}}$$

(s) $2PbO_2 + SO_4^{2-} + 4e + 6H^+ = PbO.PbSO_4 + 3H_2O$

$$E = 1.468 - 0.0886\,pH + 0.0148\,\log a_{SO_4^{2-}}$$

(t) $4PbO_2 + SO_4^{2-} + 8e + 10H^+ = 3PbO.PbSO_4.H_2O + 4H_2O$

$$E = 1.325 - 0.0739\ pH + 0.0074 \log a_{SO}^{2-}$$

(u) $PbO_2 + 2e + 2H^+ = PbO + H_2O$

$$E = 1.107 - 0.0591\ pH$$

(v) $3PbO_2 + 4e + 4H^+ = Pb_3O_4 + 2H_2O$

$$E = 1.122 - 0.0591\ pH$$

(w) $Pb_3O_4 + 2e + 2H^+ = 3PbO + H_2O$

$$E = 1.076 - 0.0591\ pH$$

(x) $4Pb_3O_4 + 3SO_4^{2-} + 8e + 14H^+ = 3(3PbO.PbSO_4.H_2O) + 4H_2O$

$$E = 1.730 - 0.1034\ pH + 0.0074 \log a_{SO_4}^{2-}$$

THE STRUCTURE OF THE LEAD DIOXIDE/AQUEOUS SOLUTION INTERPHASE

Studies of the double layer structure have been relatively few[132-145]. Kabanov et al[132] made measurements, using an electrode obtained by the anodic deposition of lead dioxide on a gold base from $Pb(NO_3)_2$ solution, in H_2SO_4 (0.001 to 0.1 N) and $HClO_4$ (0.01 N) solution. These workers estimated that potential of zero charge (p.z.c.) from a minimum in the capacitance curves (and from the presence of an inflection in the overpotential - log i curve) at 1.80 V and concluded that the diffuse double layer theory could be applied to lead dioxide electrodes. Displacement of the capacitance minimum with time was thought to be due to slow adsorption of electroactive species. Since the observed capacitance and resistance changes with time, it was con-

cluded that lead dioxide undergoes some process of surface modification. Kabanov[133] [134] reported H_2SO_4 adsorption at the lead dioxide surface of accumulator positive electrodes and lead dioxide covered lead ribbon formed in H_2SO_4. It was concluded that H_2SO_4 was specifically adsorbed at positive surface charges, the extent of the adsorption depending upon the electrode potential. Evidence was presented showing that adsorbed H_2SO_4 accelerated the o.e.r. Leikis and Venstrem[135,136] measured the hardness of lead dioxide electrodes produced anodically from pure lead in H_2SO_4. From the maximum in the hardness-potential curve the p.z.c. was estimated to be 1.9 V in 0.05 mol l^{-1} H_2SO_4 and 1.7 V for 2.5 mol l^{-1} H_2SO_4. From the sharper decrease in hardness with potential at potentials positive with respect to the p.z.c. (rational potential) it was concluded that specific adsorption of sulphuric acid occurred at positive surface charges in agreement with Kabanov[133,134].

Kokarev et al[137] have formulated equivalent electrical circuits for the impedance of the lead dioxide/0.005 mol l^{-1} H_2SO_4 solution interphase in the presence and absence of isobutanol. They estimated the p.z.c.,from the adsorption of the alcohol which occurred in the very narrow potential range 1.7 - 1.9 V, at 1.8 V. Complementary to these studies the interphase between α- and β-lead dioxide, supported on platinum bases, in a range of aqueous electrolyte solutions have recently been reported[138-142]. Measurements are presented for KNO_3, $NaClO_4$, phosphates, sulphates and sodium hydroxide, the simplest system being KNO_3. In KNO_3 solutions[138] the time-stability of the impedance data indicated no development of the surface with time of electrode/electrolyte contact. The differential capacitance curves (figure 5) resembled in shape those for mercury in sodum fluoride solution[146]. However, the potential region in the present case was about 1.5 V more positive than for the case of mercury. In the most concentrated electrolyte a well defined hump was obtained which, on dilution, became a pronounced hollow. From the magnitude of the capacitance it was suggested that the roughness factor for the lead dioxide electrodes was about 5 - 10 times that for mercury.

Such a high value of roughness factor is in agreement with the observed frequency dispersion of the capacitance. The measurements showed that the capacitance minimum was not dependent upon electrolyte concentration and hence the potential corresponding to the minimum was taken as the point of zero charge E_z. The value of E_z is 1.06 $\pm$ 0.01 V for α-lead dioxide and 1.15 $\pm$ 0.01 V for β-lead dioxide.

At all potentials the capacitance was less for β-lead dioxide than for α-lead dioxide. The capacitance curves shown in figure 5 were integrated to give the surface charge on the electrode. At constant charge density the effect of concentration changes on the differential capacitance curves theoretically follows from equation [13]. Using the connection between surface excess of adsorbed ions, $\Gamma_{\pm}$, electrode potential, $E_{\pm}$, measured with an electrode reversible to cation or anion, and charge on the electrode, q,

$$\left(\frac{\partial E_{\pm}}{\partial \mu}\right)_q = -\left(\frac{\partial \Gamma_{\pm}}{\partial q}\right)_{\mu} \qquad [13]$$

Since $\Gamma_{\pm} = q_{\pm}/z_{\pm}F$, $\partial\mu = -RT\ \partial \log a$ and [14]

$$E_R = E_{\pm} + (RT/z_{\pm}F) \ln a \qquad [15]$$

$$\left(\frac{\partial E_{\pm}}{\partial \ln a}\right)_q = -\frac{RT}{z_{\pm}F}\left(\frac{\partial q_{\pm}}{\partial q}\right)_a \qquad [16]$$

and for KNO_3 solution

$$\left(\frac{\partial E_R}{\partial \ln a}\right)_q = -\frac{RT}{F}\left\{\left(\frac{\partial q_{\pm}}{\partial q}\right)_{a^{\pm}\frac{1}{2}}\right\} \qquad [17]$$

Limiting values of $(\partial q_+/\partial q)_a$ and $(\partial q_-/\partial q)_a$ follow from the Gouy-Chapman

theory[147,148].

Charge	$(\partial q_+/\partial q)_a$	$(\partial q_-/\partial q)_a$
High positive q	0	-1
Zero q	$-\frac{1}{2}$	$-\frac{1}{2}$
High negative q	-1	0

It followed that values of $(\partial E_R/(RT/F)\partial \log a)_q$ at high positive, zero and high negative charge were 1, 0 and -1 respectively.

Figure 6 shows potential, referred to the p.z.c., E_z, as a function of activity, expressed as (RT/F) in a, indicating that specific adsorption is absent. Some divergence from the behaviour observed in the case of mercury and expected from the Gouy-Chapman theory[147,148] was apparent. In particular the magnitude of the surface charge corresponding to the various slopes of the E - log a lines is much less than the reported surface charge densities. This apparently arose since the Gouy-Chapman treatment assumes a smooth uniform electrode whereas lead dioxide is rough. At the higher electrode charge densities the magnitudes of the slopes increased. However, it has been pointed out by Delahay[149] that even for the mercury electrode at high charge density, deviations occur due to both defects in the Gouy-Chapman theory and because the contribution of the diffuse layer is relatively minor. The symmetry of the family of curves and the satisfactory slopes not far removed from E_z was taken as support for the correct choice of E_z.

It was reported that in other electrolyte solutions the double layer was complicated by adsorption. In sulphate electrolytes[139], for example, the capacitance curves were strongly influenced by pH. Figure 7 shows the results obtained. It was reported that the magnitude of the electrode capacitance rose progressively as pH was decreased. This, it was argued, indicated the participation of the H^+ ion in adsorption at the interphase. It was considered that at a high positive rational potential the direct adsorption of H^+ ion

in the experimentally polarizable region was unlikely. The SO_4^{2-} ion however was expected to be adsorbed in view of the low solubility of $PbSO_4$. As the pH is lowered the concentration of HSO_4^- at the electrode increases and it was suggested that the observed pseudo-capacitance arose from reactions of the type:-

$$H^+ + SO_{4_{ads}}^{2-} = HSO_{4_{ads}}^- \qquad [18]$$

$$4HSO_{4_{ads}}^- + PbO_2 + 2e = PbSO_{4_{ads}} + 3SO_{4_{ads}}^{2-} + H_2O \qquad [19]$$

In the case of KNO_3 reactions of the type [19] were not possible.

The difference between the behaviour of α- and β-lead dioxide electrodes in sulphate electrolytes was found to be marginal, however in nitrate electrolytes the differences were significant. It was concluded that the adsorption of sulphate and surface reactions of type [19] obscured surface structural differences between the polymorphs. Similar reactions between adsorbed species was indicated for the lead dioxide/aqueous phosphate solution interphase[140]. Here, as with sulphate[139], the magnitude of the electrode capacitance within the polarizable region was considerably greater than those observed for the nitrate system at equivalent concentrations. Further, the magnitude of the phosphate capacitances decreased progressively in the series H_3PO_4-KH_2PO_4-K_2HPO_4 and indicated the participation of the H^+ ion in the processes at the interphase. The direct adsorption of the H^+ ions at the positive rational potentials was unlikely, however, due to the low solubility of the lead phosphates, it was considered feasible that PO_4^{3-}, HPO_4^{2-} and $H_2PO_4^-$ ions were directly adsorbed according to reactions of the type:-

$$PbO_2 + 2H_2PO_{4_{ads}} + 2e = PbHPO_{4_{ads}} + HPO_{4_{ads}}^{2-} + 2H_2O \qquad [20]$$

$$PbO_2 + 4H_2PO_{4_{ads}}^- + 2e = PbHPO_{4_{ads}} + 3HPO_{4_{ads}}^{2-} + 2H_2O \qquad [21]$$

$$PbO_2 + 5HPO_4^{2-}{}_{ads} + 2e = PbHPO_4{}_{ads} + HPO_4^{3-}{}_{ads} \quad [22]$$

Such reactions are favoured by decreasing the pH of the electrolyte, thus the lower pH resulted in a greater adsorption capacitance. Both phosphate and sulphate electrolytes have been used for accumulator electrolytes. The significant difference reported between the behaviour of the lead dioxide$\left|SO_4^{2-}, H^+\right.$ system and the lead dioxide$\left|PO_4^{3-}, H^+\right.$ system was that potential excursions beyond the negative limit of the polarizable region resulted in a pronounced reduction in electrode capacitance, apparently in accord with the flat capacitor formula. For both systems the appreciable faradaic current flow at such potentials indicated lattice reduction and it was suggested that the particular lead (II) phosphate produced under these conditions had sufficient solubility to leave the electrode. Alternatively it was considered that any lead phosphate film formed was only poorly adherent to the electrode and unable to act as a dielectric.

In NaOH[142] a minimum in the capacitance curves was observed at 1.15 V for β-lead dioxide, however, for α-lead dioxide the capacitance curves were much flatter, showing no pronounced minimum.

EXCHANGE REACTIONS

The dissolution, deposition and exchange reactions at lead dioxide electrodes occur between species in the electrode surface and reduced particles on the solution side of the double layer. In certain systems where the Pb(II) ion is very insoluble such as $Pb\left|PbSO_4, H_2SO_4\right.$ system, the situation may be more complex, due to adsorption, than in systems where the Pb(II) ion is soluble since in the latter case the Pb(II) ion concentration can be determined. These simpler systems will be considered first.

Electrode Reactions in Alkaline Solutions

The electrochemical behaviour of lead dioxide in alkali was investigated by Carr,

Hampson and Taylor[150]. Galvanostatic experiments were reported for α-lead dioxide and β-lead dioxide deposited onto platinum bases. Overpotential-current density data were obtained corresponding to electrolytes based on 3 mol l^{-1} total equivalent univalent salt concentration with added KNO_3. The reaction was reported to be slow ($i_o \sim 0.1$ mA cm^{-2}). In one series of experiments [Pb(II)] was varied at constant [OH^-] and in a second [OH^-] varied at constant [Pb(II)]. Measurements were made in the temperature range 0 - 66°C. It was reported that in alkaline solutions free from Pb(II), β-lead dioxide electrodes were stable; for example, differential capacitance determinations[142] indicated a constant electrode capacitance for at least 24 hours after the initial electrode/electrolyte contact in 1 mol l^{-1} KOH. In alkaline electrolytes containing Pb(II), β-lead dioxide electrodes progressively deteriorated; mechanical strength and adhesion were affected and the deposit disintegrated[150]. It was not found possible to obtain reliable kinetic measurements on β-lead dioxide in alkaline electrolytes containing Pb(II). For α-lead dioxide, electrodes were stable. From the kinetic measurements and the concentration dependencies of both faradaic and exchange current densities the following sequence was suggested for the electrode reaction:-

$$PbO_2 + H_2O + 2e = PbO_{ads} + 2OH^- \qquad [23]$$

$$PbO_{ads} = PbO_{aq} \qquad [24]$$

$$PbO_{aq} + OH^- + H_2O = Pb(OH)_3^- \qquad [25]$$

where PbO_{ads} and PbO_{aq} represented respectively PbO adsorbed at the interphase and in solution. The potential-current density curves could be interpreted in terms of a transition of the charge transfer reaction from an effective one-step process at low overpotential to two consecutive one electron transfers at high overpotentials. This is similar to the behaviour observed for lead dioxide electrodes in perchlorate electrolytes.

The mechanism of the lead dioxide | Pb(II) exchange in acid electrolytes in which Pb(II) is uncomplexed, was reported to differ from that observed in alkali for whereas the reduction in acid involved an initial addition of two H^+ ions to the lead dioxide, viz:-

$$PbO_2 + 2H^+ = PbO_2(H^+)_2 \qquad [26]$$

in alkali the initial step is the addition of a molecule of H_2O to the electrode. It was considered that the difference was not surprising in view of the very different potentials involved.

Electrode Reactions in Perchlorate Solutions

Mark and Vosburgh[151-153] investigated the discharge of lead dioxide electrodes, electrodeposited on a gold basis, in 0.15 mol l^{-1} $HClO_4$ + 0.1 mol l^{-1} $Pb(ClO_4)_2$ and obtained overpotential data which indicated that the exchange reaction was slow ($i_o \sim$ 0.01 mA cm^{-2}). In 1.0 mol l^{-1} $HClO_4$ + 0.1 mol l^{-1} $Pb(ClO_4)_2$ the exchange current was ~ 0.4 mA cm^{-2}. β-lead dioxide electrodes were investigated by Jones et al[154]. It was shown for the cathodic (discharge) reaction that before passivation the electrode remained free of films based on Pb(II). Measurements in the low overpotential region for β-lead dioxide, where the maximum potential excursion was limited to $\pm$ 10 mV about the equilibrium potential, were made[155]. The charge transfer reaction was slow. The dependence of the exchange current on the concentration of Pb(II) indicated a charge transfer coefficient of 0.2 which was verified by an arithmetical analysis of current-potential data. Application of the order of reaction method to a study of the mechanism of exchange between β-lead dioxide and plumbous ions at high overpotentials in solution was investigated using a galvanostatic technique[156]. Interpretation of the η_D vs i data was consistent with a change in mechanism from a single two-electron transfer step to two consecutive single-electron transfer steps as the magnitude of the potential

excursion from equilibrium was increased. Analysis of the slopes obtained from the linear-logarithmic region indicated that the slow step in the reaction is that leading to the formation of a Pb(II) intermediate. The following mechanism was suggested on the basis of the kinetic data.

$$PbO_2 + 2H^+ \longrightarrow PbO_2(H^+)_{2\,ads} \qquad [27]$$

$$PbO_2(H^+)_{2\,ads} + e = [HO\cdot Pb\cdot OH]^+ \qquad [28]$$

$$HO\cdot Pb\cdot OH^+ + e = Pb(OH)_2 \qquad [29]$$

$$Pb(OH)_2 + 2H^+ \longrightarrow Pb^{2+} + 2H_2O \qquad [30]$$

In a later paper the cathodic passivation and the exchange reactions at α-lead dioxide in acid perchlorate electrolytes were reported using the galvanostatic technique[157]. The results were generally closely similar to those previously reported for β-lead dioxide but some differences occur and these were explained in terms of an α-/β-lead dioxide equilibration process. The most significant difference reported for α- and β-lead dioxide was in the order of reaction curves shown in figures 8 and 9, the cathodic data for the log i - E variation in the case of β-lead dioxide all lay on the same line whereas for α-lead dioxide they formed a parallel closely spaced set of lines. The data was interpreted as due to α-lead dioxide being unstable in acid environments and undergoing a changeover to β-lead dioxide due to the exchange reaction occurring at equilibrium.

Electrode Reactions in Nitrate Electrolytes

Mark[153] has studied the discharge of lead dioxide in nitrate electrolytes and compared the results with other soluble lead (II) systems. It appears from the results that the behaviour is similar to the behaviour in perchlorate electrolytes, although no kinetic

constants (or reaction orders) other than exchange current density was evaluated.

Temperature Dependence of Exchange Current Densities

The data reported concerning the temperature dependence of the exchange current are scanty[150,155,157], however, it is clear from the following table that the values fall ~ 31 kJ mol^{-1} for β-lead dioxide. In the case of α-lead dioxide the Arrhenius plot shows two distinct linear regions both for the exchange in alkali and acid perchlorate solutions. This break occurs at ~ 40°C. The magnitude of these enthalpies* are of the order often observed for measurements of exchange reactions at electrodes, however, such measurements are of only limited significance because of the presence of an unknown thermal junction potential. The change in slope of the Arrhenius plot at~ 40°C is particularly interesting because of a complementary behaviour in the equilibrium measurements.

Electrode Reactions in Sulphate Solutions

Because of the great technological importance a number of reviews of the reactions involved with this system, the positive plate of the lead acid battery, have been published. Those of Vinal[2] and Burbank, Simon and Willhnganz[5] appear to be the most important summaries have from time to time appeared[3,4]. For the reader concerned mainly with the technology of the reaction, a combination of references (2) and (5) appear to be adequately up to date and the early work on the discharge mechanism has been adequately reviewed.

---

*Footnote: The enthalpies calculated from Arrhenius plots are not absolute values since an unknown thermal junction potential is present in the potential measurements which cannot be measured.

Table 6

Solution	α-PbO_2	β-PbO_2	Reference
0.025 M [Pb(II)], 3 M [H^+], total [ClO_4^-] 6.85 M	12.6 kJ. mol^{-1} (low temp.) 42 kJ. mol^{-1} (high temp.)		157
0.09 M [Pb(II)], 0.5 M [H^+], total [ClO_4^-] 6.85 M		31.1 kJ. mol^{-1}	155
0.039 M [Pb(II)], 0.68 M [OH], total molar strength 3M	8.2 kJ. mol^{-1} (low temp.) 39.9 kJ. mol^{-1} (high temp.)		150

Thermodynamics of the Lead Dioxide | $PbSO_4$, H_2SO_4 Electrode

The thermodynamic reversibility of the lead-acid battery requires that the positive plate is reversible for the reaction:

$$PbO_2 + 4H^+ + SO_4^{2-} + 2e = PbSO_4 + 2H_2O \qquad [31]$$

for which at 25°C for β-lead dioxide:-

$$E_\beta = 1.6871 - 0.1182\,pH + 0.0295 \log a_{SO_4}{}^{-2} \qquad [32]$$

and for α-lead dioxide:-

$$E_\alpha = 1.6971 - 0.1182\,pH + 0.0295 \log a_{SO_4}{}^{-2} \qquad [33]$$

and

$$(dE_{\partial}/dT)_p = -0.20\ mV/^{\circ}C,\ 4.62\ M\ H_2SO_4 \qquad [34]$$

$$(dE_{\alpha}/dT)_p = -0.36\ mV/^{\circ}C,\ 4.62\ M\ H_2SO_4 \qquad [35]$$

The Kinetics of the Lead Dioxide | $PbSO_4$, H_2SO_4 Electrode

The overall reaction expressed by equation [31] is well established, however, the reaction paths and charge transfer mechanisms are not yet completely settled, partly because two electrons take part in the overall reaction whereas the theory of electrode kinetics makes a single-electron transfer step much more likely, and partly due to complications engendered by a layer of insoluble sulphate formed at the interphase. It should be mentioned in this connection that the existence of trivalent lead in a definite compound has never been observed and uncomplexed tetravalent lead ion is not detected in solution, however Russian workers[158] have described the existence of a reactive trivalent lead intermediate and indirect kinetic evidence for such a species has been presented elsewhere[155-157].

Beck, Lind and Wynne-Jones[121,122] have considered the reversible reaction from the thermodynamic viewpoint and conclude that four reactions are thermodynamically impossible as components of the electrode exchange reaction:- these are

$$H_2O \longrightarrow (OH) + H^+ + e \quad \text{(electrochemical)} \qquad [36]$$

followed by

$$PbSO_4 + 2(OH) \longrightarrow PbO_2 + H_2SO_4 \quad \text{(nonelectrochemical)} \qquad [37]$$

or

$$PbO_2 + 2e \longrightarrow PbO + O^{2-} \quad \text{(electrochemical)} \qquad [38]$$

followed by

$$PbO + H_2SO_4 \longrightarrow PbSO_4 + H_2O \quad \text{(nonelectrochemical)} \qquad [39]$$

since in order to obtain a thermodynamically reversible system the reaction mechanism cannot include any non-spontaneous non-electrochemical step. It is well known that the mechanism of complete discharge of electrodeposited lead dioxide (in the energy conversion sense) in the presence of excess electrolyte involves passivation or blocking of the available surface of lead dioxide with a deposit of $PbSO_4$[159]. Burbank et al[5] emphasised that attempts to analyse the kinetic reactions of charge and discharge on electrodes formed by anodic treatment of lead or of electrodeposited lead dioxide are complicated since the electrodes are a mixture of lead dioxide and $PbSO_4$. A kinetic study of battery plates is complicated because the reactions are diffusion-controlled, and the varying porosity and composition give a surface difficult to maintain constant, notwithstanding other ions, e.g. Sb(III), present at the electrode which may intrude on the lead dioxide$|PbSO_4, H_2SO_4$ reaction.

Fleischmann and Thirsk[160] studied the potentiostatic anodic oxidation of $PbSO_4$ to lead dioxide. At overpotentials of 0.1 V at 45°C and 0.15 V at 15°C no oxidation of the $PbSO_4$ layer occurred. At higher overpotentials, it was estimated that the voltage gradient across the $PbSO_4$ layer was of the order of 5×10^4 V/cm. At local centres of imperfection (active sites-growth sites) in the sulphate crystals electrons were ejected which acted as nucleation centres for lead dioxide. Two rate constants were determined: one for the rate of formation of nuclei of lead dioxide in the $PbSO_4$ layer: and one related to the rate of growth from a centre, the square of the age of the nucleus, and the total possible number of nuclei. The "nucleation overvoltage" showed as a peak at the leading edge of the polarization curve. Qualitatively the two rate constants were shown to be related to the consecutive processes of nucleation, spherical growth

and overlap of growing lead dioxide crystals in the $PbSO_4$ layer. Initiation of the growth began at the crystal-electrolyte interphase, however, the system was too complicated for a reaction mechanism to be abstracted from the electrometric data. For the growth of lead dioxide on $PbSO_4$ Fleischmann and Thirsk[160] reported that when sufficient nuclei had been produced, the rate of formation of additional nuclei was not significant. Mark[151] also showed that, after initial stages in the discharge had occurred, subsequent partial discharges of β-lead dioxide electrodes indicated that creation of new nuclei was not significant. Once the nucleation of $PbSO_4$ had occurred, Mark and Vosburgh[153] observed that the overpotential for the discharge reaction varied linearly with current density and did not deviate from this relation until the electrode became passivated. This was interpreted as indicating direct reduction of lead dioxide to Pb(II), the rate determining step being the transfer of two electrons. Mark investigated the reduction of α-lead dioxide and concluded that the mechanism differed from that of β-lead dioxide. The $PbSO_4$ produced remained as a tightly adhering film on the surface of the undischarged α-lead dioxide in contrast to β-lead dioxide where it was distributed as crystalline nuclei. It was suggested that the α-lead dioxide reaction occurs on the surface whereas the corresponding product in the reduction of β-lead dioxide passes into solution and then deposits on existing $PbSO_4$ crystals. Ikari et al[161] also noticed differences in the discharge behaviour of α- and β-lead dioxide as did Voss and Freundlich[41] who reported that for α-lead dioxide the discharge capacity was lower than the β-polymorph.

Wynne-Jones and co-workers[128,162,163] investigated the exchange between α- and β-lead dioxide and Pb(II) in solution using both radiometric and electrometric measurements. The exchange between Pb(II) in solution and Pb(IV) in the electrode at room temperature was attributed to the charging of the double layer and it was suggested moreover that at high temperatures the exchange is confined to disordered material in the vicinity of lattice imperfections. It was rigorously confirmed that the reaction

occurring in the cell

$$(Pt)\ H_2 \,|\, H_2SO_4\ (M),\ PbSO_4,\ PbO_2 \,|\, (Pt)$$

was:

$$PbO_2 + H_2SO_4 + H_2 \rightleftharpoons PbSO_4 + 2H_2O \qquad [40]$$

for both α- and β-lead dioxide.

The application of impedance measurements to the lead dioxide$\,|\,H_2SO_4$ system has been made by Russian workers[137,145]. Experiments have largely been exploratory and have included measurements in the oxygen evolution region, however no kinetic data were obtained. A later paper[164] describes an impedance study in which the exchange current was evaluated ($i_o \sim 0.32$ mA cm^{-2}) which was in agreement with the value obtained by other workers[155-157] for perchlorate systems.

Electrode Reactions in Phosphate Solutions

A discovery[165], on the basis of a large number of adhoc experiments, that addition of phosphoric acid to the conventional lead-acid cell electrolyte apparently improve the cycle life of the positive electrode is of some interest. The mechanism for the process cannot be regarded as settled. Feitknecht and Gaumann[101] suggested that intermediate plumbic compounds form during the charging process in the sulphuric acid accumulator which are not stable in the 40% (max.) acid, but spontaneously decay or suffer hydrolysis,

$$PbSO_4 + SO_4^{2-} + 2H_2O = \left\{\left[Pb(OH)_2(SO_4)_2\right]^{2-}\right\} + 2H^+ + 2e^- \qquad [41]$$

$$\left\{\left[Pb(OH)_2(SO_4)_2\right]^{2-}\right\} = PbO_2 + H_2SO_4 + SO_4^{2-}$$

or

$$PbSO_4 + SO_4^{2-} = \left\{ Pb(SO_4)_2 \right\} + 2e^- \qquad [42]$$

$$\left\{ Pb(SO_4)_2 \right\} + 2H_2O = PbO_2 + 2H_2SO_4$$

However Feitknecht and Gaumann[101] suggested that in the presence of additions of phosphoric acid, plumbous phosphate was formed at the electrode which was then oxidised to the corresponding plumbic phosphate, H $[Pb(OH)_2PO_4]$, which is relatively stable. It was shown by Bode and Voss that yellow plumbic phosphate (analytical composition $2PbO_2 \cdot P_2O_5 \cdot 2.5\text{-}3H_2O$) is formed in a maximum solution concentration at a molar ratio of H_2SO_4 $H_3PO_4 \sim 0.5$. At a molar ratio $H_2SO_4 : H_3PO_4 < 0.5$ the yellow compound changes, by conversion, into a difficultly soluble white plumbite compound (analytical composition $PbO_2 \cdot P_2O_5 \cdot H_2O$). Under conditions where excess phosphoric acid is present it is suggested that decomposition of the yellow compound with separation of pure α-lead dioxide takes place directly on the electrode surface owing to migration of H^+ ions into the solution. On the other hand, where excess sulphuric acid is present hydrolysis processes bring about separation of the two lead dioxide modifications, but existence of the compounds $Pb(OH)_2SO_4$ or $Pb(OH)_2(SO_4)_2^{2-}$ is hypothetical in this case. It has been established by other workers that increased α-lead dioxide content in positive plates improves the cycle life.

THE NUCLEATION OF LEAD DIOXIDE

Frequently lead dioxide is deposited from solution onto an inert metal substrate. The process of the nucleation of such a layer has been considered in great detail by Fleischmann, Thirsk and co-workers[114,160,163]. The process of electrodeposition of a new phase at an electrode involves the laying down of a number of nucleation centres followed by the growth of these centres until overlapping occurs when the

growth centres coalesce to form a complete layer of the new phase. Fleischmann and Thirsk[163] have discussed the theoretical background to such depositions and the relationships connecting the deposition current density and the time for conditions of constant potential have been fully formulated.

Two systems have been studied in depth, (i) the deposition of lead dioxide from lead acetate solutions[114] and (ii) the formation of lead dioxide from lead sulphate[160].

The Deposition of Lead Dioxide onto an Inert Basis from Lead Acetate Solution

In these solutions it is known[44,45] that α-lead dioxide is the predominantly deposited polymorph provided that the current density is not too high. Fleischmann and Liler[114] investigated the kinetics of deposition of α-lead dioxide from acetate solutions on a platinum basis. Measurements were made at constant values of the overpotential of the working electrode. The concentration dependence of the rate constants controlling the reaction were investigated. It was suggested that the formation of the lead dioxide in the non-steady state was determined by the rate of formation of nuclei, an induction period before nucleus formation and the rate of growth of formed centres. The potential and concentration dependence of these constants were studied. During the initial stages of the nucleation process, the rate equation could not be extracted but by preforming nuclei the current rose more rapidly with time at low overpotential so that the growth process may be sufficiently separated in time for the nucleation process for a limiting value of initial current above which the rate (current) at low overpotential becomes independent of the time of the preformation step. At low overpotential it was shown that the current varied as the square of the time:-

$$i = N_o \; B_3 \; t^2 \qquad [42]$$

where N_o is the original maximum number of nuclei on unit surface and B_3 a potential

dependent growth constant. Three dimensional growth is indicated. Fleischmann and Liler[114] suggested that before nucleation occurred an induction period is necessary and the current-time relationship:-

$$i = \frac{A B_3 N}{3} (t - t_o) \qquad [43]$$

where t_o is the induction period, is observed. From the variation of current density with concentration at fixed potential the orders of reaction with respect to the plumbous and hydroxyl ions were obtained and found to be non-integral. It was suggested that the slow stage of the reaction was:-

$$Pb^{2+} + OH_{ads} + OH^- - e \longrightarrow Pb(OH)_2^{2+} \equiv\equiv PbO_2 + 2H^+ \qquad [44]$$

and that the deviations of the reaction orders from whole numbers was due to adsorption on the electrode surface. Fleischmann and Liler[114] noted that the nucleation constants increased and the variation of the slopes of nucleation rates with overpotential decrease with decreasing reversible β-lead dioxide potential. These facts were interpreted as indicating an increase in the surface free energy of lead dioxide with increasing potential.

The Nucleation of Lead Dioxide on $PbSO_4$

The formation and growth of lead dioxide deposits on $PbSO_4$ bears some similarity to the deposition of lead dioxide from acetate solution. Thus it is necessary to form lead dioxide nuclei which act as active centres for the spreading of lead dioxide through the bulk of the material. Fleischmann, Thirsk and co-workers have considered the conversion of lead sulphate to lead dioxide in some detail[160,163]. The current-time data was found to obey a cubic law of the form:-

$$i = \frac{A B t^3}{3} \qquad [45]$$

where B is a potential dependent constant, A is the nucleation constant and t is time.

The rate of the oxidation was found to reach a maximum and then exponentially decay.

It was assumed that the growth of a β-lead dioxide centre was confined to discreet single lead sulphate crystals and that the decay was due to the completion of the reaction.

The relationship connecting the number of nuclei and time was shown to be:-

$$N = N_o \ (1 - \exp (-A\ t)\ ) \qquad [46]$$

where N is the number of nuclei on unit surface and N_o the maximum number of nuclei on unit surface.

It was possible to derive two rate equations:-

when $t < t_{max}$

$$i = B_3\ N_o\ (t - \frac{2t}{A^2} + \frac{2}{A^2} - \frac{2}{A^2}\ \exp (-At)\ ) \qquad [47]$$

when $t > t_{max}$

$$i = B_3\ N_o \exp (-A\ (t - t_{max})\ )\ (t_{max}^2 - \frac{2t_{max}}{A} + \frac{2}{A^2} - \frac{2}{A^2} \exp (-A\ t_{max})\ ) \quad [48]$$

Using similar reasoning to that used for the deposition of α-lead dioxide from acetate solutions it was found that the surface energy of β-lead dioxide increased with potential. For both the oxidation of $PbSO_4$ to β-lead dioxide and oxidation of plumbous salts to α-lead dioxide the variation of nucleation rate with overpotential obeyed the relationship:

$$A = k\ i_o \exp (-\frac{\kappa \sigma^3}{\eta^2}) \qquad [49]$$

where k is a frequency factor, i_o the exchange current, κ a constant determined by the shape of the nucleus and σ the surface energy.

The Oxidation of Lead to Lead Dioxide

Due to its prominent position in present day commerce the lead-acid Plante cell has been studied in considerable detail. The reaction of paramount importance to this and the lead-acid cell generally is the formation of lead dioxide on a lead substrate and it was considered sufficiently important to present day technology to warrant a fairly detailed review of this aspect of the lead dioxide electrode.

A large number of workers have studied the anodic oxidation of lead electrodes in H_2SO_4[69,84,161,166-212]. Constant current charging curves,[69,84,161,166-181] on closing the electrical circuit, show an immediate rise in potential to a potential plateau. Haring and Thomas[203] showed that the initial potential was that of the reversible $Pb|PbSO_4|$electrode. The potential then rises to a potential peak above the $PbSO_4|$ lead dioxide potential. Few workers have observed an intermediate potential arrest between the $Pb|PbSO_4$redox potential and that of the $PbSO_4|$lead dioxide electrode, however Ekler[170] inferred a potential inflection occurring at the $Pb|PbO$ or $Pb|Pb(OH)_2$ potential and Lander[182] suggested that at potentials below the reversible lead dioxide $PbSO_4|H_2SO_4$ electrode, the lead surface was oxidised with the formation of a layer of PbO on the lead and a layer of $PbSO_4$ next to the electrolyte. Between the $Pb|PbSO_4$ potential and $PbSO_4|$lead dioxide potential the sharp potential peak in the charging curves has been associated with the difficulty of nucleation of lead dioxide on the $PbSO_4$ layer[160]. Ikari and Yoshizawa[171] suggested that the peak was due to the formation of poorly conducting oxides lower than lead dioxide, and Feitknecht and Gaumann[101] associated the potential peak with the conversion of $PbSO_4$ to lead dioxide by reaction with OH radicals. At the $PbSO_4|$lead dioxide potential a plateau is observed in the charging curves in which O_2 is evolved on the lead dioxide surface and lead dioxide is continuously formed by anodic oxidation of the metallic Pb[69,121,161,168,170,180]. Lander[182] showed that the anodic oxidation of lead was a maximum as the potential approached + 1.25 V and a minimum at 1.45 - 1.75 V

(formation of a protective layer of lead dioxide). Further work by Lander[183] showed that lead dioxide and Pb underwent a solid phase reaction:-

$$PbO_2 + Pb = 2PbO \qquad [50]$$

and suggested that cracks develop which allow reaction between the lead and the electrolyte facilitating the oxidation process. At potentials below that of the $PbSO_4$|lead dioxide potential Lander[116] suggested that lead dioxide may be formed but is unstable and is converted to PbO and $PbSO_4$. At potentials close to the $PbSO_4$|lead dioxide potential $PbSO_4$ is formed and at the $PbSO_4$|lead dioxide potential lead dioxide forms and oxidation becomes minimal.

In alkaline solutions the charging curves show an initial potential plateau due to the formation of PbO[172]. Burbank[5] suggested that the PbO had a distorted tetragonal lattice and was more reactive than litharge or massicot. At higher potentials, Pb_3O_4 and $Pb_{12}O_{19}$ were formed so that a layer composed of a mixture of the three oxides was obtained before a potential peak is reached. After the peak lead dioxide was nucleated, and PbO is converted to α-lead dioxide. The lead dioxide is present at a loosely held film which can be flaked off to expose an orange layer of the lower oxides underneath. It has been suggested that the oxidation process on lead in alkaline solutions occurs by a two electron exchange mechanism[182,183,204,210].

$$Pb + 2OH^- = PbO + H_2O + 2e \qquad [51]$$

Part of the PbO is then oxidised to α-lead dioxide

$$H_2O = (O)_{ads} + 2H^+ + 2e \qquad [52]$$

$$PbO + (O)_{ads} + PbO_2 \qquad [53]$$

At potentials above the O_3/H_2O potential lead oxidises directly to lead dioxide by a tetravalent mechanism.

In H_2SO_4, both α- and β-lead dioxide are products of the oxidation of lead[69, 84,125,199], however, it has been shown that the α-lead dioxide is adjacent to the metal[190,191,199] and that oxygen is able to penetrate the β-lead dioxide layer to react with the underlying Pb[211]. Experiments[212] with labelled $(S^{35})SO_4^{2-}$ ions showed that films of $PbSO_4$ were ionic conductors and that Pb(II) ions may move across the inter-phase by a process of solid phase diffusion. Other workers[167,184] have suggested a com-plicated double salt constitution for the electrode layers. Evidence is largely from x-ray diffraction carried out on electrodes withdrawn from the electrolytic cell so that it is often difficult to judge whether results correspond to the electrode situation or to an isolated dried electrode. Since $PbSO_4$ forms a protective layer permeable to H^+ ions and H_2O molecules but not to SO_4^{2-} ions[180,183,189] an alkaline condition may be maintained next to the Pb interface which explains the detection[182,183] of PbO on lead anodes in acid solutions. Ruetschi[180] also indicated that alkaline conditions can be set up behind the $PbSO_4$ films so that PbO or basic lead sulphates may be formed at the Pb interface. As soon as the formation of α-lead dioxide is complete, O_2 evolution occurs and it is now agreed that the form of lead dioxide produced by the oxidation of $PbSO_4$ is the β-variety, however, α-lead dioxide is formed next to the lead interface in a region of high pH.

It can be concluded from the very large number of investigations that this complex reaction proceeds by the transport of charge and mass through a multiplex polyphase boundary and that the penetration of atomic oxygen from the solution side towards the metal is a major process. The study of the morphology of developing layers by potential arrest techniques is consequently likely to be greatly complicated since the potentials which are obtained depend on the role and concentration of the atomic oxygen at the interphase.

In the formation of lead dioxide on Pb by anodisation in H_2SO_4 Burbank[168] has shown that the (100) plane of β-lead dioxide lattice was orientated parallel to the (100)plane of the base. It follows that there exists a 21% mis-match in unit cell dimensions which would cause fracture of growing layers in order to relieve the the stress produced. Cahan and Ruetschi[200] studied the polarization of a Pb anode by superimposing an a.c. square wave current on the steady direct current and determined the impedance along with the potential as a function of time. When the cathodic circuit was closed, the potential dropped from the oxygen overpotential to the lead dioxide $PbSO_4$ potential, and the double layer capacity was very high (500 - 1000 $\mu F/cm^2$). After the lead dioxide step, a short arrest appeared between - 0.1 and - 0.2 V, and the capacity fell to a very low value. This step in the discharge curve may be associated with the presence of the poorly conducting PbO, $Pb(OH)_2$, or basic lead sulphates, a long $PbSO_4$ plateau is reached with a capacity value of about 75 $\mu F/cm^2$ followed by H_2 evolution. In alkaline solutions, the discharge curve exhibits steps associated with the $PbO/PbSO_4$ and the Pb/PbO potentials before H_2 evolution is reached. A small overshoot is detected just ahead of the PbO plateau. Jones and co-workers suggest that a plateau following the $PbSO_4$ step is associated with a lead hydride.

Linear Sweep Voltammetry (L.S.V.)

L.S.V. techniques would be expected to yield data complementary to the measurements discussed in the previous sections. However, there have been few reported studies on lead dioxide. Chartier and Poisson[214] studied the cathodic reduction of β- and α-lead dioxide in alkali and found that the mechanism of the reduction differed for the two polymorphs. For β-lead dioxide it was suggested that the electrode reaction mechanism consisted of two processes:-

a) A solution reaction:-

$$\beta\text{-}PbO_2 + H_2O + 2e = HPbO_2^- + OH^-$$

and

b) A solid phase reaction:-

$$\beta\text{-}PbO_2 + H_2O + 2e = PbO + 2OH^-$$

For α-lead dioxide they suggest that the reduction process occurs exclusively in the solid phase but were unable to give an exact mechanism.

Recently Carr and Hampson[142] made L.S.V. studies on α- and β-lead dioxide in alkali using faster sweep speeds than Chartier[214] ($\sim 12\ mV\ s^{-1}$). Figures 10A and 10B show typical cathodic potential sweep scans for α- and β-lead dioxide respectively.

For α-lead dioxide it was shown that for the peak corresponding to the lead dioxide reduction a linear relationship between I_m and $\sqrt{v}$ was observed passing through the origin indicating that the current limiting relationship is that of diffusion of OH^- ions in solution. From the dependence of I_m on $[OH^-]$ they concluded that for the reaction mechanism adsorption of electrode products intrudes in the electrode reaction. The suggested sequence of reactions involved:

$$\alpha\text{-}PbO_2 + H_2O + 2e = PbO_{ads} + 2OH^- \qquad [54]$$

$$PbO_{ads} = PbO_{aq} \qquad [55]$$

$$PbO_{aq} + OH^- + H_2O = Pb(OH)_3^- \qquad [56]$$

Calculation of the diffusion coefficient from their results yields a value of $\sim 10^{-7}\ cm^2\ sec^{-1}$ which is too small to be the true diffusion coefficient of the OH^- ion in aqueous

solution. These data can be interpreted by either of two explanations, diffusion of OH^- ions must occur through a layer of anodic products and the diffusion coefficient involved was that of the diffusing ion in the product phase, or alternatively the true surface area of the electrode available for diffusion was very much less than the apparent area due to the presence of a solid phase of PbO. It was found difficult to decide which of these two explanations of an adsorbed layer through which the OH^- ion must diffuse was better supported by previous experimental work than the postulation of an incomplete oxide film. For β-lead dioxide at the lead dioxide PbO potential two peaks were observed indicating the presence of α-lead dioxide in the deposit. Continuous cathodic cycling showed a decrease in peak f but increase in peak g indicating a possible modification of the β-lead dioxide on the electrode surface to α-lead dioxide.

Carr, Hampson and Taylor also reported L.S.V. measurements in H_2SO_4[215] solutions. For β-lead dioxide figure 11A shows a typical fast cathodic sweep trace. At the lowest of the sweep speeds applied a linear relationship between I_m and $\sqrt{v}$ was observed for the lead dioxide → $PbSO_4$ reaction passing through the origin. I_m was directly proportional to the concentration of H_2SO_4 throughout the whole of the experimental concentration range indicating that the faradaic current flow was controlled by a diffusion process in solution. The diffusion coefficient determined from these results $\sim 10^{-7}$ cm^2 s^{-1} was considerably higher than that reported for the SO_4^{2-} ion but it was suggested that this was due to the electrode being 'rough' as would be expected for such an electrode. At higher sweep speeds an abrupt change in the slope of the I_m vs $\sqrt{v}$ relationship was observed which occurred at progressively lower sweep speeds for increasing H_2SO_4 concentrations and gave significant intercepts on the current axis. It was suggested that there were two separate mechanisms of current limitation other than charge transfer limitation, namely (i) limitation due to shortage of SO_4^{2-} ions at the electrode and (ii) limitation due to the passage of charge through the insoluble layer of

$PbSO_4$. At lower sweeping speeds and low H_2SO_4 concentrations the current limiting process was the diffusion of the SO_4^{2-} ion in solution to the electrode interphase and at higher sweeping speeds and/or higher concentrations of H_2SO_4 the current limitation was due to the diffusion of ions in a film of $PbSO_4$ at the electrode surface. For α--ead dioxide figure 11B shows a typical fast cathodic potential scan. Repetitive cycling between the limited potential range + 2200 mV to + 1400 mV, with negligible rest time between sweeps, showed a progressive increase of the current shoulder and decrease of the main peak for the lead dioxide → $PbSO_4$ reaction. In contrast to β-lead dioxide, results of plots of I_m (peak e) vs $\sqrt{v}$ did not give linear relationships and indicated that a process other than diffusion was also involved at the electrode at this potential, for example in acid electrolytes α-lead dioxide undergoes structural modifications at its surface to give more stable β-polymorph in low pH electrolytes

$$\alpha\text{-lead dioxide} \overset{H^+}{\rightleftharpoons} Pb(IV) \rightleftharpoons \beta\text{-lead dioxide} \qquad [57]$$

Repetitive sweeps in acid solutions tended to increase the proportion of β-lead dioxide at the α-lead dioxide electrode surface until the β-polymorph is the dominant form involved in the reduction process. A tentative explanation of the appearance of two peaks at the $PbSO_4 \longrightarrow Pb$ potential for α-lead dioxide but not β-lead dioxide was the reduction of some lead compound underneath the $PbSO_4$ layer.

Panesar[216] also studied the cathodic reduction of α- and β-lead dioxide by L.S.V. but used very slow sweep speeds. Cathodic sweeps were made from + 1600 mV as shown in figure 12. The peak at ~ -800 mV was only observed in the case of α-lead dioxide, also for the anodic sweep no current maximum occurred which could indicate the oxidation of $PbSO_4$ → lead dioxide, however by cycling between + 1700 and 800 mV both the reduction and oxidation reactions were observed. Cycling also caused the oxidation/reduction peaks for α-lead dioxide to move to negative potentials

but those of β-lead dioxide remained constant indicating the conversion of α-lead dioxide to β-lead dioxide.

OXYGEN EVOLUTION REACTION ON LEAD DIOXIDE ELECTRODES

Only in H_2SO_4 solution has the oxygen evolution reaction (o.e.r.) at lead dioxide electrodes been investigated thoroughly[10,39,40,84,180,217-235]. It is well known that oxygen is evolved from lead anode only when a layer of lead dioxide has been laid down[204] and that the overpotentials are relatively high[2] being ~ 0.8 V at $\sim 1\ \mu$ A cm^{-2}. Quantitative data in H_2SO_4 electrolytes has been obtained by Ruetschi and co-workers[39,40,84,180,218-221]. It was found necessary to preanodize the electrodes at potentials more positive than that corresponding to the oxygen evolution potentials in order to obtain a time-stable electrode. The reaction was shown to be slow and exchange currents for the α-polymorph reported to be 1.77×10^{-16} A cm^{-2} and β-lead dioxide 6.2×10^{-10} A cm^{-2} in 4.4 molar H_2SO_4[39,40]. Ruetschi and co-workers used electrodeposited lead dioxide on glass sealed Pt rods for these measurements and it is clear from their results that either the β-polymorph is much more catalytically active for the o.e.r. than for the α-form or that the morphology of the polymorphs is completely different. On the basis of capacitance results, it seems to be clear that surface area factors cannot explain these differences. It has been reported[192] that using specially prepared α- and β-lead dioxide electrodes of very low surface area that identical kinetics are obtained for the o.e.r., however data is lacking as to exactly what was done in order to obtain this agreement. It is interesting to note that in H_2SO_4 electrolytes the experimentally determined equilibrium potential for the lead dioxide electrode corresponds to the lead dioxide$|PbSO_4, H_2SO_4$ potential rather than the oxygen potential. This can be traced to the presence of a layer of $PbSO_4$ on the surface of the electrode which is further evidence that the SO_4^{2-} ion, in some form or another,

is adsorbed on lead dioxide. The value of the Tafel slopes for the o.e.r. on lead dioxide have been reported in the region of 0.1 - 0.15 V/decade. For β-lead dioxide it is generally found that the Tafel slope is higher than that on α-lead dioxide . Hoare[4] considers it significant that for β-lead dioxide a slope of ~ 0.12 V/decade is typical of the o.e.r. on metals whereas for α-lead dioxide a slope of ~ 0.05 V/decade observed by Ruetschi and co-workers corresponds to the o.e.r. on metals in alkaline solution. It cannot be completely ruled out that the morphology of the electrode surface in the sense of Frumkin[237] and de Levie[6] may cause this difference which mainly arises from the effective non-uniform current distribution over the electrode surface. The o,e.r. on lead dioxide in common with the o.e.r on most metals has a negative temperature coefficient of overpotential. The small value of the exchange current and the magnitudes of the Tafel slopes shows that the o.e.r. is controlled by the charge transfer process. Ruetschi and Cahan[39,40] suggest that the magnitude of the Tafel slopes indicates a two electron change involved in the rate-determining step for the o.e.r. on α-lead dioxide whereas for the β-lead dioxide the rate determining reaction involves only a one-electron transfer[220]. Other various reaction mechanisms have been proposed. Krasil'shchikov[230] suggests that the evolution of O_2 involves the discharge of OH^- ions or H_2O molecules to form absorbed O^{2-} ions. These O^{2-} ions convert the lead dioxide to a higher oxide which decomposes, as suggested by Glasstone[224], to yield O_2 and lead dioxide. However, lead dioxide cannot be oxidized to a higher state of oxidation[218], and this mechanism is not favoured for the evolution of O_2 on Pb anodes. It is interesting in this connection to note that Burbank[210] observed O_2 evolution on Pb anodes only at potentials more positive than the O_3/H_2O potential at lower potentials lead corroded via lead monoxide in preference to O_2 evolution. Above the O_3/H_2O potential direct formation of lead dioxide takes place as a consequence of the corrosion of Pb without passing through the lead monoxide stage

and O_2 is evolved. It is now established beyond doubt that an oxide of lead higher than lead dioxide does not exist so that lead dioxide acts as an inert electrode and by analogy to the mechanism proposed for the o.e.r. on noble metals, mechanisms have been proposed which fit most of the observed facts, viz H_2O molecules or OH^- ions react to give OH radicals at the electrode to form oxygen atoms:

$$H_2O = OH_{ads} + H^+ + e \qquad [58]$$

or

$$2OH_{ads} = O_{ads} + H_2O \qquad [59]$$

followed by

$$2O_{ads} = O_{2\,gas} \qquad [60]$$

It is reasonable to suggest from the Tafel curves that the electron transfer step is rate determining[175]. It has been observed experimentally, presumably from the combination of oxygen atoms in equation [60], that oxygen atoms are able to diffuse into the lead dioxide layer[221,238]. Russian workers[137,177] have applied the impedance technique to a study of the o.e.r. at lead dioxide electrodes. It is concluded that although the general kinetic behaviour is similar to an inert metal the highly developed surface covered with a layer of intermediate products to some extent complicate the picture. It was confirmed that the products of the charge transfer reaction were OH_{ads} which may then react to form oxygen.

In alkaline solution less experimental data is available than in the corresponding H_2SO_4 solution, however Jones et al[175] have obtained overpotential-current density curves on lead anodes similar to those obtained in acid solutions although some deviations from Tafel behaviour were observed at low current densities. Over most of the experi-

mental region a slope of ~ 0.12 V/decade was obtained. The deviations could be ascribed to self discharge between lead dioxide and the underlying Pb.

The Use of Electrodeposited Lead Dioxide for Preparative Electrodes

Lead dioxide prepared electrolytically has been used from time to time to make anodes suitable in preparative chemistry. Thus iodine has been anodised to periodic acid using both supported[239-242] and unsupported[243-255] (massive) lead dioxide electrodes with high current efficiencies; sodium chlorate has been anodically oxidised to sodium perchlorate in high yield[255] using lead dioxide electrodes of a number of different constructions; iodoform has been prepared[256,257] using the reaction of acetone or ethanol at an anode in the presence of the iodide ion. In all of the investigations reported so far lead dioxide is behaving as an inert electrode in much the same way as Pt rather than showing any specific electrode catalytic activity. It is clear that lead dioxide is able to withstand prolonged high positive potentials more effectively than graphite (which undergoes degradation) and at the same time is cheaper than platinum and may be readily electrodeposited.

The Self Discharge of Lead Dioxide Electrodes

One shortcoming of the preparation of lead dioxide electrodes on a Pb basis is that reaction between the lead dioxide and the underlying Pb lattice is able to proceed in the solid phase. Due to the high electronic conductivity of lead dioxide electron exchange facilities the formation of Pb(II) ions able to react with O^{2-} ions to form a non-conducting PbO layer.

Captions to Figures

Figure 1

Packing of oxygen octahedra in α- and β-lead dioxide from reference 29. Lead-oxygen and oxygen-oxygen distances as determined in references 45 and 55.

Figure 2

Effect of concentration of anions on stress in lead dioxide electrodeposits at 23°C, 30 mA cm^{-2} from reference 110. Electrolyte:- lead nitrate 1.21 mol l^{-1}, (—) acetate; (•) tartrate; (o) citrate.

Figure 3

(A) Entropy change during reduction of PbO_2 by H_2 in x mol l^{-1} H_2SO_4 from reference 10.

(B) Entropy change in lead storage cell from reference 10.

Figure 4

Potential - pH diagram of lead in the presence of sulphate ions at unit activity and 25°C from reference 131.

Figure 5

(A) Differential capacitance vs bias potential curves for electrodeposited α-lead dioxide in aqueous KNO_3 solutions, at 23°C, 120 Hz. From reference 138.

(a) 0.307 mol l^{-1}; (b) 0.115 mol l^{-1}; (c) 0.018 mol l^{-1}; (d) 0.0121 mol l^{-1}; (e) 0.0043 mol l^{-1}. Broken line shows the electrode resistance, R_E, vs potential curve at 23°C, electrode area 4.49×10^{-2} cm^2, 0.307 M aqueous KNO_3, 120 Hz, pH 5.7.

(B) as (A) for β-lead dioxide. From reference 138.

Figure 6

(A) Potential, referred to E_z, as a function of activity $(\frac{RT}{F} \ln a_{\pm})$ for electrodeposited α-lead dioxide at constant charge. From reference 138.

(B) as (A) for β-lead dioxide.

Figure 7

(A) Differential capacitance vs bias potential curves for electrodeposited α-lead dioxide; 23°C, 0.0344 mol l^{-1} aqueous K_2SO_4 over pH range 1 - 12.

(⊖) pH 12.0; (▬) pH 6.0; (▭) pH 3.8; (▲) pH 3.4; (△) pH 3.0; (◉) pH 2.5; (○) pH 1.8; Frequency 120 Hz. From reference 139.

(B) as (A) for β-lead dioxide.

Figure 8

Anodic and cathodic current density - potential curves for electrodeposited β-lead dioxide at various Pb(II) concentrations in 3.0 mol l^{-1} $HClO_4$ at 23°C. From reference 156.

Figure 9

Cathodic and anodic current density - potential curves for electrodeposited α-lead dioxide at variable Pb(II) concentrations in 3.0 mol l^{-1} H^+ at 23°C; total $[ClO_4^-]$ 6.85 mol l^{-1}. From reference 157.

Figure 10

(A) Typical fast cathodic potential sweep on electrodeposited α-lead dioxide in aqueous NaOH solution (4.7 mol l^{-1}), 23°C, sweep rate 58.3 mV s^{-1}. Electrode area 4.9×10^{-2} cm^2. From reference 142.

(B) as (A) for β-lead dioxide.

Figure 11

(A) Typical current - potential curve for a cathodic (—) and anodic (--) potential sweep on electrodeposited α-lead dioxide in aqueous H_2SO_4 solution (4.41 mol l^{-1}) at 23°C. Electrode area 4.49 x 10^{-2} cm^2; sweep rate 58.3 mV s^{-1}. From reference 215.

(B) as (A) for β-lead dioxide in 5.56 mol l^{-1} H_2SO_4 solution.

Figure 12

Cyclic voltammetric curves for α- and β-PbO_2 electrodes in 5 mol l^{-1} H_2SO_4 at 30 mV/min (—) anodic, (---) cathodic from reference 216.

Fig. 1.

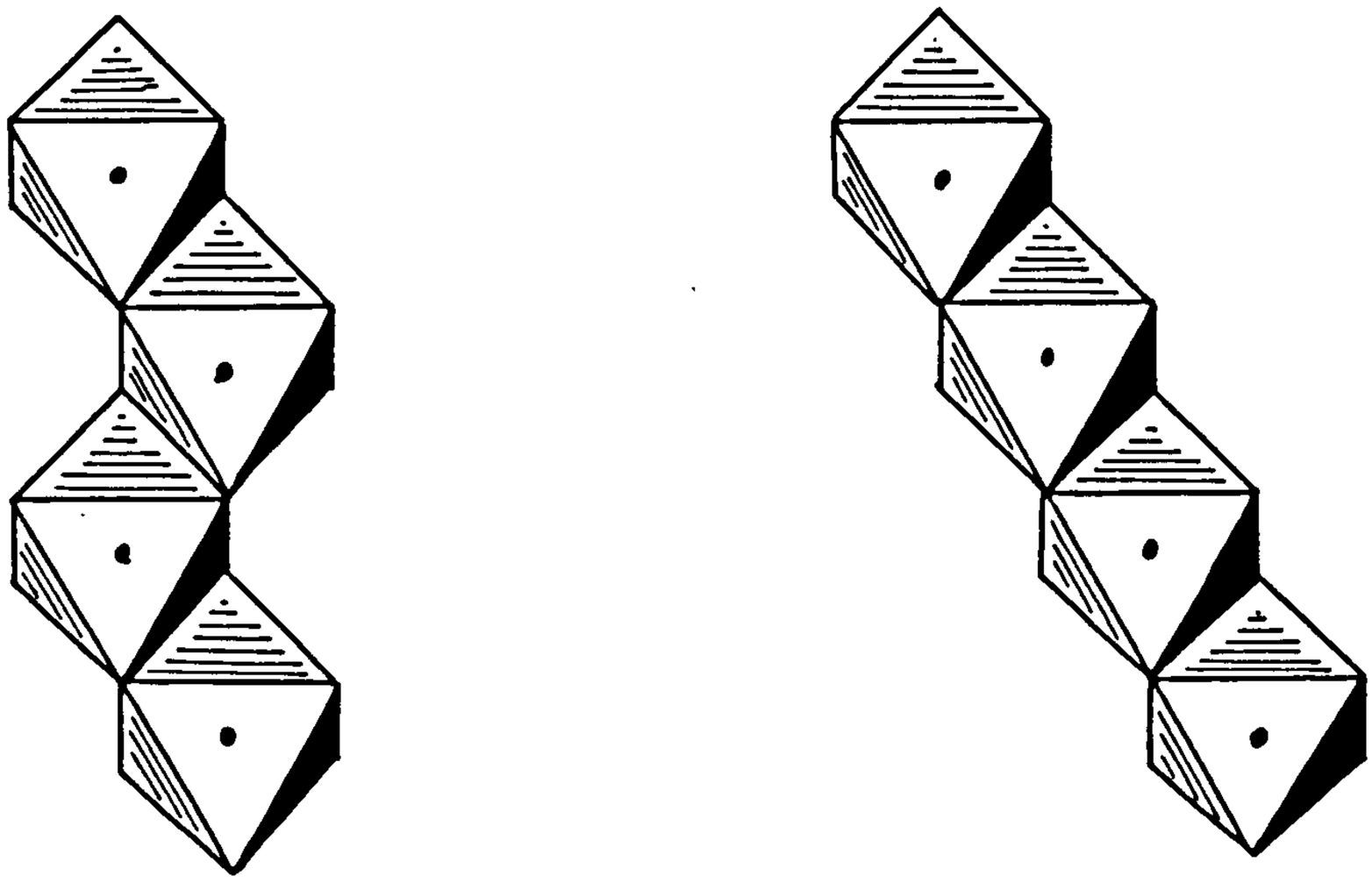

α-PbO_2 (orthorhombic)	β-PbO_2 (rutile)
6 x Pb-O = 2·16 Å	4 x Pb-O = 2·15 Å
2 x O-O = 2·59 Å	2 x Pb-O = 2·16 Å
10 x O-O = 2·92 - 3·35 Å	2 x O-O = 2·67 Å
	8 x O-O = 3·03 Å
	2 x O-O = 3·38 Å

Fig. 2.

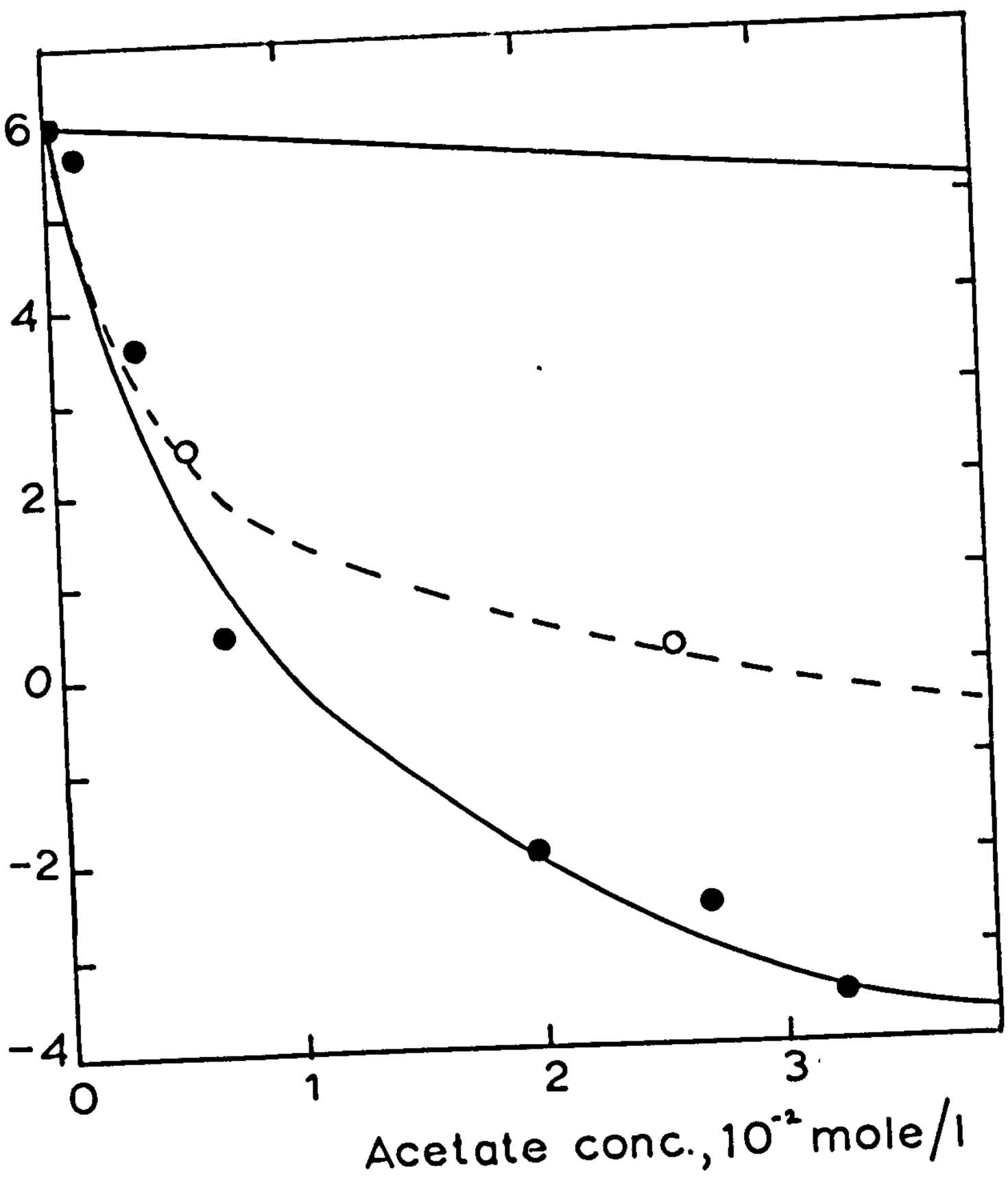

FIG. 3A

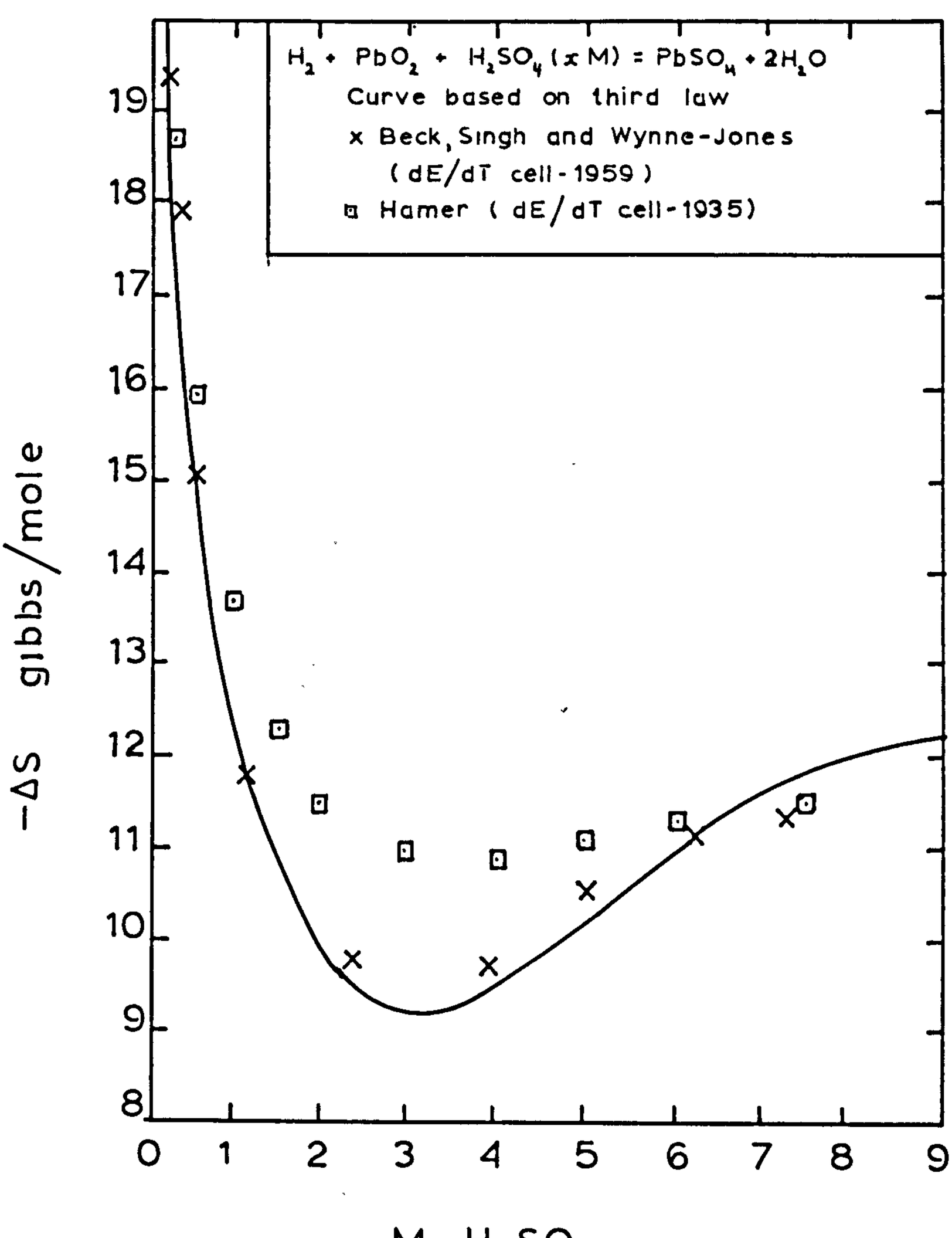
$H_2 + PbO_2 + H_2SO_4 (x\,M) = PbSO_4 + 2H_2O$
Curve based on third law
x Beck, Singh and Wynne-Jones
(dE/dT cell - 1959)
Hamer (dE/dT cell - 1935)
$-\Delta S$ gibbs/mole
19
18
17
16
15
14
13
12
11
10
9
8
0
1
2
3
4
5
6
7
8
9
M. H_2SO_4

Fig. 3B.

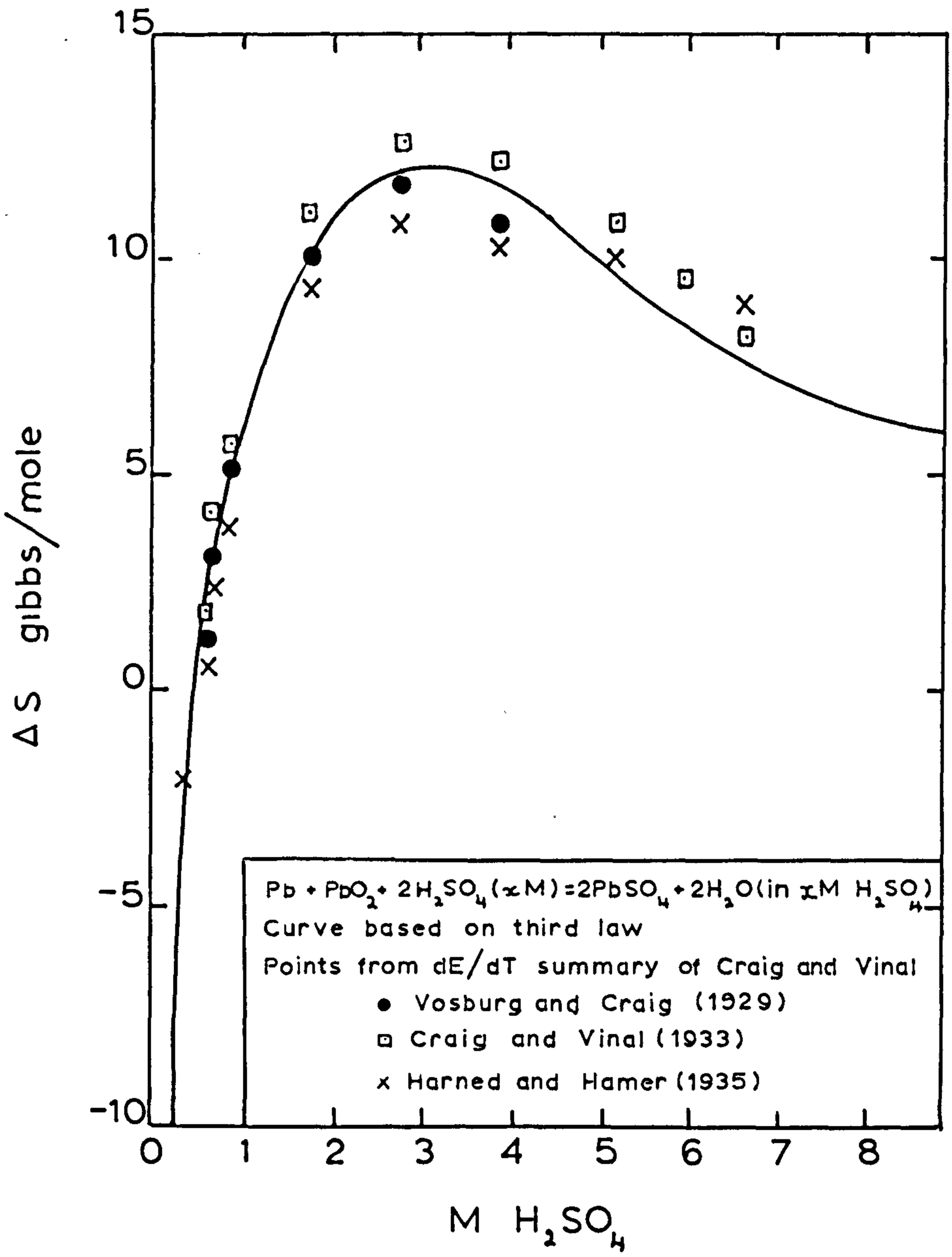
15
10
5
0
−5
−10
ΔS gibbs/mole
0 1 2 3 4 5 6 7 8
M H2SO4
Pb + PbO2 + 2H2SO4 (x M) = 2PbSO4 + 2H2O (in x M H2SO4)
Curve based on third law
Points from dE/dT summary of Craig and Vinal
● Vosburg and Craig (1929)
⊡ Craig and Vinal (1933)
× Harned and Hamer (1935)

Fig. 4.

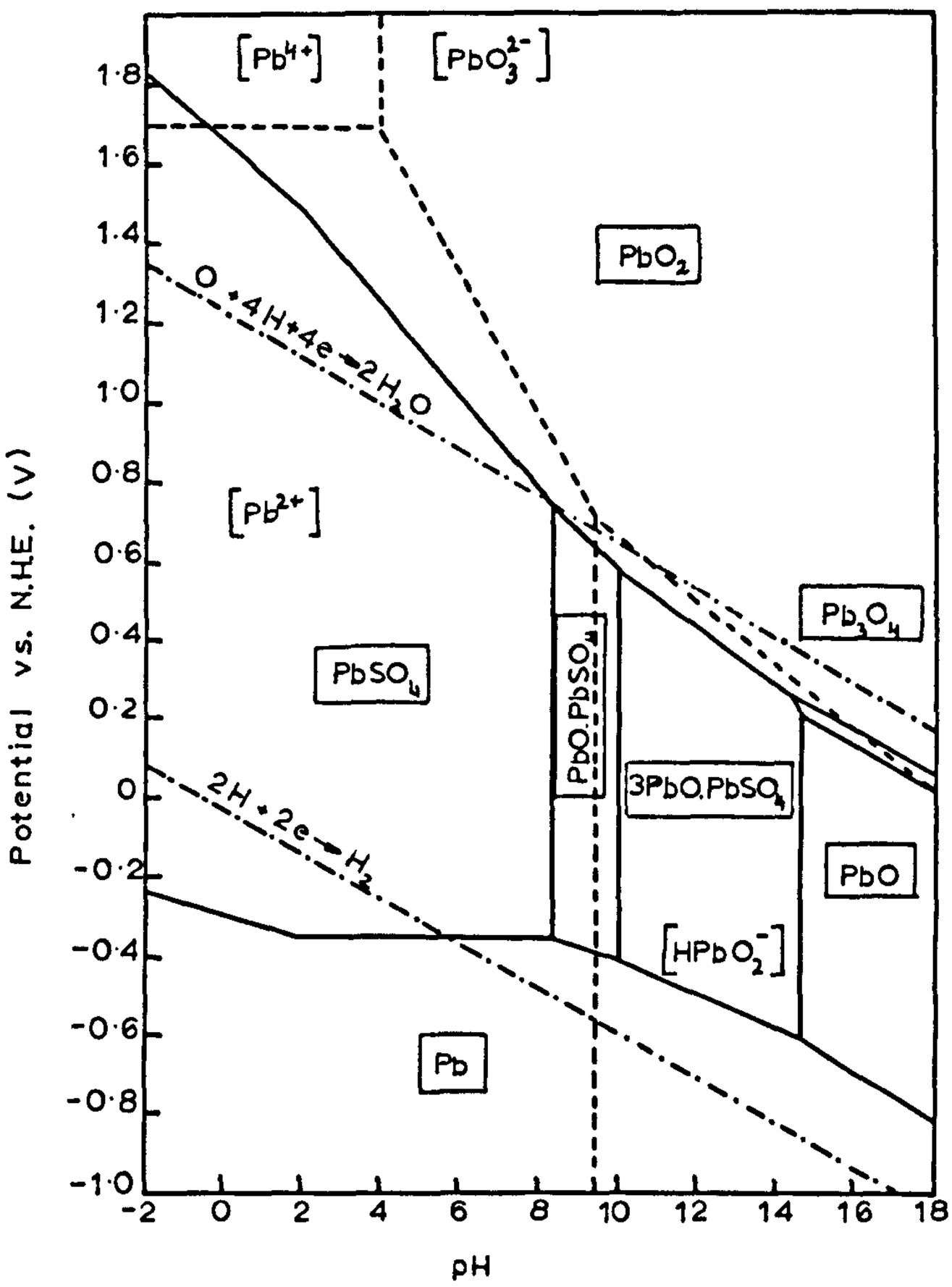
[Pb4+]
[PbO3 2-]
PbO2
O + 4H + 4e = 2H2O
[Pb2+]
PbSO4
PbO.PbSO4
3PbO.PbSO4
Pb3O4
PbO
[HPbO2-]
Pb
2H + 2e = H2
Potential vs. N.H.E. (V)
pH
1·8
1·6
1·4
1·2
1·0
0·8
0·6
0·4
0·2
0
-0·2
-0·4
-0·6
-0·8
-1·0
-2
0
2
4
6
8
10
12
14
16
18

Fig. 5A.

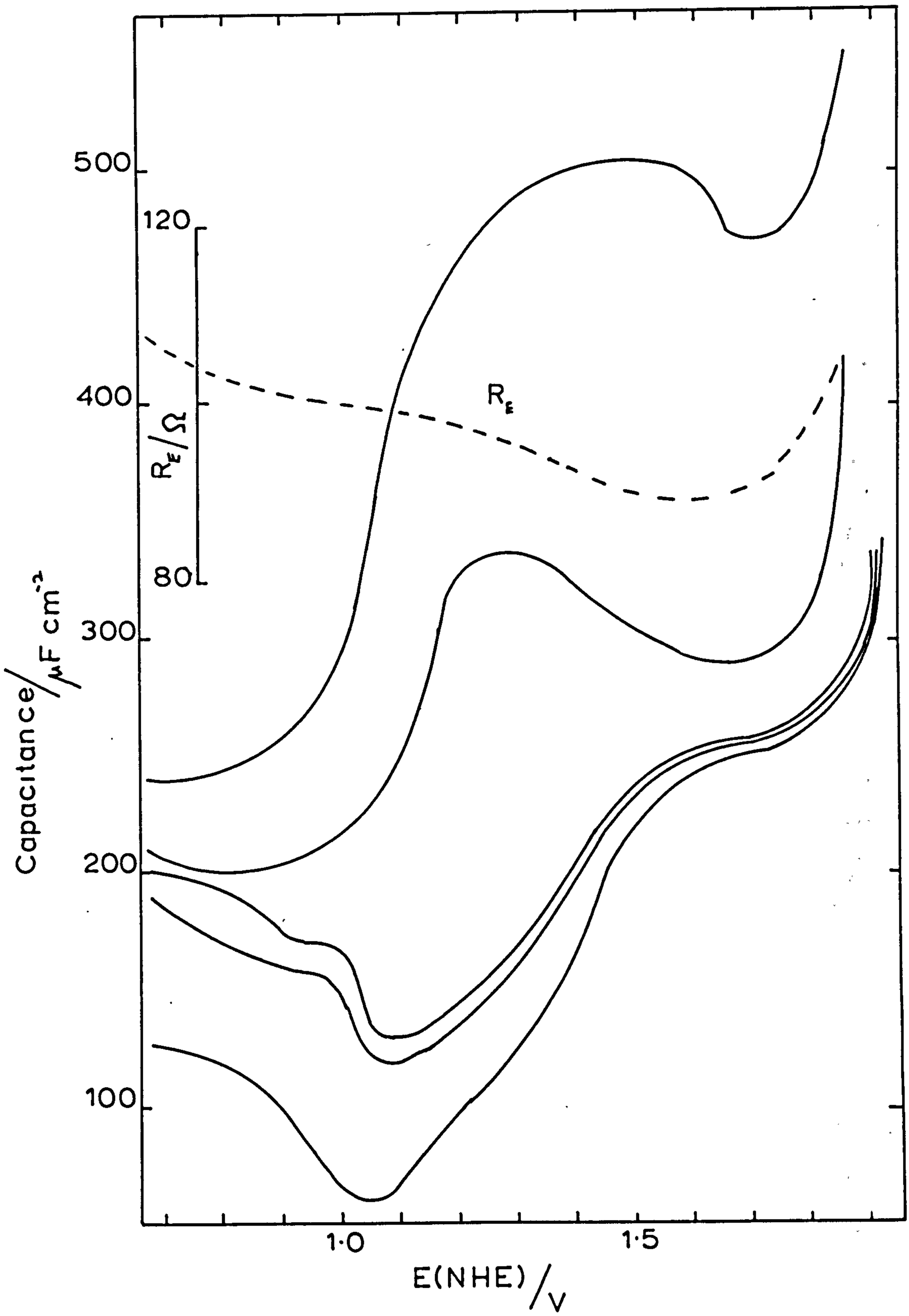
500
120
400
R_E/Ω
R_E
80
300
Capacitance/$\mu F\ cm^{-2}$
200
100
1·0
1·5
E(NHE)/V

Fig. 5B.

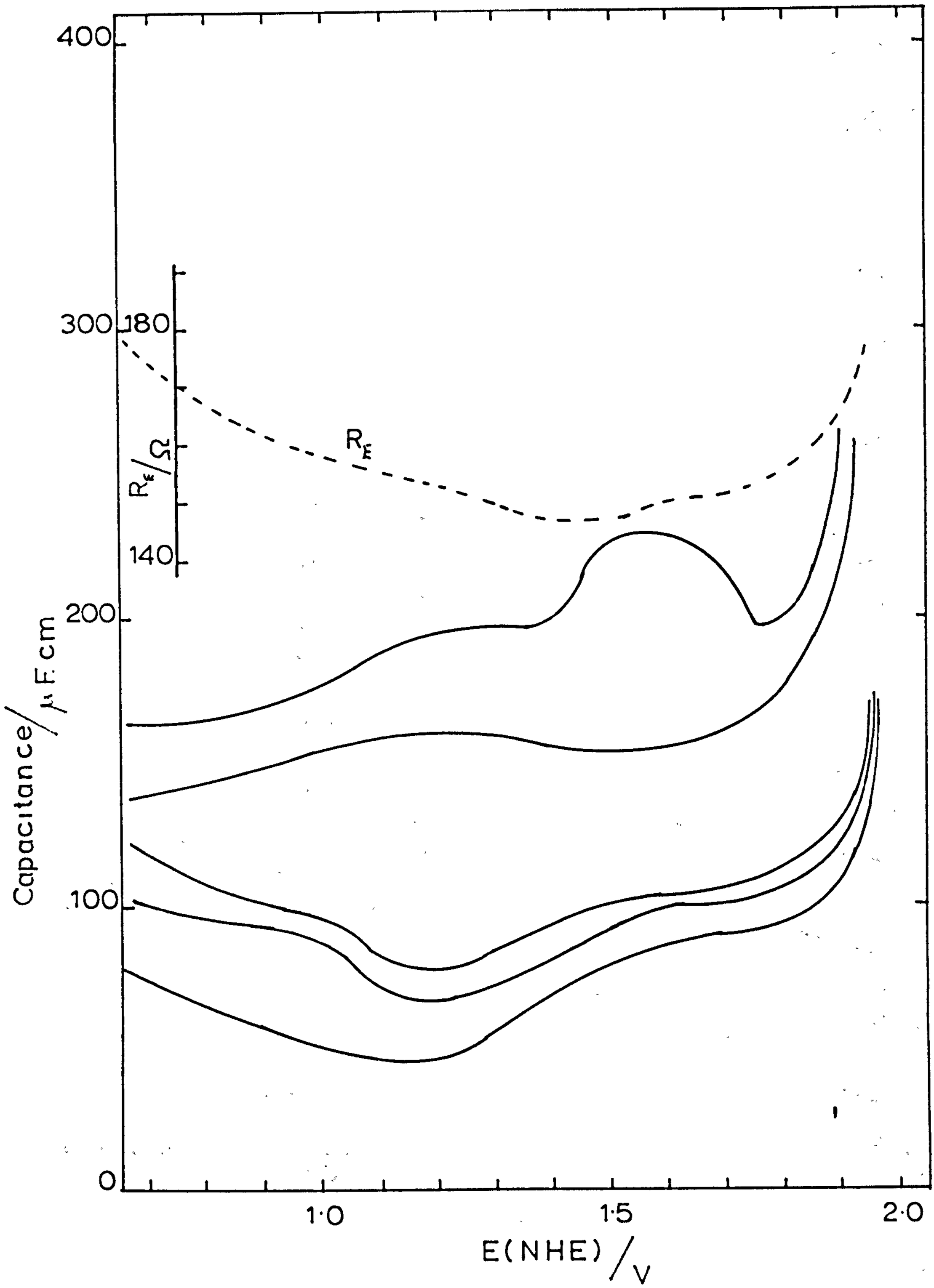
400
300
180
140
200
100
0
R_E/Ω
R_E
Capacitance/μF.cm
1·0
1·5
2·0
E(NHE)/V

Fig. 6A.

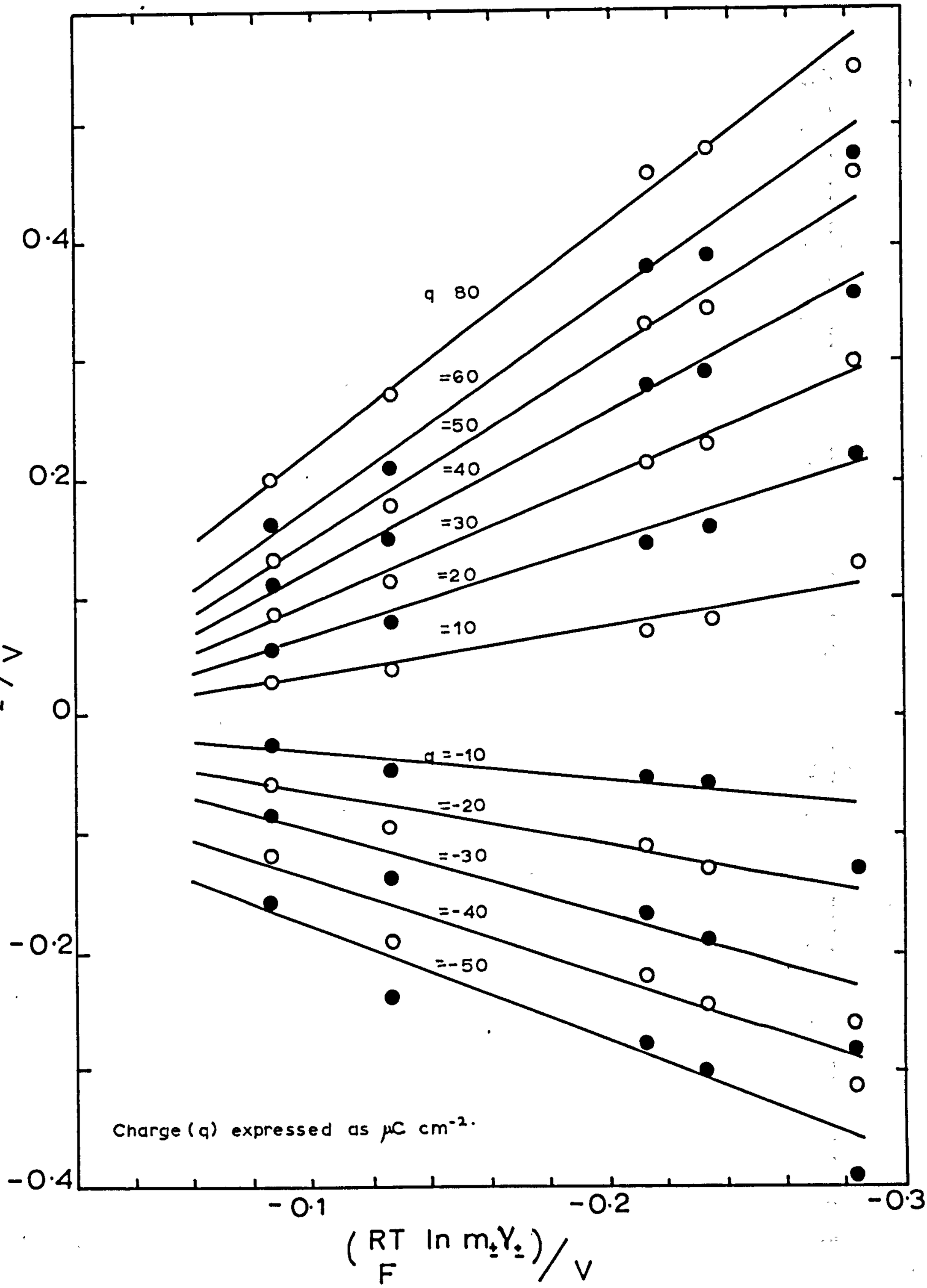
0·4
0·2
0
-0·2
-0·4
-0·1
-0·2
-0·3
$(E - E_2)/_V$
$(\frac{RT}{F} \ln m_{\pm}\gamma_{\pm})/_V$
q 80
=60
=50
=40
=30
=20
=10
q =-10
=-20
=-30
=-40
=-50
Charge (q) expressed as μC cm^{-2}.

Fig. 6B.

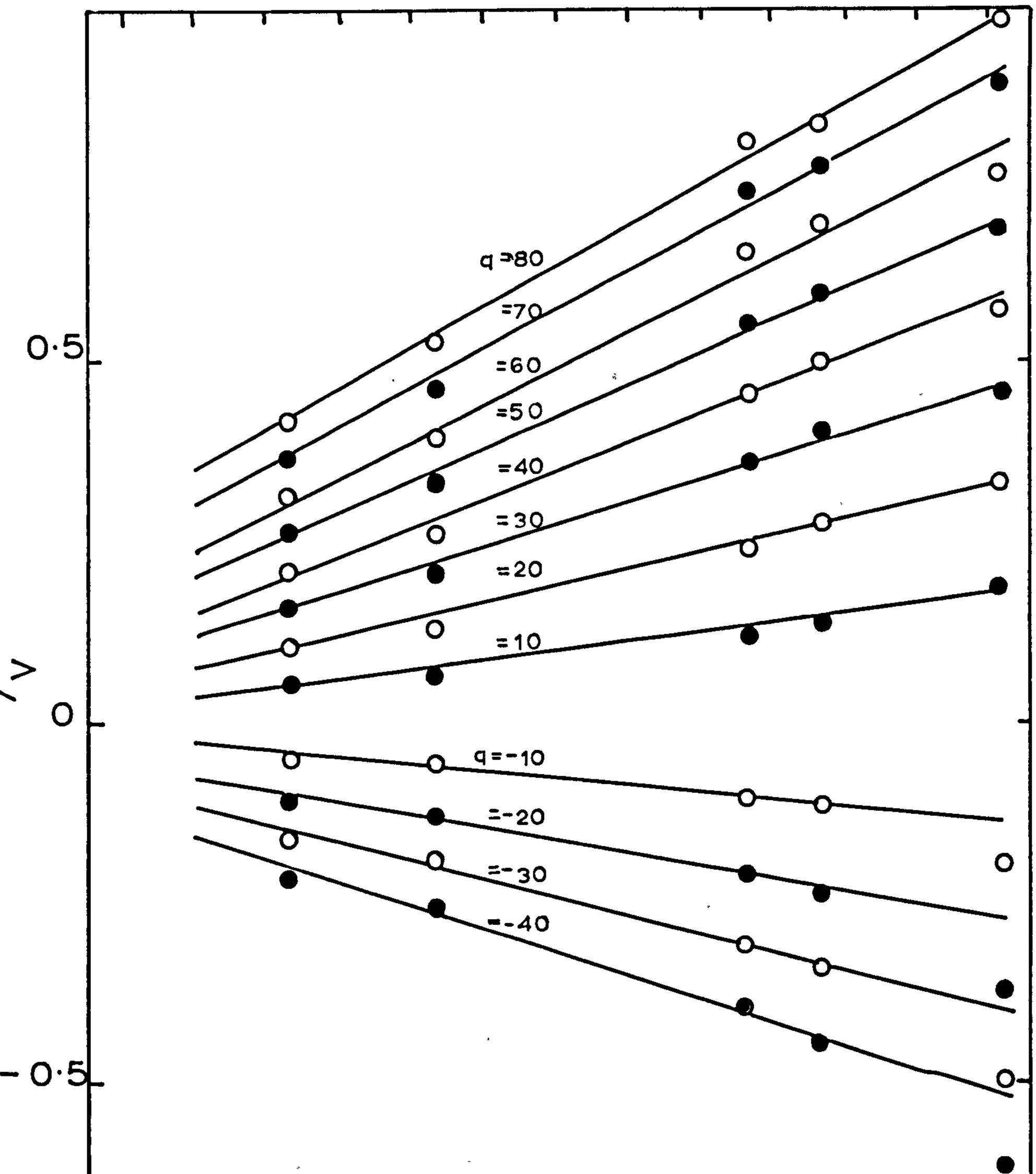
q =80
=70
=60
=50
=40
=30
=20
=10
q=-10
=-20
=-30
=-40
0·5
0
-0·5
-1·0
-0·1
-0·2
$(E - E_z)/_V$
Charge (q) expressed as $\mu C\ cm^{-2}$
$(\frac{RT}{F} \ln m_{\pm} \gamma_{\pm})/_V$

FIG. 7A.

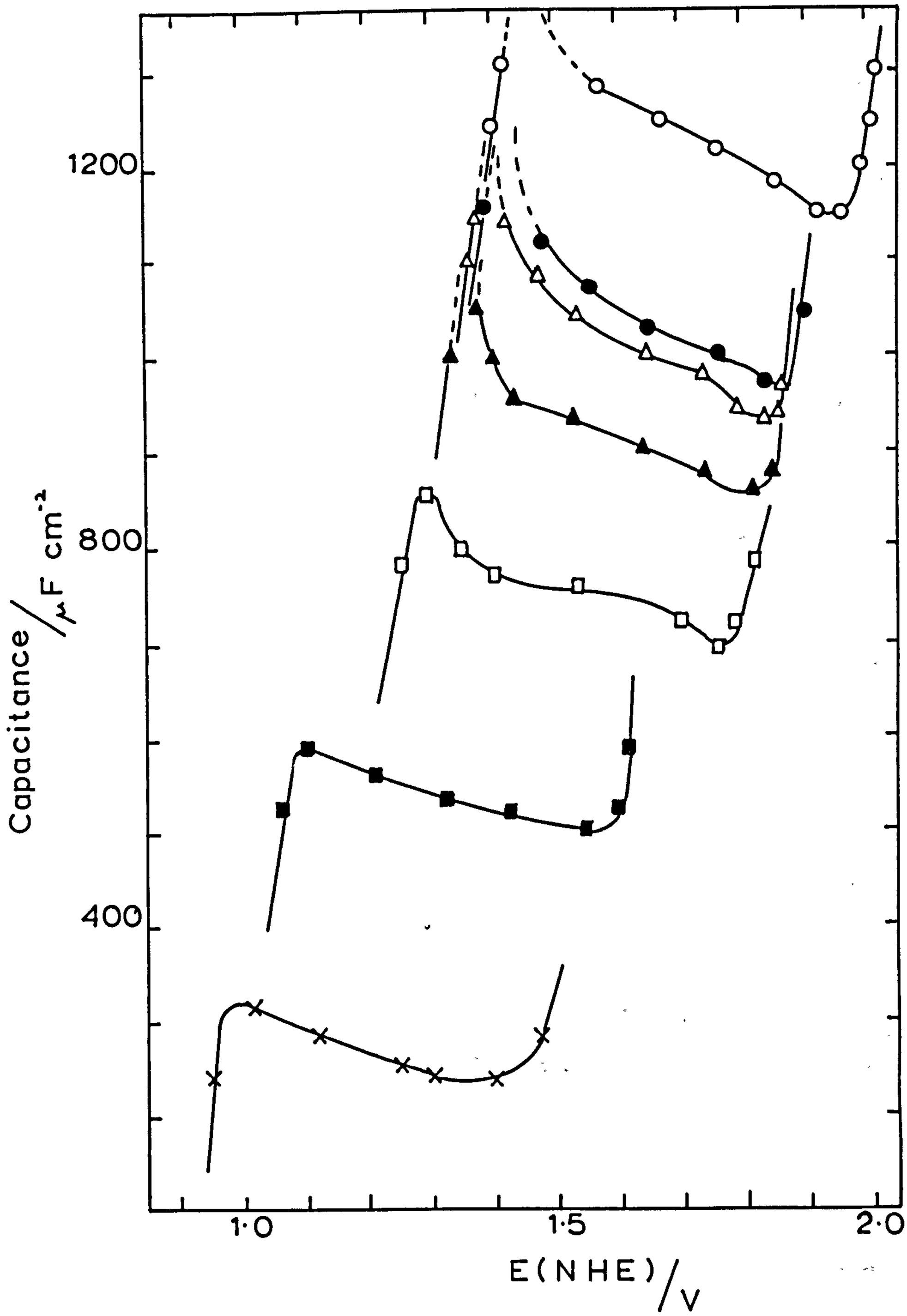

Fig. 7B.

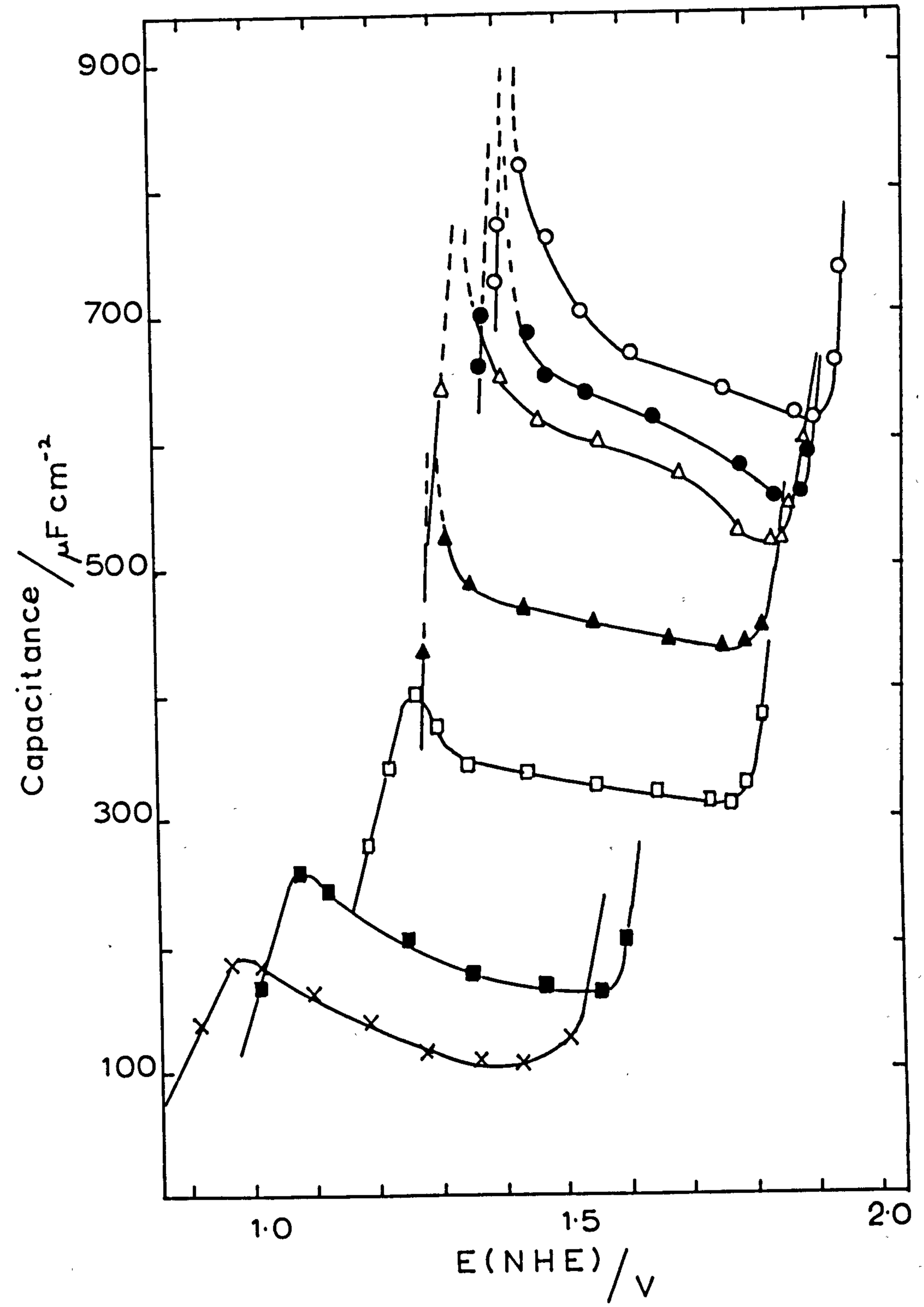

Fig. 8.

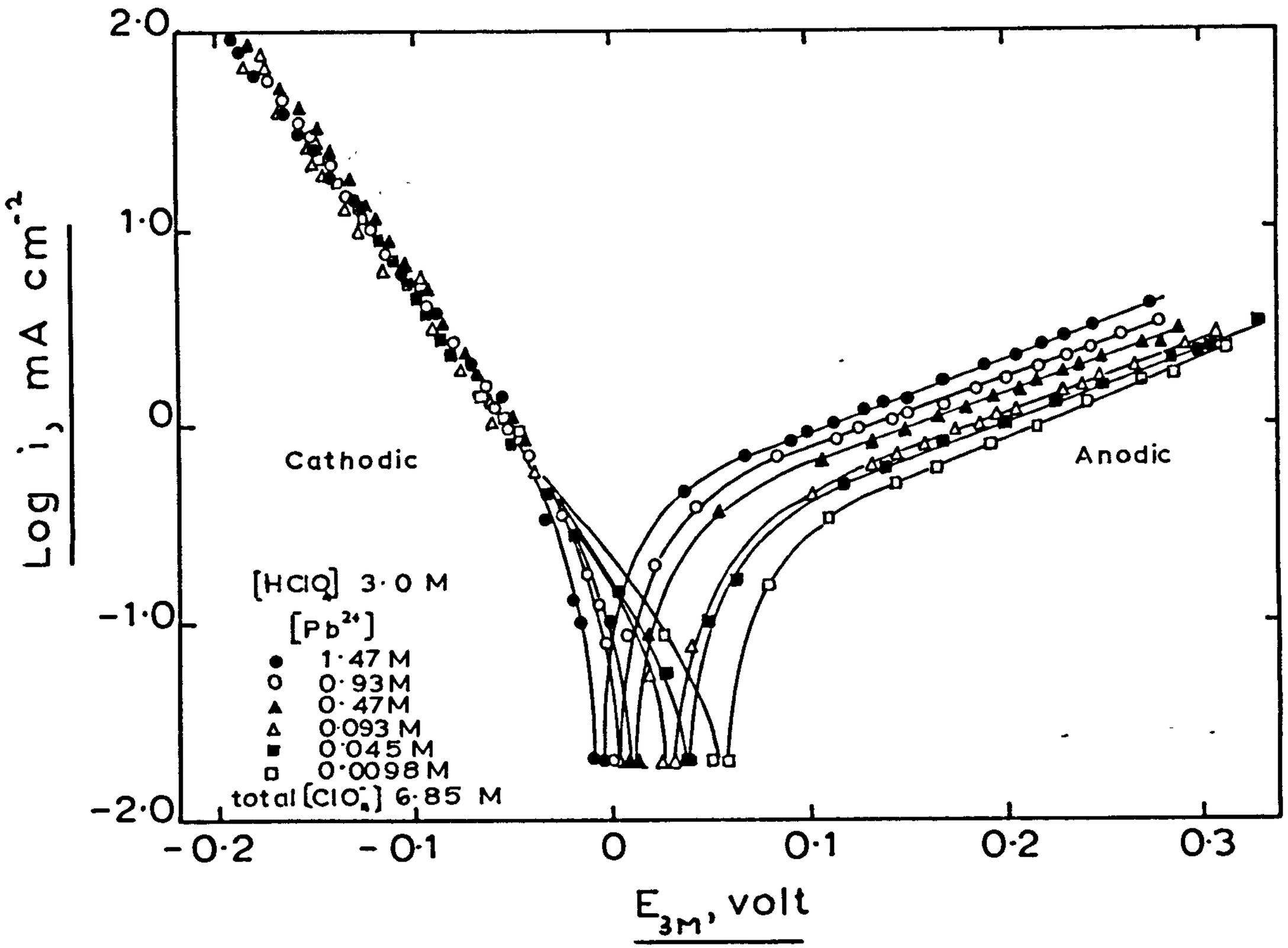
2·0
1·0
0
-1·0
-2·0
-0·2
-0·1
0
0·1
0·2
0·3
Log i, mA cm⁻²
E3M, volt
Cathodic
Anodic
[HClO4] 3·0 M
[Pb2+]
1·47 M
0·93M
0·47M
0·093 M
0·045 M
0·0098 M
total [ClO4-] 6·85 M

Fig. 9.

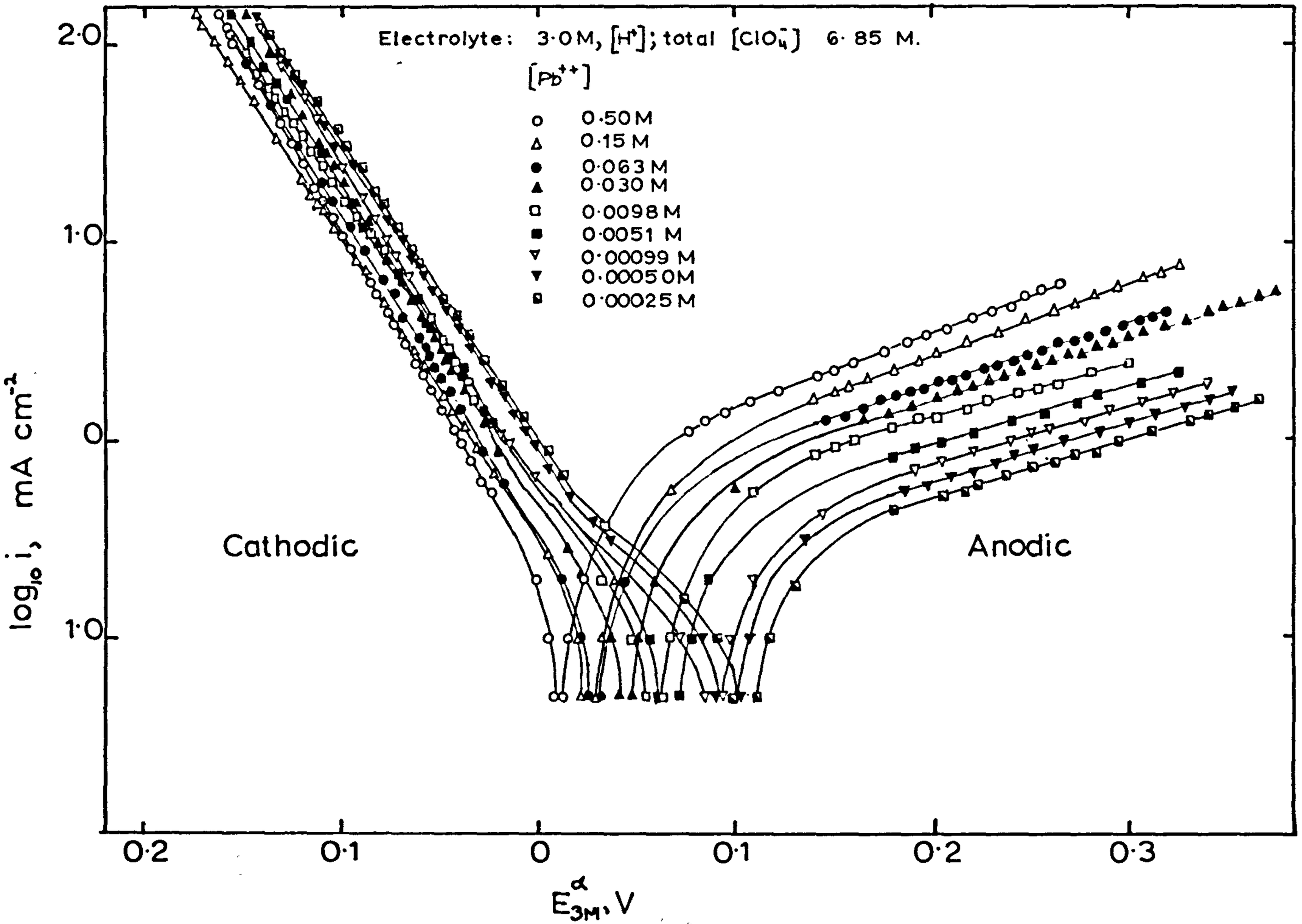
Electrolyte: 3·0 M, [H⁺]; total [ClO₄⁻] 6·85 M.
[Pb⁺⁺]
0 0·50 M
Δ 0·15 M
● 0·063 M
▲ 0·030 M
□ 0·0098 M
■ 0·0051 M
▽ 0·00099 M
▼ 0·00050 M
◘ 0·00025 M
Cathodic
Anodic
2·0
1·0
0
1·0
log₁₀ i, mA cm⁻²
0·2
0·1
0
0·1
0·2
0·3
E^α_ЗМ, V

Fig. 10A.

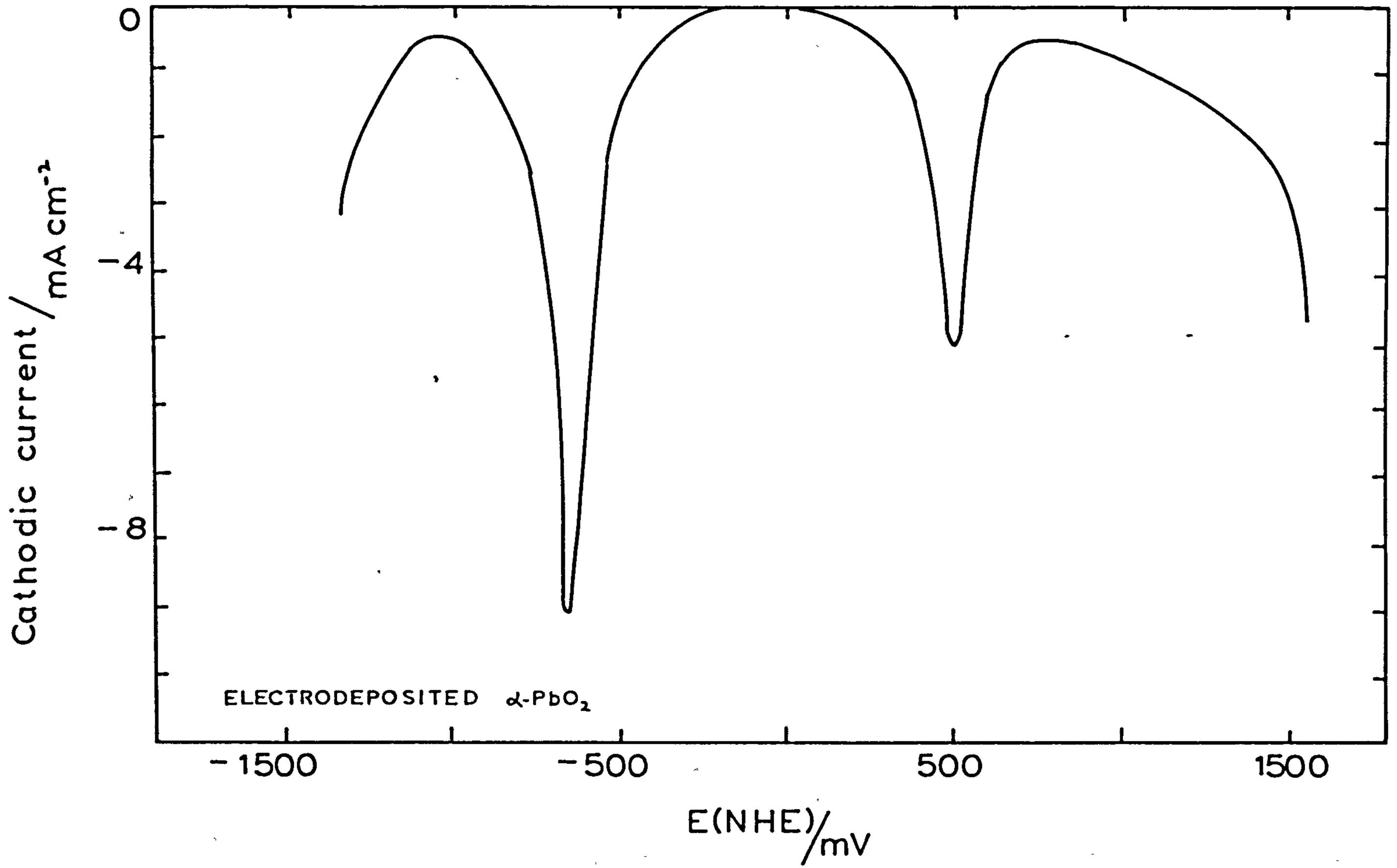
0
-4
-8
Cathodic current / mA cm⁻²
ELECTRODEPOSITED α-PbO₂
-1500
-500
500
1500
E(NHE)/mV

Fig. 10B.

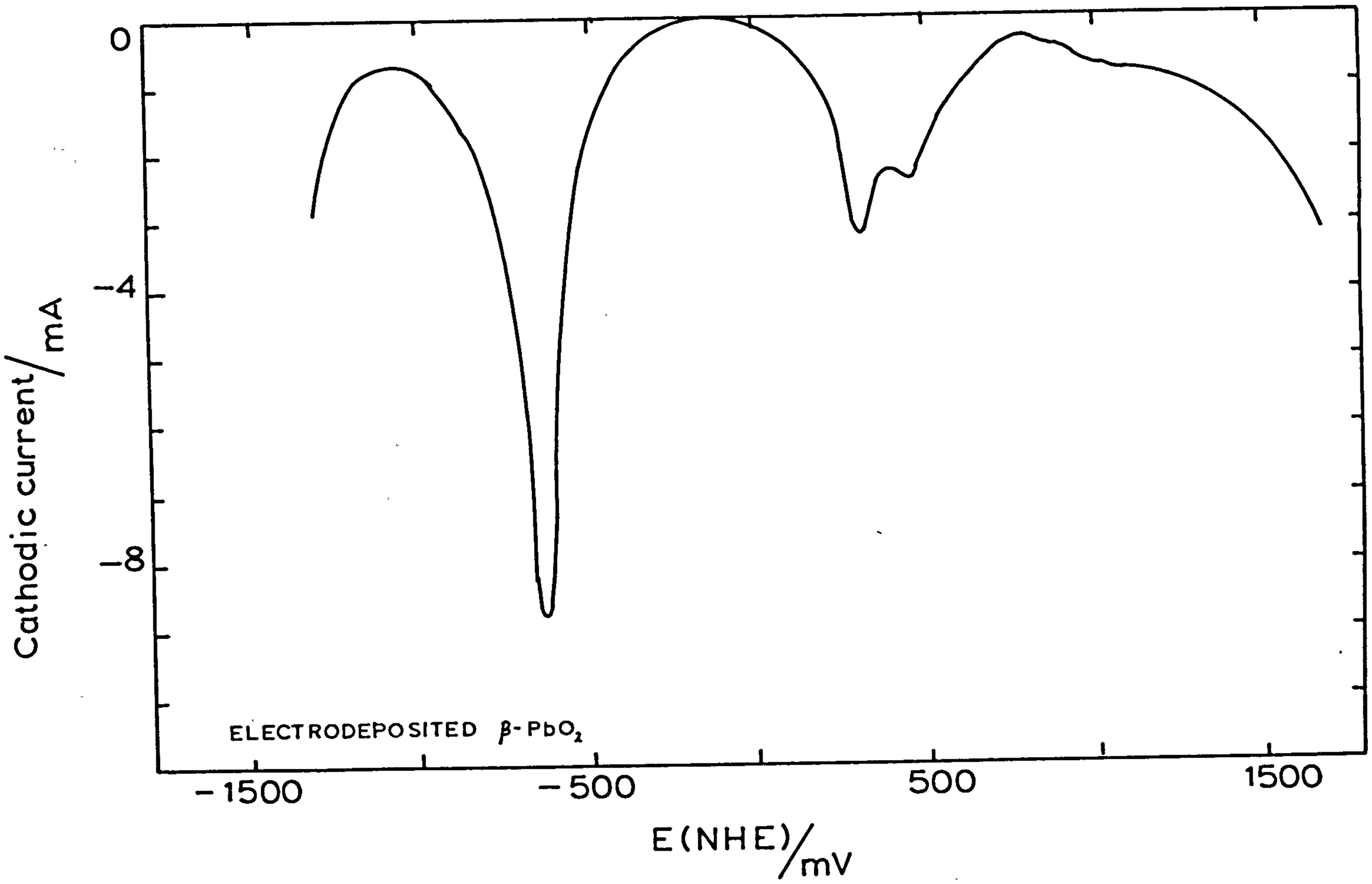
0
-4
-8
Cathodic current/mA
ELECTRODEPOSITED β-PbO₂
-1500
-500
500
1500
E(NHE)/mV

FIG. IIA.

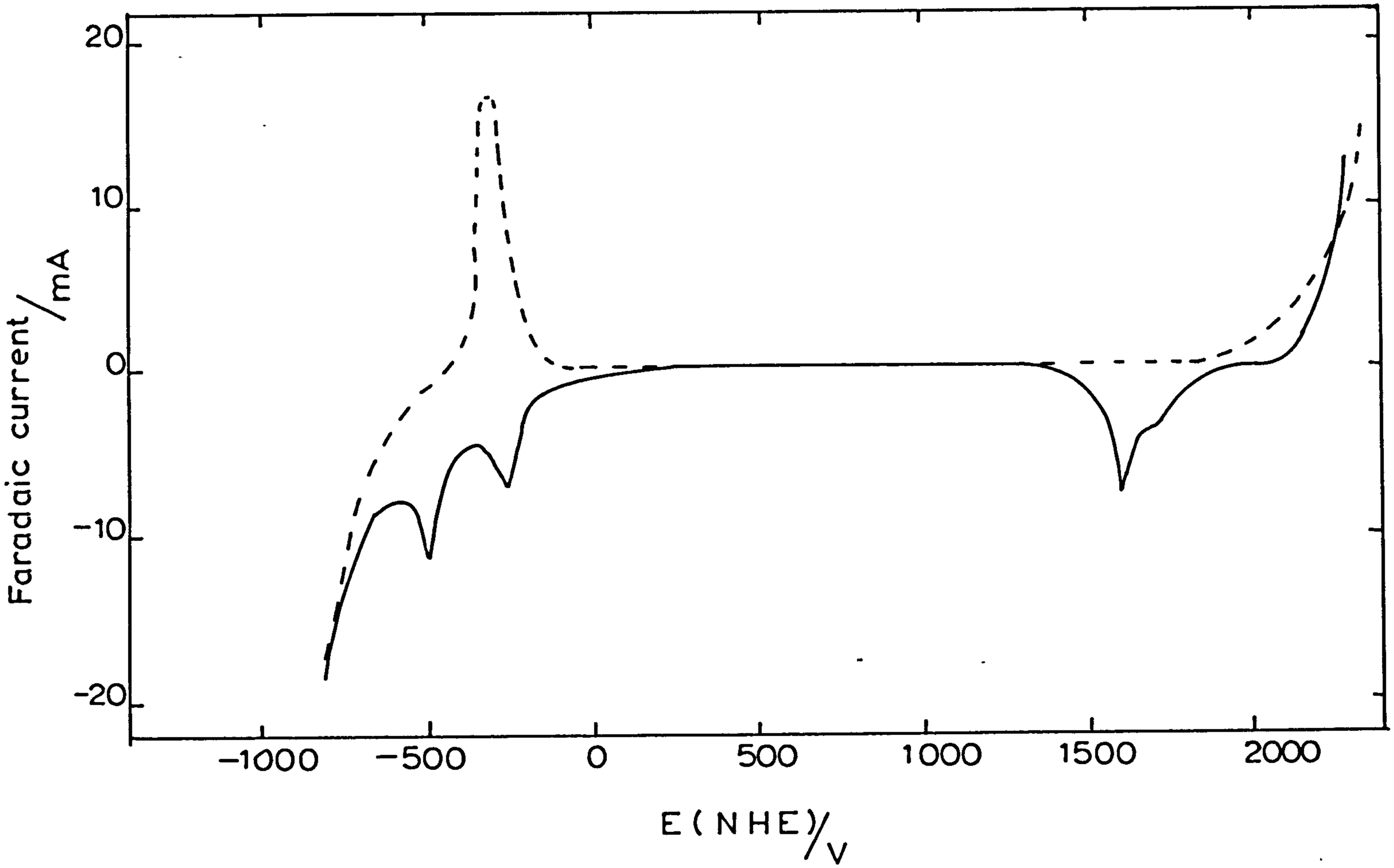
20
10
0
-10
-20
Faradaic current/mA
-1000
-500
0
500
1000
1500
2000
E(NHE)/V

FIG. 11B.

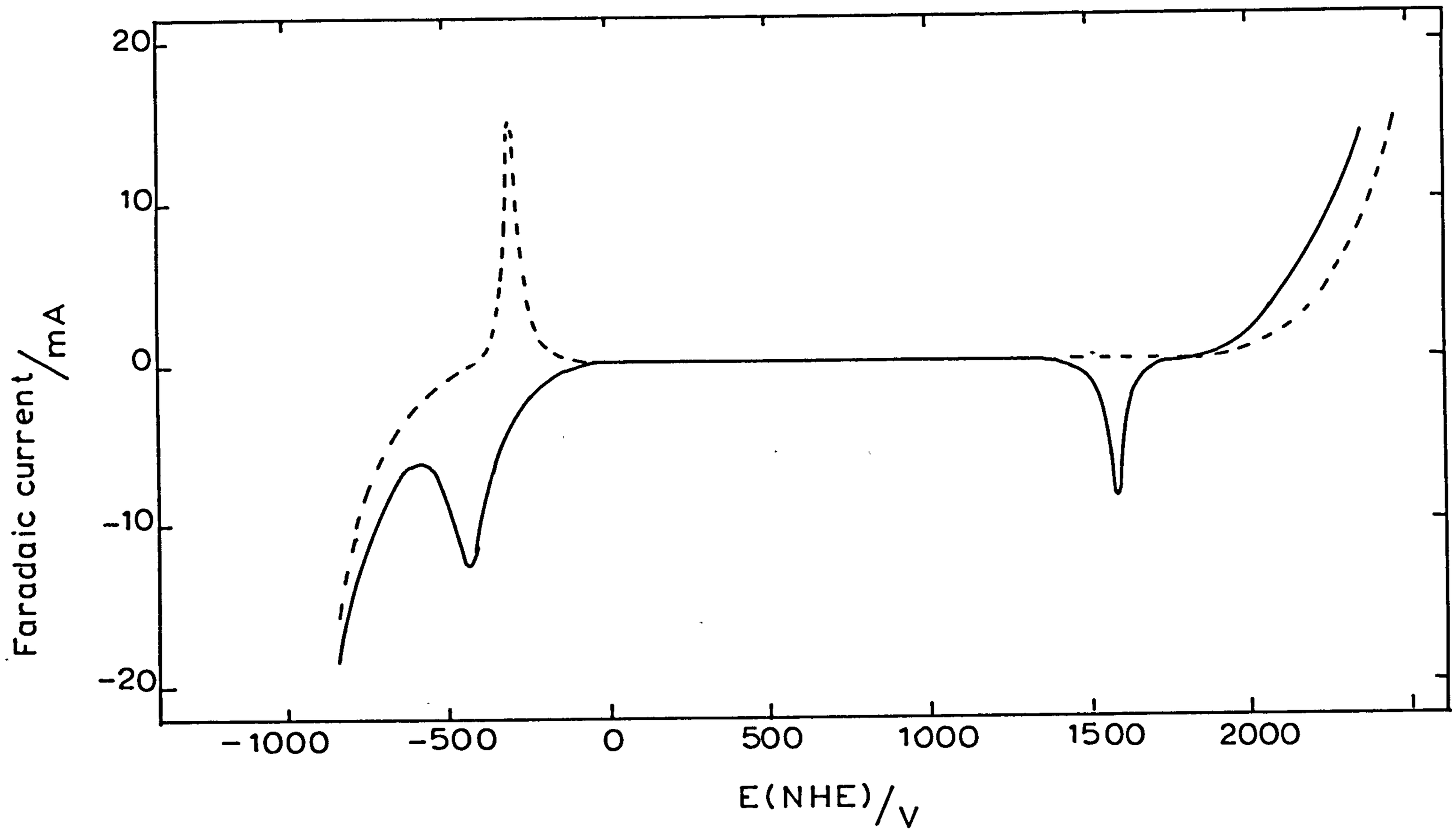
20
10
0
-10
-20
Faradaic current/mA
-1000
-500
0
500
1000
1500
2000
E(NHE)/V

Fig.12.

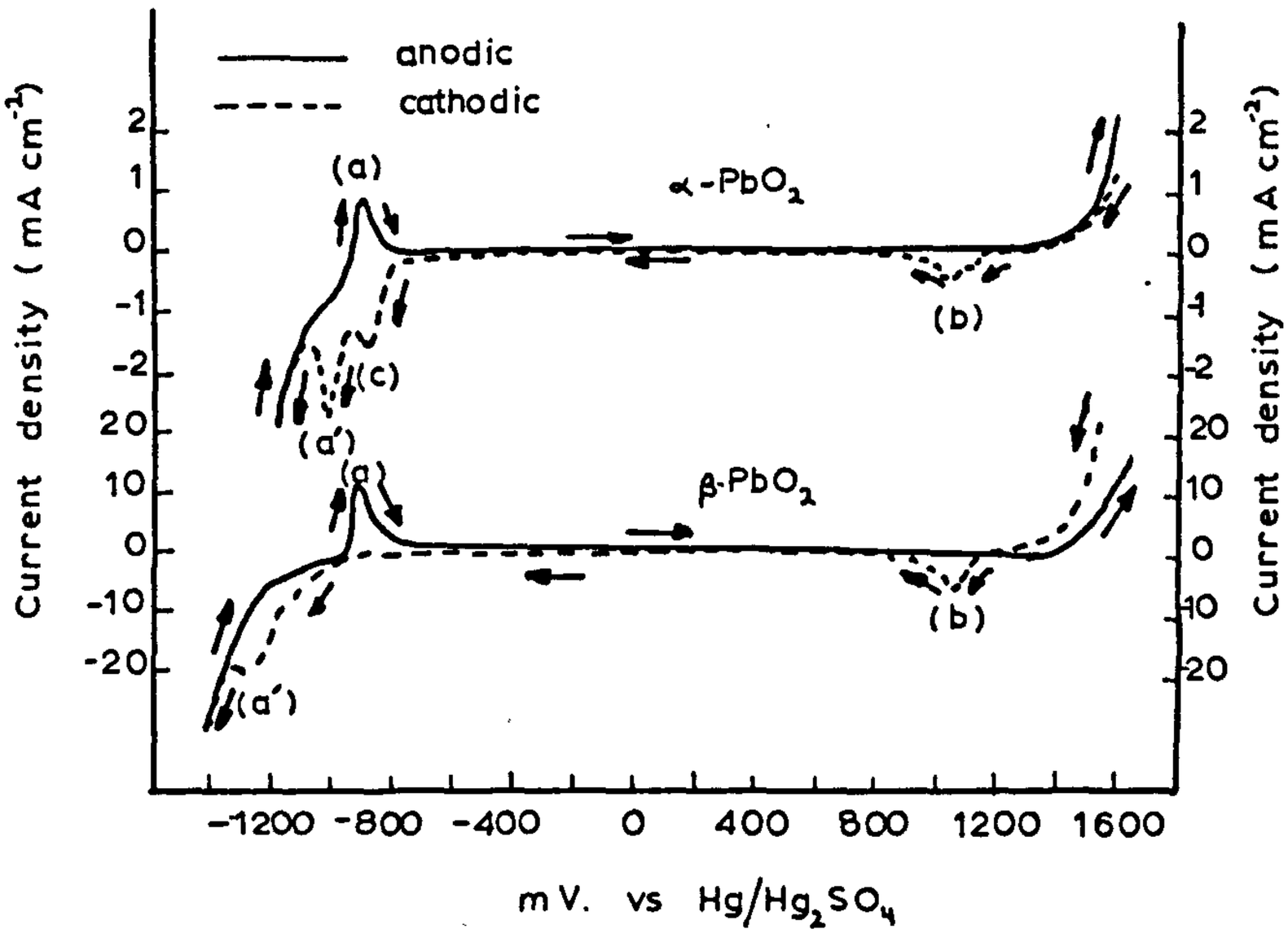
anodic
cathodic
(a)
α-PbO2
(b)
(c)
(a')
(a)
β-PbO2
(b)
(a')
2
1
0
-1
-2
20
10
0
-10
-20
Current density (mA cm-2)
-1200 -800 -400 0 400 800 1200 1600
mV. vs Hg/Hg2SO4

APPENDIX 2. DERIVATION OF THE EQUATION FOR THE DETERMINATION OF THE RATE CONTROLLING IN A MULTISTEP CHARGE TRANSFER REACTION

(B. LOVRECEK)

An overall electrode process:-

$$O + ze = R \qquad (1)$$

may involve more than one step, i.e.

$$O + z_1 e = P \qquad (2)$$

$$P + z_2 e = Q \qquad (3)$$

$$Q + z_3 e = R \qquad (4)$$

Assuming that when a net current flows, one of the steps becomes rate determining, a change in electrode potential produces a change in the ratio of activities for very step. Each step can be considered reversible.

If the activity of O, a_o, is assumed constant, then, for cathodic polarisations, the activities of the ions preceding the rate determining step will change corresponding to the potential change η

$$a_p^1 = a_p \exp(\eta z_2 F/RT) \qquad (5)$$

and

$$a_Q^1 = a_Q \exp(2\eta z_3 F/RT) \qquad (6)$$

(where a and a^1 are the activities before and after the potential change.)

Hence the activity ratios, corresponding to the change in potential can be

expressed as:-

$$a_{o/a_p^1} = a_{o/a_p} \exp\left(-\eta \frac{z/z_2 F}{RT}\right) \tag{7}$$

and

$$a_{p/a_Q^1}^1 = a_{p/a_Q} \exp\left(-\eta \frac{z_2/Z_3 F}{RT}\right) \tag{8}$$

The change in the activity ratio for each reversible step is:-

$$\exp\left(-\eta \frac{z^1 F}{RT}\right) \tag{9}$$

where z^1 represents the ratio z_{n-1}/z_n.

Hence for a general case:-

$$a^1_{n_c} = \exp\left(-\eta \frac{z_c^1 F}{RT}\right)^{n_c - 1} \cdot a_{n_c} \tag{10}$$

(n_c is the number of the step in which the respective ion will be reduced.)

If the n_c th. step is rate determining then:-

$$a^1_{n_c^*} = \exp\left(-\eta \frac{z_c^1 F}{RT}\right)^{n_c^* - 1} \cdot a_{n_c^*} \tag{11}$$

Similarly the activity of any ion involved in reduction after the rate determining step can be calculated:-

$$a_{\bar{n}_c} = \exp\left(-\eta \frac{z_c^1 F}{RT}\right)^{-(\bar{n}_c - 1)} \cdot a_{\bar{n}_c} \tag{12}$$

(where $\bar{n}_c$ is the number of the step starting from R).

For an ion produced in the rate determining step:

$$a_{\bar{n}_c^*} = \exp\left(-\eta \frac{z_2^1 F}{RT}\right)^{-(\bar{n}_c^*-1)} \cdot a_{\bar{n}_c^*} \qquad (13)$$

(where $\bar{n}_c^*$ is the number of the rate determining step).

From equation (10):

$$\log_{10} a^1_{n_c} = -(n_c-1)\, z_c^1 F\, \eta/2.3\,RT + \log_{10} a_{n_c} \qquad (14)$$

and from equation(12):

$$\log a^1_{\bar{n}_c} = (\bar{n}_c-1)\, z_c^1 F\, \eta/2.3\,RT + \log a_{\bar{n}_c} \qquad (15)$$

and for the ions involved in the slow step:-

$$\log_{10} a^1_{n_c^*} = -(n_c^*-1)\, z_c^1 F\, \eta/2.3\,RT + \log_{10} a_{n_c^*} \qquad (16)$$

and

$$\log_{10} a_{\bar{n}_c^*} = (\bar{n}_c^*-1)\, z_c^1 F\, \eta/2.3\,RT + \log_{10} a_{\bar{n}_c^*} \qquad (17)$$

Applying the general electrode kinetic equation for the cathodic rate determining step:-

$$i_c = k_c \cdot a_{\bar{n}_c^*} \exp -\alpha\, Fz/RT \qquad (18)$$

and with $z = 1$

$$\frac{\partial \log_{10} i_c}{\partial \eta} = \frac{\partial \log_{10} a_{n_c}}{\partial \eta} - \frac{\alpha F}{2.3\,RT} \qquad (19)$$

From equation (16):-

$$\frac{\Delta \log_{10} {}^{a}n^{*}_{c}}{\Delta \eta} = \frac{-(n^{*}_{c} - 1)\ F}{2.3\ RT} \qquad (20)$$

combining equations (19) and (20):-

$$\frac{\partial \log_{10} i_{c}}{\partial \eta} = \frac{-F\ (n^{*}_{c} - 1 + \alpha)}{2.3\ RT} \qquad (21)$$

Similarly for the anodic reaction the following equation can be derived:-

$$\frac{\partial \log_{10} i_{A}}{\partial \eta} = \frac{F\ (n^{*}_{A} - \alpha)}{2.3\ RT} \qquad (22)$$

APPENDIX 3. SERIES-PARALLEL CIRCUIT TRANSFORMATION AND COMPUTOR PROGRAM FOR CIRCUIT TRANSFORMATIONS

```
SHORT_LIST
SEND TO 'ED,1CLA-DEFAULT.AXXX=
PROGRAM'HO75=
INPUT1,CRO
     OUTPUT2,LPO
     TRACE O
     END
     MASTER COMPUTATION
     REAL LOGF
     DIMENSION F1'50=, RXS1'50=,  CXS1'50=
101  READ '1,2O=        N
 20  FORMAT'14=
 25  DO 21 K,1,N
201  READ '1,202=      M,NHEAD
202  FORMAT'214=
204  DO 9001,1,M
105  READ '1,1=        F1'I=, RXS1'I=, CXS1'I=
  1  FORMAT 'F4.0,F8.1,E11.4=
900  CONTINUE
     DO 901 J,1,NHEAD
103  READ '1,2=     RC,CL
  2  FORMAT 'F6.1,E11.5=
 26  WRITE'2,3=     RC,CL
  3  FORMAT '6H RC , F7.1,5XHCL , E12.5=
```

```
      WRITE'2,40=
   40 FORMAT  '///2X1HF7X3HRXS10X3HCXS10X4HBETA5X5HGAMMA6X2HRR8X2HGR7X3HR
     1RW//=
      CON1,2.*3.1415926
      DO 10 I,1,M
      RXS,RXS1 'I=
      CXS,CXS1'I=
      F,F1'I=
      RA,RXS-RC
      W,CON1*F
      IF'W*CXS*RA=45,10,45
   45 BETA,1./'W*CXS*RA=
      T1,BETA*BETA
      T2,1.IT1
      RDASH,T2*RA
      CDASH,T1/T2*CXS
      C2DASH,CDASH-CL
      GAMMA,W*C2DASH*RDASH
      RR,RDASH/'1.1GAMMA*GAMMA=
      GR,GAMMA*RR
      RRW,1./SQRTF'W=
      WRITE'2,5=      F,RXS,CXS,BETA,GAMMA,RR,GR,RRW
    5 FORMAT'F7.0,2XF8.1,2XE12.4,1XF9.4,1XF8.4,1XF9.1,1 XF10.4,1XF9.6=
   10 CONTINUE
      WRITE'2,300=
  300 FORMAT '1H1=
  901 CONTINUE
```

```
21 CONTINUE
   STOP
   END
   FUNCTION EXPF'X=
   EXPF,EXP'X=
   RETURN
   END
   REAL FUNCTION LOGF'X=
   LOGF,ALOG'X=
   RETURN
   END
   FUNCTION ABSF'X=
   ABSF,ABS'X=
   RETURN
   END
   FUNCTION SQRTF'X=
   SQRTF,SQRT'X=
   RETURN
   END
   FUNCTION SINF'X=
   SINF,SIN'X=
   RETURN
   END
   FUNCTION COSF'X=
   COSF,COS'X=
   RETURN
   END
```

```
FUNCTION ATANF'X=

RETURN

END

FINISH
```

APPENDIX 4. ANALYSIS OF ELECTROLYTES AND PREPARATION OF CHARCOAL

(a) Analysis for Pb(II)

A known volume of solution was adjusted to an estimated suitable concentration. A small amount of tartaric acid (~ 1 gm.) and pH 10 buffer were added until the solution cleared. Erichrome Black T indicator was added and the solution titrated against standard E.D.T.A. until the solution colour changed from violet to blue.

(b) Analysis of Perchlorate, Nitrate, Sulphate and Phosphate Electrolytes for Capacitance Measurements

In all cases the sodium (or potassium) content was determined. A series of standards in the range 5 - 50 p.p.m. were made. Using a flame photometer (E.E.L.), a calibration curve was obtained. The electrolyte to be analysed was diluted to ~ 25 p.p.m. sodium (or potassium) and the concentration thus determined.

(c) Analysis of Electrodeposited PbO_2

Analysis was performed using a Phillips x-ray defractometer (type PW1051) with copper K_α radiation. Freedom of β-PbO_2 deposits from α-PbO_2 was determined by the absence of a diffraction line at 2.63 Å and freedom of α-PbO_2 deposits from β-PbO_2 by the absence of diffraction lines for interplanar spacings of 2.46 Å and 1.85 Å.

(d) Preparation of Charcoal

Granular gas adsorption charcoal was extracted in a Soxlet apparatus with constant boiling HCl. The acid was changed periodically and extraction continued until the acid remained colourless (normally ~ 3 months). The charcoal was then washed with water, which was changed periodically, until the washings showed no positive test for chloride ion.

APPENDIX 5. A STUDY OF THE ANODIC OXIDATION OF POLYCRYSTALLINE LEAD IN NaOH SOLUTIONS

In Chapter 5 the cathodic reduction of PbO_2 electrodes in NaOH was recorded. In this study complementary data for the anodic oxidation of lead in NaOH are reported in order to investigate possible reaction process similarities that may exist for the two systems.

A number of studies have shown that α-PbO_2 is the main constituent of the anodic corrosion product on Pb in aqueous media[69,168,199]. Thermodynamically α-PbO_2 is the more stable form of PbO_2 in alkaline solution[127]. Recent work by Pavlov[189] has established that basic conditions are produced in the interior of the positive plates of lead acid battery systems during the initial stages of formation which would provide conditions conducive for the formation of α-PbO_2. As yet little work has been carried out concerning this aspect of the lead electrode.

Following work by Jones, Thirsk and Wynne-Jones[172], Elbs and Forsell[238] and Glasstone[225], Farr and Hampson[259] studied the anodic behaviour of polycrystalline lead in aqueous KOH and showed that the oxidation of lead is complicated by transitions between the processes:-

$$Pb + 2\,OH^- = PbO + H_2O + 2e \quad (1)$$

$$PbO + 2\,OH^- = PbO_2 + H_2O + 2e \quad (2)$$

discharge of OH^- on the PbO_2 layer. (3)

It was concluded that during oxidation, part of the oxidized lead was incorporated into a film of tetragonal lead oxide while the remainder dissolved in the electrolyte. The electrolyte in the immediate vicinity of the electrode eventually became saturated with

the anodic product, and orthorhombic lead oxide was deposited on the electrode blocking reaction 1 . α-PbO_2 was formed by the oxidation of the tetragonal lead oxide on the electrode surface.

Experimental

The lead test electrodes were prepared from 99.999% pure lead supplied by Johnson Matthey and Company Limited by drawing molten lead into a glass capillary whilst under an atmosphere of nitrogen to prevent oxidation. Good glass to lead adhesion was observed throughout. The electrode was cut square to the principle axis and polished with carbarundum paper. Before each experimental run the electrode was mechanically polished on roughened glass using conductivity water as lubricant, electrochemically etched in perchloric acid (20%) and finally chemically etched in the perchloric acid for 30 minutes.

The electrolytic cell, experimental technique and electrical circuit were as described in Chapter 3. Reproducibility of experimental results was $\pm$ 10%.

Results

Figure 1 shows the results of a typical fast anodic potential sweep on the lead electrode. The experimental potential range ($\sim$ -1300 mV to $\sim$ +1700 mV) was limited by hydrogen evolution at the negative extremity and oxygen evolution at the positive extreme. Between the potential limits two clearly defined, sharp current peaks, a and b, were observed and a minor peak, c, which appeared as a shoulder on peak b. Peak a occurred at approximately the Pb/PbO redox potential (- 585 mV) and corresponds to the anodic oxidation of Pb to PbO as given by the general reaction:-

$$Pb + 2\,OH^- = PbO + H_2O + 2e \qquad (4)$$

Fig 1 Typical anodic potential sweep on polycrystaline lead in NaOH electrolyte.

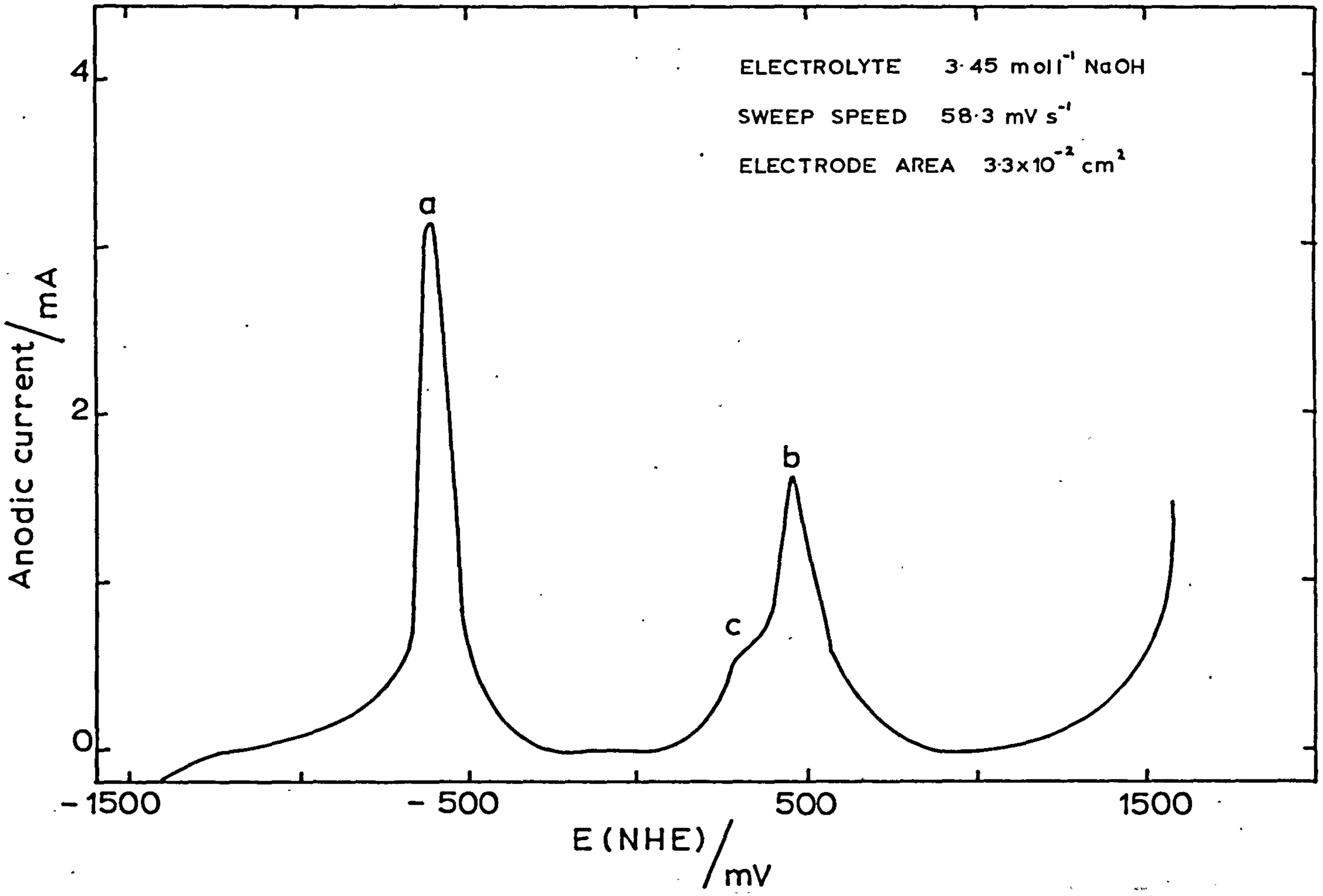

Peaks b and c occurred at a potential corresponding to the PbO/PbO_2 redox potential. From the work reported for the cathodic reduction of PbO_2 in NaOH, peak b can be associated with the formation of α-PbO_2 and peak c with the formation of β-PbO_2.

Figure 2 shows the effect of potential sweep rate on the anodic current peak height of peak a. A linear relationship between I_m and $\sqrt{v}$ was observed, the lines passing through the origin throughout the experimental concentration range. Figure 3 shows the effect of $[OH^-]$ on the current peak height of peak a. I_m is directly proportional to $[OH^-]$ in agreement with equation 2.47. Figure 4 shows the same relationship in the form of a log. - log. plot.

Discussion

It is clear from figures 1 and 2 that the process controlling the current flow for peak a is a diffusion process in solution (linear I_m vs $\sqrt{v}$ curves passing through the origin). Consideration of the species present in the solution suggests that the OH^- ion is the species involved in the diffusion process. Since I_m is directly proportional to $[OH^-]$, only one OH^- ion is involved in the diffusion process. A possible sequence of reactions involved at the electrode is:-

$$Pb + 2\,OH^- = Pb(OH)_2 + 2e \qquad (5)$$

$$Pb(OH)_2 + OH^- = Pb(OH)_3^- \qquad (6)$$

$$Pb(OH)_3^- = PbO + OH^- + H_2O \qquad (7)$$

where reactions 6 and 7 occur subsequently to produce a PbO phase at the electrode, and, at the same time, reaction 6 occurs in the absence of reaction 7 to form plumbite ions in solution. This mechanism is similar to that proposed by Farr and Hampson[259].

The apparent diffusion coefficient of the OH^- ion can be calculated from the slope

Fig 2 Anodic peak current - $\sqrt{\text{sweep rate}}$ for PbO formation on polycrystalline lead in NaOH electrolyte.

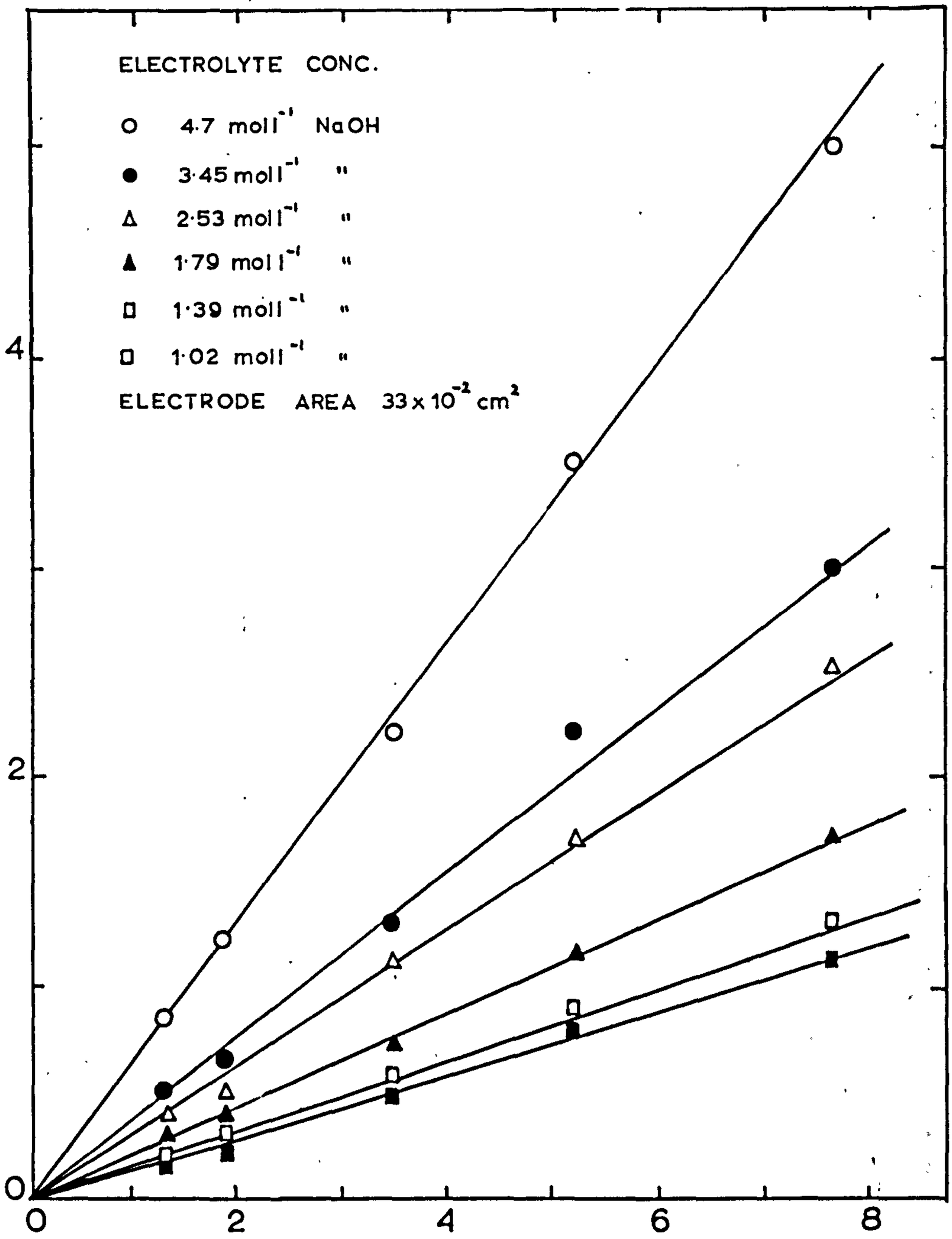

Fig 3 Anodic peak current- $[OH^-]$ for PbO formation on polycrystalline lead in NaOH electrolyte.

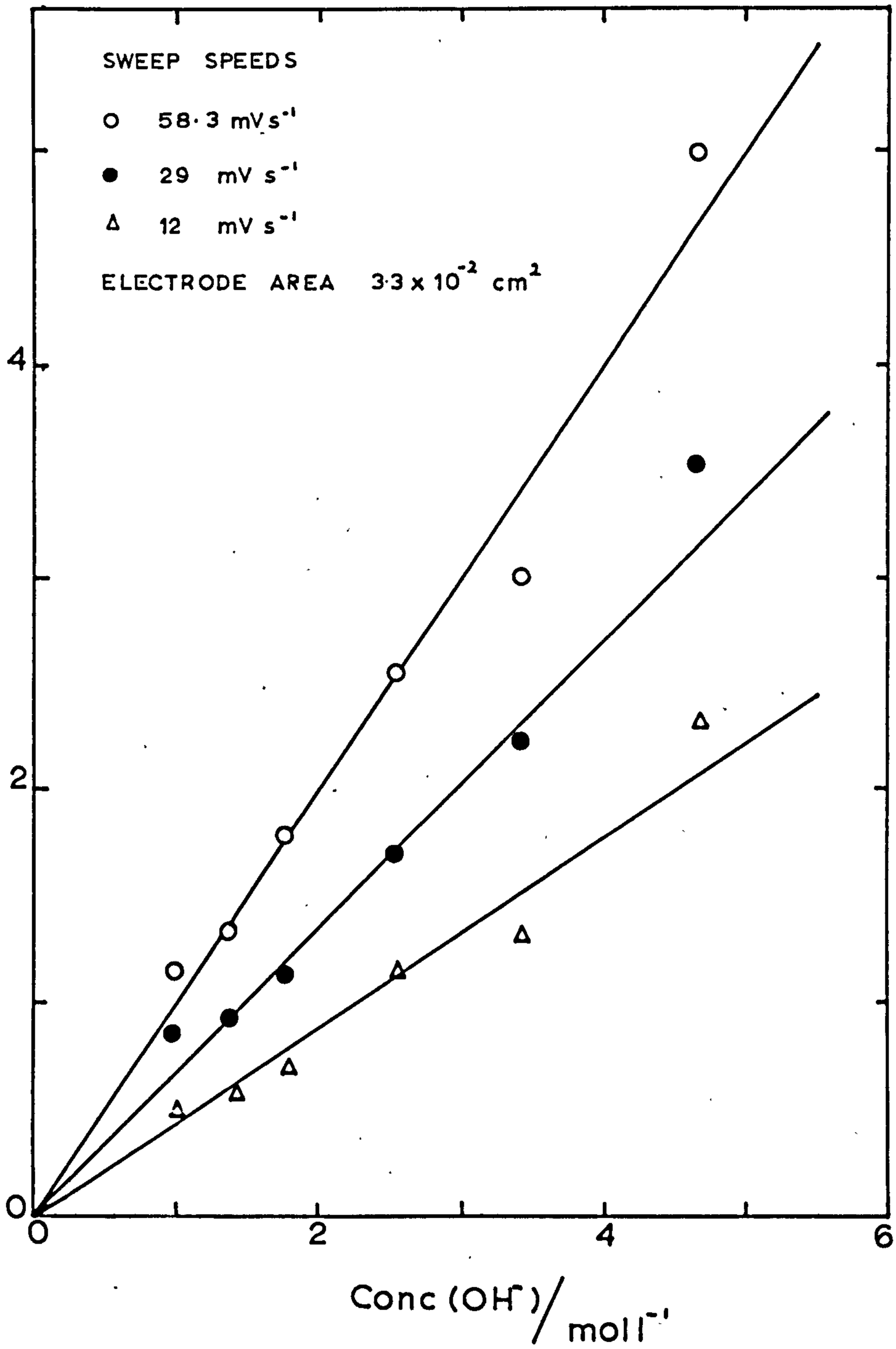

Fig 4 Variation of I_m with $[OH^-]$ for polycrystalline lead in NaOH electrolyte.

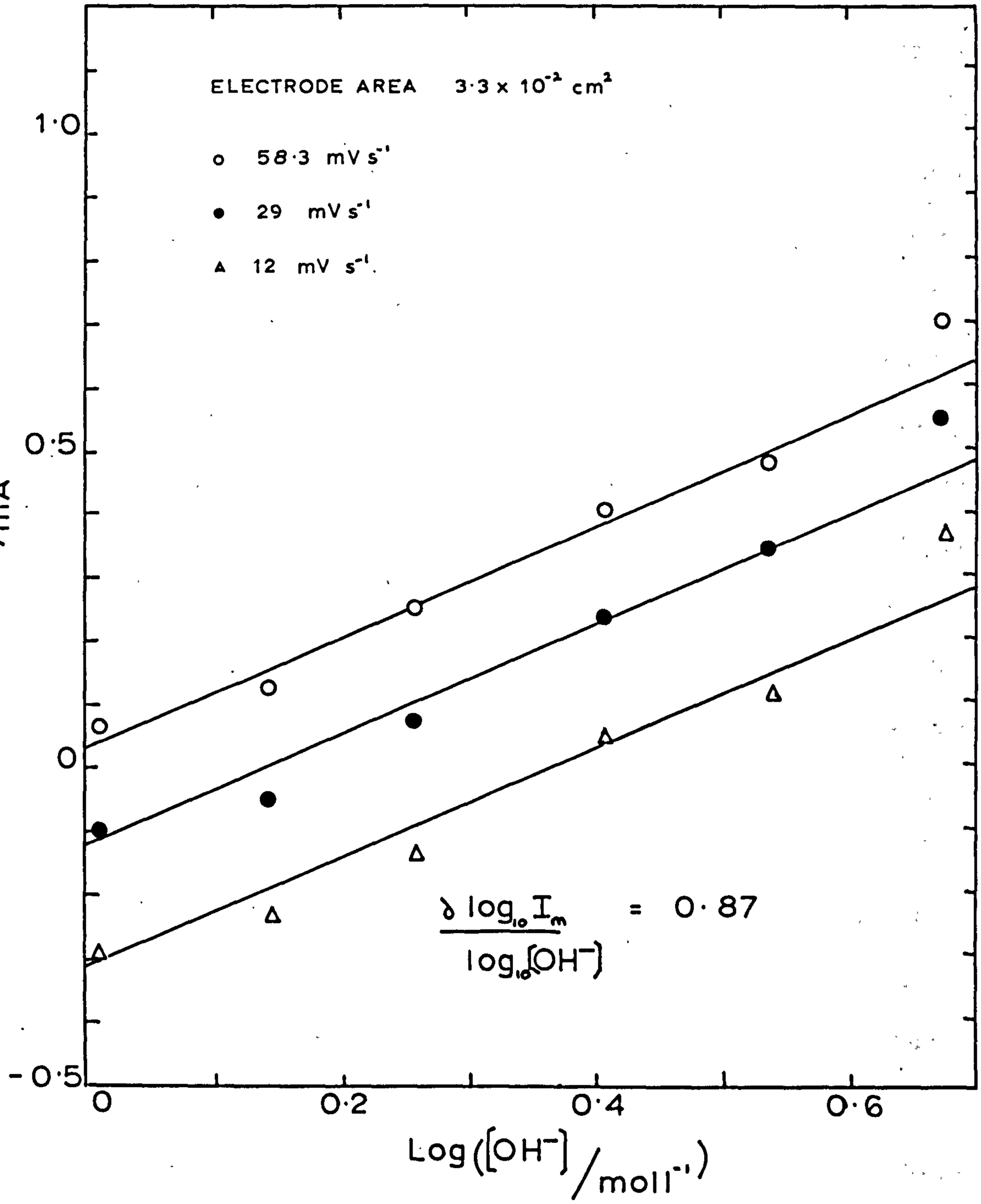

of the I_m - $\sqrt{v}$ lines, figure 5, and gives a value of ~ 10^{-7} cm^2 s^{-1} which is significantly different from the published data for the OH^- ion in aqueous solutions. It is possible that diffusion of the OH^- ion takes place through a layer of anodic products and the diffusion coefficient observed is not that of the OH^- ion in aqueous solution but that of the diffusing ion in the layer of anodic products. Alternatively the true surface area of the electrode available for diffusion is very much less than the apparent area, due to the presence of a solid phase of PbO. It is difficult to decide which explanation is correct as both indicate the well established fact that in the region of the anodic dissolution of lead in alkali, a layer of solid products exists at the electrode surface. It is not likely that a trans-passive dissolution of the electrode occurs since the potential region at which peak a is observed is too low and in any case a trans-passive dissolution would be expected to yield ions of a higher valence state.

Linear relationships between I_m and $\sqrt{v}$ for peaks b and c were not obtained within the experimental concentration range indicating that the mechanism controlling the current flow at these potentials is complex. The fact that I_m of peak b, which corresponds to the formation of α-PbO_2, was always greater than the peak current of peak c (formation of β-PbO_2) indicates that at the experimental potentials, although α-PbO_2 was the major product formed, traces of β-PbO_2 were always present. If the PbO_2 deposit was scraped from the electrode surface, after a complete anodic potential sweep, the presence of an orange coloured deposit of PbO underneath the PbO_2 was observed in agreement with Farr and Hampson[259].

Non-reproducible relationships between I_m and sweep rate for peaks b and c indicates the possibility of formation of PbO_2 by more than one mechanism, as observed previously by Ruetschi and Cahan[84] who suggest simultaneous oxidation of PbO and underlying Pb.

A slight negative shift in the potential of peaks b and c occurred with increasing sweep rate which indicates that the reaction occurring at these potentials was significantly irreversible.

Fig 5 Variation of slope of I_m-$\sqrt{v}$ curves for polycrystalline lead in NaOH electrolyte.

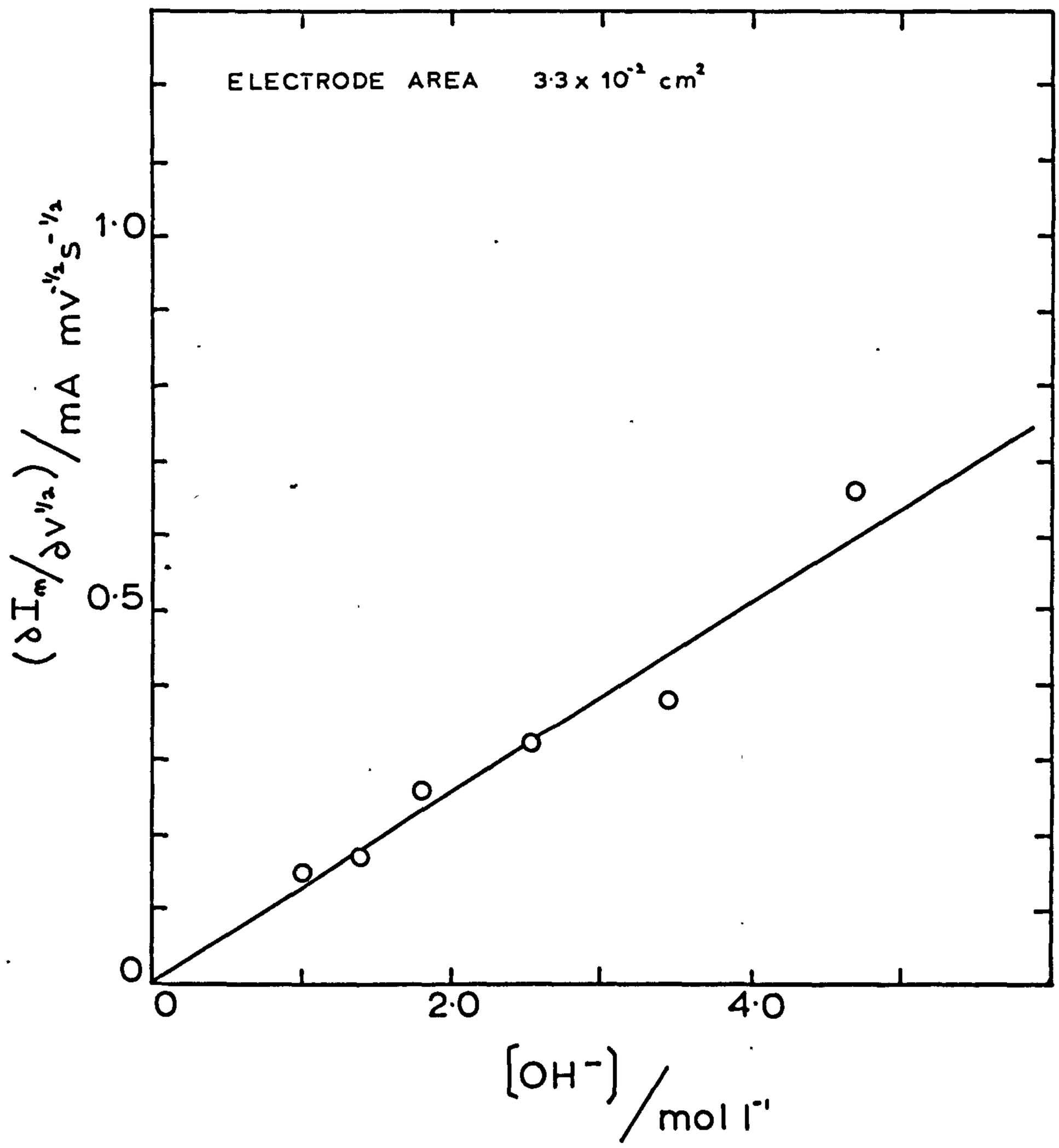

APPENDIX 6. A STUDY OF THE ANODIC OXIDATION OF POLYCRYSTALLINE LEAD IN H_2SO_4

In Chapter 7 the results of a study of the cathodic reduction of PbO_2 in H_2SO_4 solutions were recorded. In this appendix, the results of a study of the anodic oxidation of polycrystalline lead are recorded thus giving more complete picture of the possible reactions occurring in the lead acid battery system.

The electrochemical reactions of lead electrodes in H_2SO_4 have been investigated by a number of workers; a review is included in appendix 1. As yet, it is not clear which is the rate controlling reaction for the anodic oxidation of lead in H_2SO_4. Three possibilities exist:-

(1) diffusion of SO_4^{2-} ions in solution,

(2) transport of charge and mass through an insoluble layer at the electrode,

(3) charge transfer between lead atoms in the lattice and lead ions either in solution or adsorbed at the electrode.

Of these the charge transfer step, process (3), is unlikely since the specific rate constant for the Pb(II)/Pb reactions is very large. It is of interest to investigate which of these processes is rate controlling.

Experimental

Electrode preparation (appendix 5), experimental procedure, electrolytic cell and electrical circuit were as described in Chapter 3. Reproducibility of experimental results was $\pm$ 10%.

Results

Figure 1 shows a typical fast anodic potential sweep trace for Pb in H_2SO_4 solu-

tions within a potential range determined by hydrogen evolution at the negative extremity and oxygen evolution at the positive extreme. Between the potential limits one clearly defined current peak, peak a, was observed at a potential that corresponded to $Pb/PbSO_4$ potential (-342 mV), representing the formation of $PbSO_4$ as a solid phase on the electrode. At the highest sweep rates applied (> 30 mV s^{-1}) a small secondary peak, peak b, occurred at ~ -100 mV corresponding to the possible formation of a second component underneath the already formed $PbSO_4$ solid phase.

At fast sweep rates (>30 mV s^{-1}) the increase in the faradaic current observed at the positive extremity of the potential region employed corresponds to the co-formation of O_2 and PbO_2. When the electrode was removed from the system, after potential excursions to the positive limit, a definite black deposit of PbO_2 was observed on the electrode. At low sweep rates (< 10 mV s^{-1}) a current arrest, corresponding to PbO_2 formation on the electrode appeared, however, unless the sweep rate was very slow, this current arrest was very difficult to separate from the current increase due to O_2 evolution. This is a marked difference to the behaviour observed in NaOH solutions, appendix 5, where a well defined peak at the potential of PbO_2 formation was observed at all the experimental potential sweep rates.

Figure 2 shows the dependence of the current peak height of peak a on $\sqrt{v}$. A linear relationship was observed throughout the experimental concentration range, the $I_m - \sqrt{v}$ lines, for low sweep rates, passing through the origin, however, at high sweep rates an abrupt change in the slope was observed. The change in slope occurred at progressively lower sweep rates for increasing concentration of H_2SO_4. Figure 2 shows only two such relationships, at high sweep rates line a was common for all concentrations investigated greater than 4.5 mol l^{-1}. The scatter of the experimental data at high sweep rate, in the high concentration experiments was considerably greater than at low sweep rates, however, the mean slope could readily be determined as shown.

Fig 1. Typical anodic potential sweep for polycrystalline lead in H_2SO_4 electrolyte.

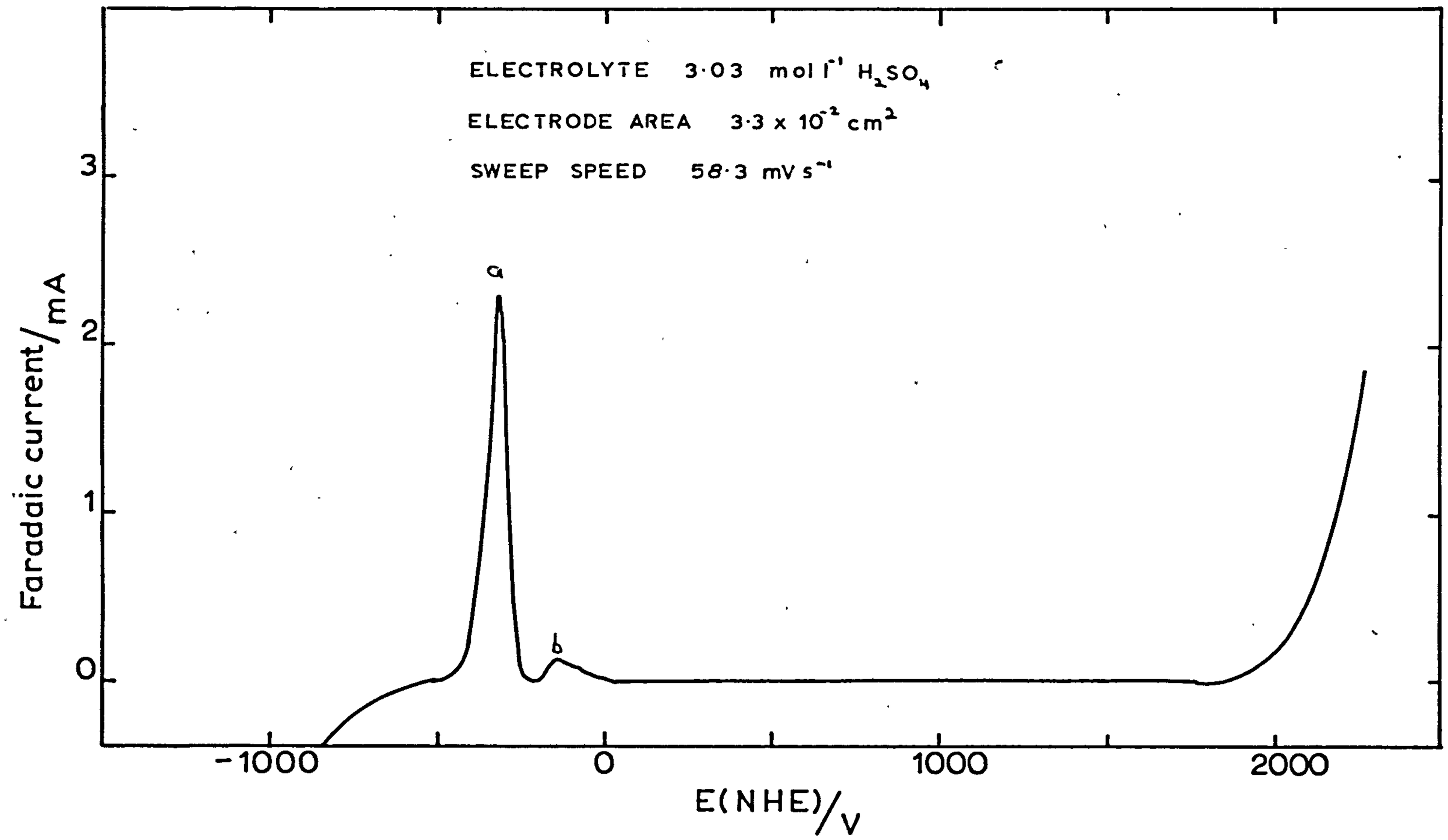

Fig. 2. Anodic peak current - $\sqrt{\text{sweep rate}}$ for $PbSO_4$ formation on polycrystalline lead in H_2SO_4 electrolyte.

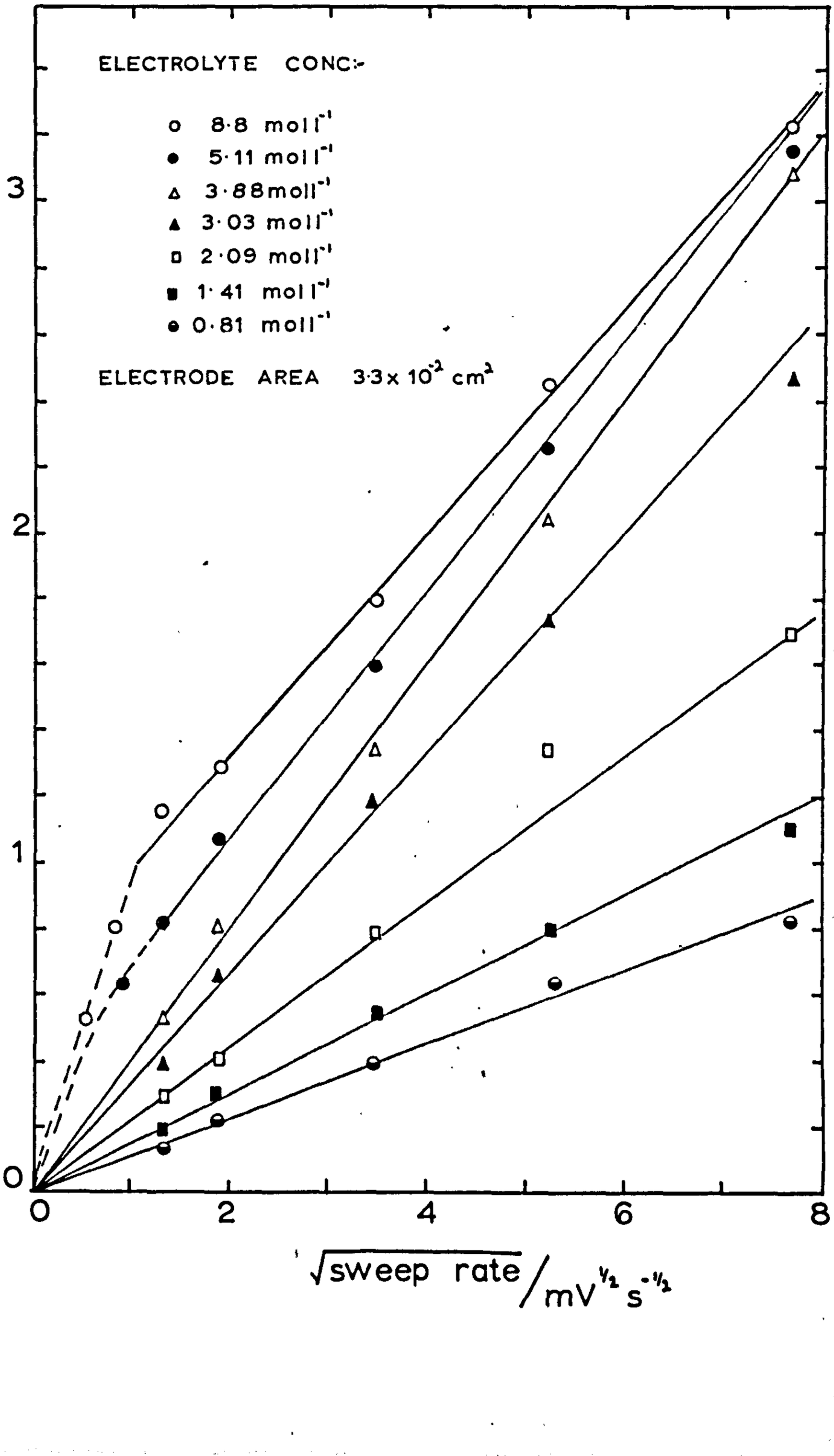

Figure 3 shows the dependence of the peak current of peak a on the concentration of H_2SO_4. At low concentrations < 4 mol l^{-1} a linear relationship was observed. Thus at concentrations of H_2SO_4 lower than 4 mol l^{-1} the concentration dependence and the linear $I_m - \sqrt{v}$ lines passing through the origin, indicate that the process controlling the current flow for peak a is a diffusion process in solution.

Figure 4 shows the relationship between the slope, $\partial I_{m/\partial} v^{-\frac{1}{2}}$, of the peak height, I_m, vs $\sqrt{v}$ curves and the concentration of H_2SO_4. A straight line plot was obtained which extrapolated through the origin as expected if the rate controlling process was diffusion in solution.

Discussion

The observed behaviour of the lead electrode in H_2SO_4 can be interpreted in terms of two processes in addition to charge transfer:-

(a) the diffusion of SO_4^{2-} and HSO_4^- ions in solution,

(b) the transport of mass and charge through an insoluble layer of $PbSO_4$ at the electrode.

Repetitive anodic sweeps around the potential of peak a, limiting the potential range to ~ -800 mV $-$ 0 mV and incorporating a 10 s rest period between each sweep, showed a slight progressive decrease in I_m. This indicates that to some extent both diffusion in solution and diffusion in the solid phase influence the rate determining process.

At the lower experimental sweep rates and low concentrations of H_2SO_4, current limitation is caused by a shortage of anions in the electrolyte layers in the immediate vicinity of the electrode, the majority of the SO_4^{2-} ions having been deposited on the electrode. At high H_2SO_4 concentrations there is always an adequate supply of SO_4^{2-}

Fig. 3. Anodic peak current - $[SO_4^{--}]$ for $PbSO_4$ formation on polycrystalline lead in H_2SO_4 electrolyte.

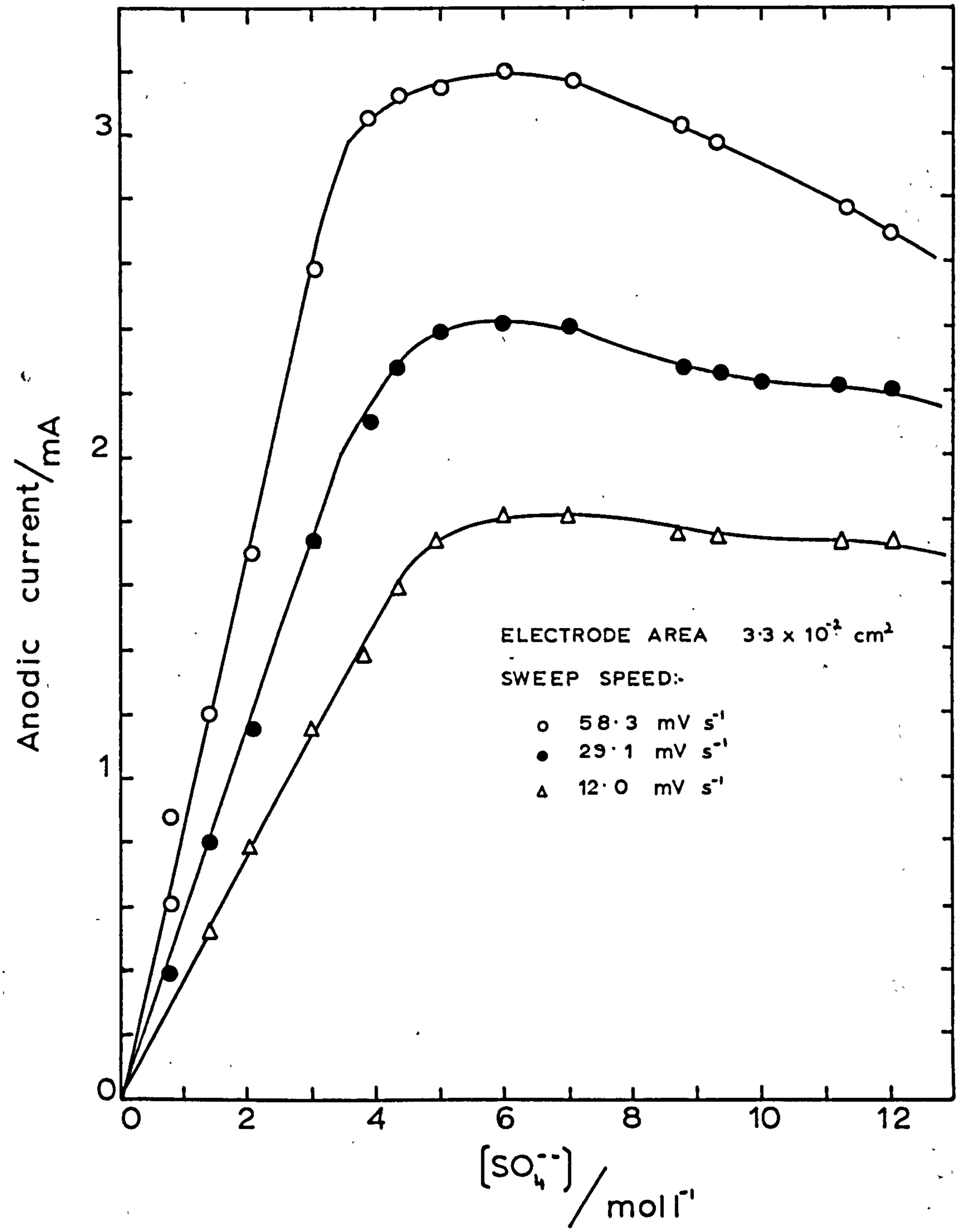

Fig.4. Slope of $I_m - \sqrt{v}$ curves for polycrystalline lead in H_2SO_4 electrolyte.

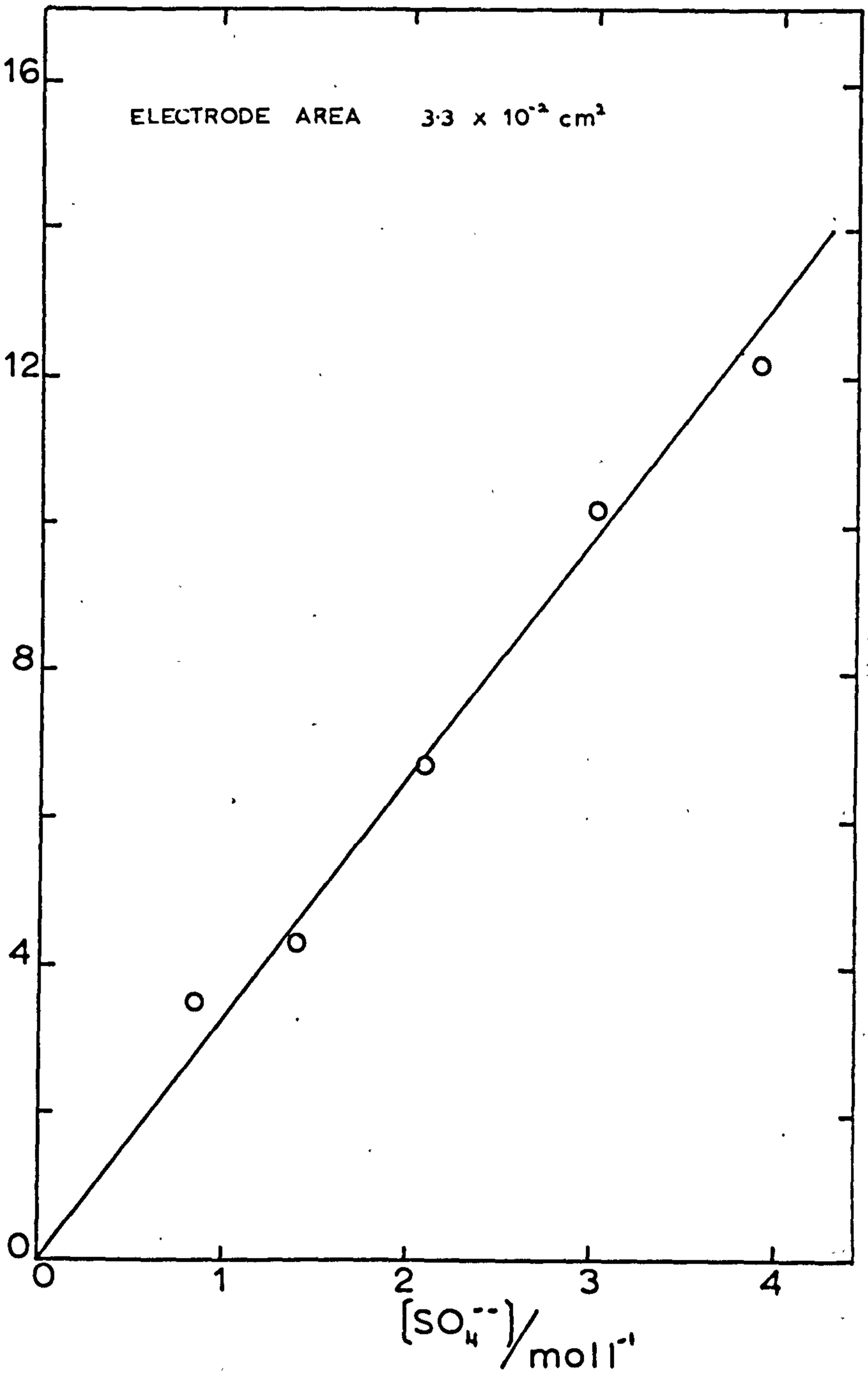

ions available at the electrode, however, the progressive growth of the $PbSO_4$ layer hinders the transport of charge through the electrode/electrolyte interphase and the current density is therefore limited. The rate controlling process is now the diffusion of ions through the $PbSO_4$ layer at the electrode so that a linear I_m vs $\sqrt{v}$ relationship would again be expected. The concentrations and diffusion coefficients of the reacting substances now refer to the solid state and the slopes of the I_m vs $\sqrt{v}$ lines undergo a change in value corresponding to the change in the mechanism of current limitation. Extrapolation of the I_m vs $\sqrt{v}$ curves, corresponding to the solid phase current limiting mechanism, to zero sweep speed do not yield zero values of I_m but a significant intercept. The magnitude of this intercept is a measure of the change necessary to cover the electrode with the solid phase of $PbSO_4$.

Increasing the concentration of H_2SO_4 causes a progressive reduction in the sweep rate at which the change over from one mechanism of current limitation to the other occurs since limitation due to a shortage of SO_4^{2-} ions becomes progressively more unlikely, as observed in figure 2.

The actual value of the sweep rate at which the change of mechanism occurs is determined by the thickness of the solid phase film and the diffusion coefficient as expressed by the physical structure of the film. Many workers have commented on structural changes that occur as concentration of H_2SO_4 increases in the range 1 - 8 mol l^{-1}. This is in the region at which I_m begins to exhibit a marked change in its relationship with concentration in the present experiments, figure 2 and figure 3, and it may be that the same factor applies in this case.

Assuming that equation 2.45 holds for the present experiments, from figure 4, the diffusion coefficient corresponding to the ion involved in the diffusion in solution rate determining process is calculated as 10^{-5} cm^2 s^{-1} which compares favourably with that reported for the SO_4^{2-} ion in aqueous solutions.

The exact composition of the secondary layer formed corresponding to peak b could not be determined from the present experiments, however, from previous work it is well established that, in H_2SO_4 the oxidation of lead produces alkaline conditions at the electrode surface which could favour the formation of tetragonal PbO,[71] [84,168,189] basic lead sulphates or $Pb(OH)_2$ on the interior of a $PbSO_4$ layer. Burbank[71,168] suggests that the formation of tetragonal PbO or $Pb(OH)_2$ is more probable at the potential corresponding to peak b and, consequently, build up of a sandwiched structure such as $Pb.PbO.PbSO_4$[167,184] rather than Pb.(oxy lead salts).$PbSO_4$ [187] at the electrode.

APPENDIX 7. A STUDY OF THE DIFFERENTIAL CAPACITANCE OF POLYCRYSTALLINE LEAD IN SOME AQUEOUS SOLUTIONS

The differential capacitance of polycrystalline lead in aqueous solutions was made so that the capacitance measurements reported for PbO_2 could be compared with what is considered a fairly "mercury like" solid metal electrode.

Preparation of test electrodes was as described in Appendix 5.

Table 1 summarizes the results of previously reported work.

Results

Figure 1 shows typical faradaic current - bias potential curves for the electrolytes investigated. The electrode was nowhere ideally polarizable, however, in each electrolyte there existed an experimental region where negligible faradaic current flowed. The limits of experimental polarizability for Pb in HNO_3, H_2SO_4, H_3PO_4, KNO_3 and NaOH were ~ -0.05 - -0.9 V, ~ -0.1 - -0.9 V, ~ -0.15 - -1.0 V, ~ -0.1 - -1.3 V and ~ -0.3 - -1.0 V respectively. The positive limit was determined by the potential of lattice dissolution and negative extremity by hydrogen evolution.

Figure 2 shows a series of differential capacitance - bias potential curves for lead in KNO_3 solution. Throughout the experimental concentration range the resistive component of the electrode impedance was fairly constant for potentials within the experimental polarizable region indicating little change in the double layer structure in this region. In the more concentrated electrolyte solutions the capacitance curves exhibited a small capacitance hump which progressively changed into a deep minimum in the more dilute solutions. The position of this minimum was concentration independent. The value of the pzc, estimated from the position of the capacitance minimum, is

Fig 1 Faradaic current-bias potential curves for polycrystalline lead in some aqueous electrolyte solutions.

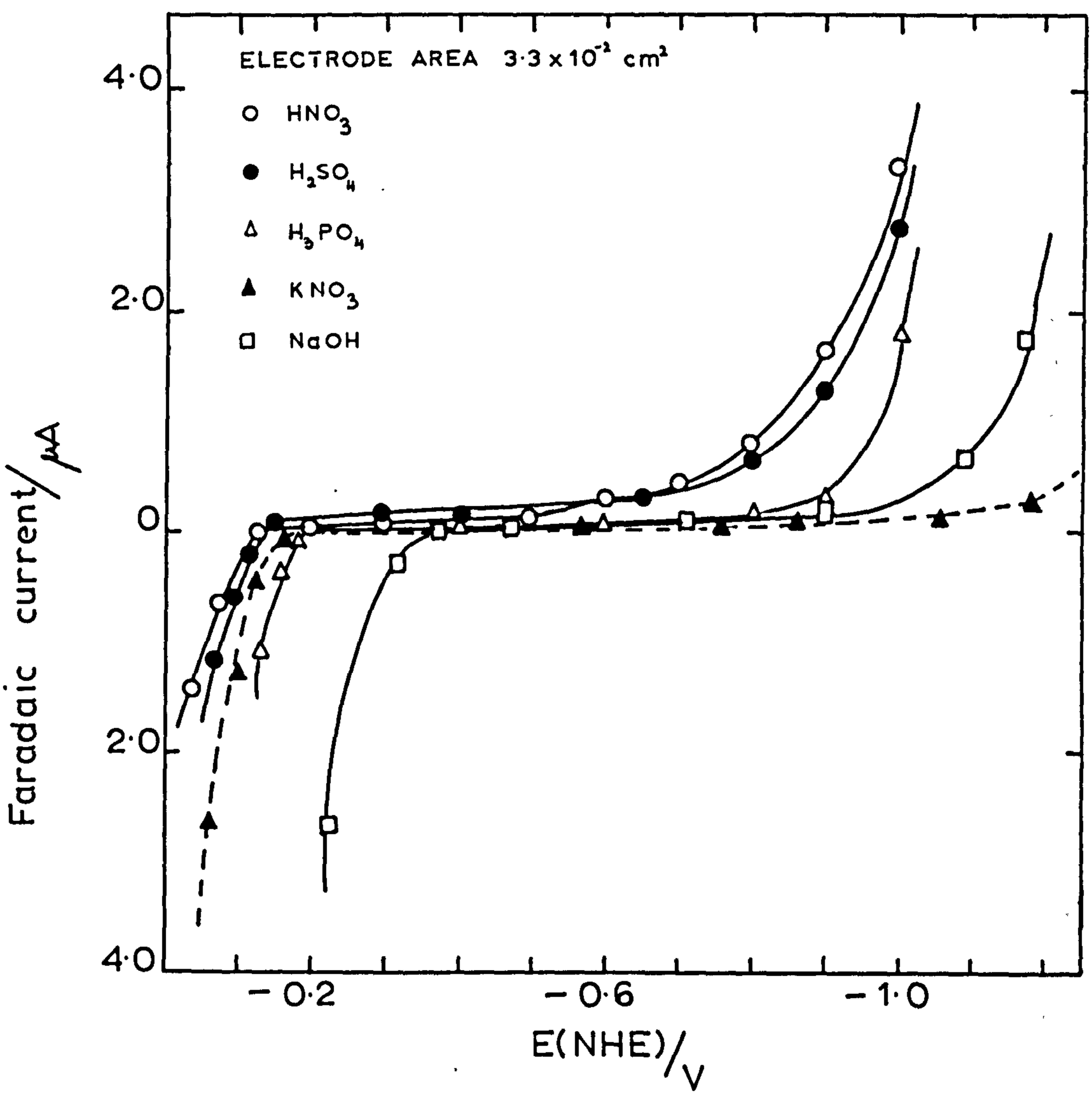

Fig 2 Differential capacitance-bias potential curves for polycrystalline lead in KNO_3 electrolyte.

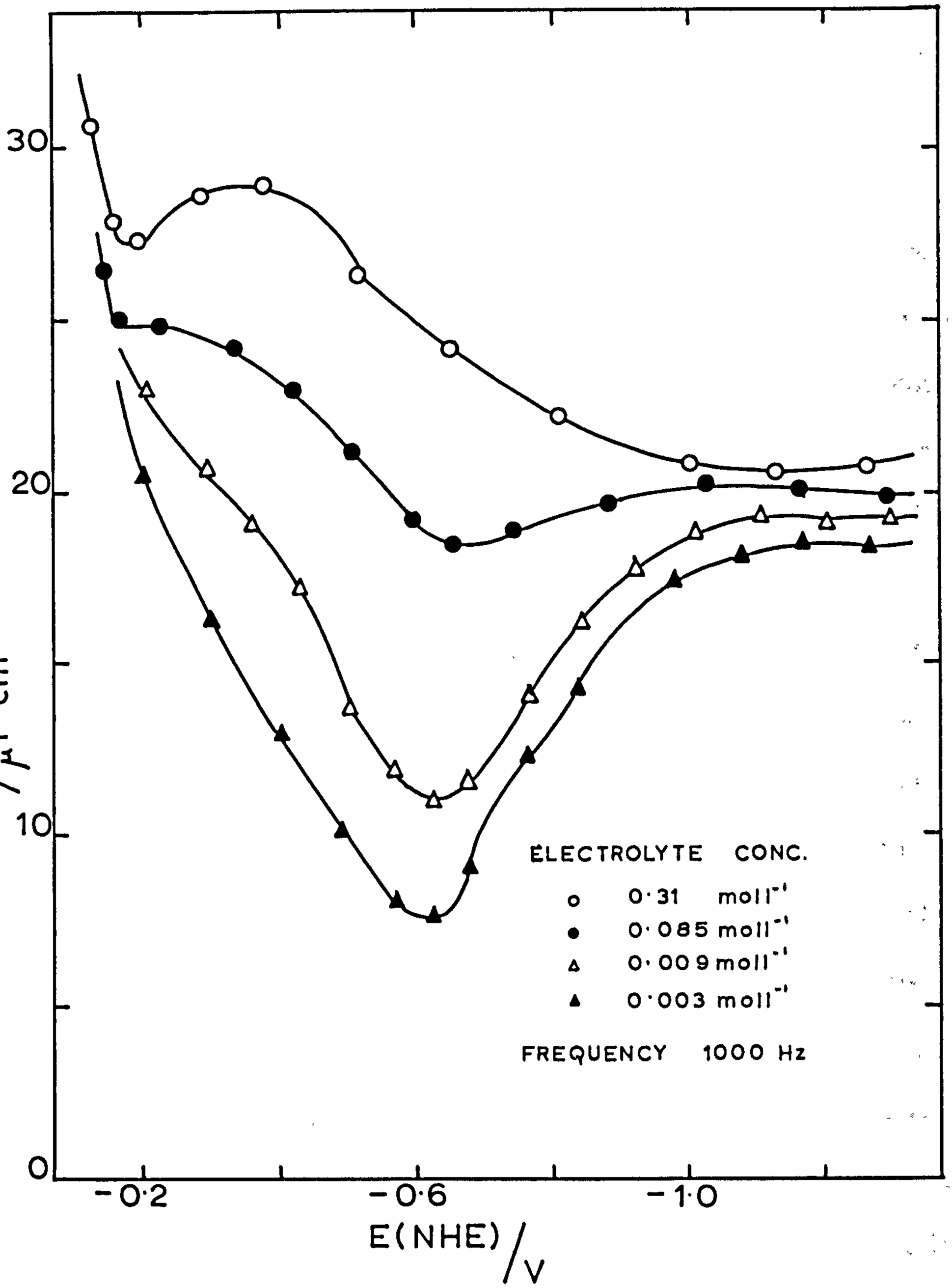

- 0.59 V in agreement with results of previously reported values in non-interacting electrolytes. (Table 1.)

Stable impedance measurements were obtained after 2 hours electrode/electrolyte contact time and showed a 5% variation about a mean.

Figures 3 and 4 show a series of differential capacitance - bias potential curves in solutions of H_2SO_4 and H_3PO_4 over the concentration range ~ 0.03 - 0.001 mol l^{-1} for electrodes held at the potential of zero faradaic current before readings were taken. The curves showed a very broad minimum indicating the probable presence of adsorption which obscures the diffuse double layer characteristics in dilute solutions and development of the compact double layer "hump" at higher concentrations. The capacitance minimum occurs at ~ - 0.5 - - 0.7 V. For lead electrodes in sulphate electrolytes, Kolotyrkin[268] suggested a slow adsorption of SO_4^{2-} ions from solution occurs which complicates the behaviour of the electrode. Accordingly, measurements were made on electrodes polarized for some time at potentials both positive and negative of the potential of zero faradaic current flow, in an attempt to restrict the adsorption of SO_4^{2-} ions

Figures 5 and 6 show the effect on the differential capacitance curves of polarizing the electrode at -0.65 V before taking readings. A fairly broad minimum is apparent from which it is clear that adsorption is still present. Comparison of these curves with the curves of figures 3 and 4, show that by polarizing the electrode at -0.65 V broader curves are obtained indicating greater adsorption. This confirms that the adsorption process involves the SO_4^{2-} and PO_4^{3-} ion in the respective electrolytes.

Figures 7 and 8 show the effect of polarizing the electrode at -1.15 V before taking readings. The capacitance curves showed a more well defined minima and were similar in form to the capacitance curves obtained in nitrate electrolyte solutions.

Table 1

P.Z.C.(NHE) Volts	Electrolyte Solution	Method of Determination	Reference
- 0.56	0.5M Na_2SO_4	Hardness	260,261
- 0.60	0.05M Na_2SO_4	Deformation of single crystal	262
- 0.64	0.005M Na_2SO_4	Capacitance minimum	272
- 0.65	0.001M Na_2SO_4	Electroreduction of anions	262,263
- 0.64 - -0.67	0.0005M K_2SO_4	Capacitance minimum	264,265, 266,267
- 0.65	0.001M $K_2S_2O_8$	Electroreduction of anions	262,263
- 0.64	0.005M H_2SO_4	Capacitance minimum	267
- 0.65	0.0005M H_2SO_4	" "	264,265, 266,267
- 0.62	0.5M H_2SO_4	" "	268
- 0.56	0.001M NaF	" "	267,272
- 0.60	1M NaCl	Hardness	260,261
- 0.69	0.01M KCl	Capacitance minimum	264,269
- 0.64	0.01M KCl	" "	270
- 0.56	0.001M KNO_3	" "	271
- 0.64	0.01M $KClO_4$	" "	271
- 0.69	0.02M $NaClO_4$	" "	266
- 0.55	1M NaOH	Hardness	260,261

Fig 3 Differential capacitance-bias potential curves for polycrystalline lead in H_2SO_4 electrolyte.

ELECTRODE HELD AT POTENTIAL OF ZERO FARADAIC CURRENT FLOW FOR 3 hrs BEFORE TAKING READINGS.

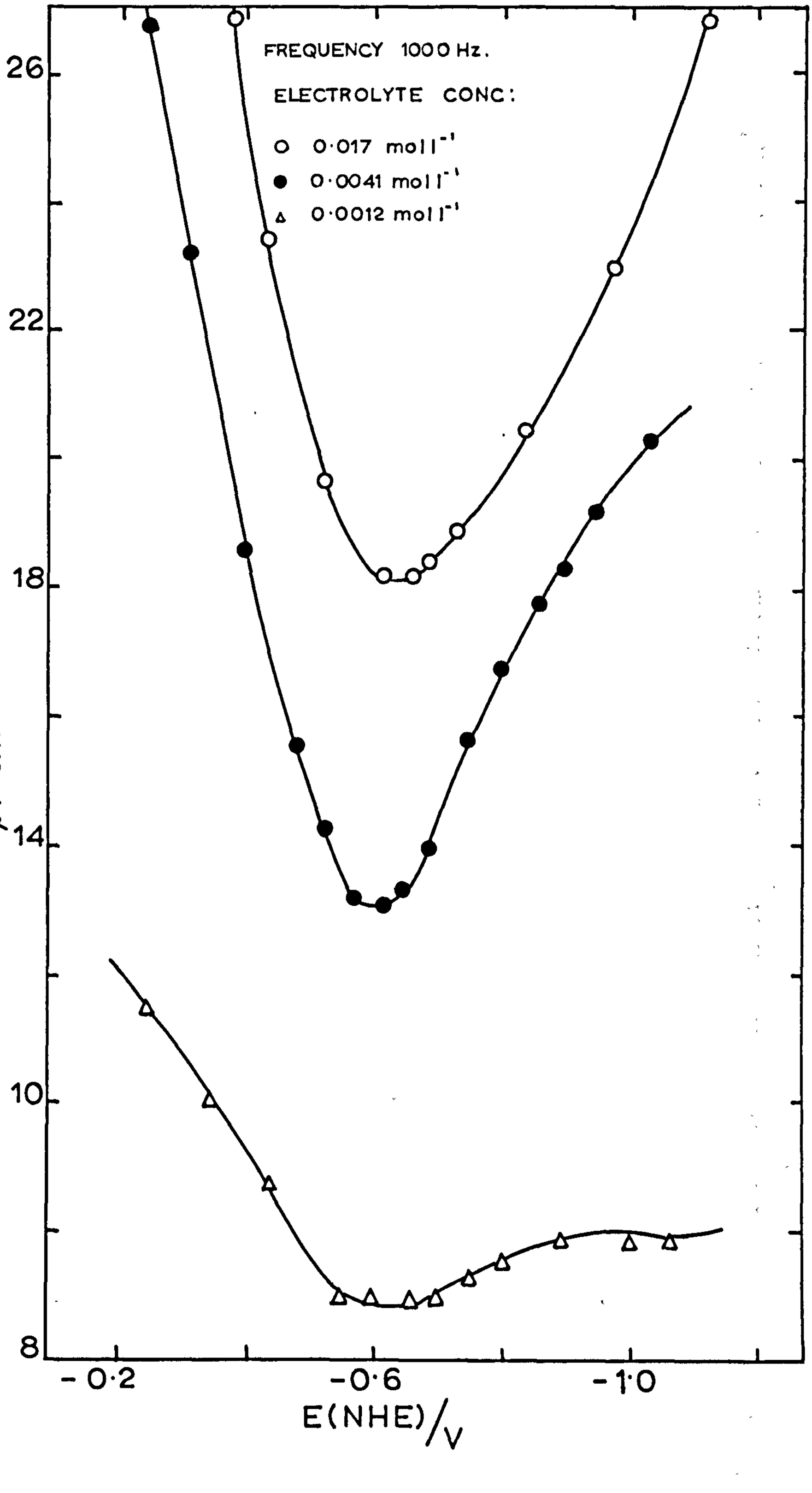

Fig 4 Differential capacitance-bias potential curves for polycrystalline lead in H_3PO_4 electrolyte.

ELECTRODE HELD AT POTENTIAL OF ZERO FARADAIC CURRENT FLOW FOR 3hrs BEFORE READINGS TAKEN.

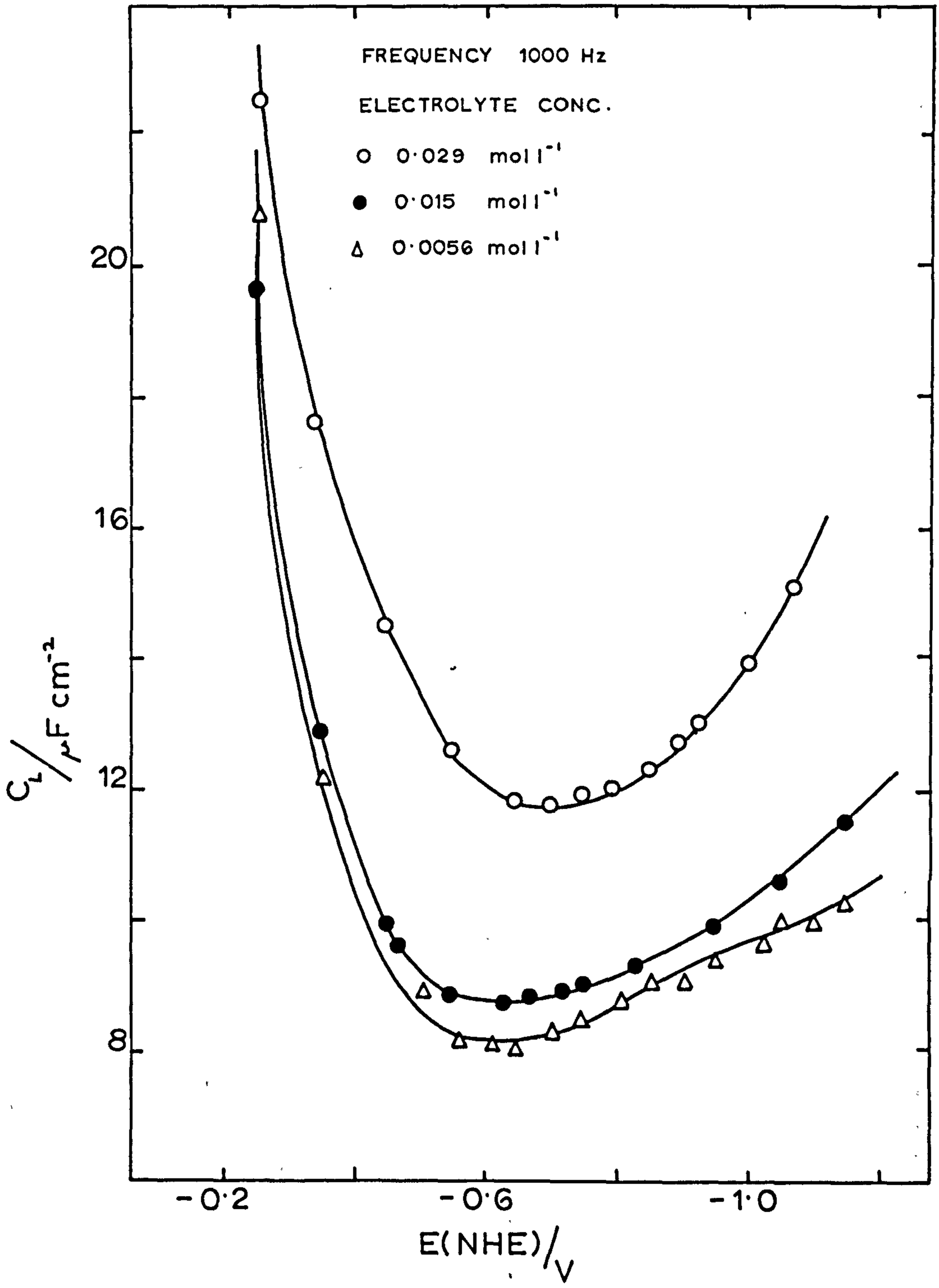

Fig 5 Differential capacitance-bias potential curves for polycrystalline lead in H_2SO_4 electrolyte.

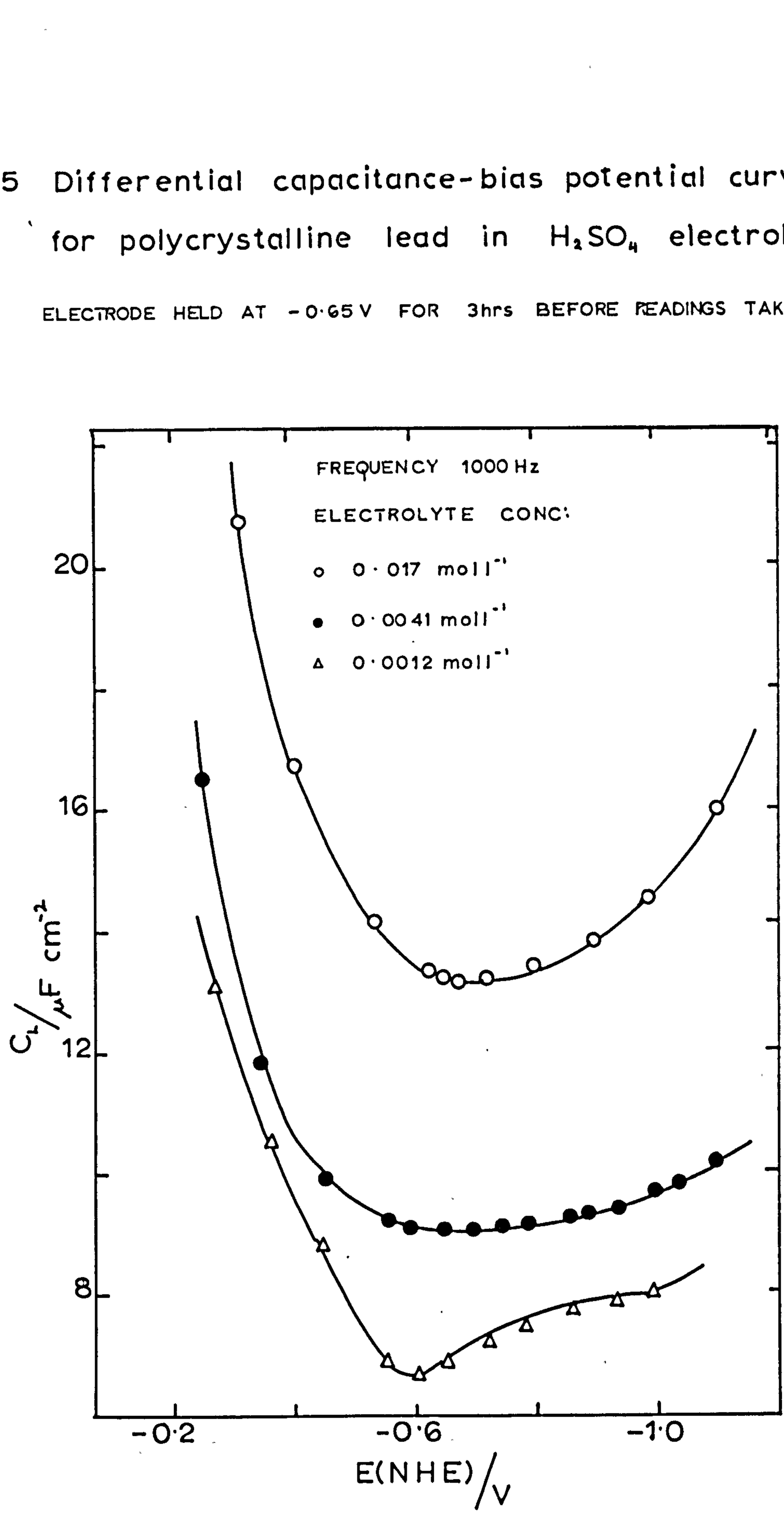

Fig 6 Differential capacitance-bias potential curves for polycrystalline lead in HPO_3 electrolyte

ELECTRODE HELD AT - 0·65 V FOR 3 hr BEFORE READINGS TAKEN

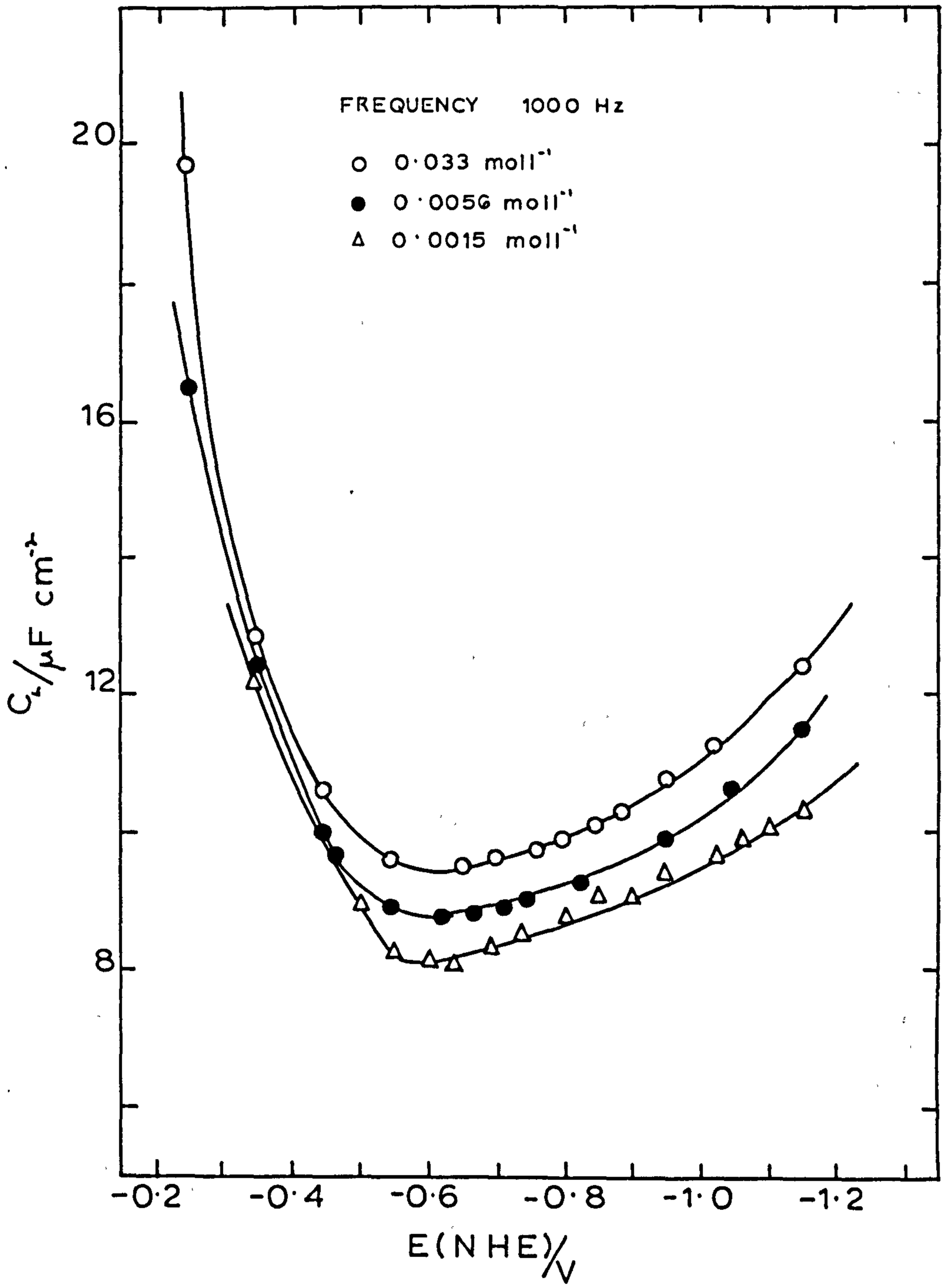

Fig 7 Differential capacitance - bias potential curves for polycrystalline lead in H_2SO_4 electrolyte.

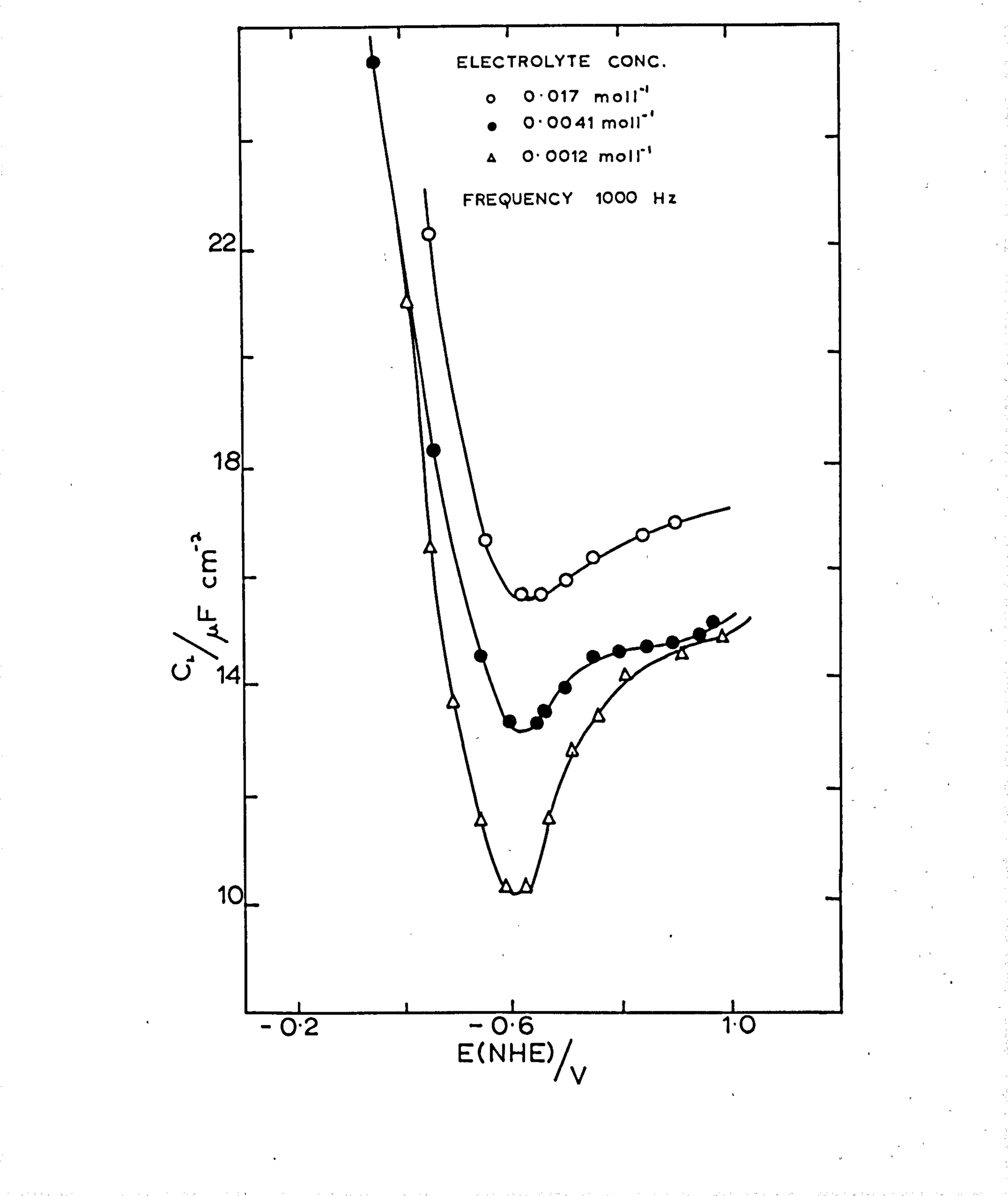

Fig 8 Differential capacitance - bias potential curves for polycrystalline lead in H_3PO_4 electrolyte.

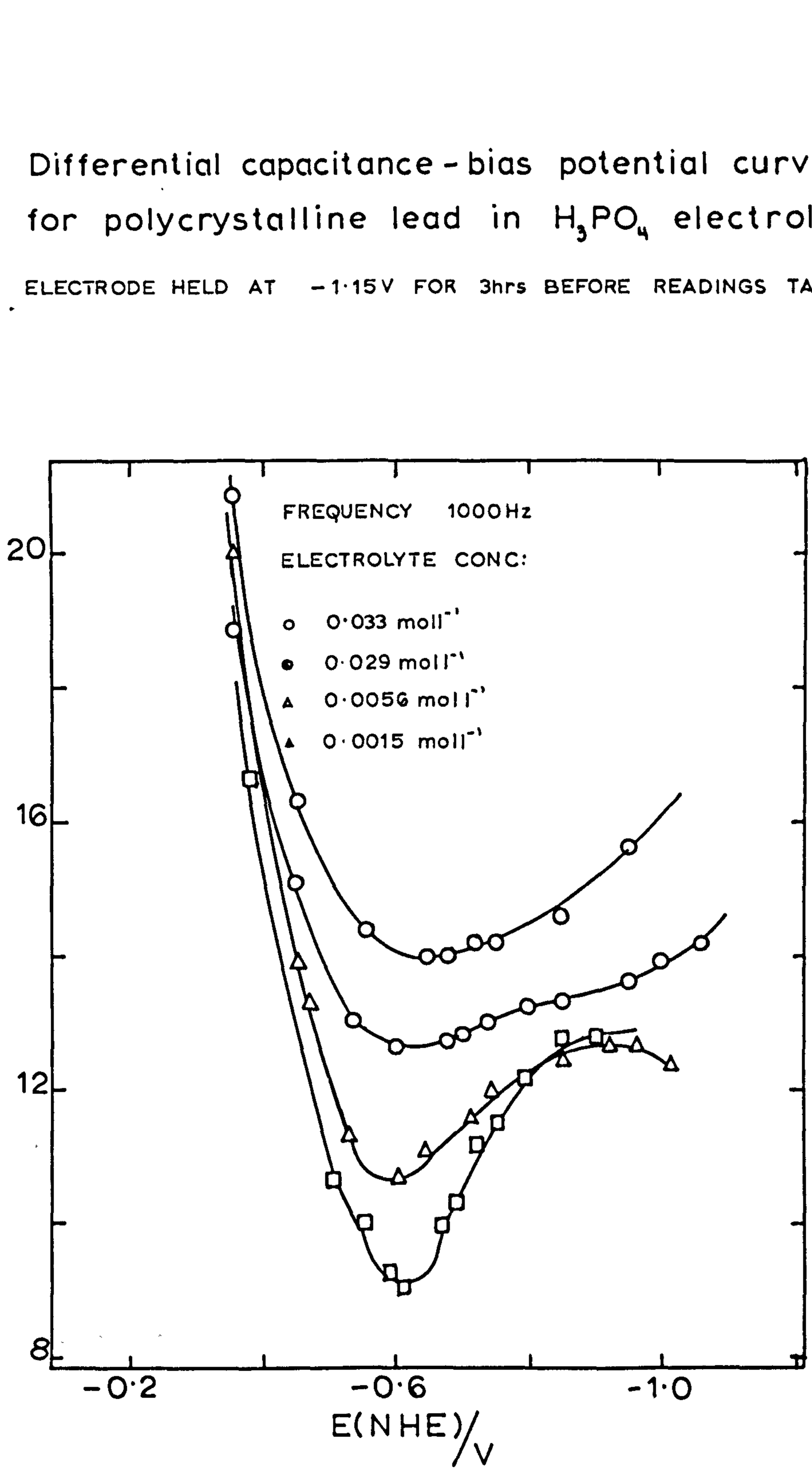

Figure 9 shows a series of differential capacitance curves for HNO_3 solutions. The deep minimum, at -0.6 V, corresponds to the minimum observed in KNO_3 solutions. Hydrogen evolution occurred at less negative potentials than in the case of KNO_3 solutions due to the lower pH.

Figure 10 shows the differential capacitance curves for solùtions of NaOH. A minimum in the curves occurs at -0.62 V. The separation of the anodic branch of the differential capacitance curves with $[OH^-]$ is a consequence of the equilibrium reaction:-

$$Pb(OH)_3^- + 2e = Pb + 3\,OH^- \qquad (1)$$

which predicts that E_o shifts by about 90 mV for each decade change in $[OH^-]$. Figure 11 shows a typical frequency dispersion of the differential capacitance curves in NaOH solutions. The extent of the dispersion amounted to $<$ 5% for a frequency change 1 kHz - 120 Hz. The observed dispersion is similar to that expected for solid metal electrodes and is probably due to a certain amount of surface roughness as discussed by De Levie[6],

Discussion

It can be concluded that the adsorption of the sulphate ion on the lead electrode can materially be affected by polarizing the electrode at high negative potentials before making measurements. The return of the'expelled' sulphate ions to the electrode surface, on returning the electrode to the experimentally polarizable region, is relatively slow. Experiments with phosphoric acid solutions gave results similar to those observed in the case of sulphuric acid. That the adsorption of SO_4^{2-} and PO_4^{3-} ions is relatively weak is supported by the electrode resistances which are equally constant with the nitrate systems.

Fig 9 Differential capacitance - bias potential curves for polycrystalline lead in HNO_3 electrolyte.

ELECTRODE HELD AT -1·15 V FOR 3hrs BEFORE READINGS TAKEN

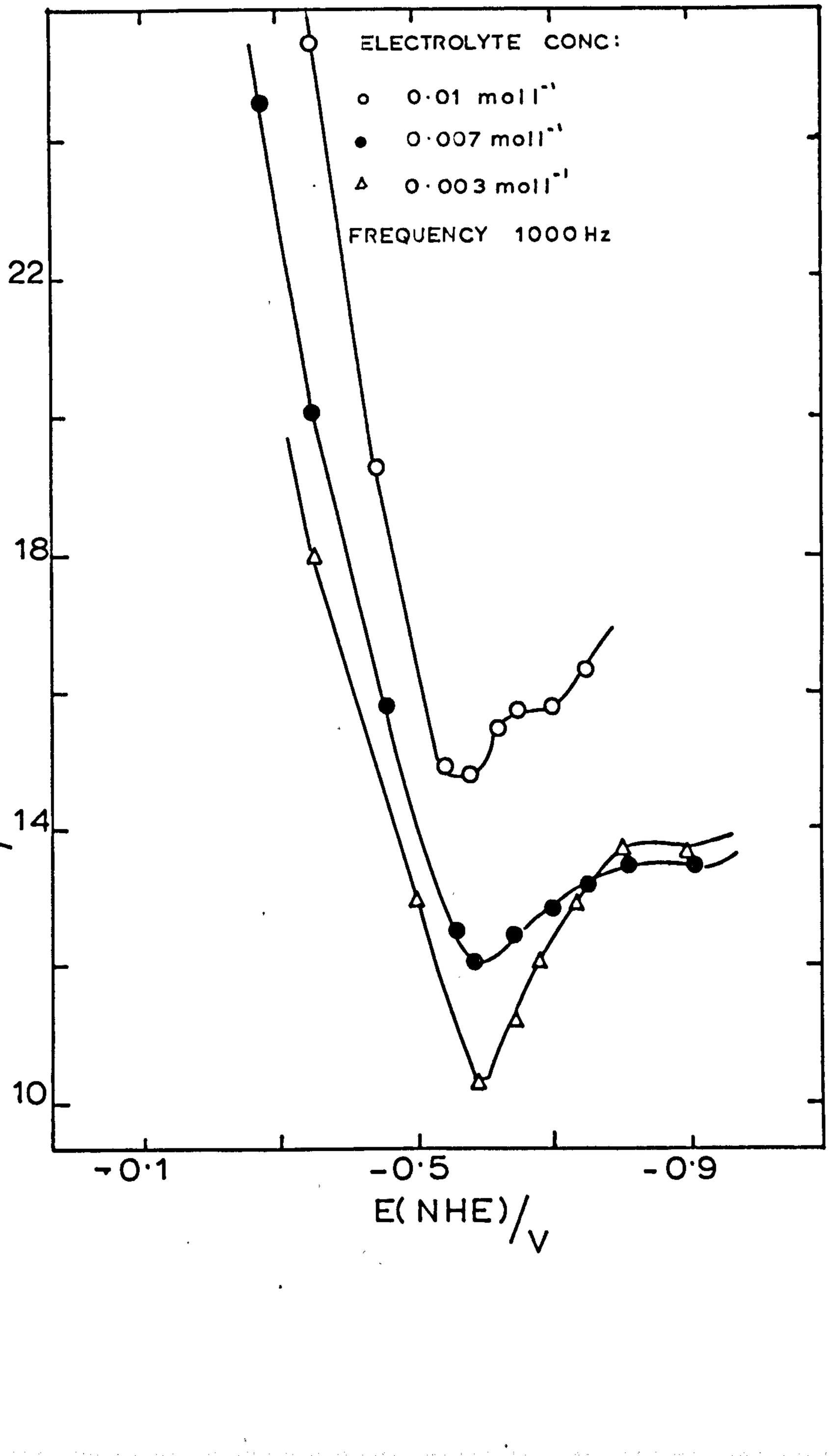

Fig 10 Differential capacitance-bias potential curves for polycrystalline lead in NaOH electrolyte.

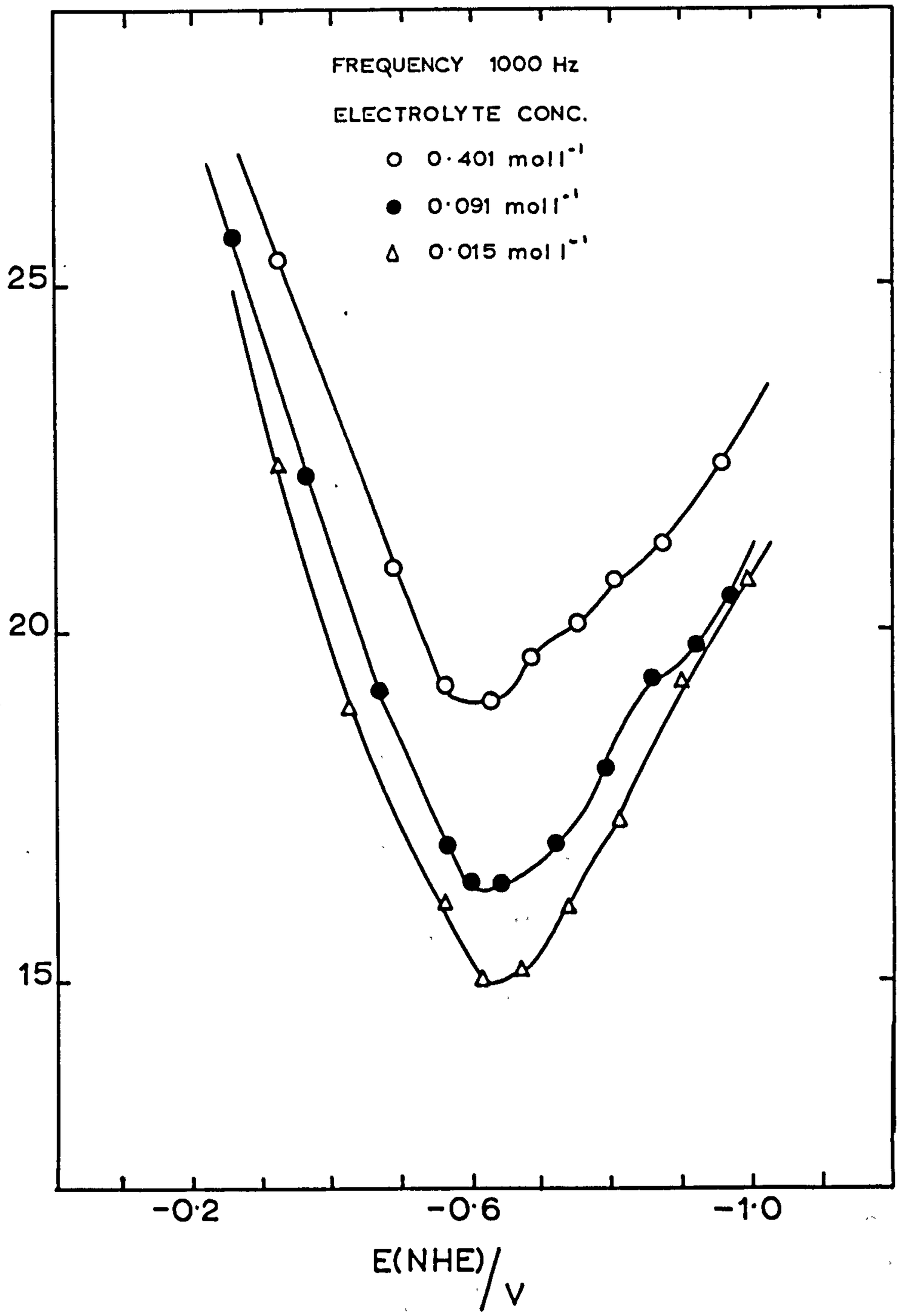

Fig 11 Typical frequency dispersion of differential capacitance curves for polycrstalline lead in NaOH electrolyte.

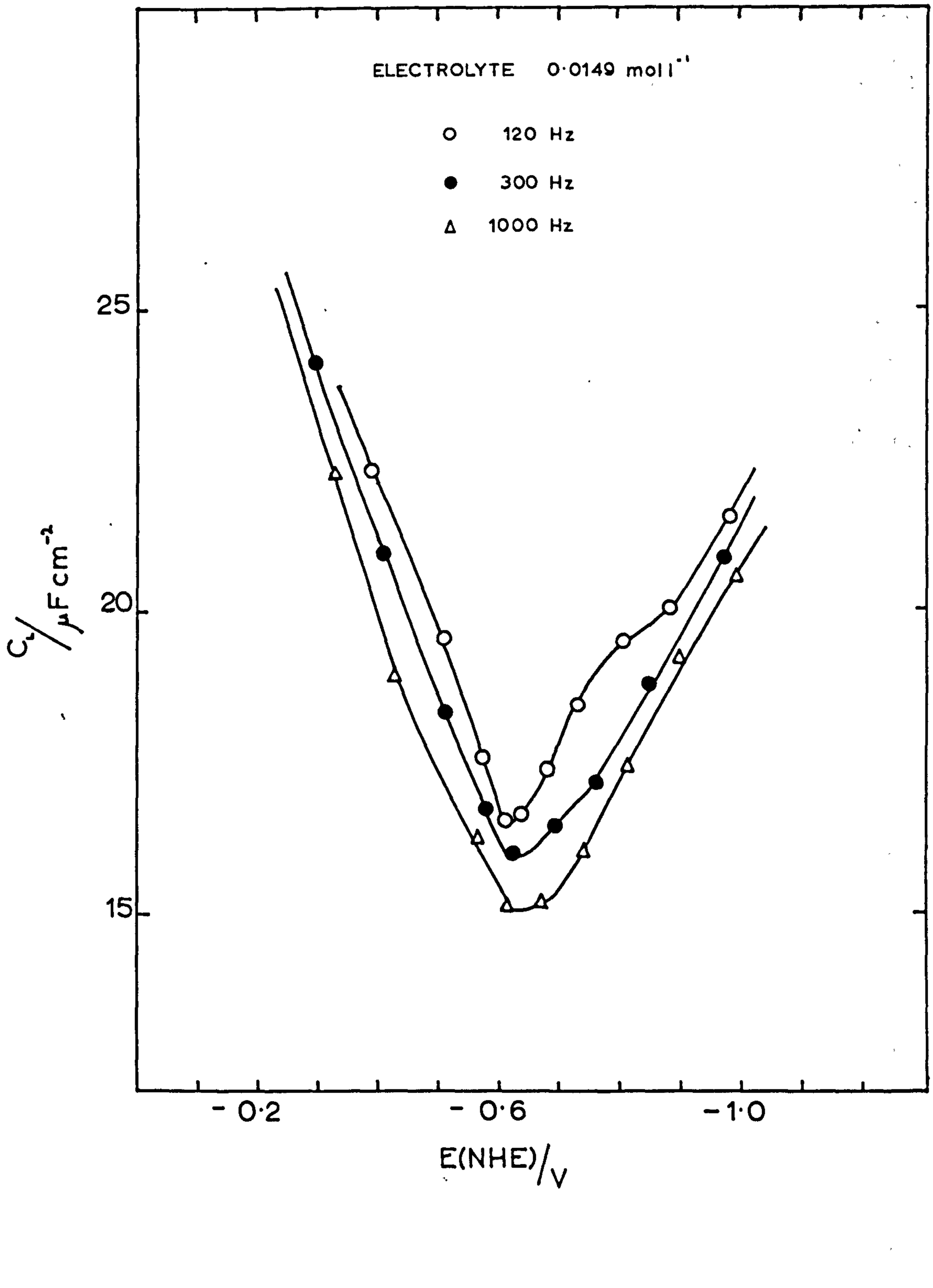

In common with all solid metal electrodes, a certain amount of initial instability of the electrode impedance was observed. In the present case it is interesting to compare the time stability curves obtained whilst holding the electrode at -1.15 V and at the potential of zero faradaic current flow. Figure 12 shows such a comparison and it is clear that suppression of adsorption of SO_4^{2-} ions onto the electrode surface significantly affects the stability curves. It can be concluded therefore that in the case of lead electrodes in H_2SO_4 solutions a certain amount of initial instability is due to the adsorption of the anion. Phosphoric acid gave similar results to sulphuric acid.

For all the electrolyte solutions, hysteresis of the impedance measurements was observed at both the negative and positive extremities of the polarizable region. Potential excursions within these limits caused little or no hysteresis. Electrodes forced to potentials outside the polarizable region and then returned to this region never reverted to their original conditions. This effect was less severe in the case of KNO_3 solutions.

Fig 12 Differential capacitance-time curves for polycrystalline lead in H_2SO_4 electrolyte.

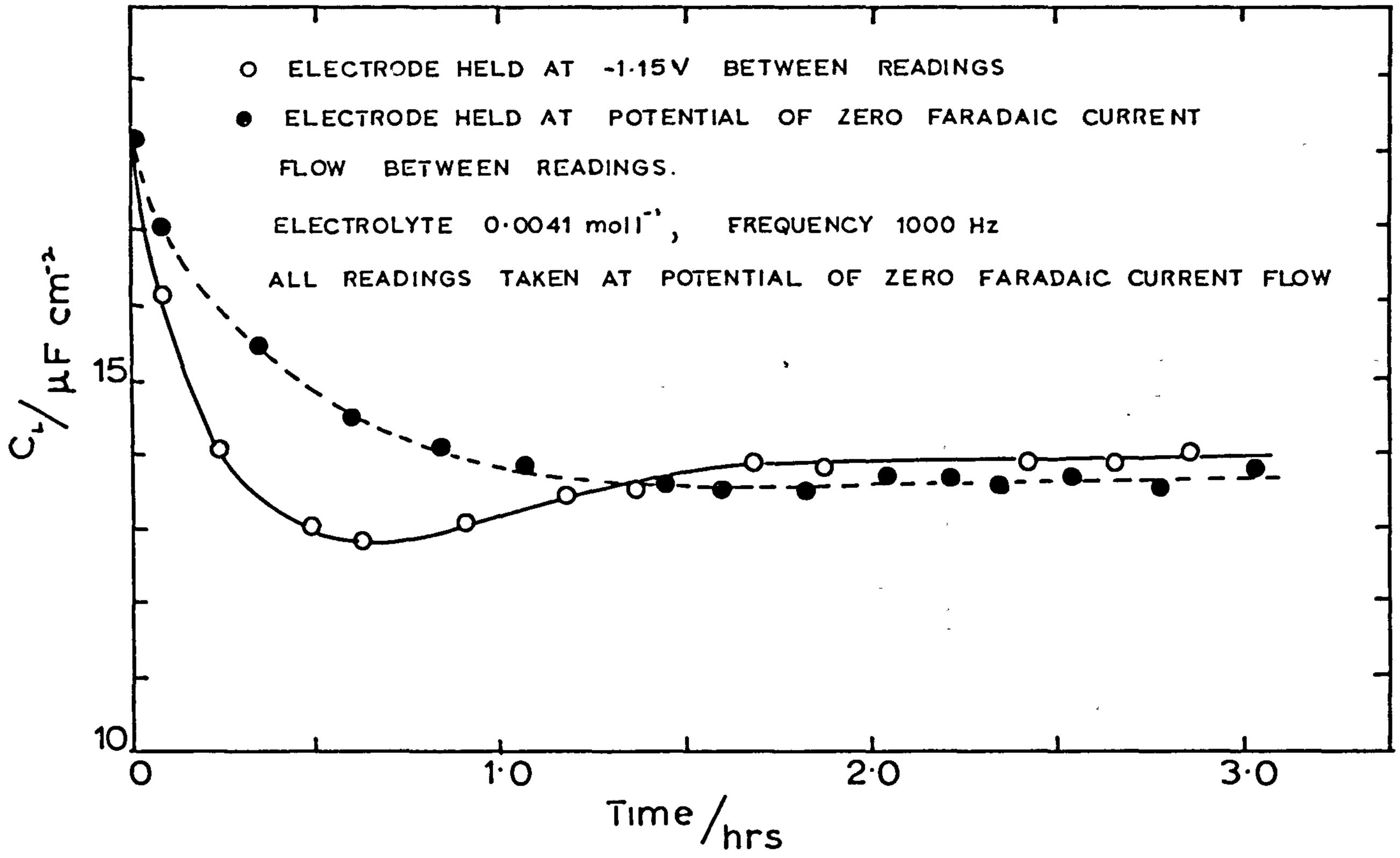

APPENDIX 8. A STUDY OF THE DIFFERENTIAL CAPACITANCE OF Pb - Sb ALLOYS IN AQUEOUS KNO_3 AND HNO_3 SOLUTIONS

Introduction

Antimony-lead alloys, in the concentration range 5% - 12% Sb, are invariably used as electrode support grids in lead-acid batteries, imparting rigidity and improving the casting properties of the lead[1]. The presence of antimony also confers desirable properties on the positive electrode, thus Burbank[98] found that the active material of positive plates with Pb-Sb alloy grids contained significant amounts of prismatic α-PbO_2 of high capacity. On the other hand, the active material on Sb-free grids had very little α-PbO_2 and with cycling rapidly lost capacity.

The disadvantage of the presence of Sb in the positive plate is to increase the self-discharge rate which Ruetschi and Cahan[84] traced to the Sb content. Since Sb has a lower hydrogen overpotential than lead, a local action commences, resulting in the formation of lead sulphate. Antimony is released from the positive plate, deposits on the negative plate, and on overcharging, is partly removed by the formation of stibine[276],

Other workers[60,99,276-280] have studied antimony elimination reactions, for example, Bushrod et al[282], from differential capacitance measurements, found no evidence for the formation of SbH_3 on pure Sb in aqueous acid electrolyte solutions. The possibility of stibine formation in commercial lead-acid batteries, due to a lead assisted reaction, has not yet been investigated.

The lead/aqueous solution interphase has been studied by a number of workers (see Appendix 7). The p.z.c. of Pb can be reliably placed at ~ -0.6 V. The antimony/aqueous solution interphase has been less well investigated[282-285], however, from available data the p.z.c. is estimated at ~ -0.15 - -0.2 V. In the

In the case of antimony complications arise due to oxide (or hydroxide) film formation under conditions of high pH[286,287]. It is of interest to investigate how Sb influences the double layer structure of lead electrodes.

Sb is not very soluble in Pb (at 247°C ~ 2.0%) thus the alloys used in this study (2 - 12% Sb) consist of two phases, a saturated solid solution of Sb in Pb and a saturated solid solution of Pb in Sb. The exact composition of the solid solutions depend upon the thermal history of the electrode. In the present study the electrode preparation initially involved rapid cooling of molten alloy so that, as far as could be arranged, the composition of the solid solution of Sb in Pb was ~ 2%. Alloys in the "unsaturated" (< 2% Sb) solid solution range were not investigated because of segregation uncertainties.

Experimental

The experimental technique, electrolytic cell and electrical circuit were described in Chapter 3. The test electrodes were prepared by drawing molten metal/alloy into glass capillary. Alloys were prepared from Tadanac Pb (> 99.98%) and Grade A Sb (>99.98%) by E.P.S. Ltd; the principle impurity in the Pb is Sb (< 0.005) the alloy purity was therefore ~ 99.99%. The electrode was mounted in polythene, good adhesion being observed, and cut at right angles to the principal axis. The test electrode was mechanically polished with carborundum paper and roughened glass, using bidistilled water as a lubricant, then chemically etched for 5 sec. in 50% HNO_3 before inserting into the electrolytic cell. This procedure was repeated before each experimental run.

Results

Figures 1 and 2 show characteristic faradaic current-bias potential curves for the electrode/electrolyte system investigated. (4% Sb was typical of all alloys.) None of the electrode systems were ideally polarizable, however experimental potential

Fig 1 Faradaic current-bias potential for polycrystalline antimony, lead and Pb-Sb alloys in KNO_3 electrolyte.

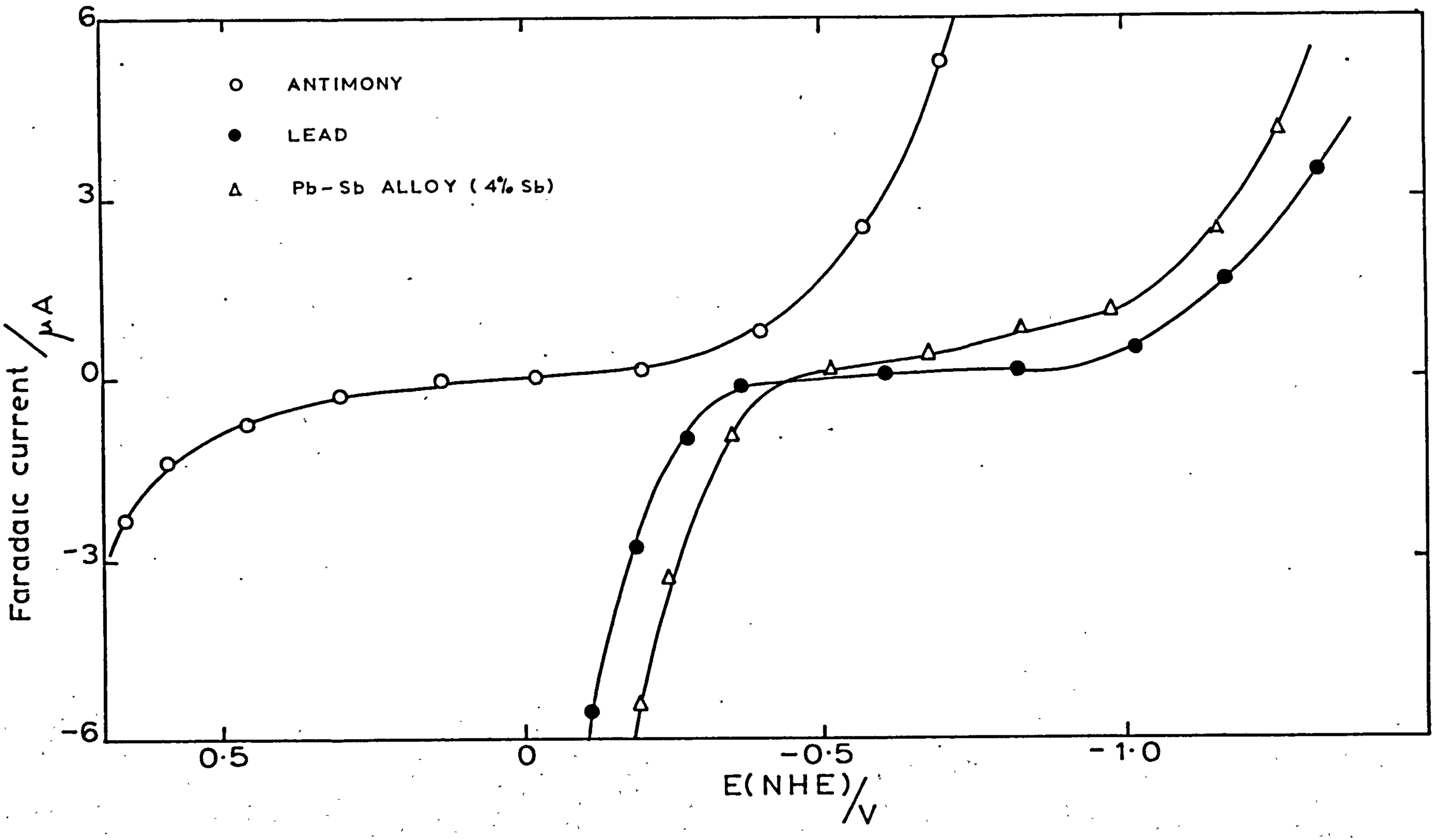

Fig 2 Faradaic current-bias potential curves for polycrystalline antimony, lead and Pb-Sb alloys in HNO_3 electrolyte.

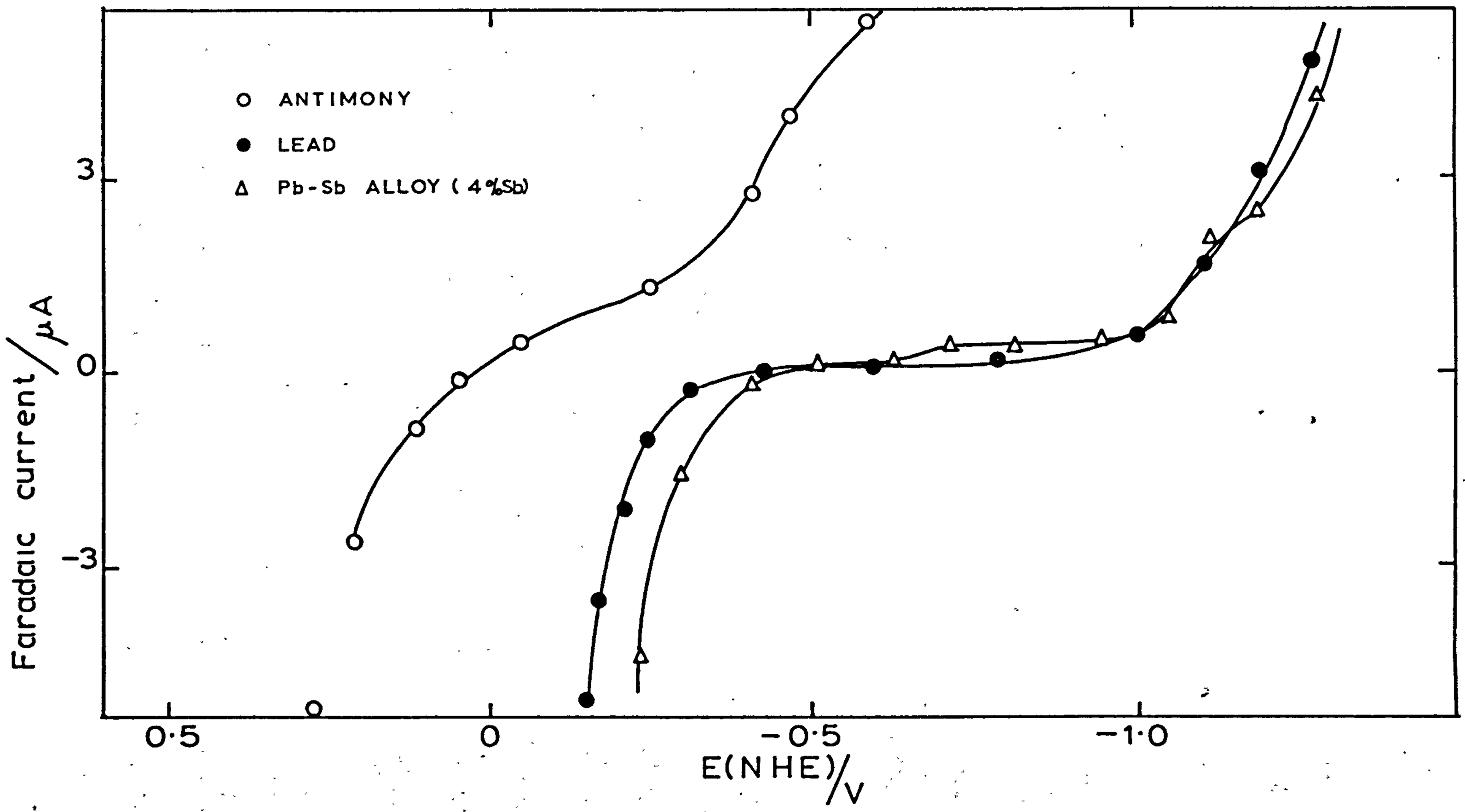

regions exist in which the faradaic current flow is negligible: ~ 0.5 - -0.2 V for Sb, ~ -0.25 - -1.2 V for Pb, and -0.3 - -1.05 V for Pb-Sb alloys in aqueous KNO_3 solutions, and 0.2 - -0.3 V for Sb, -0.3 - -1.05 V for Pb and -0.4 - -1.05 V for Pb-Sb alloys in aqueous HNO_3 solutions.

Chemically etching electrodes (50% HNO_3) gave most satisfactory impedance stability. The electrode/electrolyte contact times required for stability were ~ 2-3 hours for Pb and Pb-Sb alloys but significantly greater for Sb electrodes. Electrodes forced to potentials outside the extremes of the polarizable region required some time to return to the equilibrium (unpolarized) condition. Hysteresis was more marked at negative potentials and ~20 mins. was required for the impedance measurements to return to the initial values. Stable impedance measurements were rapidly established for small changes in the test electrode potential within the polarizable region, however longer times were required when larger capacitance changes occurred for small potential changes.

Figures 3 and 4 show a series of differential capacitance-bias potential curves for pure Pb, pure Sb and Pb-Sb alloys in aqueous KNO_3 and HNO_3 electrolyte solutions respectively. Figures 5 and 6 show a series of differential capacitance - bias potential curves for pure Sb in KNO_3 and HNO_3 solutions respectively, for varying electrolyte concentration. Complementary curves for Pb-Sb alloys (4% Sb was taken as typical of all the alloys tested) are shown in figures 7 and 8. Differential capacitance curves for polycrystalline lead were reported in Appendix 7.

In general the behaviour of Pb - Sb alloys resembled that of the pure lead. The potential of lattice dissolution of the alloys, evinced by the capacitance rise at the positive potentials, occurred at potentials more negative than for pure lead.

Discussion

The faradaic current curves for the Pb-Sb alloys resembled similar curves for pure

Fig 3 Differential capacitance-bias potential curves for Pb-Sb alloys in KNO_3 electrolyte.

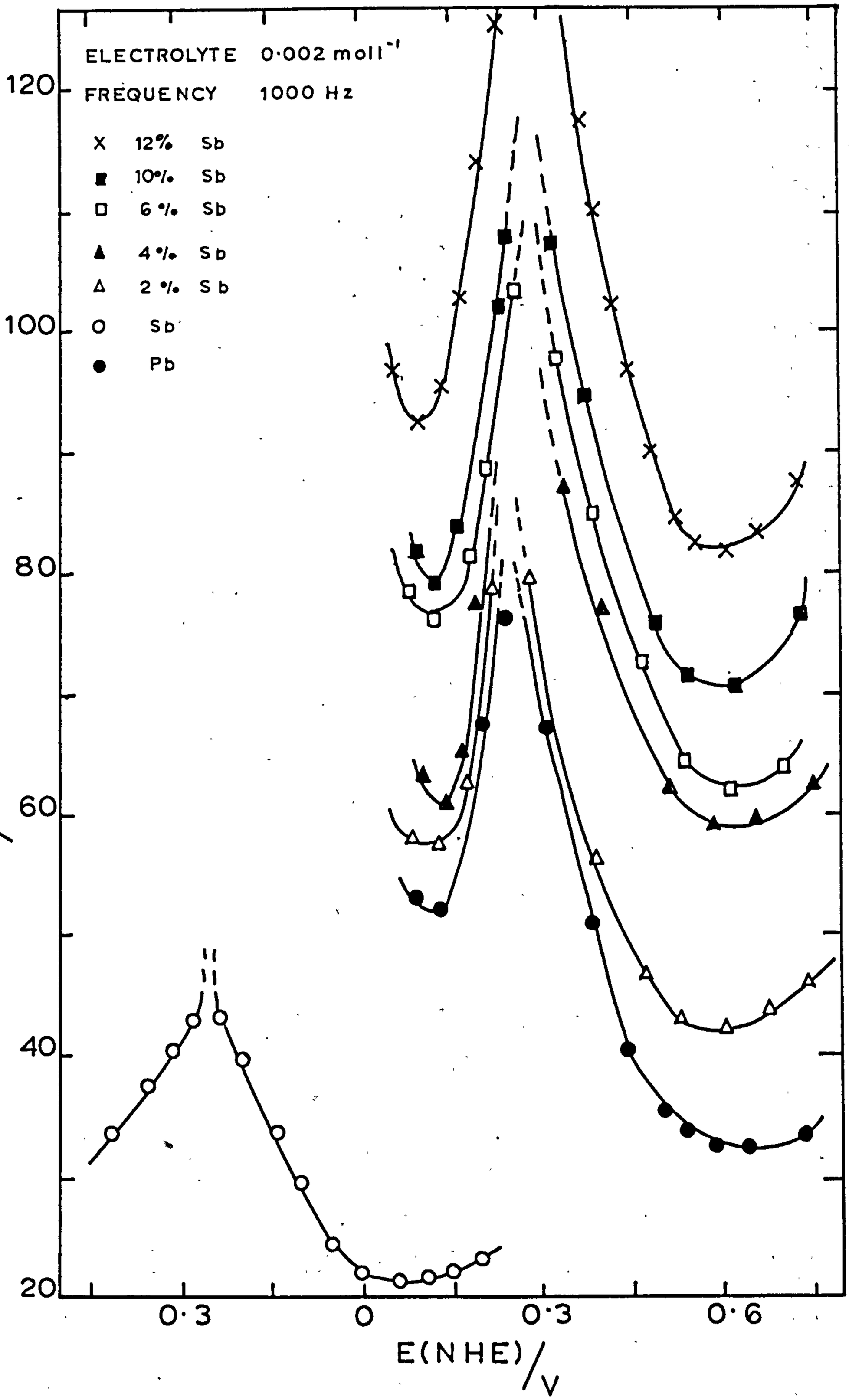

Fig 4 Differential capacitance-bias potential curves for Pb-Sb alloys in HNO_3 electrolyte.

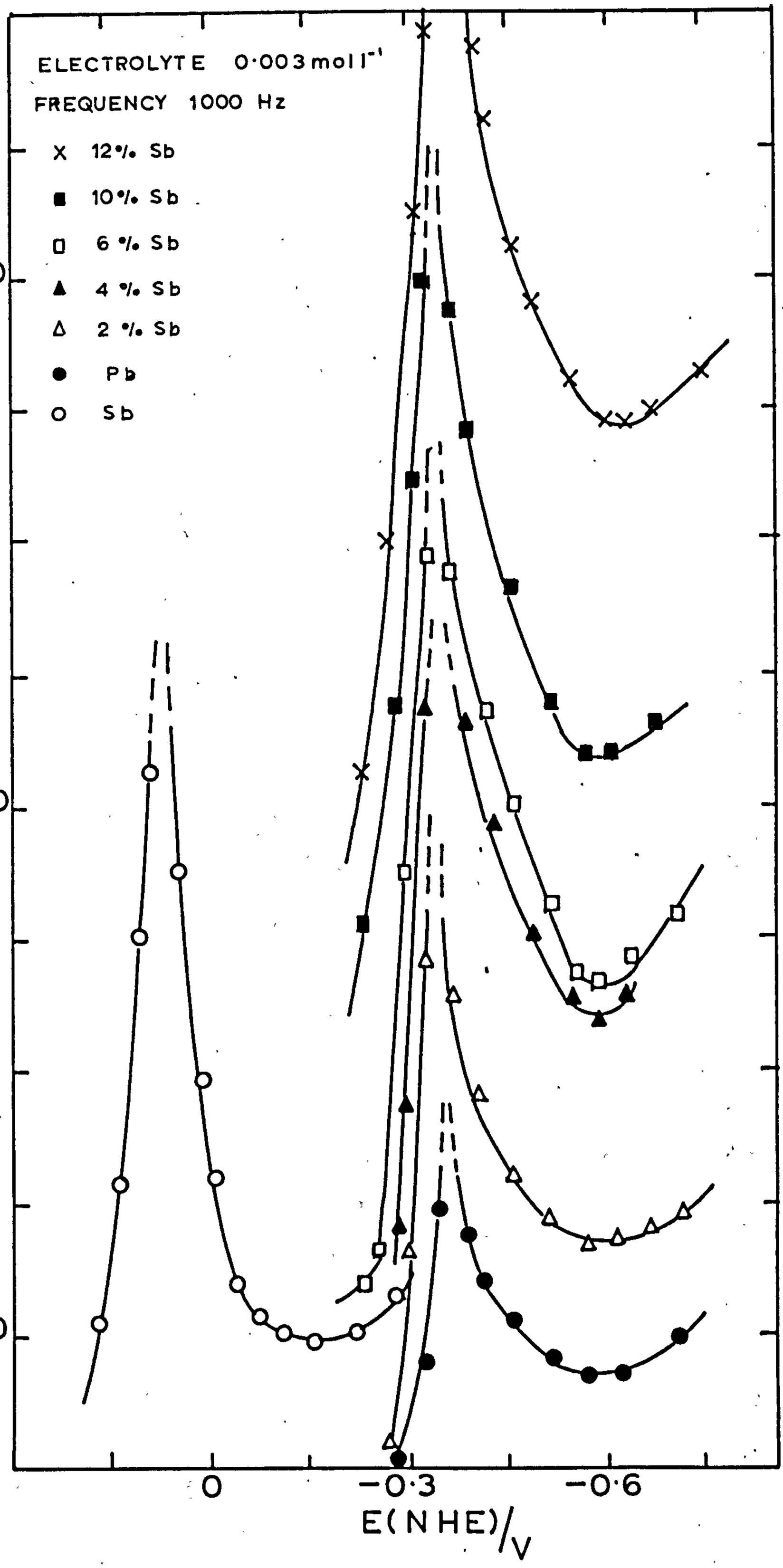

Fig 5 Variation of differential capacitance with concentration of KNO_3 for polycrystalline antimony.

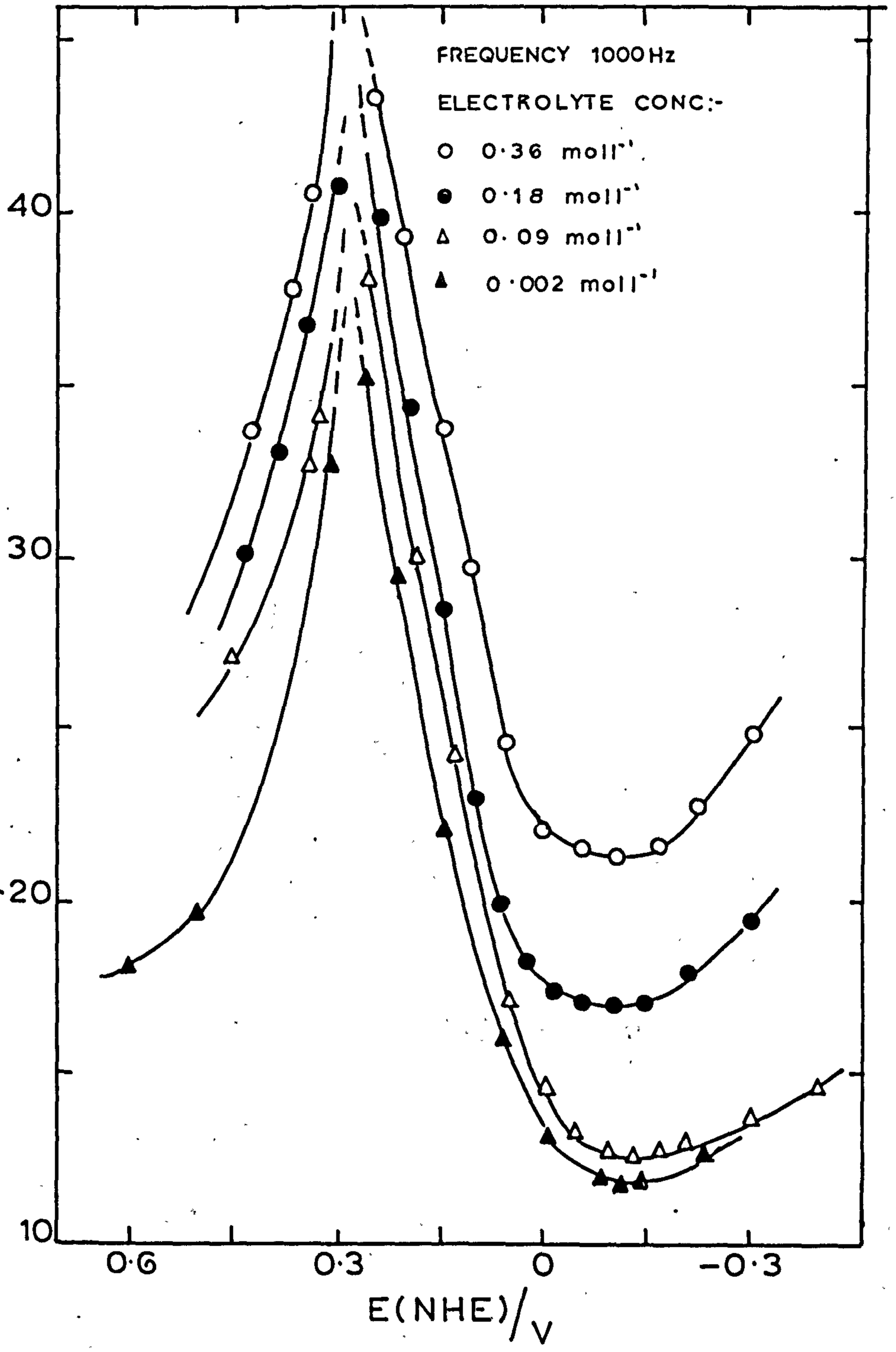

Fig 6 Variation of differential capacitance with concentration of HNO_3 for polycrystalline antimony.

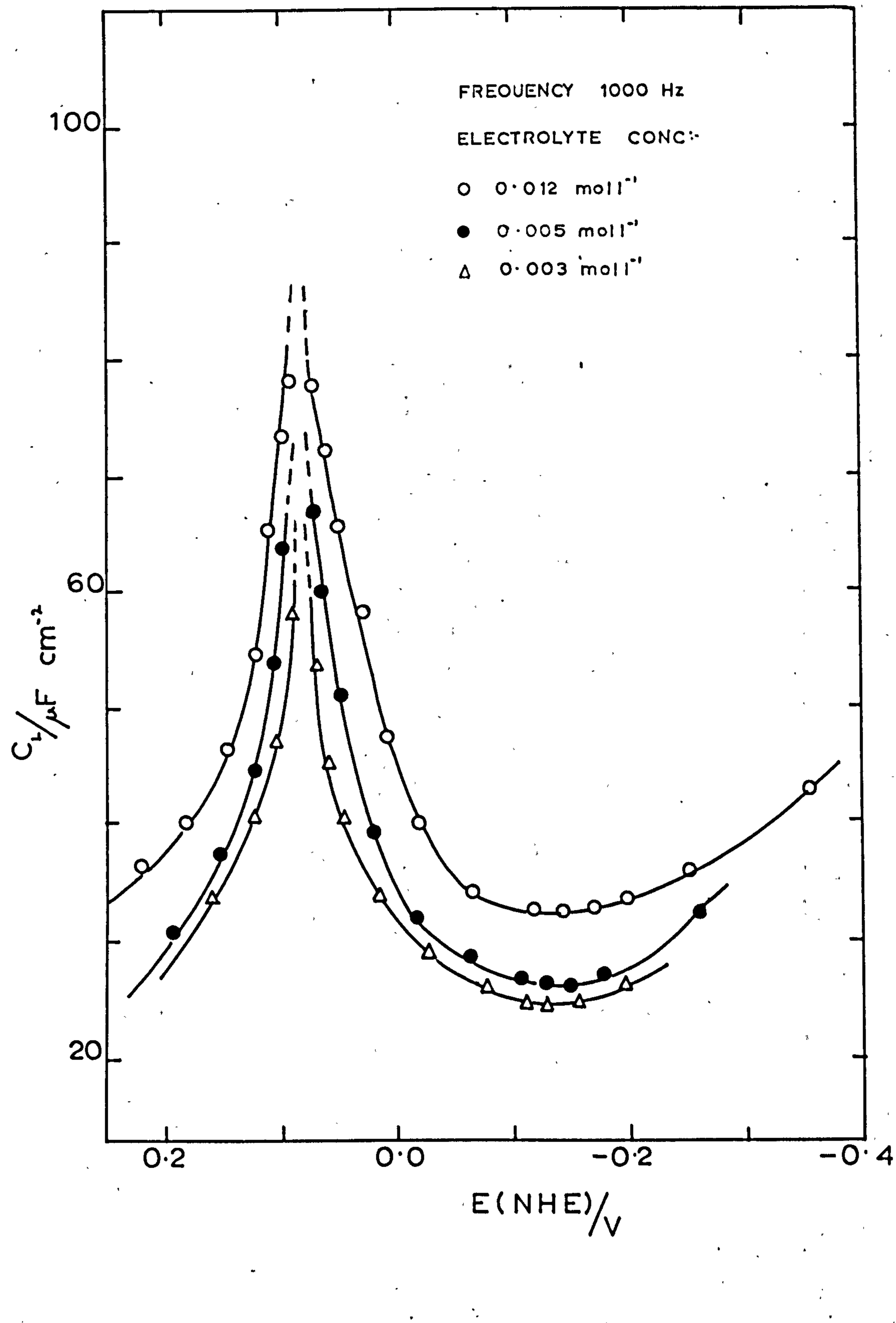

Fig 7 Variation of differential capacitance with concentration of KNO_3 electrolyte for Pb-Sb (4% Sb) alloy.

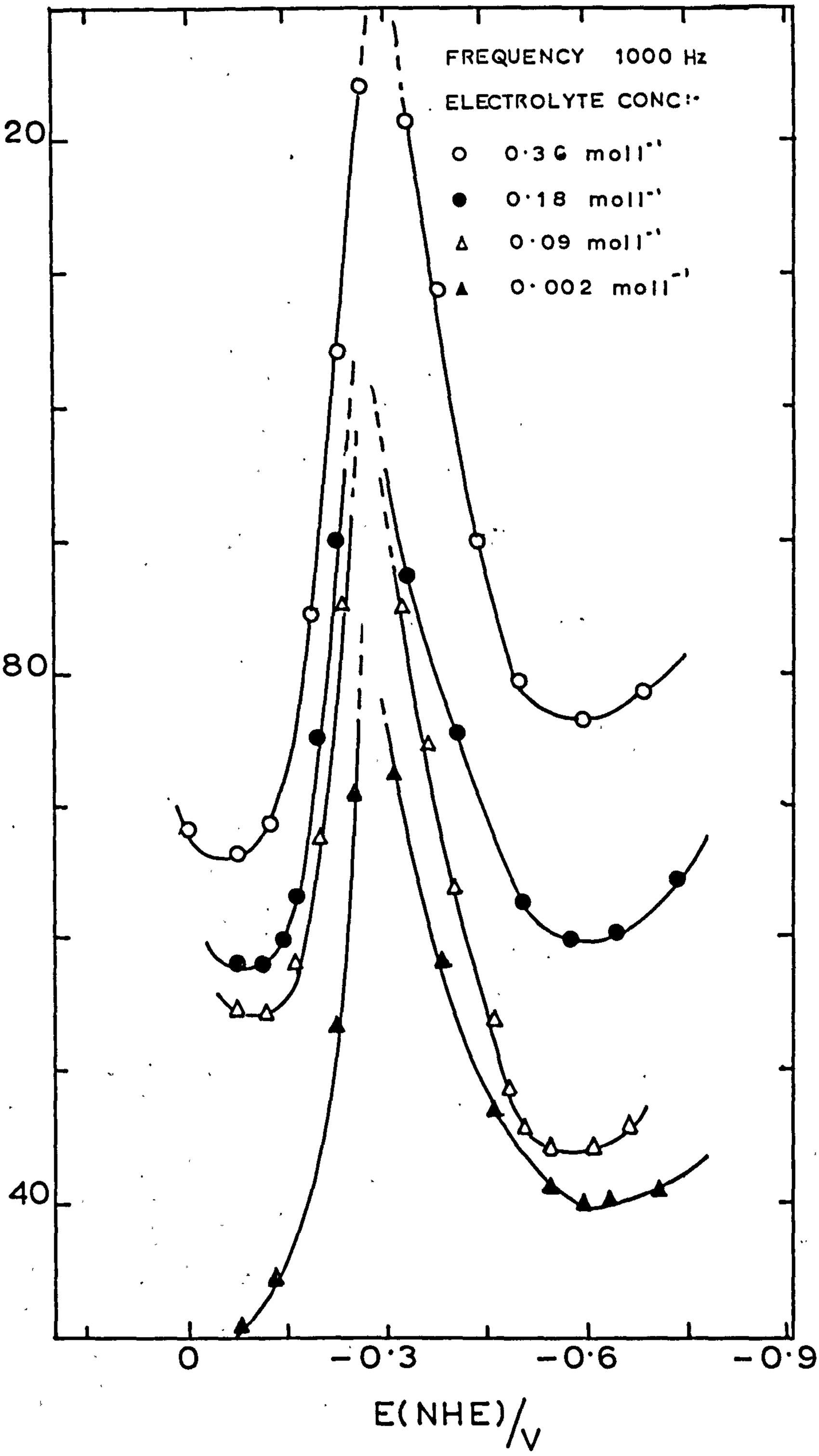

Fig 8 Variation of differential capacitance with concentration of HNO_3 for Pb - Sb (4% Sb) alloy.

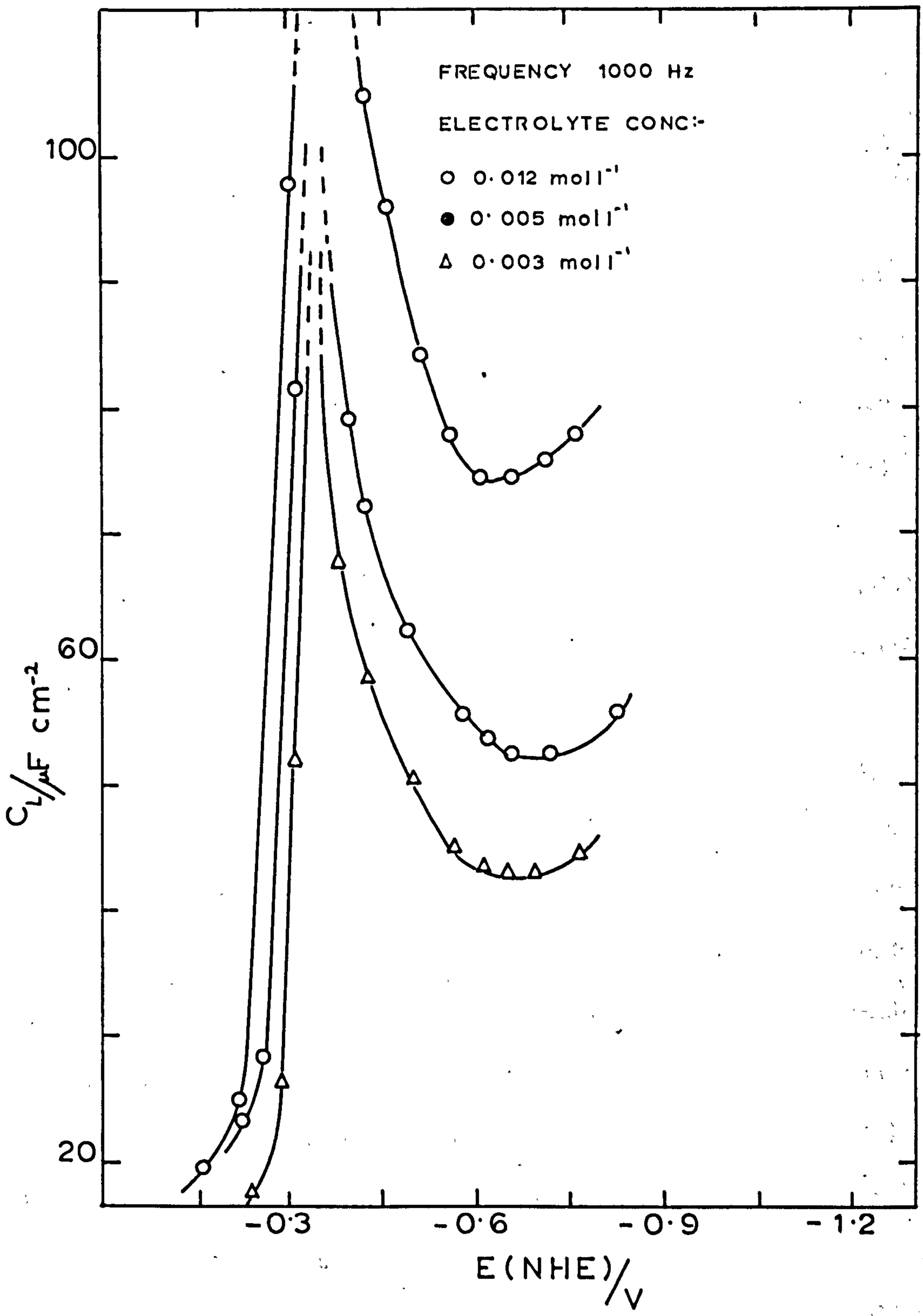

Pb rather than pure Sb. The negative extreme of the polarizable regions is determined by gas evolution and the positive extreme by lattice dissolution. A shift in the positive limit of the polarizable region to more negative potentials for Pb-Sb alloys, compared with pure Pb, is evidence of an Sb assisted lattice dissolution process, similar to the self-discharge phenomena observed in commercial lead-acid battery plates, according to equations of the type:-

$$(Pb\text{-}Sb) + NO_3^- + H_2O = \left[(Pb\text{-}Sb)\begin{matrix} OH \\ \\ NO_3 \end{matrix} \right] + H^+ + 2e \qquad (1)$$

It was not possible in the present experiments to formulate the exact composition of the products of lattice dissolution but, since the electrode capacitance was drastically and irreversibly reduced on the positive side of the potential of lattice dissolution, it was assumed that an insoluble product of basic nitrate was produced due to hydrolysis in the very dilute solution.

Further evidence for an Sb assisted Pb lattice dissolution process is obtained from the capacitance rise at positive potentials of figures 3 and 4 where Pb dissolution occurred at more negative potentials in the presence of Sb.

From the capacitance curves, figures 3 and 4, a capacitance minimum, the magnitude of which decreased with electrolyte concentration and characteristic of the pzc., was observed at -0.6 ± 0.02 V for pure Pb electrodes, in agreement with previous work (Appendix 7). Alloying Sb with Pb did not affect the position of the capacitance minimum however in both electrolyte solutions an increase in capacitance with Sb additions was observed. Reproducibility of the capacitance curves for Pb-Sb alloys was $\pm$ 10% about a mean compared and $\pm$ 5% for pure Pb and Sb. It is clear that Sb does not alter the position of the diffuse layer capacitance minimum characteristic of the Pb/aqueous solution interphase.

The metallurgical structure of the binary alloy, however, must be considered more

fully in connection with the observed capacitance magnitudes. In a binary system the eutectic mixture solidifies rapidly giving a solid containing small crystals. For Pb-Sb alloys, at Sb concentrations lower than the eutectic composition (13%), the solidification process is slow enabling large crystals of Pb (+ 2% Sb) to grow. An examination of the surface structure of the present "as cast" alloys bears this out, however, it may be that such examinations bear little relationship to the structure of the electrode surface when in contact with the electrolyte and polarized. Hence it is to be expected that the surface of the eutectic will have a high surface roughness. With decreasing Sb content the surface roughness will decrease reaching a minimum for pure Pb. The more rapid solidification process will engender a more heterogeneous constitution of the alloy. Both these factors are complementary and will favour a capacitance increase, due to greater surface roughness, with increasing Sb content up to the eutectic composition.

In contrast, it is well established that a certain amount of atomic diffusion occurs on the surface and within metals[288]. As a general rule diffusion becomes significant for an alloy when its temperature approaches or exceeds 0.4 of its melting point (in K) and is enhanced by solvation effects at the metal surface. For Pb (m.pt. $\sim$ 600 K) at room temperature diffusion is large giving a labile surface. For Pb-Sb alloys the melting point decreases with increasing Sb content until the eutectic composition is reached, consequently, increasing the Sb content would be expected to increase the atom diffusion giving a more labile and homogeneous surface and favouring a decreased capacitance. A further possibility is that the nitric acid etchant increasingly gave rise to a more localised attack as the Sb content of the range of alloys increased and consequently engendered a rougher surface. The possibility of preferential attack was tested for by varying the duration of the etch, however little change in capacitance was obtained by considerably prolonging the etching time (to 1 min.). A visual examin-

ation did not indicate any preferential attack in the case of a particular alloy composition.

It is clear from figures 3 and 4 that, for Pb-Sb alloys in aqueous solutions, the overriding factor in determining the magnitude of the capacitance is the surface heterogeneity and roughness factor caused by the rapid cooling process. Further evidence for this is found in the frequency dispersion of capacitance observed. A certain amount of dispersion was observed for Pb and Sb however for the Pb-Sb alloys the dispersion increased with Sb content being greatest for the alloy of the highest Sb content (12% Sb) thus evidencing an increasing surface roughness and electrode heterogeneity.

From the capacitance curves, figures 1 and 2, no evidence was found for SbH_3 formation at potentials of $\sim$ -0.5 V, as suggested by various workers. This confirms similar conclusions of Bushrod et al[282] for pure Sb in aqueous solutions.

APPENDIX 9. A STUDY OF THE DIFFERENTIAL CAPACITANCE OF POLYCRYSTALLINE GOLD IN AQUEOUS SOLUTIONS

Introduction

The gold/aqueous solution interphase has been studied by a number of workers[289-305] however, there is considerable disagreement regarding the position of the potential of zero charge, E_z. Reported values of E_z range from -0.47 to 0.5 V. Table 1 summarizes the previous work. The wide range of E_z values indicates that the double layer structure on gold electrodes in aqueous solutions may be complicated by oxide films and adsorption.

Studies concerning oxide formation and the anodic dissolution of gold in aqueous solutions have been reported[306-322], however, most of the work has been performed under acid conditions. In alkaline and neutral solutions there is a limited amount of such data[314,315,319]. Thermodynamically AuO_2 and Au_2O_3 can exist on gold electrodes under alkaline conditions[323] and the possibility of oxygen and OH^- adsorption has been discussed by a number of workers[318,320-322]. The absence of hydrogen adsorption was shown by Bauman and Shain[316].

Experimental

The test electrode (3.48×10^{-2} cm^2 superficial surface area) was prepared from 99.999% pure gold wire supplied by Johnson Matthey and Company and sheathed in polythene, good electrode/polythene adhesion observed throughout. Before each experimental run the electrode was mechanically polished on roughened glass using bidistilled water as a lubricant, immersed in nitric acid (50%) for 3 secs., washed with bidistilled water and placed in the test solution. The electrode was held on open circuit until stable impedance readings were obtained.

The electrolytic cell and experimental technique were as described in Chapter 3.

TABLE 1

Solution	Method	p.z.c. (volts)	Reference
1 N HCl	Calculations from work functions.	-0.45	303
0.1 N KCl 0.1 N HCl	Open circuit scrape	-0.06	296
2 N H_2SO_4	Calculation from work functions.	0.23	293
0.001 N $HClO_4$	Capacitance of single crystals.	(110) plane 0.24 (100) plane 0.19	292
0.001 mol l^{-1} $HClO_4$ and 0.001 mol l^{-1} $HClO_4$ + 1 mol l^{-1} $NaClO_4$	Organic adsorption.	0.3	294
0.001 mol l^{-1} $HClO_4$	Capacitance	0.17	299
0.1 mol l^{-1} $HClO_4$	Friction method.	0.1	299
0.01 mol l^{-1} $HClO_4$	Friction method.	0.15	299
1 N KNO_3	Deformation of wires.	0.43	289
0.02 - 0.0025 mol l^{-1} NaF	Capacitance of single crystals.	(110) plane 0.2 (100) plane 0.4 (111) plane 0.5	301
0.1 N NaF	Open circuit scrape.	0.15	296
0.1 mol l^{-1} KCl (pH = 7)	Open circuit scrape.	-0.09	295
1 N KCl	Friction and hardness measurements.	0.15	290
0.001 N KCl, 0.0005 N $La(NO_3)_3$	Crossed polarized metal threads.	0.05	291
0.1 N KBr 0.1 N NaBr	Open circuit scrape.	-0.24	296
0.1 N KI 0.1 N NaI	Open circuit scrape.	-0.47	296

Solution	Method	p.z.c. (volts)	Reference
0.001 mol l^{-1} $NaClO_4$	Capacitance	(pH3) 0.15 (pH4) 0.18	299
$NaClO_4$ (Various concs)	Organic adsorption.	0.37	299
0.02 N Na_2SO_4	Capacitance.	0.23	293
0.1 N Na_2SO_4 0.1 N Na_2SO_4	Open circuit scrape.	0.13	296
0.01, 0.005 and 0.0025 mol l^{-1} Na_2SO_4	Capacitance of single crystals.	(110) plane 0.1 (100) plane 0.02 (111) plane 0.45	300
0.0167 mol l^{-1} K_2SO_4	Capacitance.	0.1	297
0.1 N NaOH	Open circuit scrape.	-0.08	296

Results

Figure 1 shows typical faradaic current vs bias potential curves for the electrolytes investigated. The gold electrode is nowhere ideally polarizable however, there exists an experimental region in which faradaic current is negligible. The extent of the experimental polarizable region is ~ 0.9 - -0.7 V for H_2SO_4 and ~0.6 - -0.8 V for NaOH solutions. The negative extreme of the polarizable region is determined by H_2 evolution and the positive extreme by lattice dissolution.

The electrode/electrolyte contact times required for electrode impedance stability were ~ 30 mins. for both electrolytes, thereafter the electrodes remained reasonably stable for ~ 24 hrs. Electrodes forced to potentials outside the extremes of the polarizable region showed only slight hysteresis in both electrolytes, being more predominant at the negative extremity. Stable impedance measurements were rapidly established for small potential changes within the polarizable region at the test electrode, however, longer times were required when large capacitance changes occurred for small potential changes (i.e. in the region of the capacitance peak).

Figure 2 shows a series of differential capacitance vs bias potential curves for polycrystalline gold in aqueous NaOH electrolytes. The direction of the potential sweep had no significant effect on the form and magnitude of the capacitance curves. Impedance readings were reproducible to $\pm$ 3% about a mean. The capacitance curves showed a capacitance peak at ~ 0.4 V and a capacitance minimum, which intensified with dilution and was characteristic of the p.z.c., at -0.26 V. Also in figure 2 is shown a typical electrode resistance, R_E, vs bias potential curve which exhibits a rapid rise at the positive extreme of the polarizable region, a peak at ~ -0.25 V complementary to the observed capacitance min and a decrease in resistance at the negative extreme.

Figure 3 shows a typical frequency dispersion of the capacitance curves in aqueous NaOH solution. With increasing frequency, the peak observed in the capacitance

Fig 1 Faradaic current - bias potential curves for polycrystalline gold.

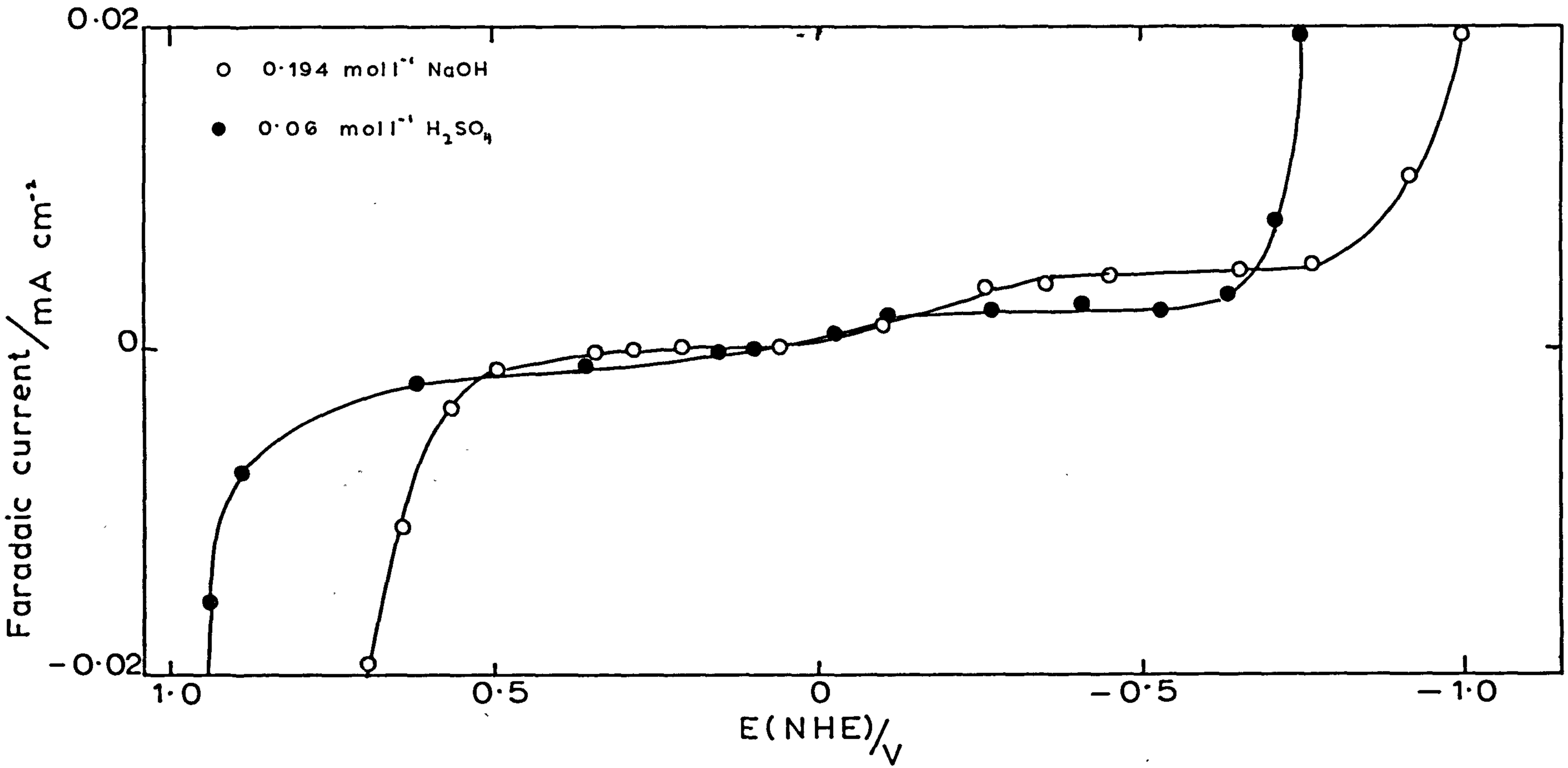

Fig 2 Differential capacitance-bias potential curves for polycrystalline gold in NaOH electrolyte.

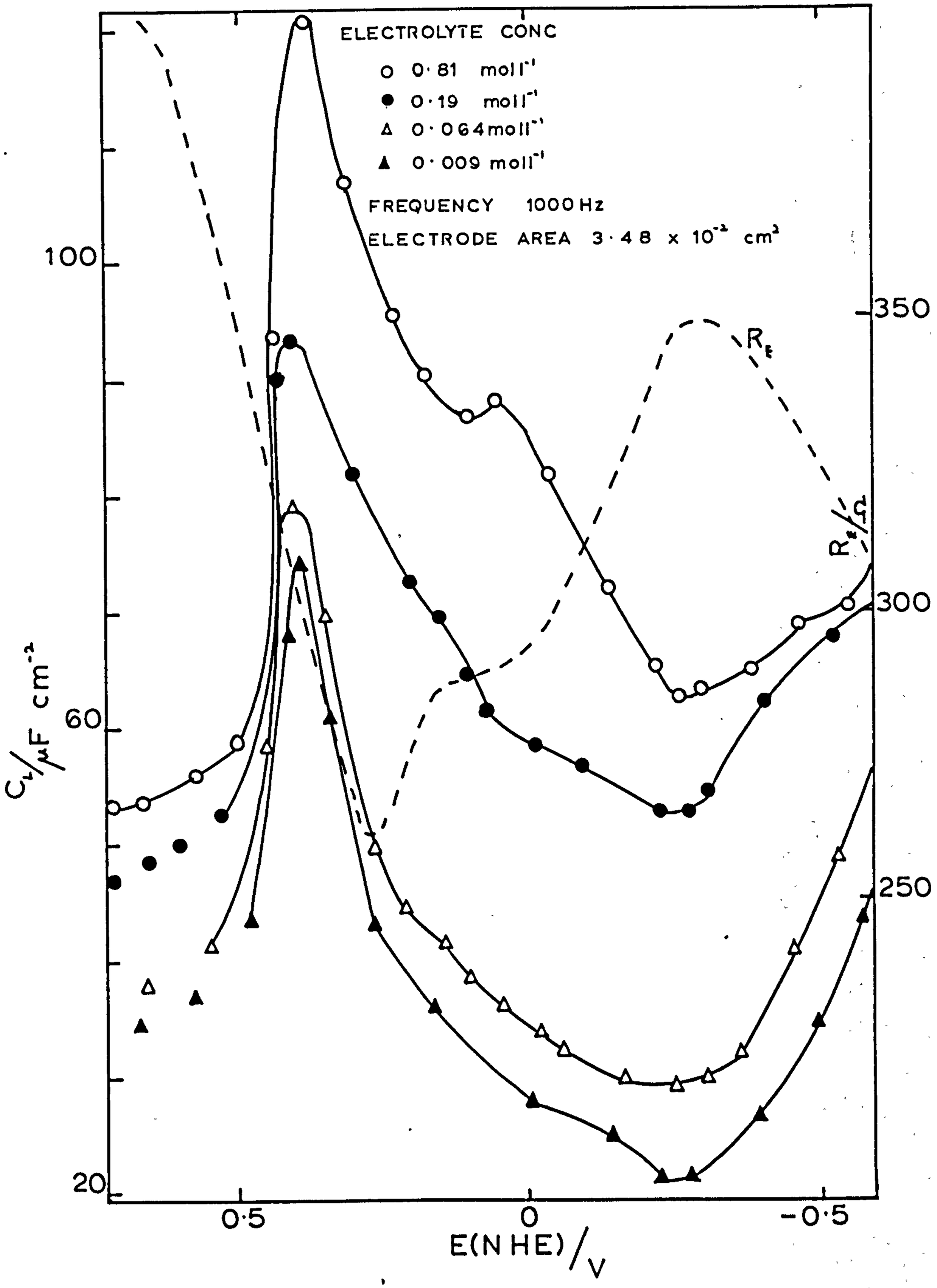

Fig 3 Dispersion of differential capacitance with frequency for polycrystalline gold in NaOH electrolyte.

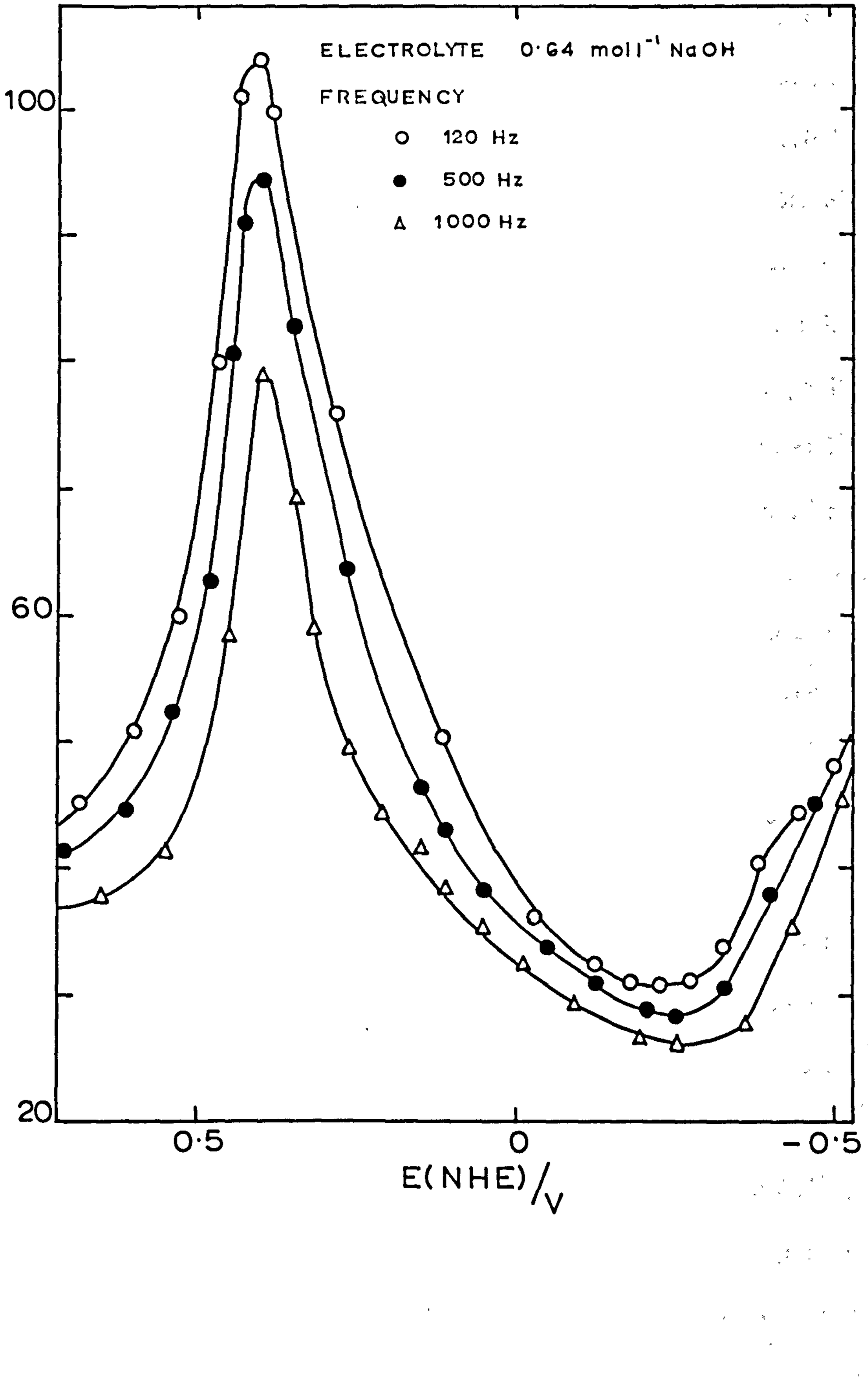

curves at ~ 0.4 V. increases in magnitude, however, for all frequencies a capacitance minimum was observed at -0.26 V for which the frequency dispersion tended to be minimal.

Figure 4 shows the influence on the differential capacitance curves of small additions of n-butylamine. In general, the magnitude of the capacitance was reduced at all potentials within the polarizable region, however, at the extremities of the experimental polarizable region, the values obtained resembled those in organic free NaOH solutions. The capacitance curves obtained when the potential was varied cathodically showed a capacitance peak at ~ 0.4 V, as in organic free NaOH solution, but were reduced in magnitude and displayed a very broad capacitance minimum at more negative potentials. Anodic potential sweeps gave capacitance curves showing a broad capacitance minimum throughout the whole polarizable region, no capacitance peak being observed at ~ 0.4 V. Further addition of n-butylamine > 0.03 mol l^{-1} had little effect on the capacitance curves. The starting potential of both anodic and cathodic potential sweeps were varied and, in the case of cathodic sweeps seemed to have little effect on the shape and magnitude of the curves, however, for the anodic sweeps with starting potentials > 0.3 V the capacitance peak could be observed whereas for starting potentials < 0.0 V no peak appeared.

Figure 5 shows a series of differential capacitance vs bias potential curves for polycrystalline gold in aqueous H_2SO_4 solution. The direction of potential sweeping had little effect on the shape and magnitude of the capacitance curves except that the small peak observed at ~ +0.15 V in the more concentrated solutions was more pronounced for cathodic sweeps. The capacitance curves were reproducible to $\pm$ 5% about a mean. All the curves showed a characteristic capacitance peak at ~ 0.8 - 0.85 V and a minimum, characteristic of the p.z.c. in H_2SO_4 solutions, at 0.33 V. Also on figure 5 is shown the electrode resistance, R_E, as a function of bias potential and is characterised by a rapid rise at both extremities of the polarizable region

Fig 4 Effect of addition of n-butylamine on differential capacitance curves for polycrystalline gold in NaOH electrolyte.

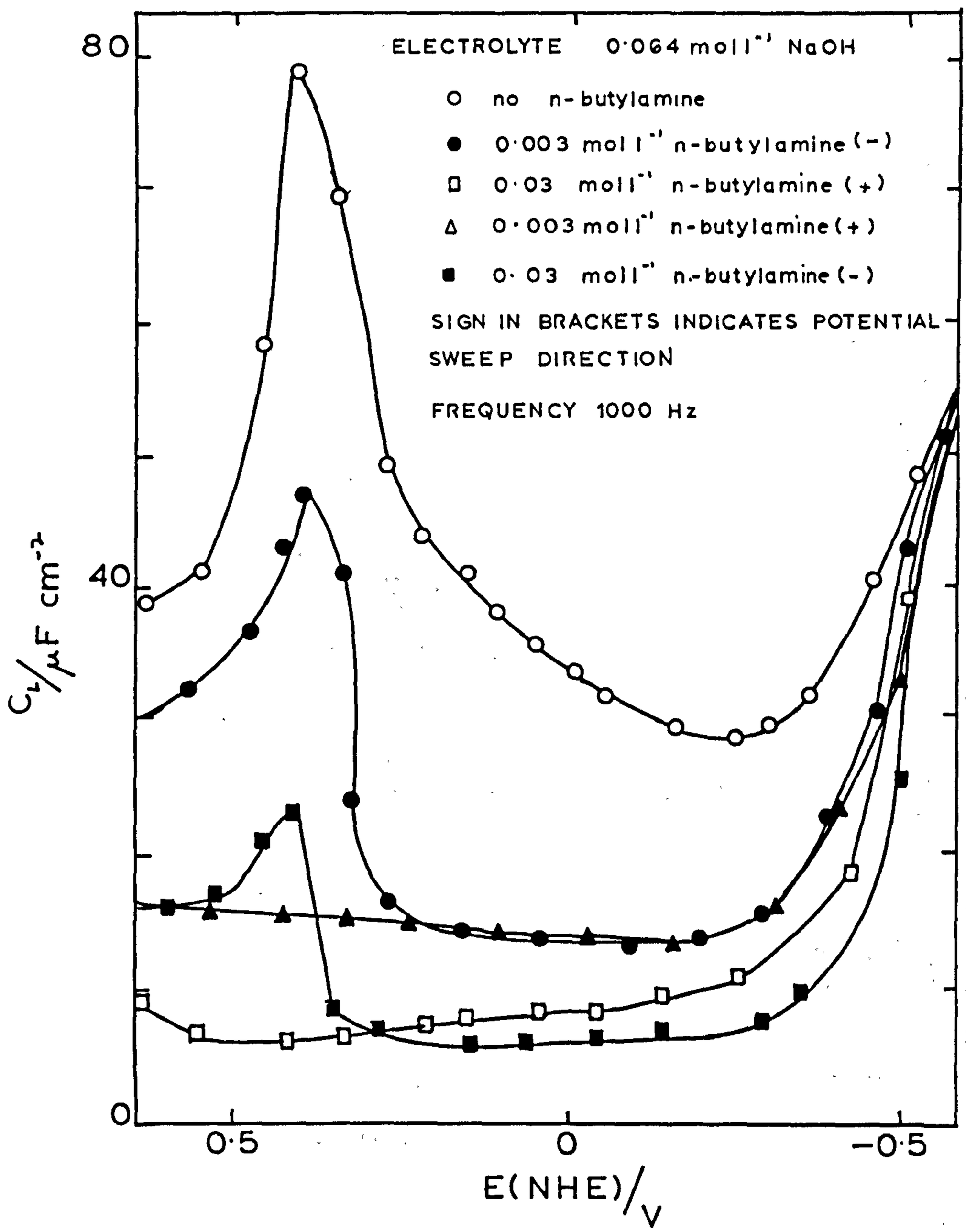

Fig5 Differential capacitance-bias potential curves for polycrystalline gold in H_2SO_4 electrolyte. Anodic potential sweeping.

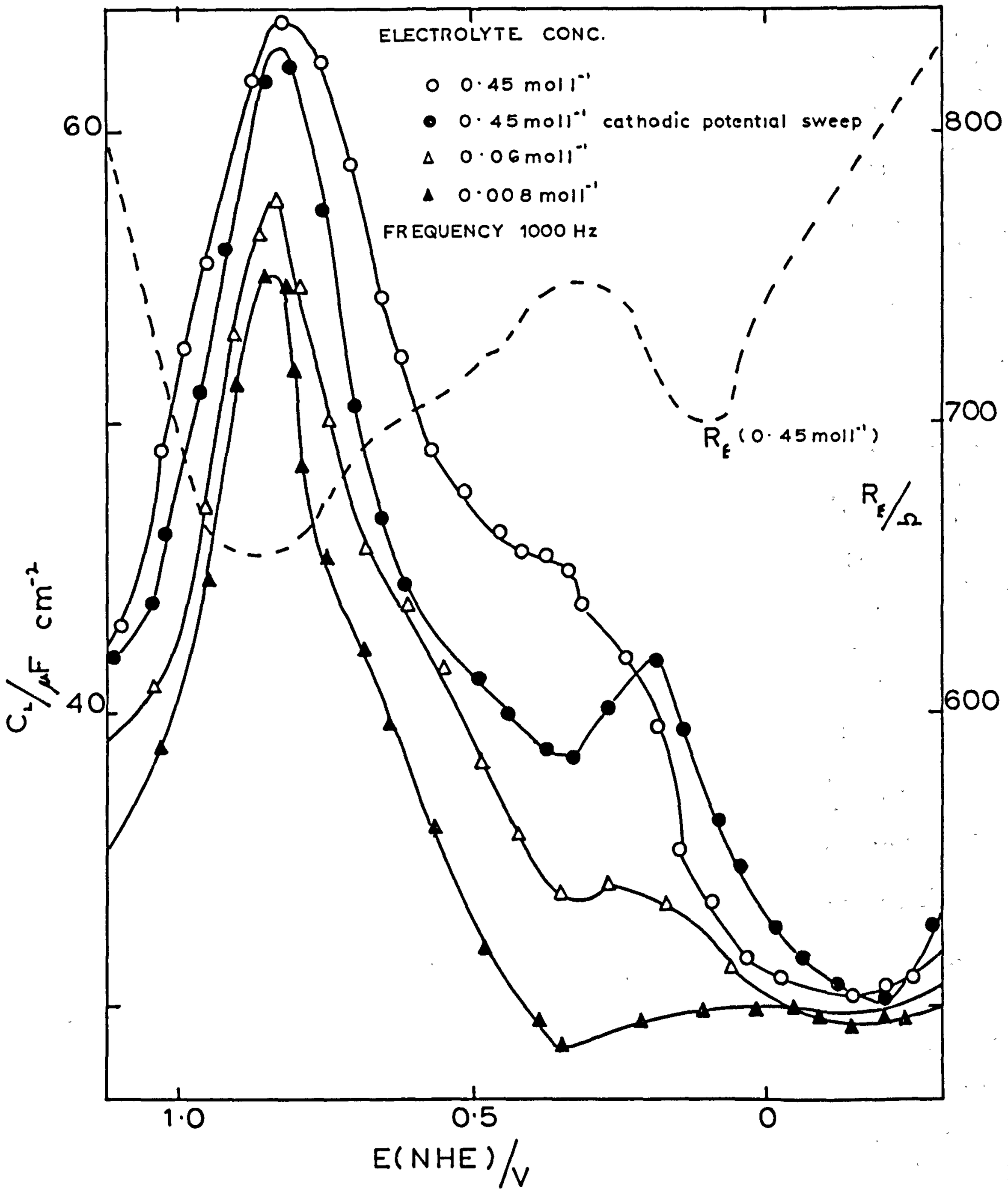

and a resistance peak at~ 0.3 V complementary to the capacitance minimum.

Figure 6 shows the influence on the differential capacitance curves of additions of n-butylamine. The curves show a progressive lowering of capacitance magnitude with concentration of n-butylamine, for potentials negative with respect to the p.z.c. up to 0.03 mol l^{-1} n-butylamine, thereafter further additions have no significant effect on the capacitance curves. At potentials positive to the p.z.c., a capacitance peak was observed at a potential corresponding to that of the capacitance peak observed in organic free H_2SO_4 solutions. The direction of potential sweeping and starting potential had little effect on the curves.

Discussion

The time stability of the electrode impedance, in all electrolytes, indicates that no chemical or structural changes occur at the surface within the polarizable region. The magnitude of the differential capacitance is similar to that observed for lead electrodes (Appendix 7) which has a low roughness factor and, from the small degree of frequency dispersion, a relatively smooth surface for the gold electrode is indicated.

The capacitance minimum in dilute NaOH solutions at -0.26 V is well removed from the value of E_z, 0.23 V, estimated from work function data[293]. In H_2SO_4 the p.z.c. occurs at 0.33 V which agrees well with previous work (cf. Table 1). Further indication of the p.z.c. in both electrolytes is given by the R_E curves for which values might be expected to reach a maximum at the p.z.c. due to solvent effects at the electrode. From figures 3 and 5 the R_E values vs bias potential reach a peak at potentials complementary to the capacitance data.

The large deviation of the diffuse layer capacitance minimum from the theoretical p.z.c. of gold in aqueous NaOH, indicates that the electrode/solution interphase is complicated by adsorption of anionic electroactive species, e.g. oxygen or OH^- ions. Similar adsorption was reported previously[318], however, from the present experiments

Fig6 Effect of addition of n-butylamine on differential capacitance curves for polycrystalline gold in H_2SO_4 electrolyte.

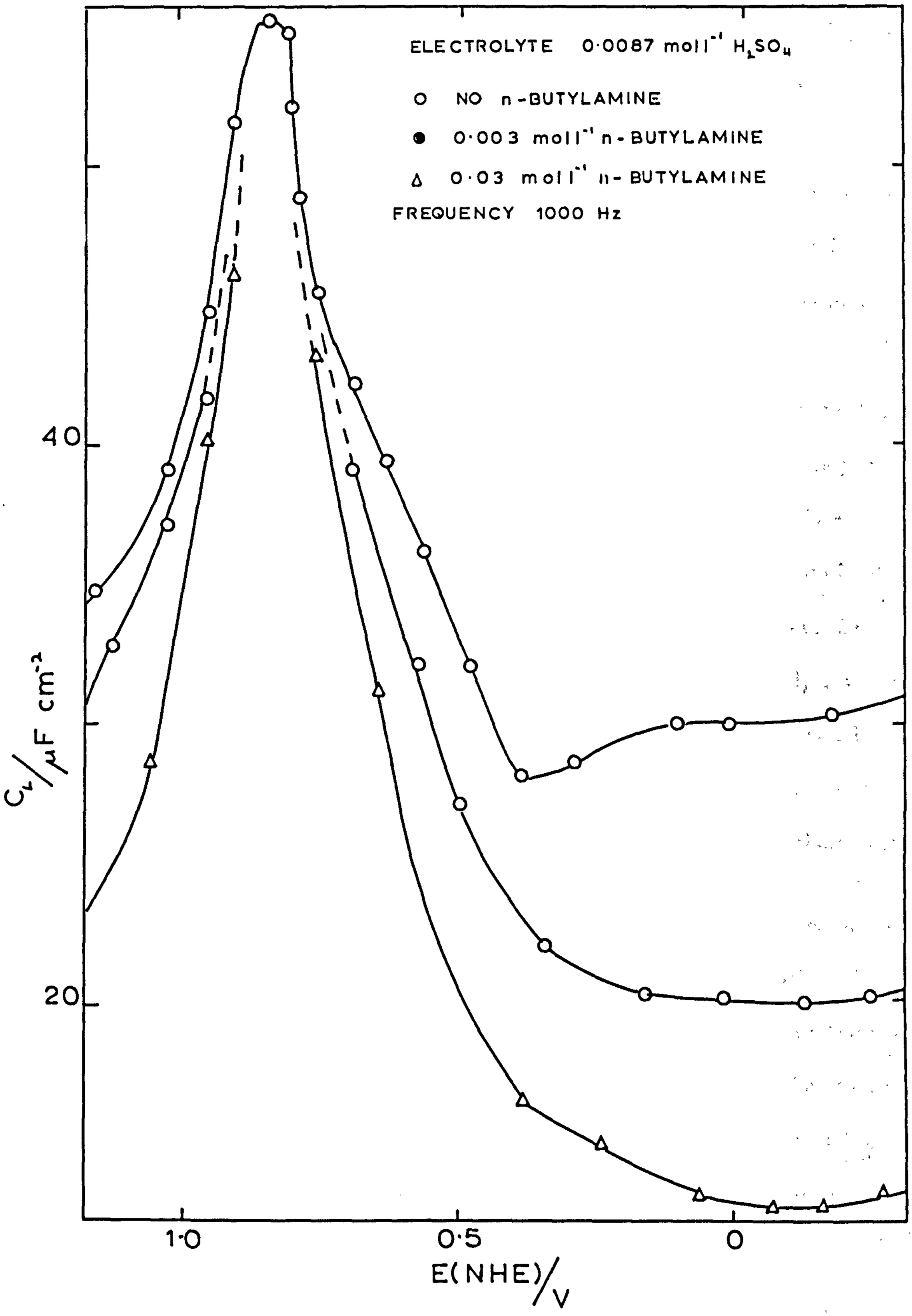

it cannot be ascertained to what extent OH^- ion adsorption is involved. From the constancy of the minimum in the capacitance curve with concentration of H^+ it seems probable that the dominant adsorbed species at the interphase is oxygen. In acid solutions the electrode interphase is relatively uncomplicated by adsorbed species.

The capacitance peaks, ~ 0.4 V and ~ 0.8 V in figures 2 and 5 are associated with adsorption of oxygen at the interphase prior to formation of an insoluble gold compound* 318,320-322, which causes the capacitance decrease at the positive extreme of the polarizable region. Confirmation of adsorption at these potentials is evidenced by the increased frequency dispersion of the capacitance in these potential regions (figure 3).

The adsorption of n-butylamine from NaOH shows differing behaviour depending on the direction of the potential sweeps. For cathodic sweeps the capacitance peak, associated with oxygen adsorption, is unaltered in potential by adsorption of n-butylamine. For anodic sweeps, however, such a peak is absent indicating an inhibition of the oxygen adsorption due to an adsorbed layer of organic molecules. By starting potential sweeps at positive potentials the gold electrode is partially covered with a layer of $Au(OH)_3$ and, on moving to more negative potentials, this layer is reduced allowing adsorption of the oxygen at the electrode. By starting the sweep from potentials negative of the polarizable region it is unlikely that negatively charged ions

---

*Footnote The exact constitution of the insoluble gold film could not be determined by these experiments but other workers have suggested the formation of $Au(OH)_2$ followed by oxidation to Au_2O_3 at more positive potentials. Impedance measurements taken at more positive values did not show any evidence for a second process, and therefore the initial insoluble $Au(OH)_3$ must cover the electrode with an insoluble layer which is further oxidised to Au_2O_3 and the gold is not directly oxidised to Au_2O_3 itself.

will initially exist in the adsorbed state at the electrode and, by moving to more positive potentials, oxygen species are partially excluded from the electrode surface by a strongly held layer of adsorbed b-butylamine.

In the case of NaOH solutions adsorption of n-butylamine is greatest around the potential of the diffuse layer minimum which is further confirmatory evidence for OH^- adsorption since it is to be expected that neutral organic molecules would be adsorbed to a greater extent where the charge on the electrode is zero. For acid solutions the formation of n-butylamine ions causes maximum adsorption at potentials negative of the p.z.c. This is borne out in the differential capacitance curves which show little adsorption of n-butylamine at potentials positive of the p.z.c.

APPENDIX 10. A STUDY OF THE DIFFERENTIAL CAPACITANCE OF POLYCRYSTALLINE PLATINUM IN AQUEOUS SOLUTIONS

Introduction

Platinum electrodes are frequently used in a wide variety of inorganic and organic synthesis, e.g. a large number of organic compounds are capable of being oxidised at platinum electrodes. It is usually assumed that the platinum behaves as an inert electrode simply providing a means of transferring electrons to and from the reactants, however, recently it has been shown that the platinum electrode is readily oxidised. Also it is only relatively recently that the control of the electrode potential in organic electrode reactions has been considered. The electrode potential, apart from determining the relative adsorption of hydrogen and oxygen species, is important in determining the adsorption of the organic reactants and products. (The adsorption depending more on the potential relative to the potential of zero charge rather than the exact potential.) Consequently, an exact knowledge of the platinum/aqueous solution interphase is important since this enables deduction of the various forces involved and the mode of approach of molecules to the electrode.

The structure of the electrical double layer at the platinum/aqueous solution interphase has been studied by a number of workers[324-375], however, poor agreement has been observed between the experimental results of different workers which has led to difficulties in the interpretation of such measurements in terms of double layer structure. The majority of interphase studies have involved acid electrolyte solutions and attempts to explain the differential capacitance measurements at platinum electrodes, by comparison with complementary results for mercury, have not been conclusive.

The surface of a platinum electrode is strongly influenced by a number of factors which include electrode pretreatment and preparation. When in aqueous sol-

utions further complications arise due to adsorption of hydrogen, oxygen and solution species. Consequently reported capacitance measurements, and the p.z.c. derived from these, must always be looked at with respect to the experimental conditions. Table 1 summarizes data reported by previous workers using a number of different experimental techniques. The reported values of the p.z.c. show quite a wide potential variation. The position of the p.z.c. is important since it determines the magnitude and sign of the charge on the electrode and consequently controls the adsorption of species and the mechanism of adsorption at the electrode to a certain extent.

The magnitude of the differential capacitance for the platinum/aqueous solution interphase in the absence of adsorption has been reported as 18 F cm^{-2} [242,376] however, Gillman[377] suggested that in aqueous solution the platinum electrode becomes partly covered with organic impurity present in the solution which results in a reduced capacitance value. Trasatti[378] showed that the capacitance decreases with time for platinum electrodes in $HClO_4$ solutions, the decrease depending upon temperature and solution stirring, and they suggested that this may be due to a surface rearrangement of the platinum atoms although they did not completely ignore the possibility of adsorption.

Studies concerning the formation and reduction of adsorbed films on platinum in aqueous solution have been numerous. Extensive reviews of the topic are available [380-384]. In both acid and alkaline solutions potential sweep measurements[385] indicate an irreversibility of the oxygen film formation/dissolution process but reversible hydrogen adsorption.

The faradaic impedance technique is suitable for investigating electrode surface phenomenon and in this study is used to investigate the behaviour of platinum electrodes in aqueous NaOH and H_2SO_4 solutions. The influence of pH and organic material are also investigated.

TABLE 1

Solution	Method	p.z.c. (V)	Reference
0.1 mol l^{-1} $HClO_4$	Immersion	0.48 ± 0.04	370
0.001N H_2SO_4	Acoustical	0.21 ± 0.01	356
0.1N H_2SO_4	Friction	0.3	332
0.2 x 10^{-4}N H_2SO_4	Double layer repulsion	0.16	329
0.01N H_2SO_4 0.005N H_2SO_4	Capacitance	0.35	337
0.001N H_2SO_4 0.01N H_2SO_4	Capacitance	0.18 ± 0.02	349
1N H_2SO_4	Capacitance	0.11 - 0.2	354
1N H_2SO_4 10^{-3} H_2SO_4	Capacitance	0.22 - 0.33	367
2 x 10^{-5}N HCl	Double layer repulsion	0.19	329
1N HCl	Capacitance	0.47	336
$HClO_4$ + $NaClO_4$	Capacitance	0.2	365
0.005N $HClO_4$ + xN $NaClO_4$	Immersion	0.1	362
$NaClO_4$ + $HClO_4$ and $NaClO_4$ + NaOH	Capacitance	linear function of pH, eg (pH 2.5) 0.47 (pH 11.2) -0.11	371
0.1N $HClO_4$ 0.01N $HClO_4$ H_2 present 0.1N $HClO_4$	Friction	0.5 0.42 0.24	371

Solution	Method	p.z.c. (V)	Reference
0.1N $HClO_4$	Adsorption	(pH 3) 0.48 (pH 12) -0.07	371
0.003N ($HClO_4$ + NaOH) and 0.003N ($NaClO_4$ + NaOH)	Capacitance	(pH 2.8) 0.41 (pH 8.1) 0.072 (pH 11.2) -0.111	357
0.1N Na_2SO_4 + 0.01N H_2SO_4 1N NaCl + 0.01N HCl 1N NaBr + 0.01N HBr 1N NaBr + 0.05N NaOH	Adsorption	0.11 0.06 -0.02 -0.26	327
0.001N Na_2SO_4 + 0.001N H_2SO_4	Adsorption	0.18	358
0.001N Na_2SO_4 + 0.001N H_2SO_4	Adsorption	0.18	351
1N Na_2SO_4	Contact angle	0.28	324,325
1N Na_2SO_4 (pH acid)	Adsorption	0.11	326
0.02N Na_2SO_4	Capacitance	(pH 2) 0.48 (pH 7) -0.21	341
0.1N Na_2SO_4	Capacitance	0.22	344
0.01N and 0.001N HCl 0.003 - 0.00001N $MgSO_4$ 0.001N H_2SO_4 0.001N $ZnCl_2$	Double layer repulsion	0.2 V	347
0.001N NaF + 0.001N H_2SO_4 0.001N Na_2SO_4 + 0.001N H_2SO_4 0.001N NaCl + 0.001N HCl 0.001N NaBr + 0.001N H_2SO_4	Adsorption	0.18 0.18 0.14 0.04	351

Solution	Method	p.z.c. (V)	Reference
0.005N NaI + 0.005N H_2SO_4 0.01N Cs_2SO_4 + 0.01N H_2SO_4 0.018N Cs_2SO_4 + 0.002N H_2SO_4	Adsorption	-0.5 0.19	351
0.01N $CdSO_4$ + 0.1N H_2SO_4 0.01N $CdBr_2$ + 0.1N H_2SO_4 0.01N CdI_2 + 0.1N H_2SO_4	Adsorption	0.65 0.45 0.01	358
0.005N Cs_2SO_4	Adsorption	(pH 2.7) 0.18	346
0.1N K_2SO_4 (pH 7) 0.0N KI	Open circuit scrape	0.05 -0.51	366
	Calculated from work function data	0.6	350,353

Experimental

The electrolytic cell, electrolyte purification and experimental technique were described in Chapter 3. The test electrode was of 99.999% pure platinum rod (4.9×10^{-2} cm^2 superficial area) supplied by Johnson Matthey and Company Limited, sealed into glass. At the commencement of each experimental run the test electrode was mechanically polished on silicon carbide paper and roughened glass lubricated with bidistilled water, chemically etched in concentrated sulphuric acid washed thoroughly with bidistilled water and test solution then placed in the cell. Reproducibility of the impedance measurements and time stability was taken as a criteria of electrode cleanliness. The electrode was held on open circuit until stable impedance measurements were obtained.

A number of different electrode pretreatments[387], as applied to the platinum electrode, have been used in the past reported work. Such procedures have ranged from immersion in strong dichromatesulphuric acid solutions which was found to oxidise the electrode, to alternate cathodic and anodic polarisation of the test electrodes before immersion in the test electrolyte solution. In the present study the most reproducible results were obtained by chemically etching the electrode in conc. H_2SO_4.

Results

Figure 1 shows typical faradaic current - bias potential curves for polycrystalline platinum electrodes in aqueous NaOH and H_2SO_4 solutions. Ideal polarizability was never obtained, however, there existed an experimental region in which the system approached ideal polarizability. The extent of the experimental polarizable region was ~ 0.9 --0.5 V for NaOH solutions and ~ 1.5 --0.3 V for H_2SO_4 solutions. In both electrolytes the negative extremity was governed by hydrogen adsorption/evolution of reactions of the type:-

Fig 1 Faradaic current - bias potential curves for polycrystalline platinum in NaOH and H_2SO_4 electrolytes.

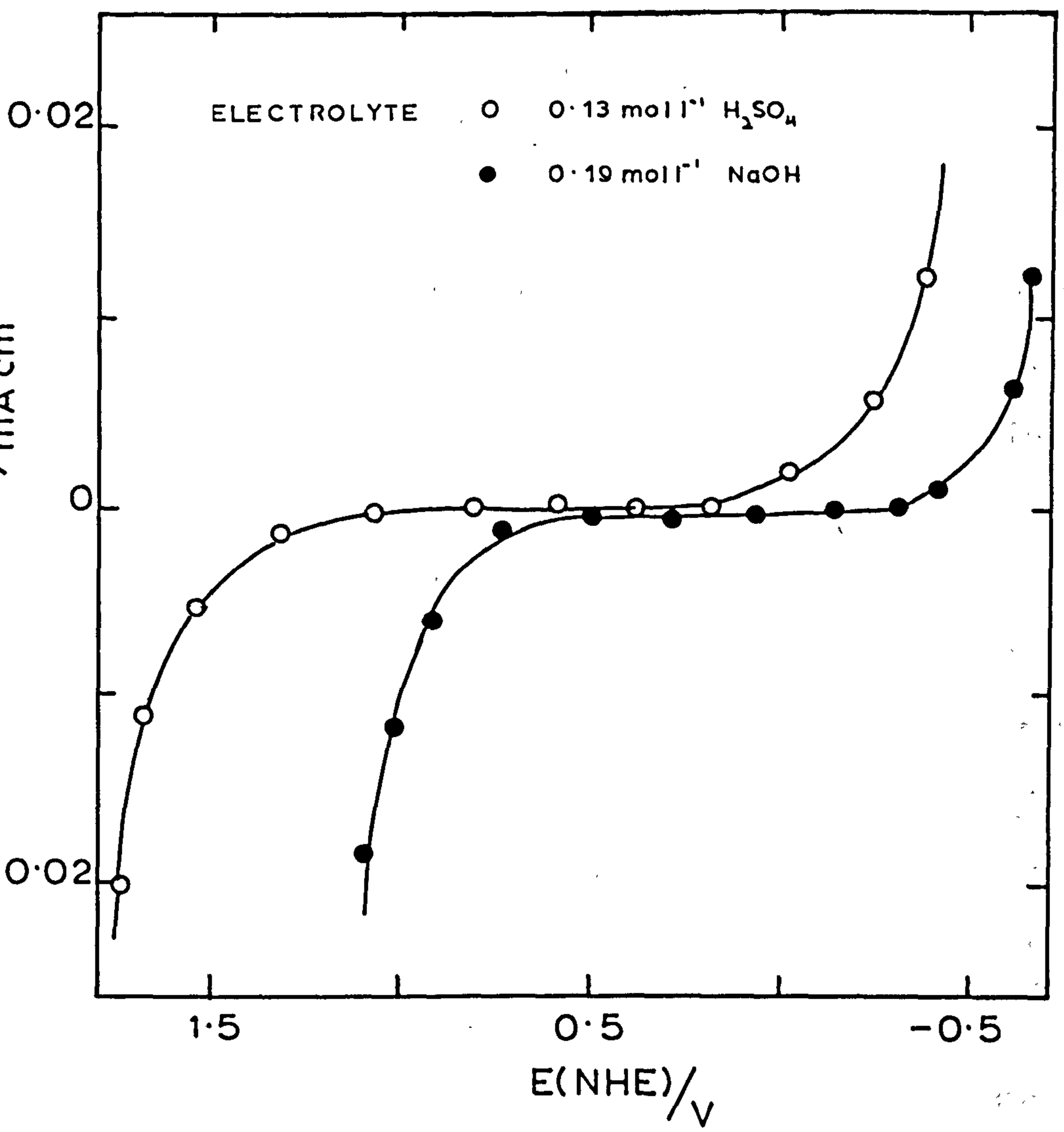

$$H^+ + e \rightleftharpoons H_{ads} \quad (1)$$

$$H_{ads} + H_2O \rightleftharpoons H_3O^+ + e \quad (2)$$

The positive extremity was governed by oxygen adsorption and film formation which may be represented by equations of the type:-

$$O^- + e \rightleftharpoons O_{ads} \quad (3)$$

$$O_{ads} + H_2O + 2e \rightleftharpoons 2\,OH^- \quad (4)$$

Figures 2 and 3 show a series of differential capacitance curves for polycrystalline platinum in aqueous NaOH solutions (figure 2 - positive potential sweeping and figure 3 negative potential sweeping.)

The curves for positive potential sweeping, figure 2, show a capacitance peak at ~ 0.3 - 0.35 V and a minimum, which intensified with dilution, at - 0.34 V Complementary results for negative potential sweeping, figure 3, showed a capacitance peak at ~ - 0.05 - -0,1 V and a minimum at - 0.34 V. The positively swept curves also show an arrest in the curves at ~ -0.15 V.

The electrode/electrolyte contact time required for electrode impedance stability was ~ 45 mins. in both solutions thereafter the electrodes remained reasonably stable (for times> 12 hrs.) Chemically etched electrodes were found to give the best stability and reproducibility. Capacitance measurements made for small electrode/electrolyte contact times showed a progressive decrease in magnitude until the stable values were obtained. Reproducibility of the capacitance curves was $\pm$ 5% about a mean. Electrodes forced to potentials outside the experimental polarizable region showed a small amount of hysteresis at the positive extremity but at negative potentials the hysteresis was more severe and quite an appreciable amount of time was required

Fig 2 Differential capacitance - bias potential curves for polycrystalline platinum in NaOH electrolyte. Anodic potential sweeping.

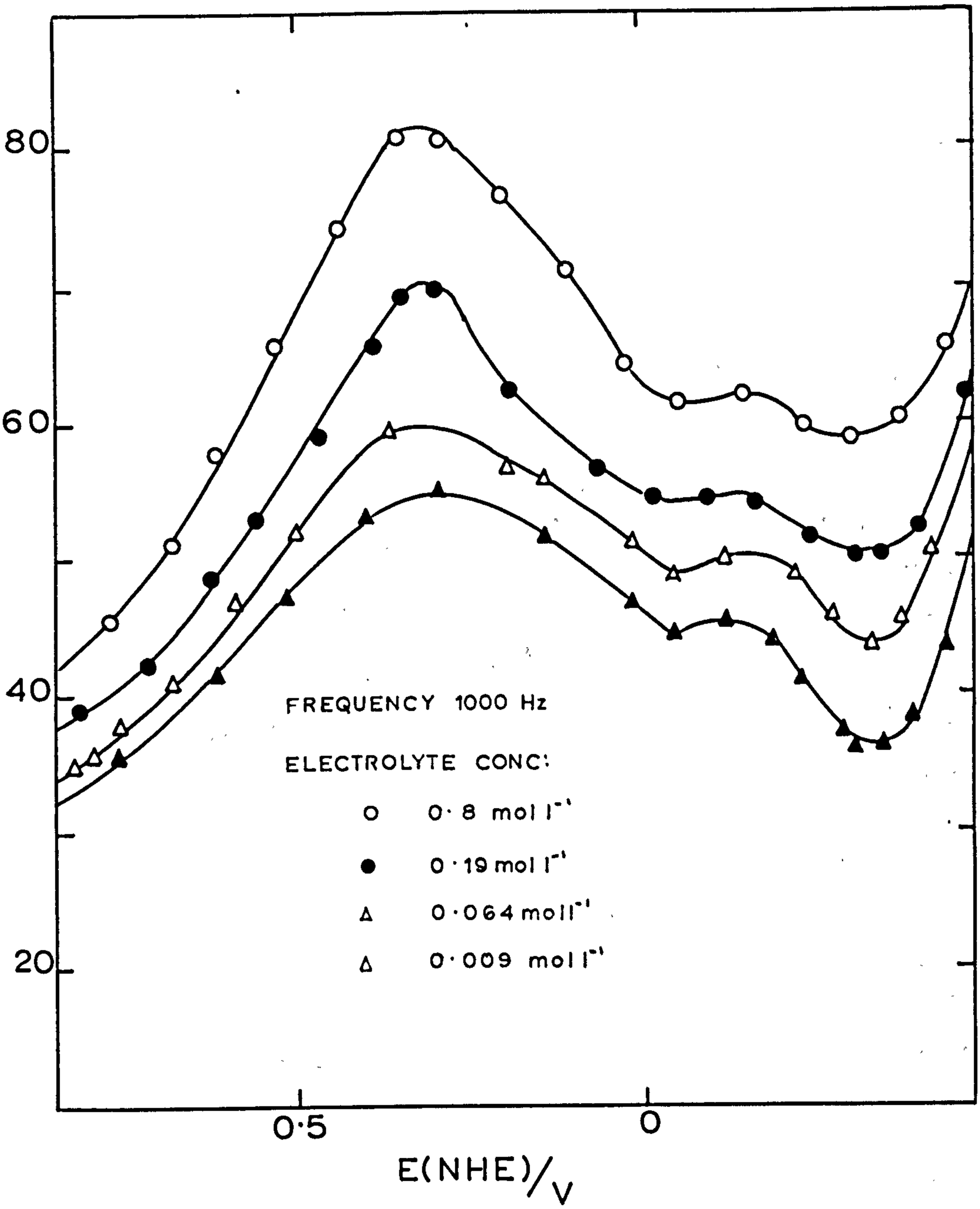

Fig 3 Differential capacitance - potential curves for polycrystalline platinum in NaOH electrolyte. Cathodic potential sweeping

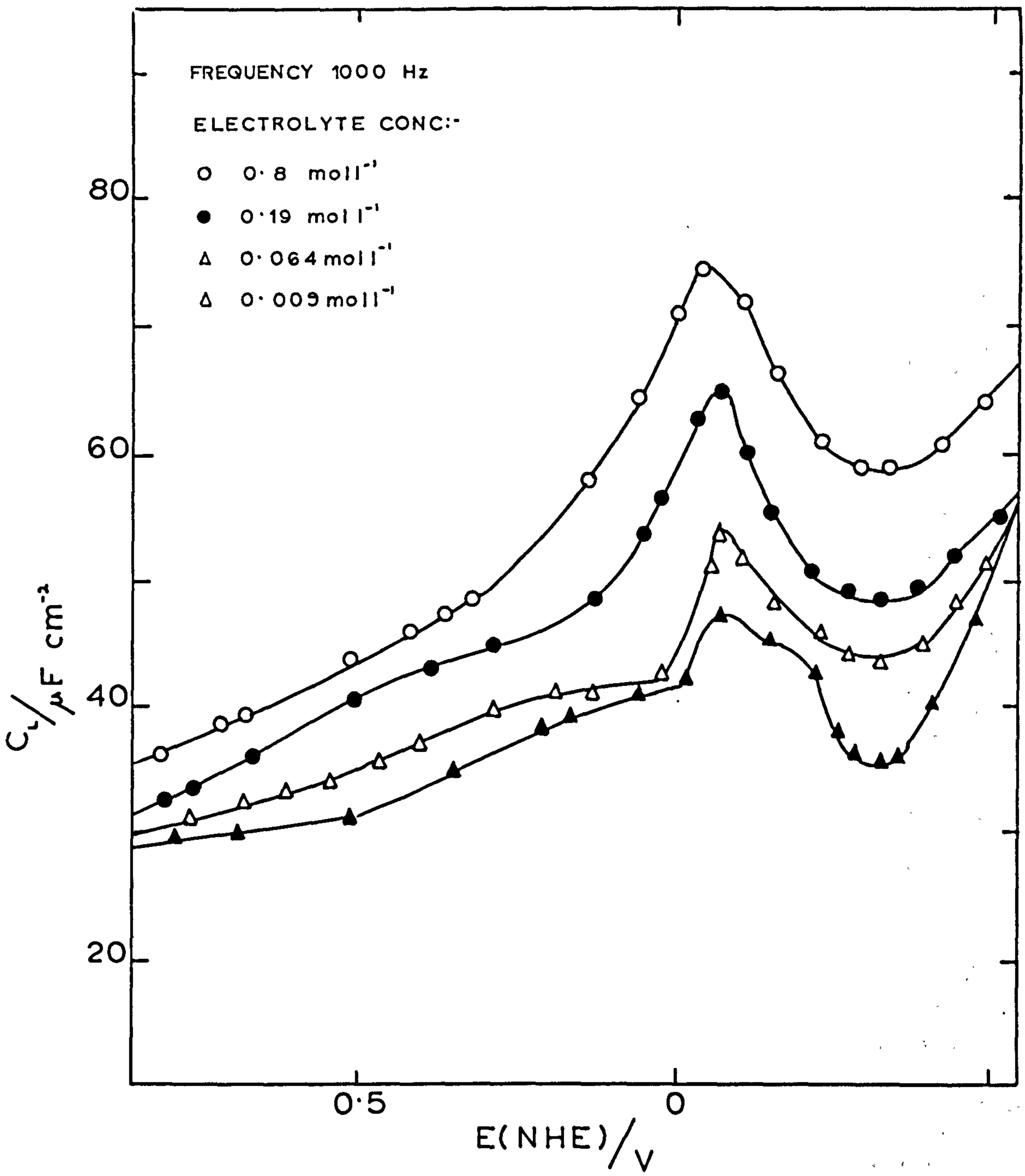

before the electrodes returned to their original condition. For small potential changes within the polarizable region impedance readings rapidly reached equilibrium but when large capacitance changes occurred for small potential changes the time to reach equilibrium was sometimes of the order of 15 mins.

Figure 4 shows a typical frequency dispersion of the positively swept capacitance curves. Frequency dispersion was largest in the potential region neighbouring the capacitance peak and smallest near the capacitance minimum. Complementary negatively swept curves showed similar behaviour.

Figures 5 and 6 show a series of positively and negatively swept differential capacitance-bias potential curves for polycrystalline platinum in NaOH solutions containing n-butylamine. These show a broad capacitance minimum, capacitance magnitudes decreasing with addition of n-butylamine up to 0.03 mol l^{-1} after which further additions had little apparent effect on the capacitance curves.

Capacitance values approached those obtained in organic-free NaOH solutions only at the extremes of the polarizable region. The negatively swept curves, figure 6, were similar in shape to those obtained in organic-free NaOH solutions but showed a considerable decrease in capacitance. Maximum adsorption occurred at potentials neighbouring the potential of the capacitance minimum.

Figures 7 and 8 show a series of differential capacitance vs bias potential curves for polycrystalline platinum in aqueous H_2SO_4 solutions. The positively swept curves show a capacitance peak at ~ 0.75 - 0.8 V and a minimum, which intensified with dilution, at 0.56 V. Complementary negatively swept curves showed a capacitance peak at ~ 0.65 - 0.7 V, a less well pronounced maximum at 0.9 V and a minimum at 0.56 V. Electrode stability and electrode/electrolyte contact times required to give stable impedances were similar to those for NaOH solutions, however, hysteresis for potential excursions negative of the polarizable region was more marked

Fig 4 Typical frequency dispersion of capacitance for polycrystalline platinum in NaOH electrolyte. Anodic potential sweeping

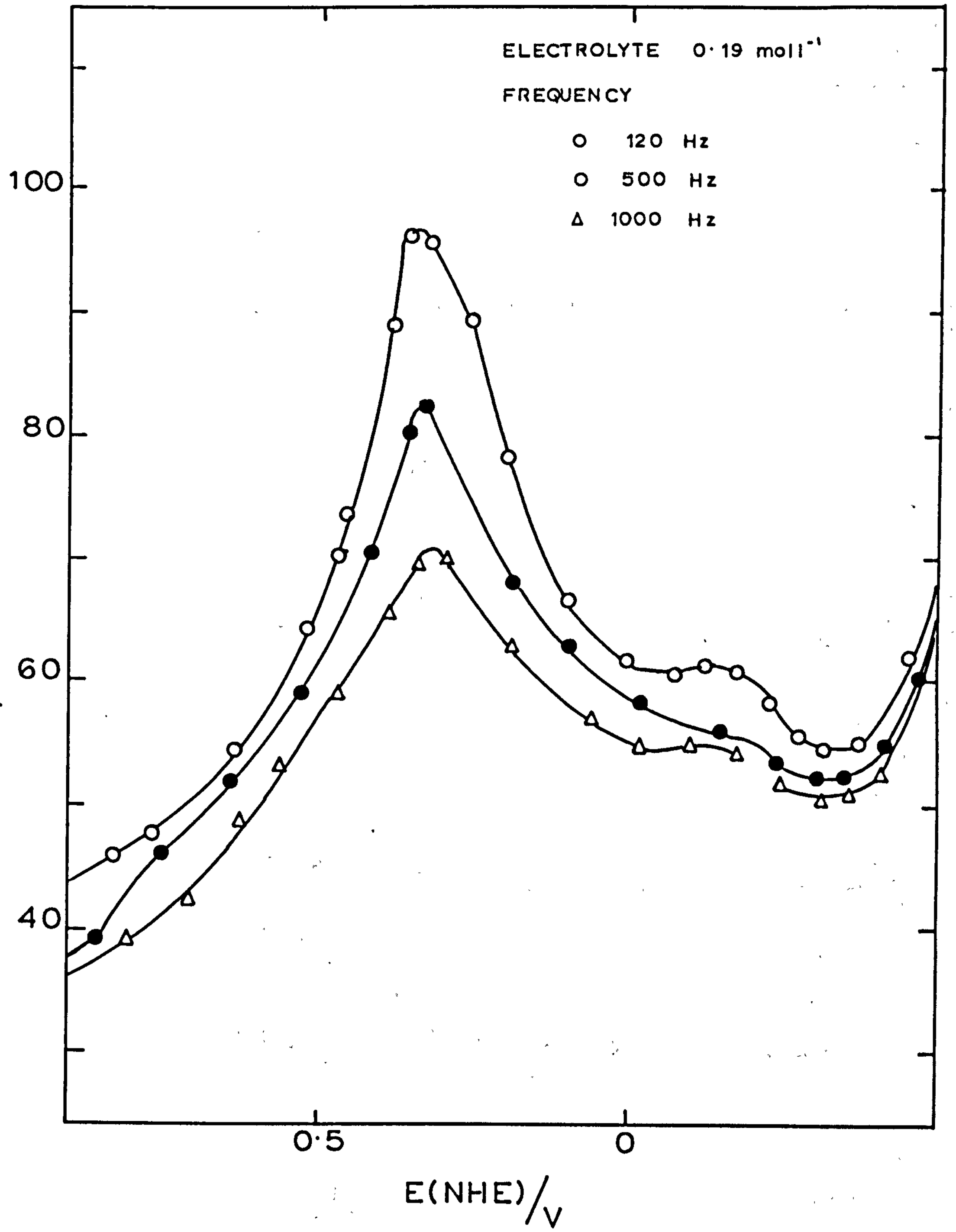

Fig 5 Effect of addition of n-butylamine on differential capacitance curves for polycrystalline platinum in NaOH electrolyte. Anodic potential sweeping.

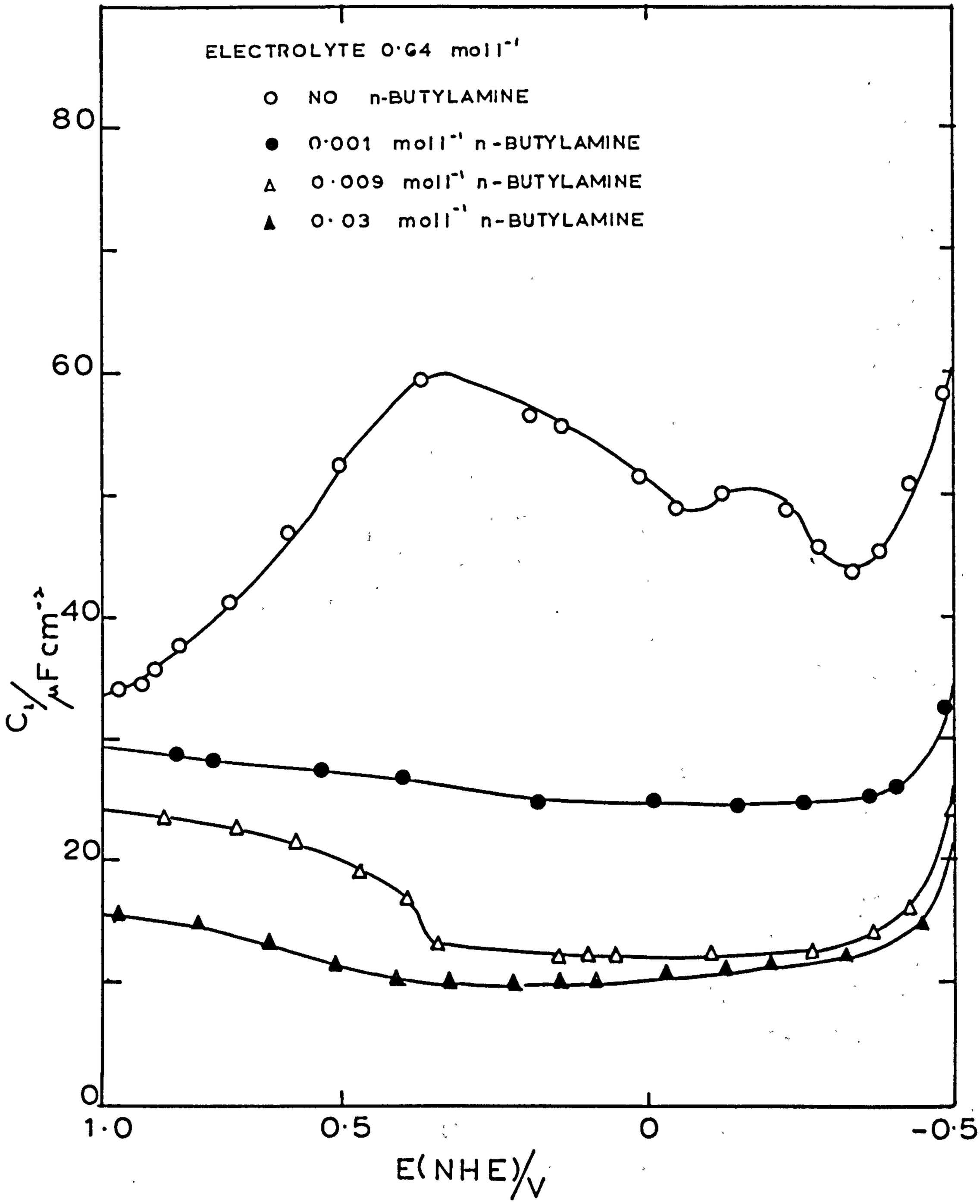

Fig 6 Effect of addition of n-butylamine on differential capacitance curves for polycrystalline platinum in NaOH electrolyte. Cathodic potential sweeping

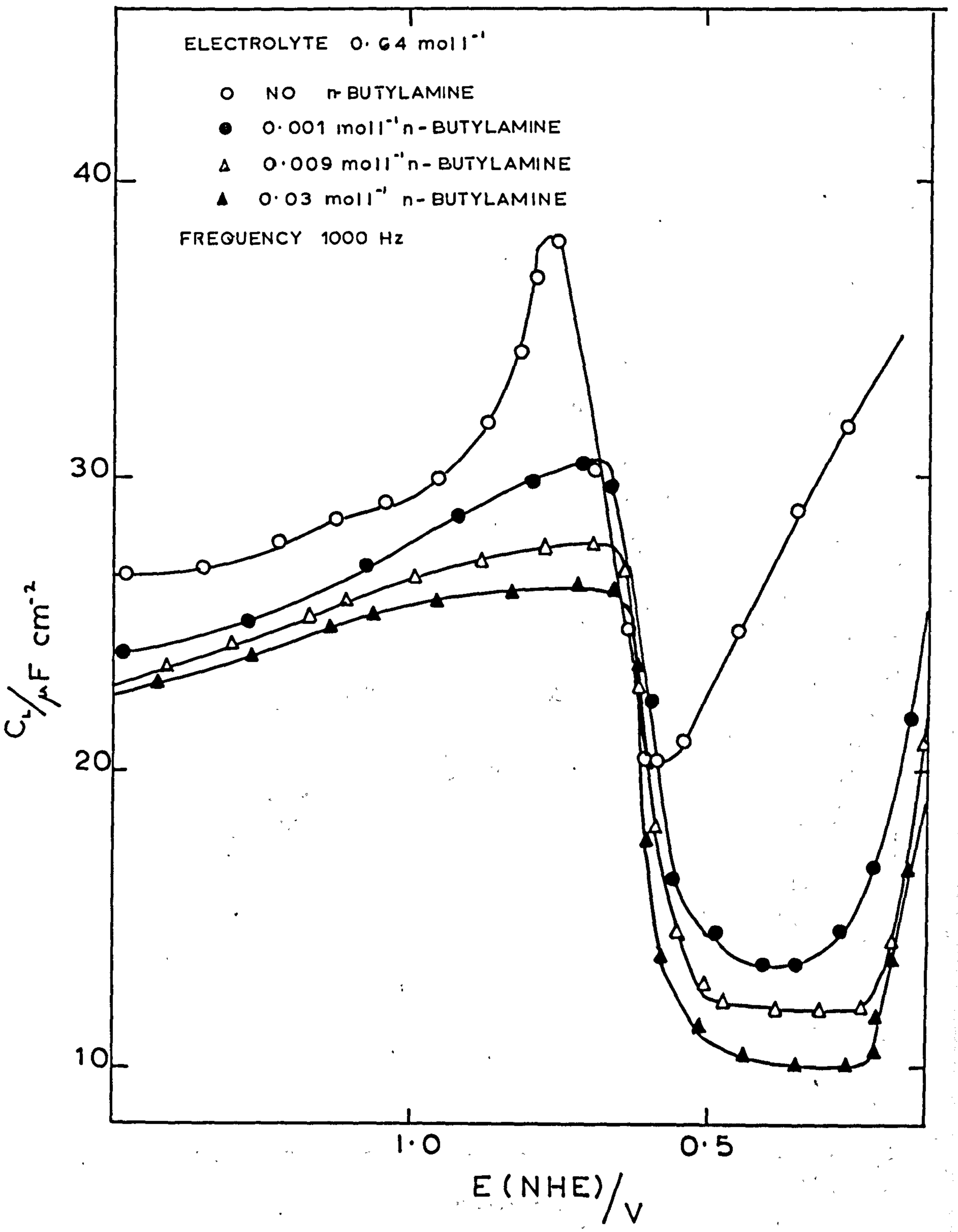

Fig 7 Differential capacitance - bias potential curves for polycrystalline platinum in H_2SO_4 electrolyte. Anodic potential sweeping.

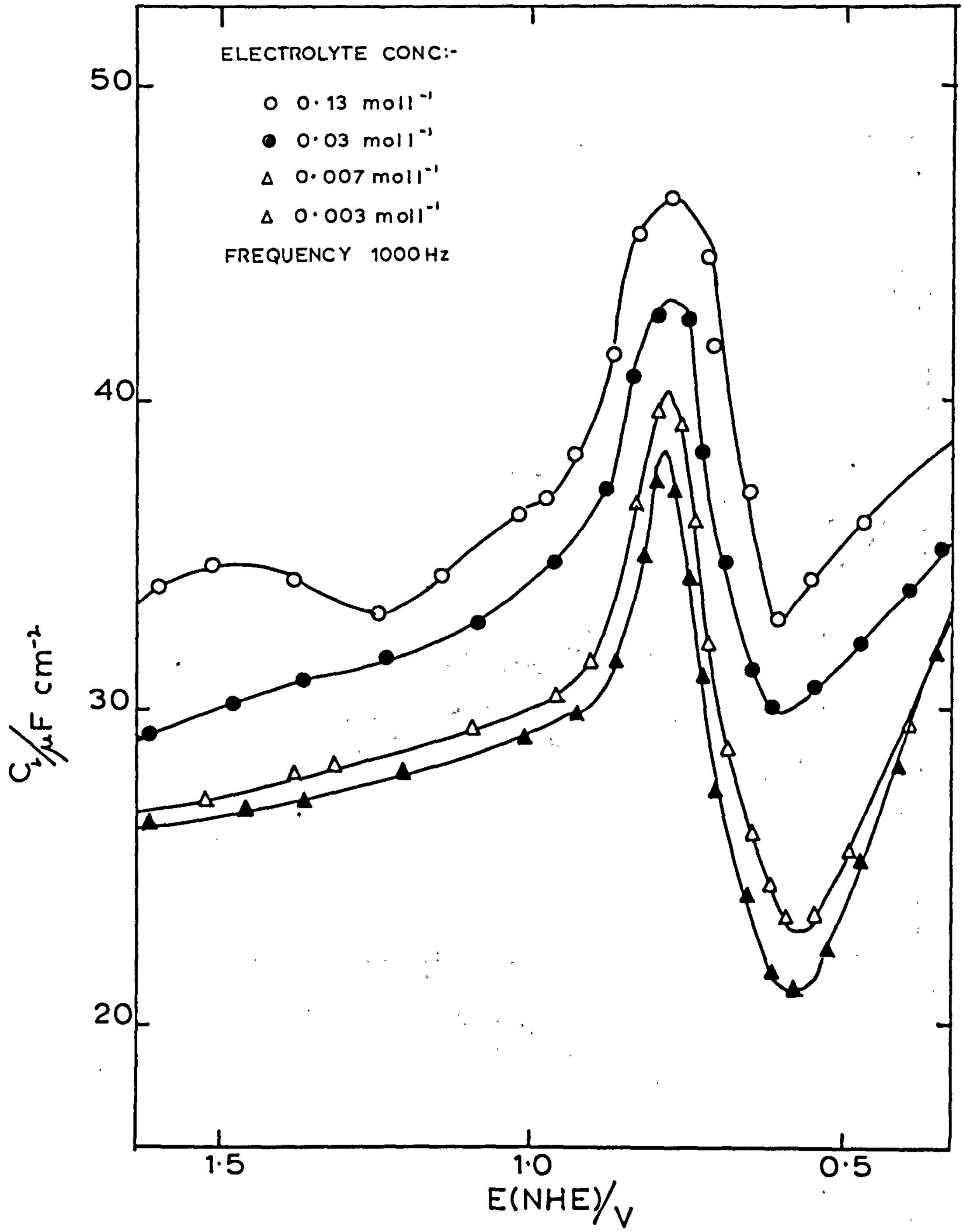

Fig 8 Differential capacitance-bias potential curves for polycrystalline platinum in H_2SO_4 electrolyte. Cathodic potential sweeping.

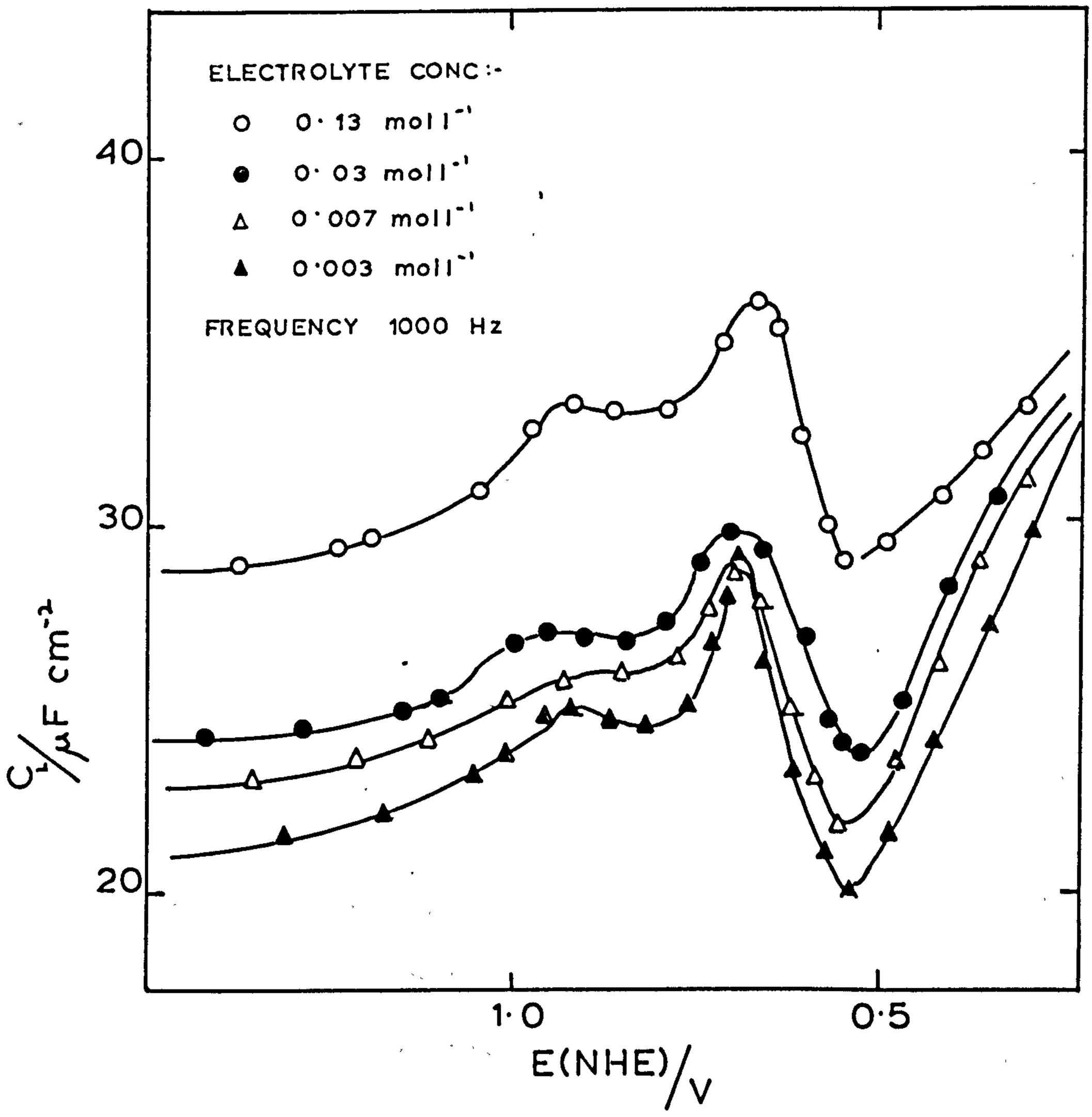

than for NaOH solutions.

Figure 9 shows a typical frequency dispersion of positively swept capacitance curves for polycrystalline platinum in H_2SO_4 solutions containing n-butylamine. The curves show a progressive lowering of the capacitance, at potentials negative with respect to the capacitance minimum with addition of n-butylamine up to 0.07 mol l^{-1}. Thereafter further additions of the organic had little visible effect upon the curves. At potentials positive with respect to the capacitance minimum the curves showed a capacitance peak corresponding to that observed in organic-free NaOH solutions but reduced in magnitude. Complementary negatively swept curves were similar to the positively swept curves but showed a slight negative shift in potential. Figure 10 shows a series of differential capacitance bias potential curves for polycrystalline platinum in H_2SO_4 solutions containing n-butylamine. The curves, which were independent of the direction of potential sweeping, were similar in shape to those obtained in organic free H_2SO_4 solutions but were considerably reduced in magnitude. Maximum adsorption, inferred from the minimum magnitude of the capacitance, was indicated in the potential region neighbouring the capacitance minimum observed in the organic free electrolytes.

Discussion

A capacitance minimum in NaOH solutions was observed at -0.34 V. Prolonged polarization at potentials close to the negative extremity of the experimental polarizable region caused a shift in the capacitance/minimum to more negative potentials indicating the possibility of hydrogen adsorption at the electrode, however, the position of the minimum returned to its original 'unpolarised' position if sufficient recovery time was allowed to ellapse. In H_2SO_4 solutions the capacitance minimum was observed at 0.56 V but at more negative potentials when the electrode was negatively polarised. Recovery of the polarized test electrode took longer than in NaOH solu-

Fig 9 Typical frequency dispersion of differential capacitance for polycrystalline platinum in H_2SO_4 electrolyte.

Fig10 Effect of addition of n-butylamine on differential capacitance curves for polycrystalline platinum in H_2SO_4 electrolyte.

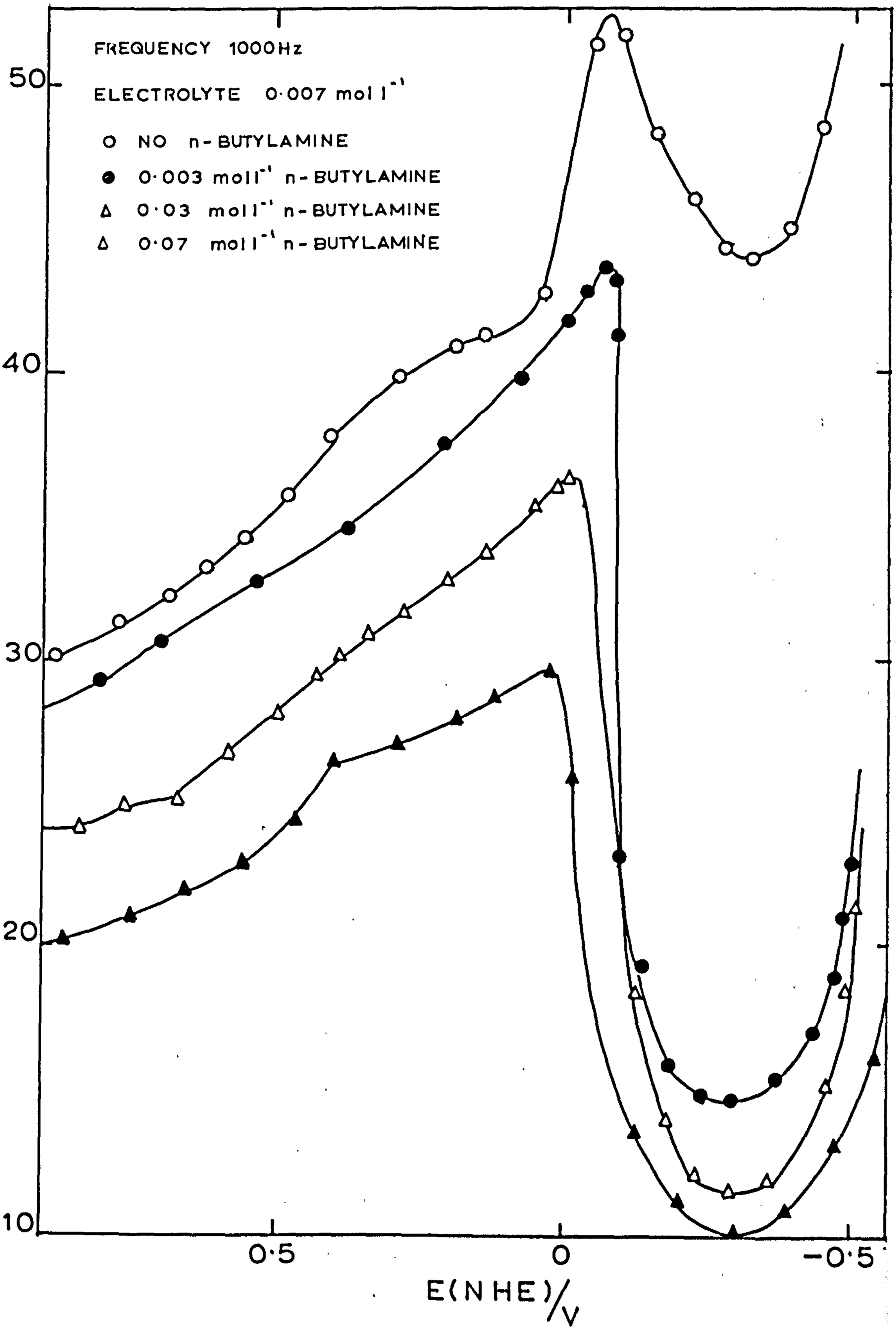

tions indicating a stronger adsorption of hydrogen.

The position of the capacitance minimum in H_2SO_4 solutions is in good agreement with the value of the pzc, 0.6 V, calculated from work function, data[350,353], however, whether or not the double layer structure of a heterogeneous metal is well enough developed to allow a meaningful calculation of the p.z.c. is doubtful.

The capacitance minima (for both NaOH and H_2SO_4 solutions) were observed in all the experimental concentrations. Bockris et al[371] did not report a capacitance minimum for platinum in $KClO_4$ solutions for concentrations greater than 5.8×10^{-3} mol^{-1} in H_2SO_4 solutions. Birintseva and Kabanov[349] and Flinn et al[357] also found no capacitance minimum in solutions of concentration greater than 1.0^{-3} mol 1^{-1}. Burshstein et al[360] showed that a capacitance minimum developed on platinum in 0.1 H_2SO_4 at 0.55 V, which shifted to 0..23 V for 0.0018 N H_2SO_4 and suggested that this was due to a pseudocapacitance associated with the ionization of hydrogen and oxygen. The position of the capacitance minima observed in the present experiments agrees quite well with that reported by Gileadi et al[357] who derived the expression:-

$$v_{pzc} = 0.56 - 2.3 \frac{RT}{F} . pH. \qquad (5)$$

where v_{pzc} is the potential of the capacitance minimum, however since the minima was observed in all the experimental concentrations and a certain degree of frequency dispersion of the capacitance in the region of the minima was observed, it is suggested that the minima does not correspond to the p.z.c. but is probably associated with the pseudocapacitance upon passing from the 'hydrogen' to the 'oxygen' potential regions.

The capacitance peaks observed in all the differential capacitance curves, at $\sim$ 0.3 - 0.35 V (positive potential sweeping) and $\sim$ .05 - 0.1 V (negative sweep-

ing) in H_2SO_4 solutions, are associated with oxygen/OH^- adsorption. The large frequency dispersion of the capacitance curves, in the potential region neighbouring the capacitance peaks, is further evidence in favour of adsorption at such potentials. It is noticeable that in both solutions a negative shift of the potential of the peaks is observed for positively and negatively swept curves:- ~ 0.4 V for NaOH and ~ 0.1 V for H_2SO_4, suggesting irreversibility of the oxygen film formation/dissolution process, and from the relative potential shifts this would appear to be greatest in NaOH solutions. Bold and Breiter[285] suggested the following reaction sequence to explain such irreversibility:-

$$Pt + H_2O \rightleftharpoons PtOH + H^+ + e^- \quad (6)$$

$$PtOH \rightleftharpoons PtO + H^+ + e^- \quad (7)$$

where reaction 7 is faster than 6. The fall in capacitance at positive potentials is due to insoluble oxide formation however it was impossible in this work to show the exact nature of the oxide film present.

For NaOH solutions containing n-butylamine, a marked difference in behaviour was observed in the capacitance measurements, resulting when the potential was positively swept, figure 5, or negatively swept, figure 6. In the positively swept curves the shape is similar to that observed in organic free NaOH, an oxygen/OH^- pseudo-capacitance occurring indicating that, for positive starting potentials, the electrode surface is not fully blocked by adsorbed n-butylamine and completely shielded from attack by oxygen species. For the negatively swept curves an absence of the oxygen/OH^- pseudocapacitance peak indicated an inhibition of adsorption of the oxygen species due to an adsorbed layer of organic molecules.

In H_2SO_4 solutions containing n-butylamine, the differential capacitance curves were similar in shape no matter which way the potential was swept and this is

probably due to complications caused by the formation of the n-butylanium ion. The relatively non-polarizability of the quaternary nitrogen accounting for the less ready adsorption of the organic molecule.

REFERENCES

1. G.W. Vinal, Storage Batteries, Wiley, New York, (1965)

2. P. Ness, Electrochim.Acta., 12, 161 (1967)

3. C.K. Morehouse, R. Glicksman and G.S. Lozier, Proc.I.R.E., 46, 1462 (1958).

4. J.P. Hoare, The Electrochemistry of Oxygen, Interscience, New York, (1969) ch. VII B.

5. J. Burbank, A.C. Simon and E. Willihnganz, Adv.Electrochem. and Electrochem.Eng., Ed.C.W.Tobias, Interscience, New York, 8, 157 (1971)

6. R. De Levie, Adv. in Electrochem. and Electrochem.Eng., Ed. P. Delahay and C.W. Tobias, Interscience, New York, 6, 329 (1967)

7. N.V. Sidgwick, The Chemical Elements and Their Compounds, Oxford Univ. Press, London, 118 (1950)

8. J.A. Darbyshire, J. Chem. Soc., 134, 211 (1932)

9. W.B. White and R. Roy, J. Am.Ceram.Soc., 47, 242 (1964)

10. J.A. Duisman and W.F. Giaque, J. Phys.Chem., 72, 562 (1968)

11. M. Fleischmann and H.R. Thirsk, J.Electrochem.Soc., 110, 688 (1963)

12. W.J. Hamer, J.Amer.Chem.Soc., 57, 9 (1935)

13. W.C. Vosburgh and D.N. Craig, J.Am.Chem.Soc., 51, 2009 (1929)

14. N.E. Bagshaw, R.L. Clarke and B. Halliwell, J.Appl.Chem., 16 (1966)

15. N.E. Bagshaw and K.D. Wilson, Electrochim.Acta., 10, 867 (1965)

16. N.G. Bakhchisaraits'yan and E.A. Dzhafarov, Nekotorye.Vopr.Khim. Technol. i Fiz.Khim.Nauk. p251 (1963)

17. N.G. Bakhchisaraits'yan, E.A. Dzhafarov and G.A. Kokarev, Tr.Mosk. Khim - Tekhnol.Inst., 32, 243 (1961)

18. N.G. Bakhchisaraits'yan and E.A. Dzhafarov, Dokl.Akad.Nauk.Azerb. SSSR, 17, 785 (1961)

19. G.L. Clark and R. Rowan, J.Am.Chem.Soc., 63, 1305 (1941)

20. V.H. Dodson, J. Electrochem.Soc., 108, 401 (1961)

21. E.A. Dzhafarov, N.G. Bakhchisaraits'yan and M.Ya.Fioshin, Byul.Izobret i Tovarnykh Znakov, 9, 20 (1963)

22. E.A. Dzhafarov, Dokl.Akad.Nauk.Azerb., SSSR, 19, 31 (1963)

23. E.A. Dzhafarov, Azerb.Khim.Zh., 3, 127 (1963)

24. A.B. Gancy, J.Electrochem.Soc., 16, 1496 (1969)

25. S. Ghosh, Electrochim.Acta., 14, 161 (1969)

26. F.D. Gibson, Chem.Abst., 67, 7537X

27. J. Giner, A.B. Gancy and A.C. Makrides, Rep.No.265, Harry Diamond Labs., (1967)

28. J.G. Kiseleva and B.N. Kabanov, Dokl.Akad.Nauk, SSSR, 122, 1042 (1958)

29. W. Mindt, J.Electrochem.Soc., 117, 615 (1970)

30. K. Sugino and V. Shibazaki, Denki.Kagaku, 16, 9 (1948)

31. A. Seidell and W.F. Linke, Solubilities of Inorganic Compounds, Wiley, New York, 4th Edition, (1958)

32. J.W. Collat and J.J. Lingane, J.Am.Chem.Soc., 76, 4214 (1954)

33. E. Eberius and M. LeBlanc, Z.Anal.Chem., 89, 81 (1932)

34. A. Bystrom, Chem.Abst., 41, 4053 (1947); Arkiv.Kemi.Min.Geol., A20 (1945)

35. T. Katz and R. LeFaivre, Bull.Soc.Chim. France, 16, D124 (1949)

36. G. Butler and G.L. Copp, J.Chem.Soc., 145, 725 (1956)

37. G.L. Clarke and R. Rowan, J.Am.Chem.Soc., 63, 1305 (1941)

38. G.L. Clarke, N.C. Schieltz and T.T. Quirke, J.Am.Chem.Soc., 59, 2305 (1937)

39. P. Ruetschi, J. Sklarchuk and R.T. Angstadt, Batteries, Ed. by D.H. Collins, Pergamon, 89 (1963)

40. R.T. Angstadt, P. Ruetschi and J. Sklarchuk, Electrochim.Acta., 8, 333, (1963)

41. E. Voss and J. Freundlich, Batteries, Ed.D.H. Collins, Pergamon,p73 (1963)

42. N. Kameyama and T. Fukomoto, J.Soc.Chem.Ind. , Japan, 46, 1022 (1943); 49, 155 (1946)

43. S.S. Tolkachev, Vestnik.Leningrad Univ., 13, No.4, Ser.Fiz i Khim, 1, 152 (1958)

44. A.J. Zaslavskii, Yu. D. Kondrashov and S.S. Tolkachev, Dokl.Akad.Nauk. SSSR, 75, 559 (1950)

45. A.J. Zaslavski and S.S. Tolkachev, Zh.Fiz.Khim., 26, 743 (1952)

46. I.M. Golovanov, Zapiski Vsesoyus. Mineral. Obshchestva, 8, 333 (1959)

47. U.B. Thomas, Trans.Electrochem.Soc.,94, 42 (1948)

48. M.L. Huggins, Phys.Rev., 21, 719 (1923)

49. L.Pauling and J.H. Stur divant, Z. Krist., 68, 239 (1923)

50. H.J. Goldschmidt, Metallurgia, 62, 211, 241 (1960)

51. R.G. McQueen, J.C. Jamieson and S.P. Marsh, Science, 155, 1401 (1967)

52. K. Sasvari, Acta.Phys.Acad.Sci.Hung., 11, 333, 345 (1960)

53. W.B. White, F. Dachille and R. Roy, J.Am.Ceram.Soc., 44, 170 (1961)

54. A.I. Zaslavskii and S.S. Tolkachev, Uchenye Zapiski Leningrad Gosudarst Univ.in A.A. Zhdanova, No. 163, Ser.Khim.Nauk., 12, 186 (1953)

55. J. Leciejewicz and I. Padlo, Naturwissenschaften, 49, 373 (1962)

56. A.S.T.M. index. Powder Diffraction File, Card 8 - 185

57. L. Alexander and H.P. Klug, Anal.Chem., 20, 886 (1948)

58. N.N. Fedorova, I.A. Aguf, L.M. Levinson and M.A. Dasoyan, Ind.Lab., 30, 914 (1964)

59. N.N. Fedorova, I.A. Aguf, L.M. Levinzon and M.A. Dasoyan, Sb.Rab. Khim. Isotochnikam Toka, 252 (1966)

60. D. Kordes, Chem.Ingr.Tech., 38, 638 (1966)

61. D. Fouque, P. Foulloux, P. Buisiere, D. Weigel and M. Prettre, J.Chim.Phys., 62, 1088 (1965)

62. A.S. Brar and R.F. Dapo, J. Electrochem.Soc., 116, (1969) Ab.No.361

63. B. Dickens, as in N.E. Bagshaw, R.L. Clarke and B. Halliwell[14]

64. R.G. Acton, Power Sources, Ed.D.H. Collins, Pergamon, London,p133 (1967)

65. V.A. Kirkinskii, Zh.Neorg.Khim., 10, 1966 (1965)

66. J. Burbank, Power Sources, Ed. D.H. Collins, Pergamon, New York,p147 (1967)

67. E.J. Ritchie, "The Transition of the Polymorphic Forms of Lead Monoxide" Eagle-Picher Res.Labs., Fourth Quarterly Rep. (1967)

68. G. Perrault and J. Brenet, Compt.Rend., 250C, 325 (1960)

69. P. Ruetschi and B.D. Cahan, J. Electrochem.Soc., 104, 406 (1957)

70. S. Anderson and M. Sterns, J.Inorg.Nucl.Chem., 11, 272 (1959)

71. J. Burbank, J. Electrochem.Soc., 106, 369 (1959)

72. R. Baroni, Gazz.Chim.Ital., 68, 387 (1938)

73. K.V. Krishna Rao and S.V. Nagender Naider, Current Sci.(India), 33, 708 (1964)

74. E. Renker, Bull.Soc.Chim. France, 3, 981 (1936)

75. P. Moles and L. Vitoria, An.Fiz.Quin., 27, 52 (1929)

76. C. Holtermann and P. Laffitte, Compt.Rend., 204C, 1818 (1937)

77. M.I. Gillibrand and B. Halliwell, Power Sources, Ed.D.H. Collins, Pergamon, London,p179 (1967)

78. W.H. Palmaer, Z. Elektrochem., 29, 415 (1923)

79. I.A. Aguf, A.J. Rusin and M.A. Dasoyan, Zashchita.Metal i Oksiduye Poktytiya, Korroziya Metal i Issled v Obl.Elektrochim.Akad.Nauk., SSSR, Otd.Obshch i Tekhn.Khim.Sb.Statei, 328 (1965)

80. F. Lappe, J.Phys.Chem.Solids, 23, 1563 (1962)

81. L.H. Piette and H.E. Weaver, J.Chem.Phys., 28, 735 (1958)

82. J.M. Rocard, M. Bloom and L.B. Robinson, Can.J.Phys., 37, 522 (1959)

83. D.A. Frey and H.E. Weaver, J. Electrochem.Soc., 107, 930 (1960)

84. P. Ruetschi and B.D. Cahan, J.Electrochem.Soc., 105, 369 (1958)

85. A. Kittel, Diss.Prague, Czech. (1944)

86. V.J. Veselovskii, Zh.Fiz.Khim., 22, 1302 (1948); Chem.Abst., 43, 2503f (1949)

87. R.A. Baker, J.Electrochem.Soc., 109, 337 (1962)

88. C. Drotschmann, Batteries, 17, 472 (1963); ibid 17, 569 (1964); ibid 19, 85 (1966); ibid 20, 276, 899 (1966)

89. D.G. Thomas, Semiconductors, Ed. N.B. Hannay, Reinhold, New York, (1960)

90. W. Mindt, J.Electrochem.Soc., 116, 1076 (1969)

91. J.R. Pierson, Electrochem.Tech., 5, 323 (1967)

92. S.M. Caulder, J. Electrochem.Soc., 116, (1969) Ab.No. 40

93. J.E. Busbirk, P.D. Boyd and V.V. Smith, Houston meeting of Electrochem. Soc., 9, (Oct. 1960)

94. I.J. Astakhov, I.G. Kiseleva and B.N. Kabanov, Dokl.Akad.Nauk. SSSR, 126, 1041 (1959)

95. A.C. Simon, Batteries 2, Ed. D.H. Collins, Pergamon, New York, 63, (1965)

96. A.C. Simon and E.L. Jones, J. Electrochem. Soc., 109 760 (1962)

97. J. Burbank, Batteries, Ed. D.H. Collins, Pergamon, New York, 43 (1963)

98. J. Burbank, J. Electrochem.Soc., 111, 765 (1964)

99. J. Burbank, J. Electrochem.Soc., 111; 1112 (1964)

100. J. Burbank, Power Sources, Ed. D.H. Collins, Pergamon, New York,p147 (1966); Naval Res.Lab.Rep. 6613 (1967)

PAGE NUMBERING AS ORIGINAL

101. W. Feitknecht and A. Gaumann, J. Chim. Phys., 49 C135 (1952)

102. W. Feitknecht, Z. Elektrochem., 62, 795 (1958)

103. J. Burbank and E.J. Ritchie, J. Electrochem.Soc., 116, 125 (1969)

104. N.G. Bakhchisaraits'yan, K.G. Samoskenkova and G.P. Grechina, Tr.Mosk.Khim-Tekhnol.Inst., 54, 156 (1967)

105. N.P. Fedot'ev and Yu.M. Pozin, Zh.Fiz.Khim., 31, 419 (1958)

106. A.T. Vagramian and Yu. S. Petrova, Physico-Mechanical Properties of Electrolytic Deposits, M. Izd.Akad.Nauk., SSSR (1960)

107. M. Ya. Popereka, Fiz.Metallov i Metallovendenie, 20, 754 (1965)

108. N.G. Bakhchisaraits'yan, V.A. Oshchimskii, A.A. Gfebenkina, E.M. Vasileva and D.D. Cemenov, Tr.Mosk.Khim - Tecknol.Inst., 54, 149 (1967)

109. N.G. Bakhchisaraits'yan, V.A. Oshchinski and V.A. Volgina, Tr. Mosk. Khim - Tekhnol.Inst., 49, 135 (1965)

110. C.J. Bushrod and N.A. Hampson, Br.Corros.J., 6, 129 (1971)

111. I.K. Nishikara, M. Kurachi, M. Hayashi and T. Hashimoto, Suiyokai-Shi, 16, 211 (1967)

112. Y. Shibasaki, Denki Kagaku, 33, 269 (1965)

113. U.R. Evans, The Corrosion and Oxidation of Metals, Arnold, London (1960) Ch.XV

114. M. Fleischmann and M. Liler, Trans.Faraday Soc., 54, 1370 (1958)

115. Y. Shibasaki, J. Electrochem.Soc., 105, 624 (1958)

116. J.J. Lander, J. Electrochem.Soc., 103, 1 (1956)

117. P. Delahay, M. Pourbaix and P. Van Rysselberghe, J. Electrochem.Soc., 98, 57 (1951)

118. H.S. Harned and W.J. Hamer, J.Am.Chem.Soc., 57, 27 (1935)

119. S. Shankman and A.R. Gordon, J.Am.Chem.Soc., 62, 2370 (1939)

120. R.H. Stokes, J.Am.Chem.Soc., 69, 1291 (1947)

121. W.H. Beck, R. Lind and W.F.K. Wynne-Jones, Trans.Faraday Soc., 50, 136 (1954)

122. W.H. Beck and W.F.K. Wynne-Jones, Trans.Faraday Soc., 112, 1133 (1965)

123. C.D. Craig and G.W. Vinal, J.Res.Natl.Bur.Std., 24, 482 (1940)

124. D.J.G. Ives and F.R. Smith, Reference Electrodes, Ed. D.J.G. Ives and G.J. Janz, Academic Press, New York (1961)

125. H. Bode and E. Voss, Z. Elektrochem, 60, 1053 (1956)

126. P. Ruetschi, R.T. Angstadt and B.D. Cahan, J. Electrochem.Soc., 106, 547 (1959)

127. R.T. Angstadt, C.J. Venuto and P. Ruetschi, J. Electrochem.Soc., 109, 177 (1962)

128. S.J. Bone, K.P. Singh and W.F.K. Wynne-Jones, Electrochim.Acta, 4, 288 (1961)

129. W.H. Beck, K.P. Singh and W.F.K. Wynne-Jones, Trans.Faraday Soc., 55, 331 (1959)

130. M. Pourbaix, Atlas of Electrochemical Equilibrium, Gauthiers-Villars, Paris (1963)

131. S.C. Barnes and R.T. Mathieson, Batteries (2), Ed. D.H. Collins, Pergamon London,p41 (1965)

132. B.N. Kabanov, I.G. Kiseleva and D.I. Leikis, Dokl.Akad.Nauk., SSSR, 99, 805 (1054)

133. B.N. Kabanov, Prace Electrochem.Conf., Warsaw,p515 (1957)

134. B.N. Kabanov, 4th Edition Treatise of Electrochemistry, Izd-vo, Akad,Nauk, SSSR, 252 (1959)

135. D. Leikis and E.K. Venstrem, Proc.Acad.Sci., USSR, Phys.Chem.Sect., 112, 17 (1957)

136. D. Leikis and E.K. Venstrem, Dokl.Akad.Nauk., SSSR, 112, 97 (1957)

137. G.A. Kokarev, N.G. Bakhchisaraits'yan and G.J. Medvedev, Katal. Reakts.Zhidk.Faze., Tr.Vses.Konf. 2nd Alma-Ata, Kaz, SSSR, 406 (1966) (Pub. 1967)

138. J.P. Carr, N.A. Hampson and R. Taylor, J. Electroanal.Chem., 27, 109(1970)

139. J.P. Carr, N.A. Hampson and R. Taylor, J. Electroanal.Chem.,27, 201(1970)

140. J.P. Carr, N.A. Hampson and R. Taylor, J. Electroanal.Chem.,28, 65 (1970)

141. J.P. Carr, N.A. Hampson and R. Taylor, J. Electroanal.Chem., 27 466(1970)

142. J.P. Carr and N.A. Hampson, J. Electrochem.Soc., 118, 1262 (1971)

143. Ya M. Kolotyrkin and G.J. Medvedev, Zh.Fiz.Khim., 25, 1355 (1951)

144. F.J. Kukoz and S.A. Semenchenko, Electrokhimiya, 2, 74 (1966); 1, 1454 (1965)

145. G.A. Kokarev, N.G. Bakhchisaraits-yan, A.N. Smirnova and G.J. Medvedev, Tr.Mosk.Khim.Tekhnol.Inst. 54, 169 (1967)

146. D.C. Grahame, J.Am.Chem.Soc., 76, 4819 (1954)

147. G. Gouy, J.Phys.Radium, 9, 457 (1960); Compt.Rend., 149, 654 (1910)

148. D.L. Chapman, Phil.Mag., 25, 475 (1913)

149. P. Delahay, Double Layer and Electrode Kinetics, Interscience, New York, (1965), Ch.2.

150. J.P. Carr, N.A. Hampson and R. Taylor, Ber.Bunsenges physik.Chem., 74, 557 (1970)

151. H.B. Mark, J.Electrochem.Soc., 109, 634 (1962)

152. H.B. Mark, J.Electrochem.Soc., 110, 945 (1963)

153. H.B. Mark and W.C. Vosburgh, J.Electrochem.Soc., 108 615 (1961)

154. N.A. Hampsön, P.C. Jones and R.F. Phillips, Can.J.Chem., 45, 2039 (1967)

155. N.A. Hampson, P.C. Jones and R.F. Phillips, Can.J.Chem., 45,2045 (1967)

156. N.A. Hampson, P.C. Jones and R.F. Phillips, Can.J.Chem., 46, 1325 (1968)

157. N.A. Hampson, P.C. Jones and R.F. Phillips, Can.J.Chem., 47, 2171 (1969)

158. V.N. Varypaev and N.P. Fedot'ev, Tr.Leningr.Tekhnol.Inst. im Lensoveta, 46, 103 (1958)

159. B.N. Kabanov, D.I. Leikis and E.I. Krepakova, Dokl.Akad.Nauk., SSSR, 98, 989 (1954)

160. M. Fleischmann and H.R. Thirsk, Trans.Faraday Soc., 51, 71 (1955)

161. S. Ikari, S. Yoshizawa and S. Okada, J.Electrochem.Soc., Japan, Overseas Ed., 27, E223 (1959)

162. S.J. Bone, M. Fleischmann and W.F.K. Wynne-Jones, Trans.Faraday Soc., 55, 1783 (1959)

163. M. Fleischmann and H.R. Thirsk, Electrochim.Acta, 1, 146 (1959)

164. I.A. Aguf, Elektrokhimiya, 4, 1130 (1968)

165. H. Bode and E. Voss, Electrochim.Acta., 6, 11 (1962)

166. R.T. Angstadt, C.J. Venuto and P. Ruetschi, J.Electrochem.Soc., 109, 177 (1962)

167. W.H. Beck, R. Lind and W.F.K. Wynne-Jones, Trans.Faraday Soc, 50, 147 (1954)

168. J. Burbank, J.Electrochem.Soc., 103, 87 (1956)

169. P. Delahay, C.F. Pillon and D. Perry, J. Electrochem.Soc., 99, 414 (1952)

170. K. Ekler, Can.J.Chem., 42, 1355 (1964)

171. S. Ikari and S. Yoshizawa, Denki.Kagaku, 28, 675 (1960)

172. P. Jones, H.R. Thirsk and W.F.K. Wynne-Jones, Trans.Faraday Soc., 52, 1003 (1956)

173. B.N. Kabanov and D.I. Leikis, Z. Elektrochem., 62, 660 (1958)

174. R. Lorenz and E. Lauber, Z. Elektrochem., 15, 157 (1909)

175. P. Jones, R. Lind and W.F.K. Wynne-Jones, Trans.Faraday Soc., 50, 972(1954)

176. M. Maeda, Denki Kagaku, 25, 195 (1957)

177. M. Maeda, Acta.Met., 6, 66 (1958)

178. K. Nagel, R. Ohse, and E. Lange, Z.Elektrochem., 61, 795 (1957)

179. R. Piontelli and G. Poli, Z. Elektrochem., 62, 320 (1958)

180. E.F. Wolf and C.F. Bonilla, Trans.Electrochem.Soc., 79, 307 (1941)

181. J.J. Lander, J. Electrochem.Soc., 98, 213 (1951)

182. J.J. Lander, J. Electrochem.Soc., 98, 220 (1951)

183. J.J. Lander, J. Electrochem.Soc., 98, 522 (1951)

184. R. Ohse, Werkstoffe u. Korrosion, 11, 220 (1960)

185. D. Pavlov and N. Iordanov, J. Electrochem.Soc., 117, 1103 (1970)

186. D. Pavlov, Electrochim.Acta., 18, 2051 (1968)

187. D. Pavlov, C.N. Poulieff, E. Klaja and N. Iordanov, J.Electrochem.Soc., 16, 316 (1969)

188. D. Pavlov, Ber.Bunsenges.Phys.Chem., 71, 398 (1967)

189. D. Pavlov, Electrochim.Acta., 13, 2051 (1968)

190. D. Pavlov and R. Papova, Electrochim.Acta., 15, 1483 (1970)

191. D. Spahrbier, Diss.Stuttgart, (1960)

192. E. Tarter and K. Ekler, Can.J.Chem., 47, 2191 (1968)

193. H.R. Thirsk and W.F.K. Wynne-Jones, J.Chim.Phys., 49, 131 (1952)

194. S. Ikari and S. Yoshizawa, Denki Kagaku, 28, 503 (1960)

195. L.V. Vanyukova, M.M. Isaeva and B.N. Kabanov, Dokl.Akad.Nauk, SSSR, 143, 377 (1962)

196. I. Astakhov, E.S. Vaisberg and B.N. Kabanov, Dokl.Akad.Nauk., SSSR, 154, 1414 (1964)

197. M.C. Boswell and R.K. Iler, J.Am.Chem.Soc., 58, 924 (1936)

198. J. Burbank, N.R.L. Report, 6613 (1967)

199. J. Burbank, J.Electrochem.Soc., 104, 693 (1957)

200. B.D. Cahan and P. Ruetschi, J.Electrochem.Soc., 106, 543 (1959)

201. G. Grube, Z.Elektrochem., 28, 273 (1922)

202. S. Ikari, S. Yoshizawa and S. Okada, J.Electrochem.Soc., Japan, 27, E247 (1959)

203. H.E. Haring and U.B. Thomas, Trans.Electrochem.Soc., 48, 293 (1935)

204. S. Glasstone, J.Chem.Soc., 121, 2091 (1922)

205. D.F.A. Koch, Electrochim.Acta, 1, 32 (1959)

206. E.V. Krivolapova and B.N. Kabanov, Trudy Soveshchaniya Elektrokhim.Akad. Nauk. SSSR, Otd.Khim.Nauk, 1950, 539 (1953)

207. W.J. Muller, Kolloid - 2. Z.Polym., 86, 150 (1939)

208. V.J. Goncharov, F.I. Kukoz and M.F. Skalozubov, Issled.Obl.Khim. Istchnikov Toka, 193 (1966)

209. A. Ragheb, W. Machu and W.H. Boctor, Werkst.Korros., 16, 676 (1965)

210. J. Burbank, J.Electrochem.Soc., 106, 369 (1959)

211. P. Ruetschi and R.T. Angstadt, J.Electrochem.Soc., 111, 1323 (1964)

212. M. Maeda, J.Electrochem.Soc., Japan, 25, 197 (1957); Oversead ed., 26, E21; E183 (1958)

213. F.I. Kukoz and M.F. Skalozubov, Zh.Prikl.Khim., 33, 177 (1960)

214. P. Chartier and R. Poisson, Bull.Soc.Chim. France, 7, 2255 (1969)

215. J.P. Carr, N.A. Hampson and R. Taylor, J.Electroanal.Chem., 33, 109 (1971)

216. H.S. Panesar, Power Sources 3, Ed. D.H. Collins, Oriel Press, Newcastle (1971)

217. S. Sekido and S. Katoh, Denki Kagaku, 37, 550 (1969)

218. R.F. Amilie, J.B. Ockerman and P. Ruetschi, J. Electrochem.Soc., 108, 377 (1961)

219. P. Ruetschi, J.B. Ockerman and R. Amilia , J.Electrochem.Soc., 107, 325 (1966)

220. P. Ruetschi and P. Delahay, J.Phys.Chem., 23, 596 (1955)

221. P. Ruetschi, R.T. Angstadt and B.D. Cahan, J. Electrochem.Soc., 106, 547 (1959)

222. S.H. Chin, Y.C. Chu, C.W. Chin and K.T. Yuan, Chung-Kuo K'O Hseuh Yuan, Ying Yung Hua Hsueh Yeu Chin Chi K'an, 16, 34 (1966)

223. M.I. Gillibrand and G.R. Lomax, Trans.Faraday Soc., 55, 643 (1959)

224. S. Glasstone, J.Chem.Soc., 121, 2091 (1922)

225. S. Glasstone, J.Chem.Soc., 121, 1459 (1922)

226. B.N. Kabanov, E.S. Weisberg, J.L. Romanova and E.V. Krivolapova, Electrochim.Acta, 9, 1197 (1964)

227. B.N. Kabanov, Trudy Chetvertogo Sov.Elektrokhim Moscow, 252 (1956) (Pub. 1959)

228. I.G. Kiseleva and B.N. Kabanov, Dokl.Akad.Nauk. SSSR, 108, 864 (1956)

229. P. Kivalo and V. Vuorio, Suomen Kenu - stilehti, 34, 1079 (1962)

230. A.J. Krasil'shchikov, Zh.Fiz.Khim., 37, 531 (1963)

231. E.V. Krivolopava, E.S. Vaisberg and B.N. Kabanov, Trudy Chetvertogo Sov., Elektrochim. Moscow, p757 (1956) (Pub. 1959)

232. A.C. Makrides, J. Electrochem.Soc., 113, 1158 (1966)

233. E.M. Otto, J. Electrochem.Soc., 113, 525 (1966)

234. M.S.V. Pathy and H.V.K. Udupa, Electrochim.Acta., 10, 1185 (1965)

235. K. Sugino, T. Tomonari and M. Takahashi, J.Chem.Soc.Japan, Ind.Chem. Sect., 52, 75 (1949)

236. G.A. Kokarev, N.G. Bakhchisaraits'yan and V.V. Panteleeva, Tr.Mosk. Khim.Tekhnol.Inst., 54, 161 (1967)

237. A.N. Frumkin, Zh.Fiz.Khim., 23, 1477 (1969)

238. K. Elbs and J. Forrsell, Z.Electrochem., 62, 795 (1958)

239. H. Willard and R.R. Ralston, Trans.Electrochem.Soc., 62, 239 (1932)

240. C.L. Mehltretter, U.S. Patent, 2, 830, 941 (1958)

241. C.L. Mehltretter and C.S. Wise, Ind.Eng.Chem., 51, 511 (1959)

242. V.F. Pfeifer, V.E. Sohns, H.F. Conway, E.B. Lancaster, S. Dabie and E.L. Griffin, Ind.Eng.Chem., 52, 201 (1960)

243. Y. Aiya, S. Fujii, K. Sugino and K. Shirai, J.Electrochem.Soc., 109, 419 (1962)

244. T. Osuga and K. Sugino, J.Electrochem.Soc., 104, 448 (1957)

245. E. Torigai and E. Ishii, Bull.Osaka Ind.Res.Inst., 7, 195 (1956)

246. Y. Kato, K. Sugino, K. Koizumi and S. Kitahara, Electrotech.J.Japan, 5, 45 (1941)

247. S. Kitahara and T. Osuga, J.Electrochem.Soc.,Japan, 10, 409 (1942)

248. K. Sugino, Bull.Chem.Soc., Japan 23, 115 (1950)

249. J. Mizuguchi, J. Electrochem.Soc., Japan, 17, 294 (1947)

250. Y. Kato and K. Koizuim, J.Electrochem.Soc., Japan, 2, 309 (1934)

251. T. Osuga and K. Sugino, J.Electrochem.Soc., 104, 448 (1957)

252. G. Angel and H. Mellquist, Z.Elektrochem., 40, 702 (1934)

253. J.C. Grigger, H.C. Miller and F.D. Loomis, J.Electrochem.Soc., 105, 100 (1958)

254. K.C. Narasimham, S. Sundarajan and H.V.K. Udupa, J.Electrochem.Soc., 108, 798 (1961)

255. H. Debange, Brit.Pat. 148, 760 (1919); C.A. 15, 212 (1921); Ital.Pat. 172, 916 (1919)

256. K.C. Narasimham and H.V.K. Udupa, Proc.Symp. "Electrolytic Cells" p.22, Central Electrochem.Res.Inst., Karaikudi - 3,5. Rly.India (1961)

Indian 66, 95 (1958)

257. R. Ramaswamy, M.S. Venkatochalapathy and H.V.K. Udupa, J.Electrochem Soc., 110, 294 (1963)

258. B. Lovrecek, J. Phys.Chem., 63 (1959) 1759

259. J.P.G. Farr and N.A. Hampson, Electrochem.Tech., 6, 10 (1968)

260. E.K.Venstrem and P.A. Rehbinder, Dokl.Akad.Nauk,SSSR, 68, 329 (1949)

261. E.K. Venstrem, P.A. Rehbinder and V. Hikchtman, Dokl.Akad.Nauk,SSSR., 107, 105 (1956)

262. E.K. Venstrem and P.A. Rehbinder, Zh.Fiz.Khim., 26, 1847 (1952)

263. A.N. Frumkin, Z. Elektrochem., 59, 807 (1955)

264. T. Borisava, B. Ershler and A.N. Frumkin, Zh.Fiz.Khim., 22, 925 (1948)

265. N.V. Nikolaeva, N.S. Shapino and A.N. Frumkin, Dokl.Akad.Nauk, SSSR, 86, 581 (1952)

266. G.M. Deriaz, Ph.D. Thesis, University of Birmingham (1951)

267. A.N. Frumkin, J.Res.Inst.Catal., Hokkaido Univ., 15, 61 (1967)

268. Ya.Kolotyrkin, C.I.T.C.E. Rept.,9th Mtg., Butterworths, London (1958) 406; Trans.Faraday Soc., 55, 455 (1959)

269. D.I. Leikis and B.N. Kabanov, Tr.Inst.Fiz.Khim.Akad.Nauk, SSSR., 6, Nov. Metody Fiz.Khim.Issled., 2, 5 (1957)

270. D. Lowe, Final year project thesis, Loughborough University of Technology, 1966

271. J.E.B. Randles, Private communication

272. K. Rybalko and D.I. Leikis, Electrokhimiya, 3, 383 (1967)

273. Ya.Kolotyrkin and A.N. Frumkin, Zh.Fiz.Khim., 15, 346 (1941)

274. Ya.Kolotyrkin and N. Bune, Zh.Fiz.Khim., 21, 581 (1947)

275. Ya.Kolotyrkin, Zh.Fiz.Khim., 20, 667 (1946)

276. J.L. Dawson, PhD Thesis, University of Salford, 1970

277. E.J. Ritchie and J. Burbank, J. Electrochem.Soc., 117, 299 (1970)

278. D.W. Jones, J.Soc.Chem.Ind., 47, 151 (1928)

279. G. Osterheld and A. Portmann, Hlev.Chim.Acta., 24, 389 (1941)

280. V.P. Mashovets and A.F. Layanders, Zh.Prikl.Khim., 21, 441 (1948)

281. J. Burbank, U.S. Naval Res.Lab.Report 6078, 1964

282. C.J. Bushrod, M.A. Goulden, N.A. Hampson and R.J. Latham, J.Electroanal.Chem., 30, 59 (1971)

283. E.S. Sevastpyauov and D.I. Leikis, Isv.Akad, Nauk, SSSR, Ser.Khim., 450 (1964)

284. Wu.Hao-Tsing and Lin Chin-Cheng, Acta.Chim.Sinica., 29, .95 (1963)

285. M.E. Khaga and V.E. Past, Soviet Electrochemistry, 5, 574 (1969)

286. M. Pourbaix, Atlas of Electrochemical Equilibria in Aqueous Solutions, Pergamon,London, New York, 1966, p.52

287. A.J. Bethune and N.A.S. Land in C.A. Hampel (Ed), Encyclopedia of Electrochemistry, Reinhold, New York, 1964

288. B. Chalmers, Physical Metallurgy, Wiley, New York, (1959) 371

289. A.P. Sfutzenreuter and G. Masing, Z. Metalk, 42, (1951) 361

290. E.K. Venstrem, V.J. Likhtman and P.A. Rehbinder, Dokl.Akad.Nauk., SSSR., 107 (1956) 106

291. T.N. Koropaeva, B.V. Deragin and B.N. Kabanov, Koloidn.Zh., 24 (1962) 396; Izv.Akad.Nauk.SSSR, Otd.Khim.Nauk., (1963) 257

292. G.M. Schmid and N. Hackerman, J.Etectrochem.Soc., 109 (1962) 243; 110 (1963) 440

293. B.S. Krasikov, Zh.Prikl.Khim., 37 (1964) 2420; The Potentials of Zero Charge of Metals and Alloys, LDNTP, Leningrad 1963

294. M. Green and H. Dahms, J.Electrochem.Soc., 110 (1963) 466

295. T.N. Anderson, R.S. Perkins and H. Eyring, J.Am.Chem.Soc., 86 (1964) 449

296. D.D. Bode, Jr. T.N. Anderson and H. Eyring, J.Phys.Chem., 71 (1967) 792

297. M.Petit and J. Clavilier, Compte Rendus, 264, Series C, 1967, 145

298. J. Clavilier, A. Hamelin and G. Valette, Compte Rendus, 265, Series C, 1967, 221

299. J. O'M. Bockris, S.D. Argade and E. Gileadi, Electrochim.Acta, 14 (1969) 1259

300. A. Hamelin, M. Sotto and G. Valette, Compte Rendus, Series C, 268, (1969) 213

301. A. Hamelin, and J. Lecoeur, Coll.Czech.Chem.Comms., 36 (1971) 714

302. J. Clavilier and N. Van Huong, Compte Rendus, Series C, 270 (1970) 982

303. V.S. Fomenko, The Emission Properties of the Chemical Elements and their Compounds, Naukova Dumka, 1964

304. V. Jendrasic, J. Electroanal.Chem., 32 (1969) 157

305. T.R. Beck, Paper presented at the 19th meeting of CITCE, Detroit, September 1968

306. F.H. Jeffery, Trans.Faraday Soc., 11 (1915) 172

307. F. Jirsa and O. Buryanek, Z.Elektrochem., 29 (1923) 126

308. F. Jirsa and H. Jelinek, Z. Elektrochem., 30 (1924) 286, 534

309. R.H. Gerke and M.D. Rourke, J. Maer.Chem.Soc., 49 (1927) 1855

310. T.F. Buehrer and W.E. Roseveare, J.Amer.Chem.Soc., 49 (1927) 1989

311. W.I. Shutt and A. Walton, Trans.Faraday Soc., 30 (1934) 914

312. G. Armstrong, F. Himsworth and I. Butler, Proc.Roy.Soc., 143A (1934) 89

313. G. Deborin and B. Ershler, Acta.Physicochem. URSS, 13 (1940) 347

314. A. Hickling, Trans.Faraday Soc., 42 (1946) 518

315. S. Wakkad and A. Din, J.Chem.Soc., 9 (1954) 3098

316. F. Bauman and I. Shain, Anal.Chem., 29 (1957) 303

317. S. Barnatt, J. Electrochem.Soc., 106 (1959) 722

318. H. Laitenen and M. Chao, J.Electrochem.Soc., 108 (1961) 726

319. S. Brummer and A. Makrides, J.Electrochem.Soc., 111 (1964) 1122

320. G.M. Schmid and R.W. O'Brien, J.Electrochem.Soc., 111 (1964) 832

321. F.F. Faizullin and N.P. Nikandrov, Elektrokhimiyia, 3 (1967) 988

322. J.N. Gaur and G.M. Schmid, J.Electroanal.Chem., 24 (1970) 279

323. M. Pourbaix, Atlas dpequilibres Electrochimique, Paris 1963, 399

324. A.N. Frumkin, A.W. Gorodetzkaya, B.N. Kabanov and N.A. Balashova, Phys.Z.Sowjetunion, 1 (1932) 225

325. A.N. Frumkin and B.N. Kabanov, Phys.Z.Sowjetunion, 5 (1934) 4

326. A.N. Frumkin, Actualites sci.et ind., (1935) 373

327. A. Slygin, A.N. Frumkin and V. Medvedovsky, Acta Physicochim, URSS, 4 (1936) 911

328. B.V. Ershler, Acta Physicochium, URSS, 7 (1937) 327

329. N.A. Balashova and A.N. Frumkin, Dokl.Akad.Nauk., SSSR, 20 (1938) 449

330. P. Dolin, B.V. Ershler and A.N. Frumkin, Zhur.Fiz.Khim., 14 (1940) 886, 907; Acta Physicochim, URSS, 13 (1940) 747, 779; Zhur.Fiz.Khim., 22 (1948) 925

331. T.I. Borisova and B.V. Ershler, Zhur.Fiz.Khim., 24 (1956) 337

332. F.P. Bowden and L. Young, Research, 3 (1950) 235

333. A. Eucken and B. Weblus, Z. Electrochem., 55 (1951) 114

334. S. Schuldiner, J.Electrochem.Soc., 99 (1952) 488; Ibid, 101 (1954) 426

335. A.N. Frumkin, V.S. Bagotskii, Z.A. Jofa and B.W. Kabanov, Kinetics of electrode processes, Moscow State University Press, 1952

336. W.D. Robertson, J.Electrochem.Soc., 100 (1953) 194

337. T.I. Borisova and V.J. Veselovskii, Zh.Fiz.Khim., 37 (1953) 1195

338. A. Ruis, J. Llopis and F. Colom, Proc.of the Int. Com. on Electrochemical Thermodynamics and Kinetics, 6th meeting, Butterworths, London, 1955, p.280, and 414.

339. M. Brieter, H. Kamnermaier and C.A. Knorr, Z.Electrochem., 60 (1956) 37

340. E.O. Ayazyan, Dokl.Akad.Nauk., SSSR, 100 (1955) 473

341. V.L. Kheifets and B.S. Krasikov, Dokl.Akad.Nauk., SSSR, 109 (1956) 586; Zh.Fiz.Khim., 31 (1957) 1992

342. J.N. Sarmousakis and M.J. Prager, J.Electrochem.Soc., 104 (1957) 454

343. P.V. Popat and Hackerman, J.Phys.Chem., 62 (1958) 1148

344. J.J. McMullen and N. Hackerman, J.Electrochem.Soc., 106 (1959) 341

345. H.A. Laitenen and C.G. Enke, J.Electrochem.Soc., 107 (1960) 773

346. N.A. Balashova and N.S. Merkulova, Soviet Electrochemistry, 1 (1961) 23

347. T.M. Voropaeva, B.V. Deryagin and B.N. Kabanov, Dokl.Akad.Nauk., SSSR, 128 (1959) 981; Koloidn.Zh., 24 (1962) 396; Izv.Akad.Nauk.,; SSSR, Otd., Khim.Nauk, 2 (1963) 257

348. M. Brieter, Trans.Symp. on Electrode Processes, Ed. E. Yeager, Wiley, New York, 1961, p.307; Electrochem.Soc., 109 (1962) 42, 425, 622; Electrochim.Acta, 8 (1963) 925

349. T.P. Birintseva and B.N. Kabanov, Zh.Fiz.Khim., 37 (1963) 2600

350. B.S. Krasikov, The Potentials of Zero Charge of Metals and Alloys, L.D.N.T.P., Leningrad, 1963

351. V.E. Kazarinov and N.A. Balashova, Dokl.Akad.Nauk., SSSR, 157 (1964) 1174: Uspekhi Khim., 31 (1965) 1721; Coll.Czech.Chem.Comm., 30 (1965) 4184

352. M.C. Banta and N. Hackerman, J.Electrochem.Soc., 111 (1964) 114

353. V.S. Fomenko, The Emission Properties of the Chemical Elements and Their Compounds, Nauk.Dauk.Kiev. (1964)

354. A.N. Frumkin, Svensk.Kem.Tidskr., 77 (1965) 300

355. N.A. Balashova, V.E. Kazarinov, Elektrochimiya 1 (1965) 512

356. F.I. Kukoz, S.A. Semenchenko and V.J. Bagdanov, Issled.Obl.Khim. Istochnikov.Toka (1966) 201

357. E. Gileadi, S.D. Argade and J.O'M. Bockris, J.Phys.Che., 70 (1966) 2044

358. A.N. Frumkin, G. Mausurov, V.Kazarinov and N.A. Balashova, Coll. Czech. Comms., 31 (1966) 806; Elektrokhimiya 2 (1966) 1438

359. T.B. Warner and S. Schuldiner, Electrochim.Acta, 11 (1966) 307

360. R. Burstein, H.G. Pshenichnikov and L.A. Shevchenko, J.Electrochem.Soc., 113 (1968) 1022

361. A.N. Frumkin, J.Electrochem.Soc., 113 (1966) 1022

362. A.N. Frumkin, N.A. Balashova and V.E. Kazarinov, J.Electrochem.Soc., 113 (1966) 1011

363. D.J. Ben Daniel and F.G. Will, J.Electrochem.Soc., 114 (1967) 909

364 L. Formaro and S. Trasatti, Electrochim.Acta, 12 (1967) 1457

365. R. Kh. Burshtein, H.G. Pshenichnikov and L.A. Shevchenko, Elektrokhimiya, 5 (1969) 332

366. T.N. Andersen, J.L. Anderson, D.D. Bode Jr., and H.Eyring, J.Res.Inst. Catalysis, Hokkaido Univ., 16 (1968) 449

367. M. Rosen, D.R. Flinn and S. Schuldiner, J.Electrochem.Soc., 116 (1969) 1112; Coll.Czech.Chem.Comms., 36 (1971) 454

368. R.Kh. Burshtein and A.G. Pshenichnikov, Elektrokhimiya, 5 (1969) 332

369. C. Bernard, Electrochim. Acta, 14 (1969) 143

370. V. Jendrasic, J. Electroanal.Chem., 22 (1969) 157

371. J. O'M. Bockris, S.D. Argade and E. Gileadi Electrochim.Acta., 14 (1969) 1259

372. V.I. Luk'yanycheva, E.M. Strochkova and V.S. Bagotskii, Elektrokhimiya, 6 (1970) 701

373. S.Ya. Vasina and O.A. Petrii, Elektrokhimiya, 6 (1970) 242

374. A.N. Frumkin and O.A. Petrii, Electrochim.Acta, 15 (1970) 391

375. L.Fomaro and S. Trasatti, Electrochim.Acta, 15 (1970) 729

376. J.P. Hoarė, Nautre, London, 204 (1964) 71

377. J. Gillman, Electrochim. Acta, 9 (1964) 1025

378. J. Llopis and F. Colom, Anr.Soc.Esp.Fis.Quim., 52A (1956) 233

379. S. Trasatti, Electrochim.Metall., 1 (1966) 267

380. L.Young, Anodic Oxide Films, Academic Press, New York, 1961, ch.22

381. J.A.V. Butler, Electrical Phenomena at Interfaces, Methuen, London, 1961, Ch. IX

382. P. Delahay, Double Layer and Electrode Kinetics, Wiley-Interscience, New York, 1965

383. K. Vetter, Electrochemische Kinetik, Springer, Berlin, 1961, Ch.4.

384. S. Gilman, Electroanalytical Chemistry, Vol.2., ed. A.J. Bard, Arnold London 1967, pp.111

385. W. Bold and M.W. Breiter, Electrochim.Acta, 5 (1961) 169

386. S.W. Feldberg, C.G. Enke and C.E. Bricker, J.Electrochem.Soc., 110 (1963) 826

387 R.N. Adams, Electrochemistry at Solid Electrodes, Dekker

388. G. Archdale and J.A. Harrison, J.Electroanal Chem.,